Application of the cross-metathesis reaction as alternative methodology for the synthesis of *para*-methoxycinnamate analogues as sunscreen components.

Dissertation submitted in fulfillment of the requirements for the degree

Magister Scientiae

in the

Department of Chemistry

Faculty of Natural and Agricultural Sciences

at the

University of the Free State

Bloemfontein

by

Marthinus Rudi Swart

Supervisor: Dr C. Marais

Co-supervisor: Prof. B. C. B. Bezuidenhoudt

January 2016

Acknowledgements

I would hereby like to convey my sincere gratitude to the following people:

Prof. Ben Bezuidenhoudt and Dr Charlene Marais for their amazing guidance, advice and assistance as supervisors. I strive to someday have the insight and knowledge you possess.

My beautiful wife and daughter, Carla and Lana, for your unconditional love and support. The joy and happiness I possess is mainly due to your roles in my life. Thank you for making me the man I am today.

My parents, Piet and Lena, for the foundation of Godly wisdom, love, loyalty, hard work and dedication, but to mention a few, you laid within me. Love you always.

My in-laws, Frans and Hanna, for accepting me as part of the family from day one. Your support, motivation and food is always appreciated.

All of my siblings: Morné, Tewie, Francois, Frieda and Marie, for always standing by me and showing an interest in my research, even though I lose you after the first sentence.

My family and friends for your humor and patience during the course of this degree.

My colleagues in the Chemistry department, especially the members of the IPC group, past and present, for your encouragement and assistance.

Dr Linette Twigge for all of your help and insight into NMR techniques.

Finally, all praise to God for the strength and wisdom He has bestowed upon me.

“The more I study science, the more I believe in God.”

- Albert Einstein

Table of Content

List of Abbreviations

A	:	acetone
ADMET	:	acyclic diene metathesis polymerization
anh.	:	anhydrous
aq.	:	aqueous
ARCM	:	asymmetric ring-closing metathesis
b	:	broad (spectral)
bp	:	boiling point
$CDCl_3$	:	deuterated chloroform
CFC	:	chlorofluorocarbon
CM	:	cross-metathesis
CNSL	:	cashew nut shell liquid
COSY	:	correlation spectroscopy
Cy	:	cyclohexyl
d	:	doublet (spectral)
DEPT	:	distortionless enhancement by polarization transfer
EE	:	erythemal effect
eq.	:	equivalent
FCC	:	flash column chromatography
Grubbs II / GII	:	Grubbs 2^{nd} generation catalyst
H	:	hexane
HMBC	:	heteronuclear multiple bond correlation
HRMS	:	high-resolution mass spectrometry
HSQC	:	heteronuclear single-quantum correlation
IR	:	infrared spectroscopy
J	:	Joule; coupling constant (NMR)
lit.	:	literature value
m	:	multiplet (spectral)
m/z	:	mass-to-charge ratio
MALDI	:	matrix-assisted laser desorption ionization

MALDI-TOF MS	:	MALDI-time of flight mass spectroscopy
MED	:	minimal erythema dose
Mes	:	2,4,6-trimethylphenyl
MS	:	mass spectrometry
NMR	:	nuclear magnetic resonance
NOESY / NOE	:	nuclear overhauser effect spectroscopy
OMC	:	octyl methoxycinnamate
Ph	:	phenyl
PLC	:	preparative thin-layer chromotography
ppm	:	parts per million
q	:	quartet (spectral)
RCM	:	ring-closing metathesis
R_f	:	retention factor (chromatography)
ROM	:	ring-opening metathesis
ROMP	:	ring-opening metathesis polymerization
rt	:	room temperature
s	:	singlet (spectral)
SM	:	self-metathesis
SMes	:	1,3-bis(2,4,5-trimethylphenyl)-4,5-dihydroimidazol-2-ylidene
SPF	:	sun protection factor
t	:	triplet (spectral)
TLC	:	thin-layer chromatography
TMS	:	tetramethylsilane
TON	:	turn over number
UV; UV-Vis	:	ultraviolet ; ultraviolet-visible spectroscopy
wt	:	weight
δ	:	chemical shift in ppm downfield from TMS

List of Figures

List of Tables

LITERATURE SURVEY

Chapter 1: Introduction

Due to the increase in the concentration of halogens in the atmosphere[1] which results in the depletion of the ozone layer, increasing amounts of harmful UV-B rays are radiating the earth's surface.[2] This may account for the increase in the number of people being diagnosed with skin cancer.[3] Although many compounds are being, and can be used to protect the skin from UV rays, organic substances like octyl methoxycinnamate (OMC) (**7**),[4] are very popular and are widely used in sunscreen lotions and creams. While several technologies have been published to prepare OMC, current commercial production for almost 80% of the OMC consumption is by BASF according to the ketene route indicated in Figure 1.1.[5,6,7] A possible alternative to the ketene process, which is based on the Heck reaction,[8] and currently represents the only catalytic process, has been developed by IMI, Hoechst and other companies[7,9,10,] (Figure 1.1(a)) and modified by Lipshutz and Taft (Figure 1.1(b)).[8]

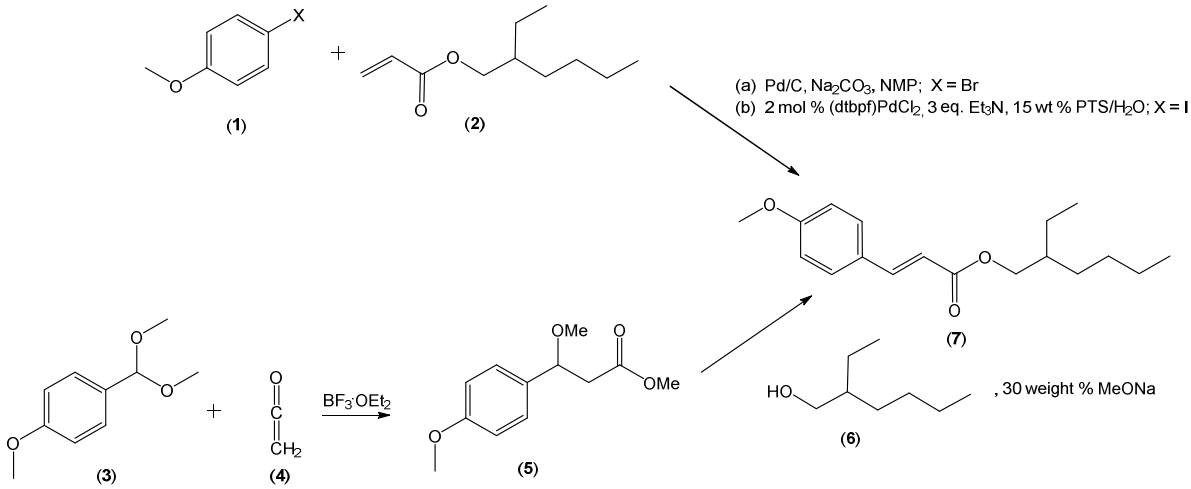

Figure 1.1: Reaction sequences for the preparation of OMC.

Due to the abundance of naturally occurring essential-oil phenylpropenoids like estragole (**8**), eugenol (**9**) and safrole (**10**), which can easily be transformed into anethole (**11**), isoeugenol (**12**) and isosafrole (**13**) by catalytic double bond isomerisation, the possibility of utilizing one of these β-methylstyrenes, *i.e*. anethole (**11**) as starting material in the synthesis of new metathesis based methodology for the preparation of OMC looked promising. Using anethole rather than methoxy substituted styrene in a cross-metathesis reaction with an acrylate derivative like (**2**) (Figure 1.3) would have the added advantage that working with styrene, which is notorious for auto-polymerization, could be eliminated. The aim of the study therefore was to investigate metathesis reactions as alternative catalytic method for the preparation of OMC and related α,β-unsaturated aromatic compounds. If successful, the methodology could also be extended to other industrially important compounds[11,12,13,14] while the possibility of finding another potent UV-B blocker could, in principle, also be realized.

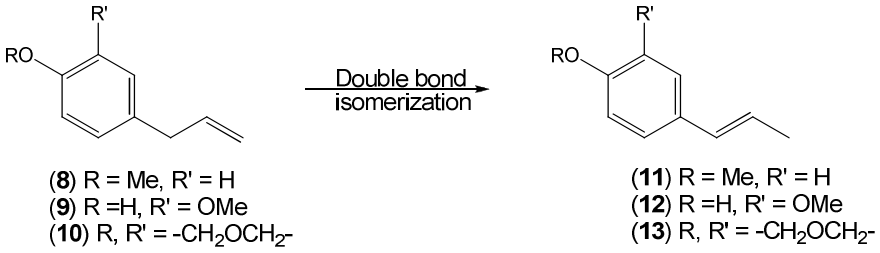

Figure 1.2: Available essential-oil based phenylpropenoids.

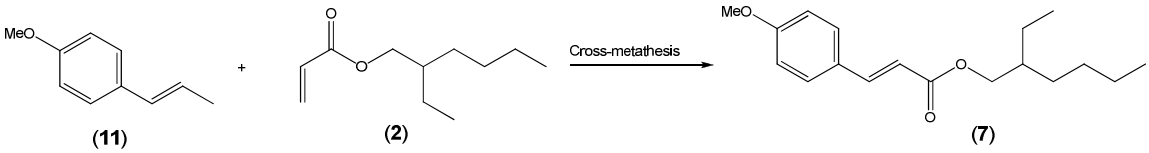

Figure 1.3: Envisaged cross-metathesis based preparation of OMC.

References

[1] Newman, P. A.; Daniel, J. S.; Waugh, D. W.; Nash, E. R. *Atmos. Chem. Phys*. **2007**, *7*, 4537 – 4552.

[2] U. S. Environmental protection agency, Ozone Layer Protection – Science: Health and Environmental Effects of Ozone Depletion. http://www3.epa.gov/ozone/science/effects (accessed Dec 09, 2015)

[3] Skin cancer foundation: Nonmelanoma skin cancer incidence jumps by approximately 300 percent http://www.skincancer.org/skin-cancer-information/skin-cancer-facts/nonmelanoma-skin-cancer-incidence-jumps-by-approximately-300-percent. (accessed Dec 09, 2015)

[4] Dutra, W. D.; da Costa e Oliveira, D. A. G.; Kendor-Hackmann, E. R. M.; Santero, M. I. R. M. *Braz. J. Pharm. Sci*. **2004**, *40*, 381 – 385.

[5] Hùllmann,M.; Gnad, J.; Becker, R. DE 40 39 782, 1990

[6] Nedlac: Study into the establishment of an aroma and fragrance fine chemicals value chain in South Africa, https://www.thedti.gov.za/industrial_development/docs/fridge/Aroma_Part3.pdf (accessed Dec 16, 2015)

[7] Cosmetics & toiletries: Ingredient profile – Ethyl methoxycinnamate, http://www.cosmeticsandtoiletries.com/formulating/function/uvfilter/premium-Ingredient-Profile-Ethylhexyl-Methoxycinnamate.html (accessed Dec 16, 2015)

[8] Lipshutz, B. H.; Taft, B. R. *Org. Lett*. **2008**, *10*, 1329 – 1332.

[9] Eisenstadt, A. In *Catalysis of Organic Reactions*; Herkes, F.E., Ed.; Marcel Dekker: New York, **1998**; p 416.

[10] Li. J. J.; Gribble, G. W. *Palladium in Heterocyclic Chemistry: A guide for the Synthetic Chemist*; Gulf Professional Publishing, **2006**, p599.

[11] Sheldon, R. A. *Catal. Today* **2011**, *167*, 3 − 13.

[12] Mol, J. C. *Green Chem*. **2002**, *4*, 5 − 13.

[13] Corma, A.; Iborra, S.; Velty, A. *Chem. Rev*. **2007**, *107*, 2411 − 2502.

[14] Biermann, U.; Bornscheuer, U.; Meier, M. A. R.; Metzger, J. O.; Schafer, H. J. *Angew. Chem. Int. Ed*. **2011**, *50*, 3854 − 3871.

Chapter 2:
Sunscreen Lotions and Active Components Therein

2.1 Introduction

Although the sun is an essential part of life as we know it, too much exposure can lead to undesirable health defects which may include photoallergies, skin wrinkles, immune system alterations, sunburn, eye damage and skin cancer.[1] This is mainly due to the effect UV light has on skin cells and the corresponding DNA damage. As much as 90 percent of non-melanoma and 65 percent of melanoma skin cancers is estimated to originate from UV radiation.[2]

According to the American Cancer Society,[3,4] ~74 000 new melanoma cancer patients would have been diagnosed in 2015, and for ~10 000 of these it would have been fatal. They also found that different skin types are affected differently and that the overall risk for a lighter pigmented person to be diagnosed with melanoma is 1 in 50 whereas darker skinned people, this figure becomes 1 in 1000. Lastly, their findings showed that the average age for one to be diagnosed with cancer is 61, but melanoma is not uncommon for people younger than 30. In fact, it is the most common cancer in that age range.

These figures will only increase as depletion of the ozone layer increases, so it is critical that precautions are taken to prevent unnecessary exposure of the skin to the sun.[5]

2.2 Ultraviolet radiation[6,7]

Continuous thermonuclear reactions that take place in the sun's core generate electromagnetic radiation that is emitted as photons with wave- and particle-like properties.

The energy (E) associated with a particular photon is dependent on the wavelength of the light and can be described by the Planck-Einstein relation (Equation 2.1) where h is Planck's constant (6.623×10^{-34} J.s), c is the speed of light (2.998×10^{8} m.s^{-1}) and λ is the wavelength of the light in meters.

Equation 2.1:

$$E = \frac{hc}{\lambda}$$

Since the thermonuclear reactions in the sun take place in an uncontrolled way, the electromagnetic radiation generated by these reactions, called the electromagnetic spectrum (Figure 2.1),[8] span a wide range of wavelengths/frequencies. According to the wavelength of the photons, the electromagnetic spectrum can be divided into several regions.

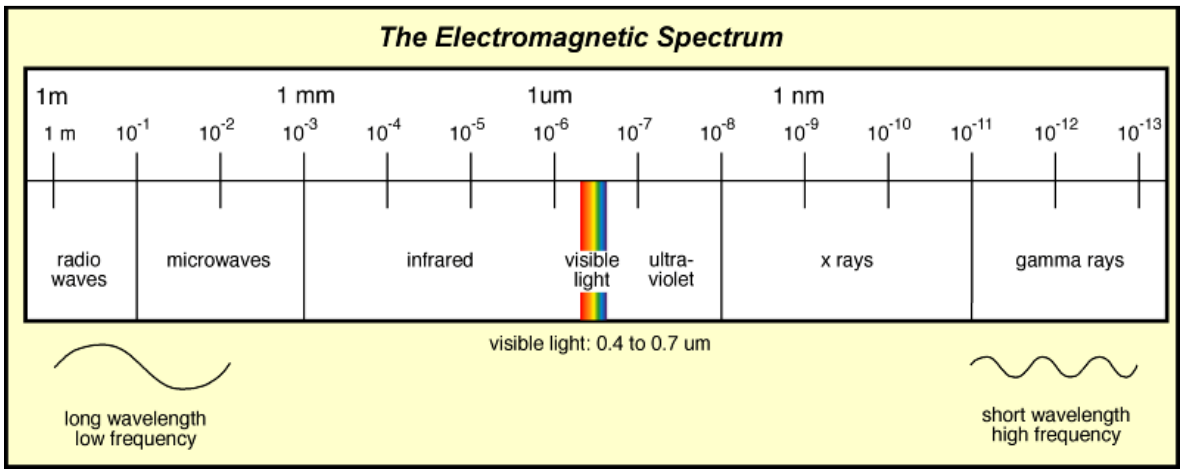

Figure 2.1: The Electromagnetic spectrum.

The 400 – 700 nm part of the electromagnetic spectrum is visible to the human eye and is therefore referred to as the visible light region. Photons in the visible light region can penetrate through human skin, but are not harmful as they do not alter or damage skin tissue. Next to red light in the visible light spectrum, lies the invisible infrared region (700 – 1000 nm) followed by microwaves and radio waves (> 1000 nm); all with longer-wavelengths and lower energy.

Next to violet in the visible light spectrum, is the invisible ultraviolet (UV) region (10 – 400 nm), followed by X-rays, gamma rays and cosmic rays (< 10 nm) with shorter wavelengths and higher energy. Both infrared and ultraviolet light are capable of penetrating the skin, causing different biological effects due to differences in energy.

When a photon penetrates the skin, its energy is absorbed by an atom or molecule in its direct vicinity. While infrared photon excitation affects the rotational and vibrational states of the atom or molecule, visible light and ultraviolet photons lead to higher vibrational or electronic excitation states, whereas X-rays, gamma rays and cosmic rays can cause ionization of the atom or molecule. The ultraviolet region of the electromagnetic spectrum is sub-divided into various sub-regions, like UV-A, UV-B, UV-C, etc.

While radiation of wavelengths shorter than 200 nm is not important since it is absorbed by the air, photons with wavelengths between 200 nm and 290 nm, known as the UV-C region, may cause erythema (redness) of normal skin and inflammation of the cornea. As these photons have the ability to kill one celled organisms, it is also known as germicidal radiation. Photons in this region are also absorbed by the ozone layer of the earth and may not reach the earth's surface.

Light in the UV-B region consists of photons with wavelengths between 290 nm and 320 nm, may cause sunburn of human skin and has been shown to induce skin cancer and mutations in bacteria. Fortunately these photons reach the earth in relatively low quantities and are absorbed by glass. The UV-A region is generally known to contain photons in the region 320 to 400 nm, may cause redness of the skin and may add to the effects of UV-B radiation.

Although UV radiation may cause skin damage, it is needed in small quantities as it converts 7-dehydrocholesterol to vitamin D_3, which again is needed by the

human body as it enhances absorption of calcium and calcification of bones, thereby preventing osteoporosis.

2.3 Overexposure to UV radiation

Ultraviolet radiation is regarded as the most prominent physical carcinogen found in nature. It is extremely genotoxic, but fortunately does not penetrate the body any deeper than the skin.[9] While darker human skin types in general are rather well adapted to constant UV strain, lighter skin types on the other hand are not that resistant towards UV radiation, which may in some instances lead to skin cancer.[10] Although a lot of emphasis is placed on educating the general public on skin cancer, few give any ear to the dangers of over-exposure to the sun and the extremity of the consequences.

Although organic molecules containing conjugated multiple bonds absorb UV radiation in the region of 200 nm, it does not render great concern as radiation in this region is absorbed by the air. If the molecule has linear repeats or ring structures, the absorption shifts higher to the 250 – 300 nm region where not all of these rays are absorbed by the ozone layer around the earth and may therefore cause damage to the skins of people. An example of this is the difference in UV absorption of ethylene (**14**), butadiene (**15**), 1,3,5-hexatriene (**16**), benzene (**17**) and naphthalene (**18**) as depicted in Table 2.1.[11,12]

The depletion in the ozone renders even greater concern as more of these dangerous wavelengths are permitted through to the earth's surface.

After absorption of the radiant energy, molecules may become either chemically or photochemically reactive and may be modified or damaged. These modifications in molecules cause irregular and often undesired reactions.

Table 2.1: UV absorption peaks of some organic molecules.

Compound	Structure	UV absorption peak (nm)
Ethylene (**14**)		180
Butadiene (**15**)	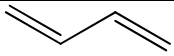	217
1,3,5-Hexatriene (**16**)		258
Benzene (**17**)	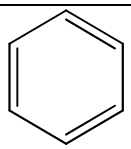	255
Naphthalene (**18**)	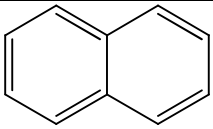	286

The most persistent disturbance in cells caused by these reactions is the synthesis of dysfunctional signaling proteins or by a complete lack of synthesis of such proteins from miscoding or lost genes. Such defects are passed on to daughter cells, propagating the problem of controlling cell growth. Since UV radiation damages DNA in exposed skin cells,[13] there is a continuous threat to the integrity of genes in skin cells. The fact that humans do not develop skin cancer more readily is proof of impressive adaptations of human skin cells.

There are predominately three different types of skin cancers, namely basal cell carcinoma, squamous cell carcinoma and malignant melanoma.[10] Basal cell carcinoma is the most common form of skin cancer and presents itself as a clear spot or a small bump that occurs on the head, neck or hands of the patient. Squamous cell carcinoma normally starts as nodules or as a red, patchy area on the face, lips or tops of the ears and often manifests itself as wart-like growths, rough skin lesions or fast growing bumps.[14] Both basal cell carcinoma and squamous cell carcinoma are classified under non-melanoma

skin cancer and are associated with cumulative sun exposure. Malignant melanoma, being associated with brief, intense sun exposure or blistering sunburns, is the least common of skin cancers, but also the most fatal. Risk factors for melanoma include light skin colour, family and/or personal history of melanoma, large number of skin moles, percentage of freckles and sunburn history in the early stages of life.

The first experimental proof of UV radiation being carcinogenic, came from experiments done on mice by Findlay in the 1920's.[9] Roffo then proved that sunlight can induce skin cancer in rats and also found that UV-B rays are blocked by both coloured and colourless glass.[6] In the 1940's, Blum, Kirby-Smith and Grady[13] found a relationship between tumor formation and chronic UV exposure, which were similar to the effect of the chronic application of chemical carcinogens to the skin and bone cancer induction by radium application.

Based on analysis of wavelength dependency, Gates[15] concluded in 1928 that the bactericidal effect of UV radiation corresponded to the absorption thereof by DNA, and later a similar analysis by Hollaender and Emmons[16] led to the conclusion that UV-induced mutation in fungi were also related to UV absorption by DNA. Beuker sand Berends[17] then identified a UV-induced modification of DNA bases in 1960.

2.4 Sunburn Protection Factor

The possibility of getting skin cancer from exposure to the sun, led to the recent trend of adding a UV protecting agent to the formulation of almost all sunscreen lotions, sunbalms, bodycreams, moisturizers and concealers. The effectiveness of these suncare products and the protection against the sun given by these products is usually indicated by the so-called Sun Protection Factor (SPF) of the product.

SPF is determined by the dosage of the active sun protection agent required to induce a delay in erythema – the turning red of skin when exposed to sun radiation - between treated and untreated skin. The amount of UV radiation that will produce erythema, is known as the minimal erythema dose (MED) and the ratio between MED (protected) and MED (unprotected skin) is defined as the SPF (Equation 2.2).[18]

The SPF is the ratio between the minimal erythema doses of sunscreen-protected and unprotected skin, where the minimal erythema dose (MED) is the shortest time interval (or lowest dosage) of UV light required to produce minimal discernible erythema (redness) of the skin.

Equation 2.2:

$$SPF = \frac{MED\ (\text{protected skin})}{MED\ (\text{non} - \text{protected skin})}$$

SPF values can be determined *in vivo* or *in vitro*, but is ideally determined by phototesting on human volunteers. Since this method is time consuming and costly, much effort went into the development of *in vitro* techniques for determining the protection given by sunscreen compounds.[14] Two general methods have been developed in this regard: The first method measures absorption or transmission of UV radiation through a film of sunscreen compound, while the second measures the absorption characteristics of diluted solutions of the sunscreen agent. Liandhajani *et al*.[19] developed a simple mathematical equation (Equation 2.3), derived from that of Mansur *et al.,*[19] based on the absorption of the sunscreen, the erythemal effect (EE) and the solar intensity (I), that could be used during *in vitro* methods to quantify/determine the SPF of a particular sunscreen agent.[19]. The value of EE x I is a constant at a specific wavelength and can be found in the work published by Sayre *et al*.,[20] whereas CF is a correction factor with a value of 10.

Equation 2.3:

$$SPF = CF \times \sum_{290}^{330} EE(\lambda) \times I(\lambda) \times Abs(\lambda)$$

CF = correction factor of 10

EE = erythemal effect spectrum

I = Solar intensity

Abs = Absorbance of sunscreen

Although SPF values have been assigned by the United States Food and Drug Administration (FDA) since 1978,[16] it only gives an indication of the lotion's UV-B blocking ability and not the protection against UV-A rays. Currently sunscreen agents/lotions with SPF values between 2 and 50 are available. The rule of thumb is that a compound with an SPF of 15 will block out 93% of UV-B rays and will allow you to stay in the sun 15 times longer than with unprotected skin before the skin is sunburnt, i.e. the minutes to burn without sunscreen multiplied by the SPF number gives the maximum time of sun exposure[2] before reapplication is needed. A lotion with SPF 30, however, does not work twice as well as its 15 counterpart. It provides 97% protection against UV-B ray absorption and will allow a period 30 times longer in the sun before erythema sets in compared to unprotected skin.[2] The SPF of a particular lotion is also dependant on altitude, proximity to the equator and skin fairness and is therefore not the same for everyone, so its requirement for reapplication will differ from one person to the next.

The efficacy of a sun care agent, its substantivity, is not only related to its SPF, but also to its ability to remain effective under extreme conditions, like prolonged exposure to sweating and water. For this reason, three major recommendations, *i.e.* sweat-resistance, water-resistance and waterproof, are indicated on the labels of sunscreens to help clarify substantivity. The term sweat-resistant is an indication that the lotion will give protection for up to 30 minutes to a person with continuous heavy perspiration. Water-resistant means that during continuous exposure to water, it will protect a subject for up to 40

minutes, while waterproof indicates protection for up to 80 minutes during continuous water exposure.[11] It is, however, recommended that sunscreens be reapplied after swimming or perspiring but reapplication, however, does not extend the period of protection.[2]

Although the importance of the SPF of a particular sunscreen lotion cannot be underestimated, the application thickness of the lotion also plays a significant role. Internationally it is agreed that sunscreens should be applied at 2 mg/cm^2 in order to fully benefit from the SPF,[21] so a standard sized adult should apply about 30 mL of sunscreen to protect the whole body. On average, people, however, do not use even one-fifth of this quantity, therefore severely limiting the protection ability of these products.[22]

The ideal sunscreen lotion should have good optical and physical properties (such as absorption of light over a broad UV spectrum), have good adhesion to the skin, have good water resistance and lack phototoxicity.[23]

2.5 Active components in sunscreens

Sunscreen lotions contain active compounds that provide protection by either absorbing, reflecting and/or scattering UV radiation. According to their action of protection, these compounds are usually divided into two categories, *i.e.* compounds giving chemical protection and those rendering physical protection.[20] Compounds with a chemical mode of protection are usually UV absorbers and are available in a variety of formulations. These compounds are usually only protective against UV-B radiation with very few also showing UV-A absorption.

Compounds that are categorized as physical protectors are usually thick opaque substances that give protection by their ability to scatter sunlight and are usually messy and unappealing, but provide protection against both UV-A and -B radiation.

The effectiveness of sunscreens was originally achieved by the incorporation of soluble organic UV absorbers into cosmetic formulations. Cinnamates, benzoates and salicylates (Table 2.2)[2] are some of the more general UV absorbers.

Table 2.2: SPF effectiveness of some sun protection compounds.

Sunscreen Ingredient	**Structure**	**Protection**		**Chemical (C) or Physical (P) Protection**
		UV-A	UV-B	
Aminobenzoic acid (PABA) (**19**)	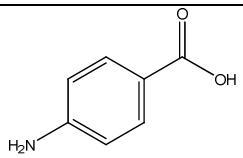	○	●	C
Avobenzone (**20**)	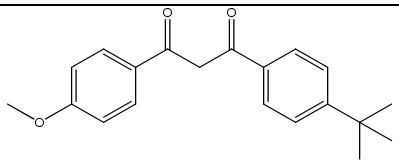	●	◌	C
Cinoxate (**21**)	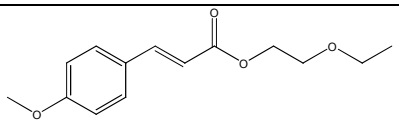	◌	●	C
Dioxybenzone (**22**)	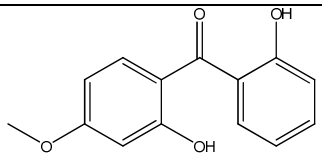	◌	●	C
Ecamsule (**23**)	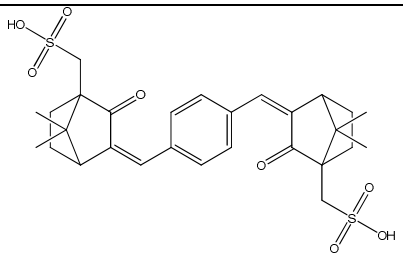	●	◌	C

Homosalate (**24**)	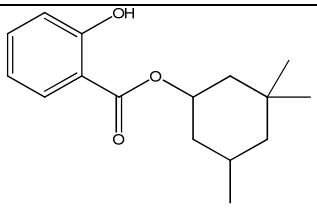	○	●	C
Methyl anthranilate (**25**)	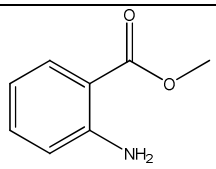	●	●	C
Octocrylene (**26**)	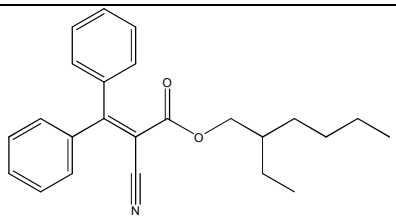	●	●	C
Octyl methoxy-cinnamate* (**7**)	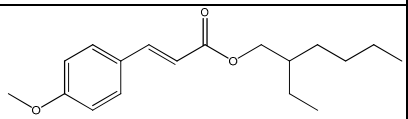	●	●	C
Octyl salicylate (**27**)	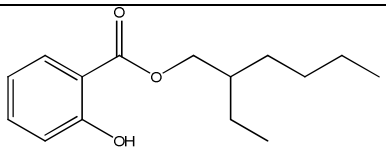	○	●	C
Benzophenone-3** (**28**)	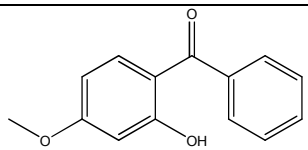	●	●	C
Padimate O (**29**)	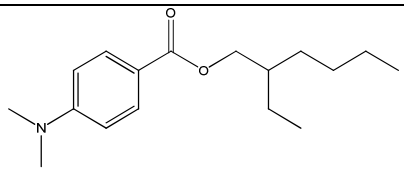	○	●	C
Phenylbenz-imidazole (**30**)	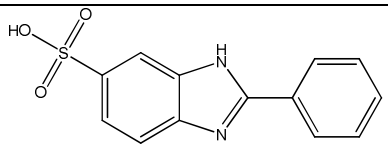	○	●	C
Sulisobenzone (**31**)	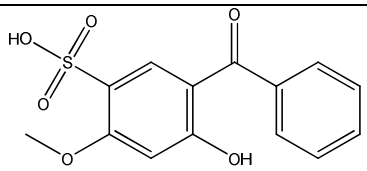	●	●	C

Titanium dioxide (**32**)	TiO_2	●	●	P
Trolamine salicylate (**33**)	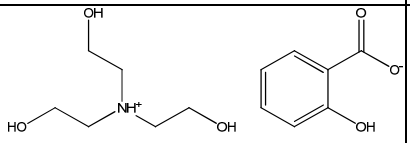	○	●	C
Zinc oxide (**34**)	ZnO	●	●	P

● : Extensive Protection

● : Considerable Protection

● : Limited Protection

○ : Minimal Protection

*****Commercial name for 2-ethylhexyl 4-methoxycinnamate (OMC); also known as octinoxate or ethylhexyl methoxycinnamate

******Commercial name for oxybenzone

Although cinnamates, benzoates and salicylates have excellent abilities to absorb UV rays, these compounds pose a safety risk when used in high concentrations. For this reason, micronized metal oxides such as titanium dioxide, zinc oxide,[24] cerium oxide[25] and talc have been added to some cosmetic formulations containing these organic compounds (Table 2.3)[14] to assist with sun protection as it has UV protection abilities too. Another advantage of these metal oxides is that they are not absorbed by the epidermis and remain deposited on the outermost surface of the skin, regardless of their particle size or shape. Advances in the formulation of these UV filters using nanotechnology have resulted in them now coating the skin as a thin film. Commercially this is of great importance as it appears transparent rather than opaque, whilst still providing the desired UV protection. It was however found that small amounts of Zn from the ZnO, when applied outdoors, is absorbed into the skin[26]. For this reason the concentration of these metal oxides should only be between 4 – 30% wt/wt of the sunscreen lotion.

Table 2.3: SPF labeled and found in commercially available samples.

Commercial sample (means of protection)	**Active ingredients**	**Composition** (%)	**SPF**	
			Labelled	**Found**
A (Emulsion for body)	Benzophenone-3 (**28**) OMC (**7**)	4.0 7.5	15.00	16.24 ±0.05
B (Emulsion for body)	Benzophenone-3 (**28**) OMC (**7**)	3.0 8.0	15.00	15.35 ±0.05
C (Emulsion for body)	Benzophenone-3 (**28**) OMC (**7**) Titanium dioxide alkylbenzoate	2.8 6.8 0.7	15.00	14.90 ±0.03
D (Emulsion for body)	Benzophenone-3 (**28**) OMC (**7**) Octyl salicylate (**10**) Titanium dioxide (**32**)	3.5 7.0 2.0 2.0	15.00	14.65 ±0.04
E (Sunblock lotion)	Benzophenone-3 (**28**) OMC (**7**) Titanium dioxide alkylbenzoate	2.1 5.7 0.6	8.00	12.20 ±0.06
F (Emulsion for body)	Benzophenone-3 (**28**) OMC (**7**) Octyl salicylate (**27**) Titanium dioxide (**32**)	1.5 5.5 1.0 1.0	8.00	10.94 ±0.04
G (Emulsion for body)	Benzophenone-3 (**28**) OMC (**7**) Octyl salicylate (**27**) Titanium dioxide (**32**)	2.75 6.5 1.0 1.0	15.00	13.65 ±0.04
H (Emulsion for body)	Benzophenone-3 (**28**) OMC (**7**) Octyl salicylate (**27**)	5.0 7.5 5.0	30.00	19.00 ±0.07

I (Emulsion for body)	Benzophenone-3 (**28**) OMC (**7**) Titanium dioxide (**32**) Zinc oxide (**34**)	Not specified	20.00	14.15 ±0.04
J (Emulsion for face)	Benzophenone-3 (**28**) OMC (**7**) Octyl salicylate (**27**)	Not specified	23.00	20.30 ±0.05

Despite their effectiveness in preventing sunburn and erythema, sunscreens proved ineffective to provide free radical protection. This prompted the synthesis of a compound which displayed both UV absorbing and antioxidant properties in the same molecule. 2-Ethylhexyl 4-methoxycinnamate (OMC) (**7**), known for its UV-B protection abilities, was therefore transesterified with piperidine nitroxide TEMPOL (**36**), a compound with antioxidant properties[27] (Figure 2.2). This new nitroxide-based sunscreen (MC-NO) (**37**) proved to absorb radiation in the UV-B region, act as a free radical scavenger, strongly reduced UV-A and sunlight induced lipid peroxidation in liposomes, and has comparable antioxidant activities to Vitamin E commonly used in skin care formulations.

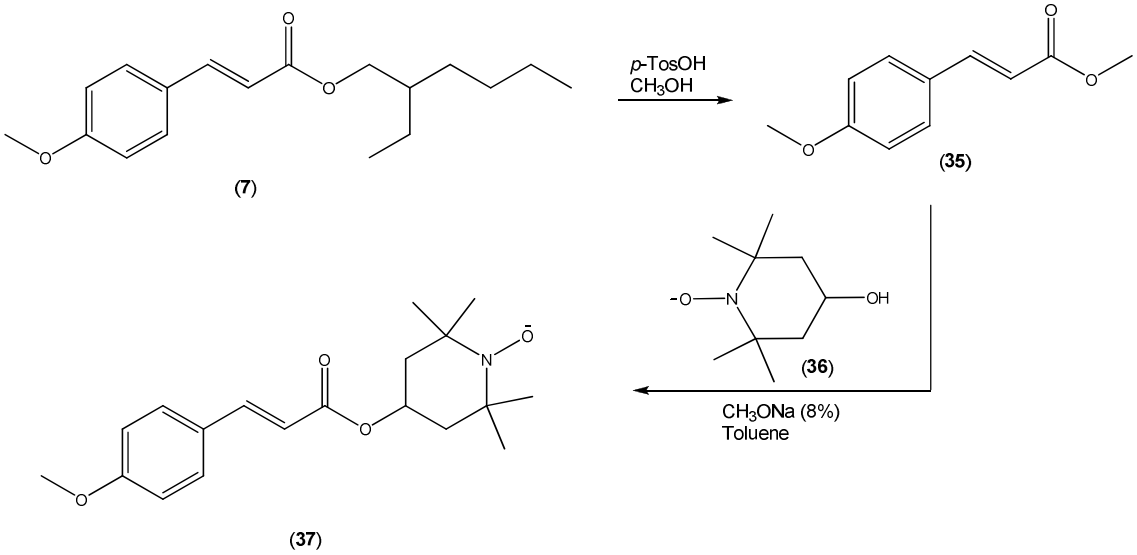

Figure 2.2: Preparation of MC-NO.

2.6 Decomposition of sunscreen agents

With all the benefits of sunscreen agents being identified and advocated, some major concerns[28,29,30] were raised regarding the photostability of these agents. Avobenzone (**2**) and 2-ethylhexyl 4-methoxycinnamate (OMC) (**7**) are renowned for being photolabile, with irradiation leading to fragmentation, photodimerization, photooxidation and *trans-cis* isomerization.[31] Salicylates and methylbenzylidene camphor (**38**), on the other hand, are reported to enhance the photostability of sunscreen formulations.[31]

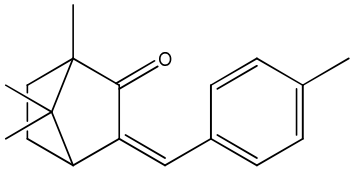

(**38**)

Figure 2.3: Structure of camphor.

Sayre *et al*.[23] found that the higher the concentration of sunscreen agents are, the more readily they decompose. In their studies, they found that a 0.2 MED (minimal erythemal dose) film of a sunscreen containing 7.5% 2-ethylhexyl 4-methoxycinnamate (octinoxate, OMC) (**7**), 3% oxybenzone (2-hydroxy-4-methoxybenzophenone) and 3% avobenzone (4-*t*-butyl-4'-methoxydibenzoyl methane) (**20**) maintains 75% of its protection after *ca*. 100 minutes of irradiation. A 2.0 MED film, however, only maintains 25% of its initial protection. Avobenzone (**2**) decomposed into radical fragments during irradiation (*cf*. Figure 2.3), which resulted in the photolysis of 2-ethylhexyl 4-methoxycinnamate (**7**). When irradiated, 2-ethylhexyl 4-methoxycinnamate (**7**) is known to split into two radicals (Figure 2.4) that can be quenched by a hydrogen donor to form 4-methoxybenzaldehyde and 2-ethylhexyl alcohol.[32,33]

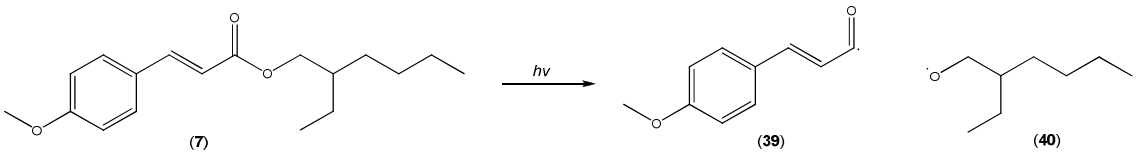

(**7**) (**39**) (**40**)

Figure 2.4: Radical fragments formation when 2-ethylhexyl 4-methoxycinnamate (**7**) is irradiated.

Schwack and Rudolph[34] subjected dibenzoyl methanes, including avobenzone (**20**), to irradiation by a solar simulator and identified the photoproducts (Figure 2.6) as the corresponding benzaldehydes (**44**), benzoic acids (**46**), acetophenones (**17.13**), phenyl glyoxals (**51**), benzils (**47**), dibenzoyl methanes (**41**) and dibenzoyl ethanes (**48**).

Kockler *et al*.[24] found that the physical sunscreen nano-TiO_2 induces photodegeneration of some chemical sunscreen agents (avobenzone (**20**) and octocrylene **26**)) due to the formation of reactive oxygen species such as hydroxyl radicals and superoxide radical anions (Figure 2.5). Gonzalez *et al*.,[25] however, reported that commercial sunscreens containing TiO_2 were more stable than those without.

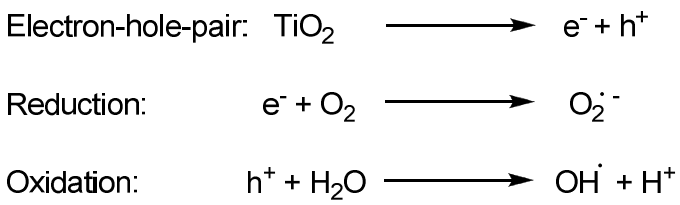

Figure 2.5: Irradation of TiO_2 with *hv* (λ <400nm).

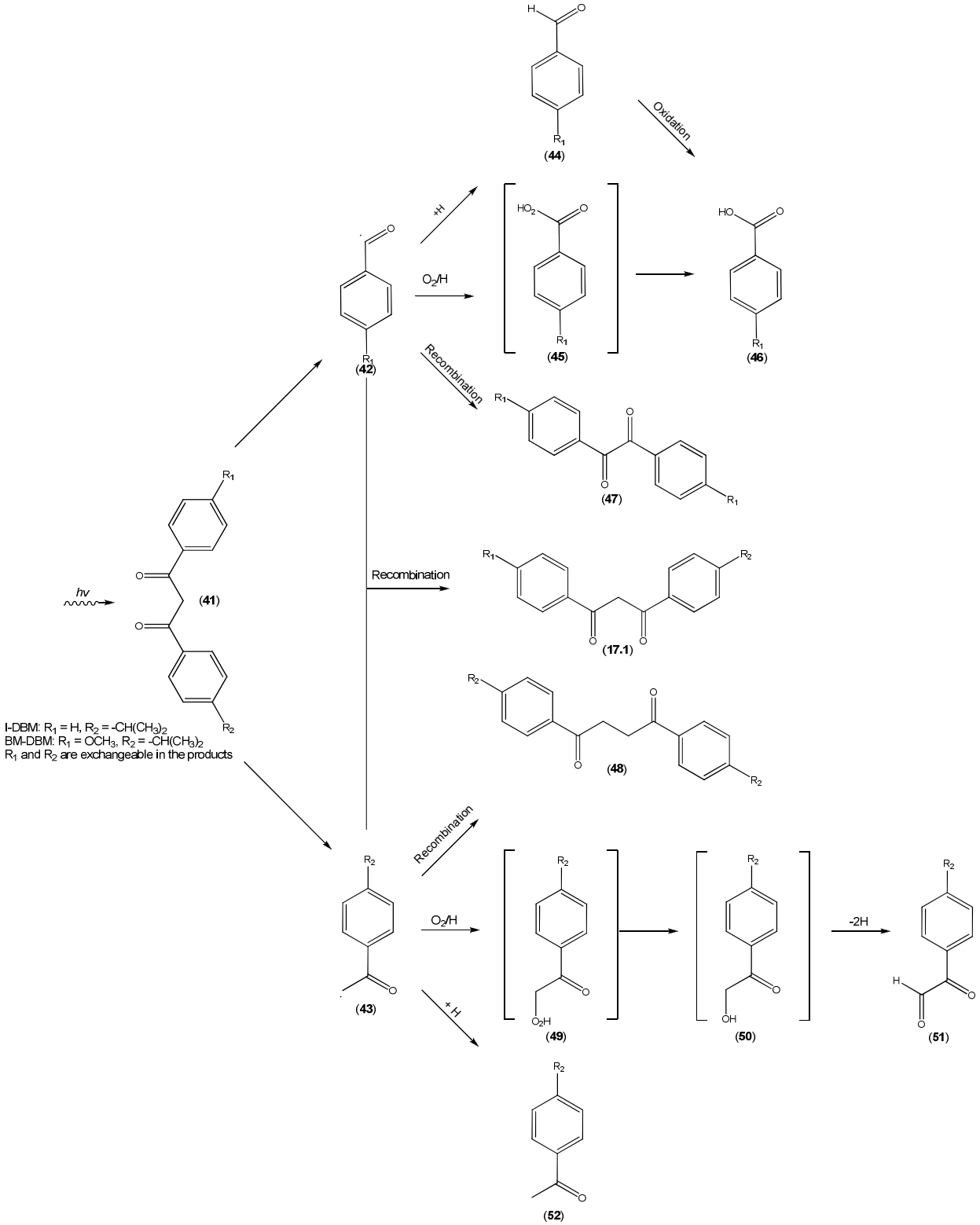

Figure 2.6: Photoproducts of dibenzoyl methanes, 4-isopropyldibenzoyl methane (I-DBM) and 4-*t*-butyl-4'-methoxydibenzoyl methane (BM-DBM or avobenzone[23] (**20**)).

2.7 Preparation of the active components in sunscreen lotions

Since 2-ethylhexyl 4-methoxycinnamate (**7**), octyl salicylate (2-ethylhexyl-2-hydroxybezoate) (**27**) and benzophenone-3 ((2-hydroxy-4-methoxyphenyl)-phenylmethanone) (**28**) have been proven to be amongst the best UV absorbers,[2] these compounds are widely used in sunscreen lotions (Table 2.3). They were also found to exhibit anti-inflammatory properties[35] that could assist in their effectiveness in these lotions. Benzophenone-3 (**28**) and 2-ethylhexyl 4-methoxycinnamate (**7**) are also used as light stabilizers in plastics, while octyl salicylate (**27**) is used as a fragrance ingredient. Economically viable preparations of these compounds have been the objective of several attempts and investigations.

2.7.1 Benzophenone-3 (2-hydroxy-4-methoxybenzophenone) (28)

Benzophenone-3 (**28**), also known as oxybenzone, can easily be prepared by means of Friedel-Crafts methodologies. Two variations of this method have been studied. The first variant[36] (Figure 2.7) is a benzoylation followed by a Fries rearrangement. The extreme temperatures needed for this reaction and the use of strong acids and bases along with an overall yield of 60%, all contribute to rendering this reaction undesirable.

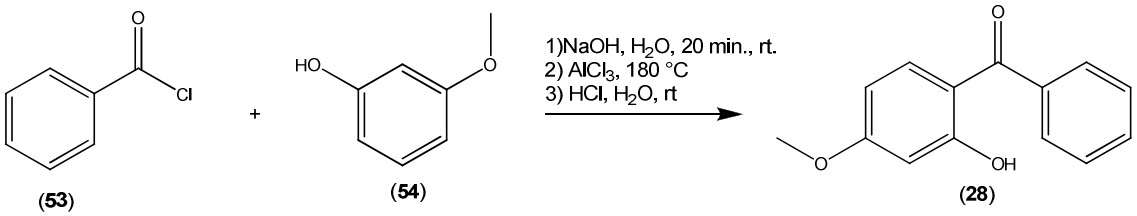

Figure 2.7: Benzoylation-Fries rearrangement variant of Friedel-Crafts acylation.

The second variant is a Friedel-Crafts acylation[37] followed by methylation with dimethylsulphate (**58**) (Figure 2.8). Economically this procedure is more favorable by far as the starting materials, benzoic acid (**55**), resorcinol (**56**) and dimethyl sulfate (**58**) combined, cost almost a tenth of the price per kg (or L) of

the reagents used in the first method. This, however, does not compensate for the extremely low yields (25% for each of the steps).

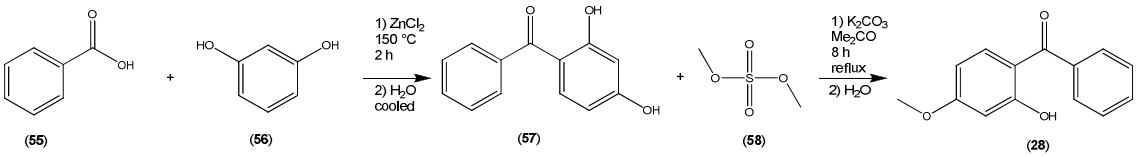

Figure 2.8: Preparation of benzophenone-3 (**28**) Friedel-Crafts acylation, followed by methylation.

An alternative route for the production of benzophenone-3 (**28**) is a palladium catalyzed aryl iodide coupling with an aromatic aldehyde[38] (Figure 2.9) to give the desired product in 82% yield.

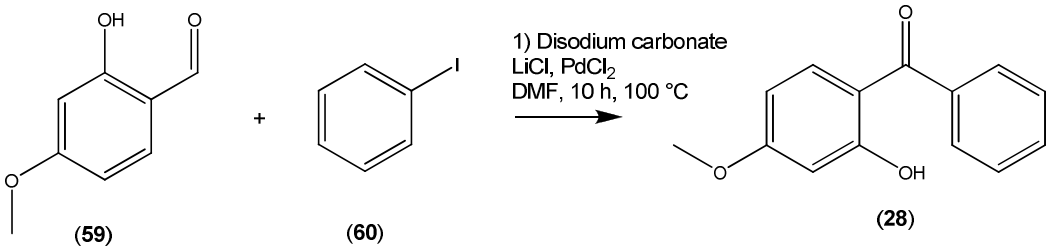

Figure 2.9: $PdCl_2$ catalyzed benzophenone-3 (**28**) preparation.

2.7.2 Octyl salicylate (2-ethylhexyl 2-hydroxybenzoate) (27)

Octyl salicylate (**27**) is industrially prepared by employing an esterification[39] of the corresponding carboxylic acid (Figure 2.10). Few new advances have been made regarding the preparation of this compound since 1988.[39] Most of the research conducted focused on the catalyst, which included *p*-$MeC_6H_4SO_3H$,[40] SO_4^{2-}-La^{3+}/TiO_2[41] (350 W, 3min) and $NaHSO_4$[42] (360 W, 30 min) (Figure 2.10). Yields of these reactions are excellent (98%, 95%, and 89%, respectively), but the techniques used are not industrially viable as they make use of microwave irradiation and/or solid super acids.

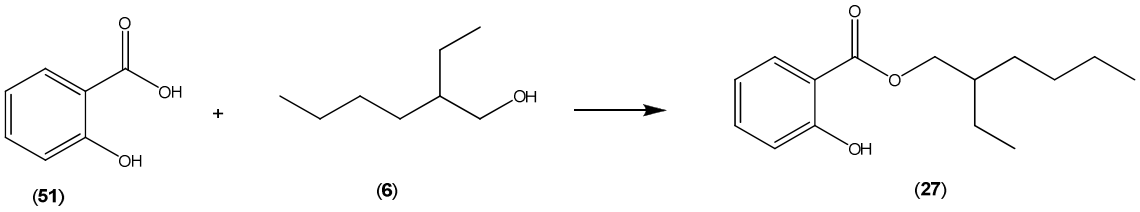

Figure 2.10: Esterification of 2-hydroxybenzoic acid with 2-ethylhexan-1-ol.

Two new methodologies, however, were studied, namely transesterification (Figure 2.11)[43,44] and *O*-alkylation of carboxylate anions in the presence of a solid-liquid phase transfer agent (Figure 2.12).[45] The transesterification approach (Figure 2.11) increased the overall yield, but require high temperatures.

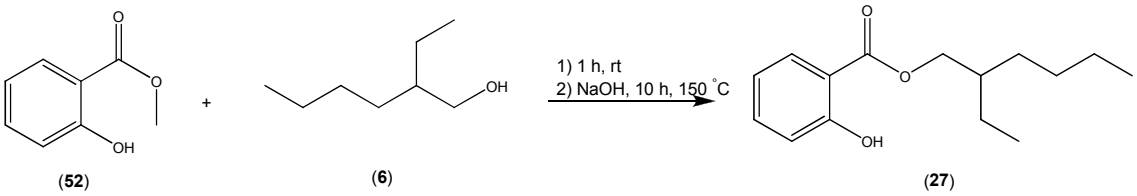

Figure 2.11: Transesterification of methyl-2-hydroxybenzoate with 2-ethylhexan-1-ol.

The alkylation approach (Figure 2.12) gave an excellent yield (95%) after 10 minutes, but as microwave irradiation (300 W) was applied, it is not industrially compatible.

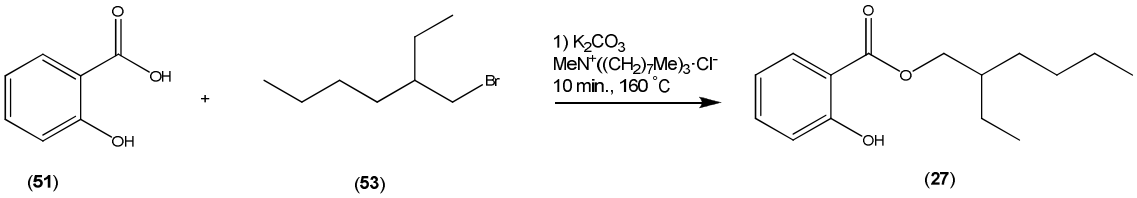

Figure 2.12: Alkylation of 2-hydroxybenzoic acid with 3-(bromomethyl)heptanes.

2.7.3 2-Ethylhexyl 4-methoxycinnamate (OMC)

The raw materials for the preparation of 2-ethylhexyl 4-methoxycinnamate (**9**) originate from propylene and phenol or *para*-cresol petrochemical feedstocks.[46]

2-Ethylhexanol (**6**) can be derived from propylene (**54**) (Figure 2.13) and can be used as such, or in its acetate or acrylate esters form, depending on the synthetic route.

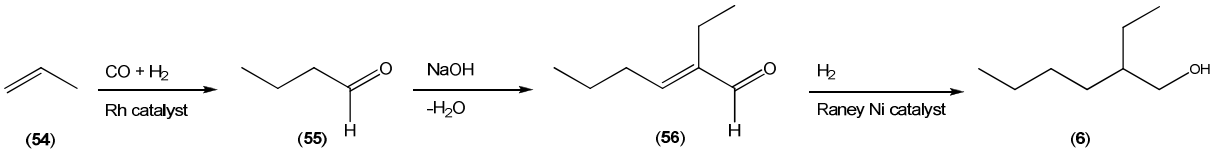

Figure 2.13: Synthesis of 2-ethylhexanol from propylene.

The aromatic moiety of the cinnamate, which may include *p*-anisaldehyde or *p*-bromoanisole, on the other hand can derived from *p*-cresol or phenol *via* oxidation or substitution, and methylation of the hydroxyl group.[46]

Traditional processes for the synthesis of 2-ethylhexyl *p*-methoxycinnamate (**7**) involves the aldol reaction of *p*-anisaldehyde (**57**) with 2-ethylhexyl acetate (**58**) (Figure 14(a)) or the aldol reaction of *p*-anisaldehyde (**57**) with methyl acetate (**59**), followed by transesterification with 2-ethylhexanol (**6**) (Figure(b)).[46]

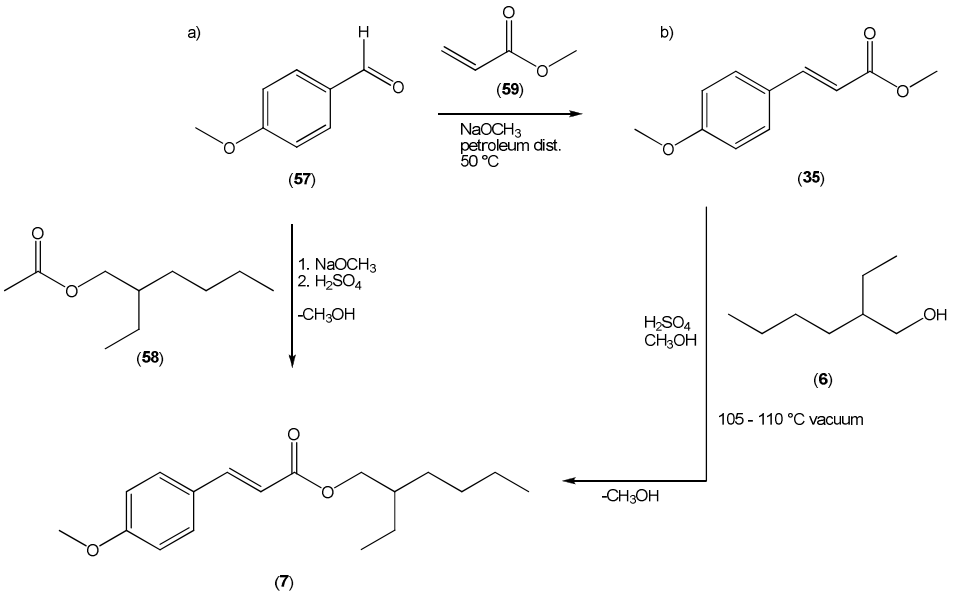

Figure 2.14: Synthesis of OMC from *p*-anisaldehyde via, a) direct aldol condensation with 2-ethylhexyl acetate, and, b) aldol condensation with methyl *p*-methoxycinnamate followed by transesterification with 2-ethylhexanol.

Another attempt at producing this compound industrially centered around application of the Verley-Doebner modification of the Knoevenagel condensation reaction to form *p*-methoxycinnamic acid (**61**), followed by *O*-alkylation and transesterification (Figure 2.15). [41,47,48]

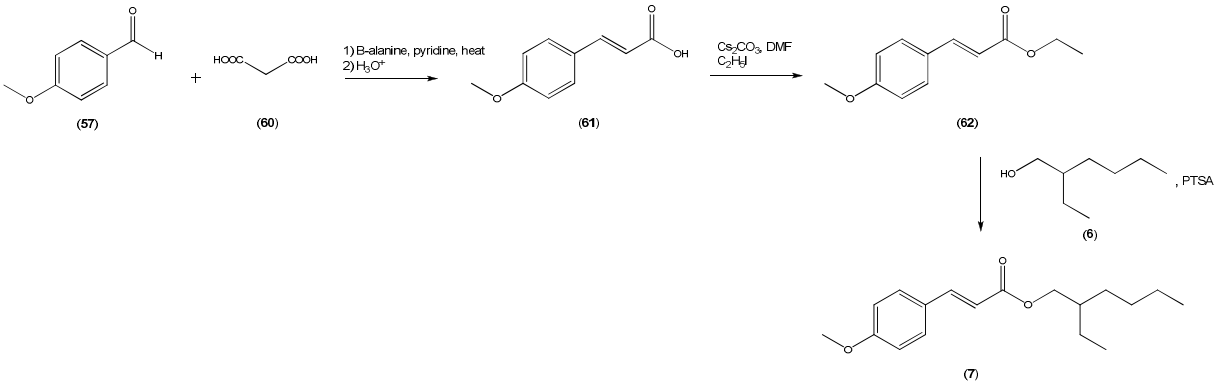

Figure 2.15: Verley-Doebner modification of Knoevenagel condensation.

Apart from *p*-anisaldehyde (**57**) being expensive, the processes above produce many by-products and large volumes of waste.

Former Hoechst AG Company, now trading under the name Aventis Deutshland, IMI[49] and other companies developed Heck reaction based methodology[50] between *p*-bromoanisole (**1**) and 2-ethylhexyl acrylate (**2**) with Pd/C and sodium carbonate in refluxing *N*-methylpyrrolidone to form 2-ethylhexyl *p*-methoxycinnamic acid (**7**) in 80 – 90% yield (Figure 2.16). Carbon dioxide and sodium bromide were generated as by-products, but the latter could be recycled for *p*-bromoanisole (**1**) synthesis.[46]

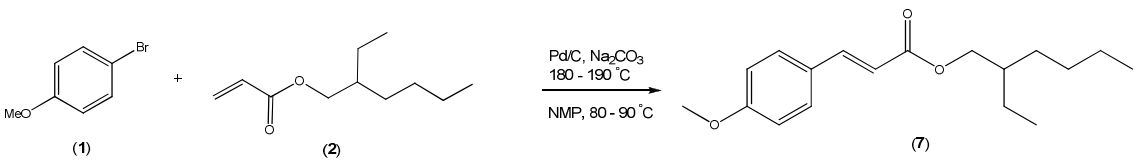

Figure 2.16: Heck reaction using Pd/C as catalyst.

Lipshutz *et al.*[51] later modified this reaction to be conducted at room temperature by reacting *p*-iodoanisole (**63**) and 2-ethylhexyl acrylate (**2**) in the

presence of the Johnson-Matthey catalyst [1,1'-bis(di-*tert*-butylphosphino)ferrocene dichloropalladium (II) [(dtbpf)$PdCl_2$] and obtained the desired cinnamate product in 84% yield (Figure 2.17).

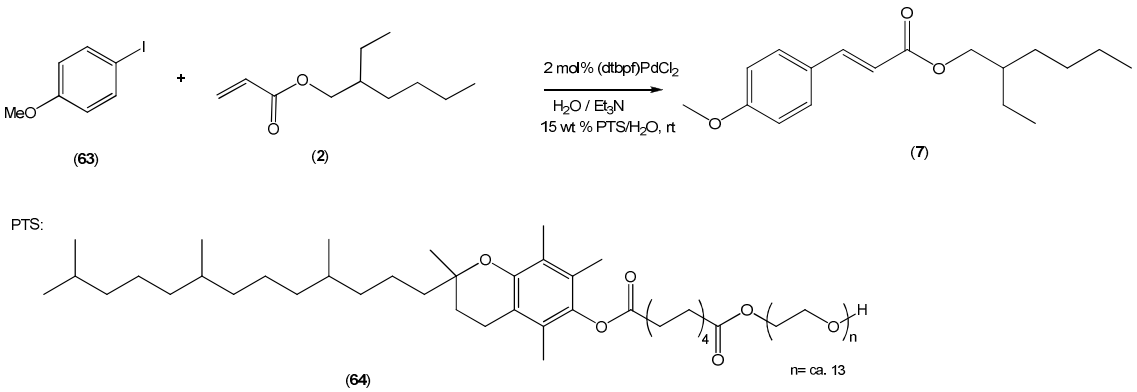

Figure 2.17: Heck reaction using (dtbpf)$PdCl_2$ as catalyst.

Alternatively, Heck methodology can be used to prepare *p*-methoxycinnamic acid (**61**) from *p*-bromoanisole (**1**) and acrylic acid (**65**). Esterification of *p*-methoxycinnamic acid (**61**) and 2-ethylhexanol (**6**) subsequently gives the desired 2-ethylhexyl 4-methoxycinnamate (**7**).[52]

In 2000, the ketene approach was introduced in a BASF plant,[46,53] delivering 4500 metric ton of 2-ethylhexyl 4-methoxycinnamate (7) per year. This approach involves a two-step anisole dimethylacetal (**3**) based process, with ketene (**4**) and 2-ethylhexanol (**6**) as co-building blocks (Figure 2.19).

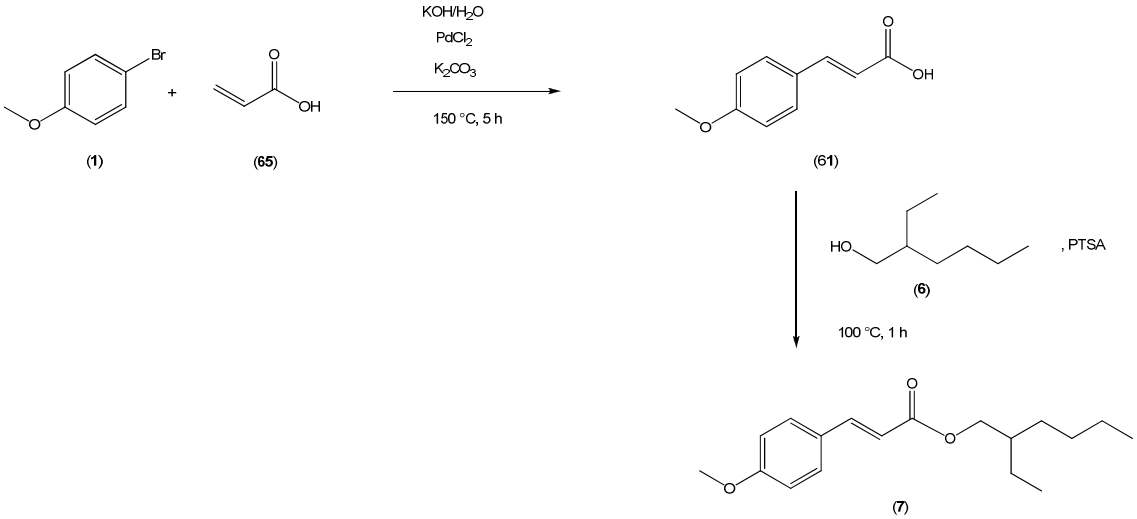

Figure 2.18: Preparation of OMC via a Heck methodology followed by esterification.

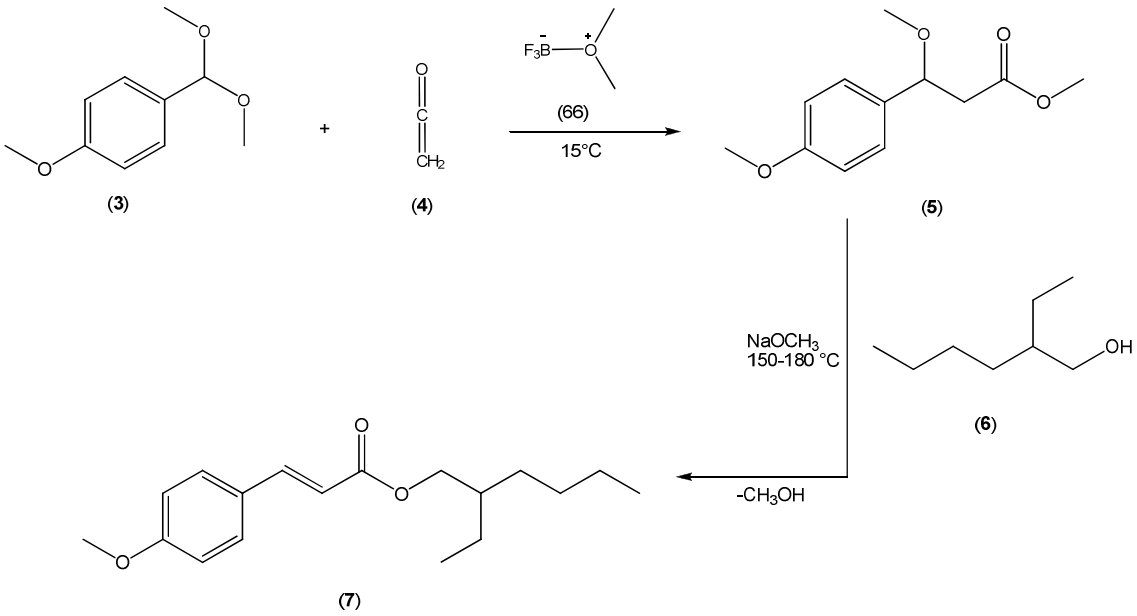

Figure 2.19: Ketene approach for OMC formation.

The highly reactive ketene (**4**) is prepared by the pyrolysis (700 – 800 °C) of acetic acid in the presence of a polyalkylphospate catalyst, whereas the *p*-anisaldehyde dimethyl acetal (**3**) is obtained from *p*-cresol and methanol *via* electrochemical oxidation.[46]

References

[1] Schultz, *J. et al. Advanced Drug Delivery Reviews* **2002**, *54*, S157 – S163.

[2] United States Environmental Protection Agency: The burning facts. http://www.epa.gov/sunwise/doc/sunscreen.pdf (accessed Nov 09, 2011)

[3] American Cancer Society: Melanoma skin cancer. http://www.cancer.org/cancer/skincancer-melanoma/detailedguide/melanoma-skin-cancer-key-statistics (accessed Feb 16, 2015)

[4] American Cancer Society: Cancer facts & figures 2015. http://www.cancer.org/acs/groups/content/@editorial/documents/document/acspc-044552.pdf (accessed Dec 16, 2015)

[5] Thompson, S. C.; Jolley, D; Marks, R. *N. Engl. J. Med.* **1993**, *16*, 1147 – 1151.

[6] Parrish, J. A.; Anderson, R. R.; Urbach, F.; Pitts, D. *UV-A, Biological Effects of Ultraviolet Radioation with Emphasis on Human Responses to Longwave Ultraviolet*; Plenum Press: New York, **1978**, pp 1-6, 107 – 109, 157 – 159 and 248 – 251.

[7] Fundamentals of Photonics, Module 1.1: Nature and Properties of Light https://spie.org/Documents/Publications/00%20STEP%20Module%2001.pdf (accessed Dec 08, 2015)

[8] The electromagnetic spectrum. http://www.columbia.edu/~vjd1/electromag_spectrum.htm (accessed Jan 17, 2013)

[9] de Gruijl, F.R. *Eur. J. Cancer* **1999**, *35*, 2003 – 2009.

[10] Arora, A.; Attwood, *J. Surg. Clin. North Am.* **2009**, *89*, 703 – 712.

[11] Absorption of light by organic molecules. http://archives.library.illinois.edu/erec/University%20Archives/1505050/Organic/Arenes/Chapter%205/sec5-14/5-14.htm (accessed Nov 4, 2015)

[12]Shimadzu: The relationship between UV-VIS absorption and structure of organic compounds. http://www.shimadzu.com/an/uv/support/uv/ap/apl.html (accessed Nov 4, 2015).

[13] Ravanat, J.-L.; Douki, T.; Cadet, J. J. *Photochem. Photobiol. B*. **2001**, *63*, 88 – 102.

[14] Ahmed, A. H.; Soyer, H. P.; Saunders, N.; Boukamp, P.; Roberts, M. S*. Drug Discov. Today* **2008**, *5*, 55 – 62.

[15] Gates, F.I. *Science* **1928**, *68*, 479 – 480.

[16] Hollaender, A.; Emmons, C.W. *Cold Spring Harbor Symp. Quant. Biol.* **1941**, *9*, 179 – 186.

[17] Beukes, R.; Berends, W. *Biochem. Biophys. Acta* **1960**, *41*, 550 – 551.

[18] Dutra, W. D.; da Costa e Oliveira, D. A. G.; Kendor-Hackmann, E. R. M.; Santero, M. I. R. M. *Braz. J. Pharm. Sci*. **2004**, *40*, 381 – 385.

[19] Liandijani, L.; Iwo, M. I.; Sukrasno, Soemardji, A. A.; Hanafi, M. *J. Appl. Pharm. Sci.* **2013**, *3*, 70 – 73.

[20] Sayre, R. M.; Agin, P. P.; LeVee, G. J.; Marlowe, E. *Photochem. Photobiol.* **1979**, *29*, 559 – 566.

[21] Oliveira, S. L.; Mansanares, A. M.; da Silva, E. C.; Barja, P. R. *Eur. Phys. J.* **2008**, *153*, 475 – 478.

[22] Autier, A.; Boniol, M.; Serveri, G.; Doré, F-J. *Br. J. Dermatol*. **2001**, *144*, 288 – 291.

[23] de Freitas, Z. M. F.; dos Santos, E. P.; da Rocha, J. F.; Dellsmora-Ortiz, G. M.; Goncalves, J. C. S. *Eur. J. Pharm. Sci.* **2005**, *25*, 67 – 72.

[24] Mirchnick, M. A., Fairhurst, D.; Pinnell, S.R. *J. Am. Acad. Dermatol*. **1999**, *40*, 85 – 90.

[25] Yabe, S.; Sato, T. *J. Solid State Chem*. **2003**, *171*, 7 – 11.

[26] Gulson, B.; McCall, M.; Korsch, M.; Gomez, L.; Casey, P.; Oytam, Y.; Taylor, A.; McCulloch, M.; Trotter, J.; Kinsley, L.; Greenoak, G. *Toxicol. Sci*. **2010**, *118*, 140 – 149.

[27] Damiani, E.; Astolfi, P.; Cionna, L.; Ippoliti, F.; Greci, L. *Free Radical Research* **2006**, *40*, 485 – 494.

[28] Sayre, R. M.; Dowdy, J. C.; Gerwig, A. J.; Shields, W. J.; Lloyd, R. V. *Photochem. Photobiol.* **2005**, *81*, 452 – 456.

[29] Kockler, J.; Oelgemöller, M.; Robertson, S.; Glass, B. D. *Cosmetics* **2014**, *1*, 128 – 139.

[30] Gonzalez, H.; Tarras-Wahlberg, N.; Strömdahl, B.; Juzeniene, A.; Moan, J.; Larkö, O; Rosén, A.; Wennberg, M. *Dermatology* **2007**, 1 – 9.

[31] Chatelain, E.; Gabard, B. *Photochem. Photobiol.* **2001**, *74*, 401 – 406.

[32] MacNanus-Spencer, L.; Tse, M. L.; Klein, J. L.; Kracunas, A. E. *Environ. Sci. Technol*. **2011**, *45*, 3931 – 3937.

[33] Gackowska, A.; Przybytek, M.; Studzinski, W.; Gaca, J. *Cent. Eur. J. Chem*. **2014**, *12*, 612 – 623.

[34] Schwack, W.; Rudolph, T. *J. Photochem. Photobiol. B: Biol.* **1995**, *28*, 229 – 234.

[35] Couteau, C.; Chauvet, C; Paparis, E.; Coiffard, L. *PLOS ONE* **2012**, *7*, 1 – 6.

[36] Raja, N.; Ramesh, R.; Liu, Y. *Polyhedron* **2012**, *31*, 196 – 201

[37] Wang, X.; Liu, J.; Wang, J. *Yao Xue Xue Bao* **2012**, *47*, 72 – 76.

[38] Moure, M. J.; SanMartin, R.; Dominguez, E. *Angew. Chem. Int. Ed.* **2012**, *51*, 3220 – 3224.

[39] Muntean, M.; Harles, L. RO 93627, 1988.

[40] Ding, Y. *Hauxua Shijie* **2001**, *42*, 432 – 434.

[41] Wang, Y.-X.; Gong, J. *Jingxi Haugong* **2004**, *21*, 115 – 117.

[42] Du, C.-Y.; Wang, Y.K.; Guo, J. *Hauxua Shijie* **2010**, *51*, 176 – 178.

[43] Wang, J.J. *Hauxue Shiji* **2004**, *26*, 243 – 244.

[44] Sun, B.; Wang, Y.; Xu, B.; Zuo, R. CN 102775311, 2012.

[45] Villa, C.; Baldassari, S.; Gambaro, E.; Loupy, A*. Int. J. Cosmet. Sci*. **2005**, *27*, 11 – 16.

[46] Cosmetics and Toiletries: Ingredient profile – Ethyl methoxycinnamate. http://www.cosmeticsandtoiletries.com/formulating/function/uvfilter/premium-Ingredient-Profile-Ethylhexyl-Methoxycinnamate.html (accessed Dec 16, 2015)

[47] Hùllmann, M.; Gnad, J.; Becker, R. DE 4039782, 1990.

[48] Yadav, V. G.; Chandalia, S. B. *Indian J. Chem. Technol.* **1999**, 6, 19 – 23.

[49] Herkes. F. E. *Catalysis of Organic Reactions*; Marcel Dekker Inc.: New York, **1998**; p 416.

[50] Li. J. J.; Gribble, G. W. *Palladium in Heterocyclic Chemistry: A guide for the Synthetic Chemist*; Gulf Professional Publishing, **2006**, p599.

[51] Lipshutz, B. H.; Taft, B. R. *Org. Lett*. **2008**, *10*, 1329 – 1332.

[52] Ewenson, A.; Croitoru, B.; Shushan, A. US 5728865, 1998.

[53] Triumph Venture Capital: Study into the establishment of an aroma and fragrance fine chemicals value chain in South Africa. https://www.thedti.gov.za/industrial_development/docs/fridge/Aroma_Part3.pdf (accessed Dec 7, 2015)

Chapter 3:
Metathesis Reactions

3.1 Introduction

The word metathesis originates from the Greek word *metatithemi*, meaning to put one thing in the place of another.[1] In chemistry terms, it means to replace or rather exchange part of a molecule by another. Olefin metathesis is achieved by allowing two alkenes to react with each other, forming two new olefin products after redistribution of the groups attached to the two double bonds (Figure 3.1).

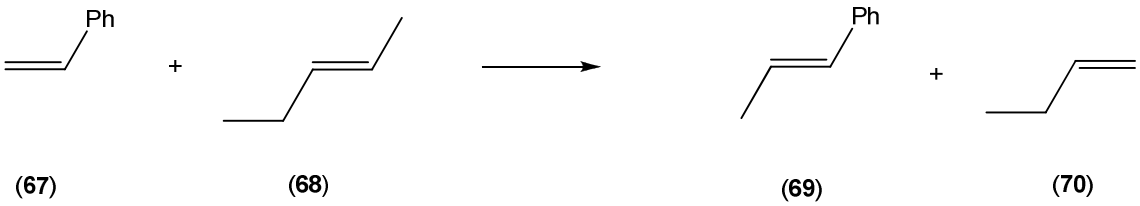

(**67**) (**68**) (**69**) (**70**)

Figure 3.1: General cross-metathesis reaction.

Although generally thought to be discovered in the mid 1960's, these reactions were actually already patented by Eleuterio[2] in 1957 when he observed as he knew it to be, the polymerization of cyclic olefins to polymeric products during hydrogenation with a molybdenum on alumina - lithium aluminium hydride catalyst system (Figure 3.2).

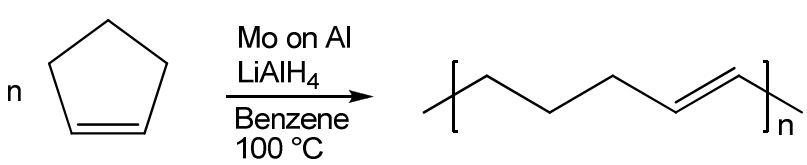

(**71**) (**72**)

Figure 3.2: Polymerization of cyclic olefins.

The scientific community, however, only became aware of the alkene metathesis reaction when Banks and Bailey[1,3,4] applied it to the transformation of propene into ethene and 2-butene in the Phillips Triolefin Process.

Alkene metathesis has since these early days erupted into a field with a myriad of applications both in academia and industry. The current importance of the alkene metathesis reaction is amply illustrated by the fact that the 2005 Nobel Prize in Chemistry[5] was awarded to three of the leading scientists in this field, *i.e*. Yves Chauvin, Robert H. Grubbs and Richard R. Schrock.

3.2 Types of metathesis reactions[5,6,7]

Metathesis reactions include various well known basic types, amongst others cross-metathesis, self-metathesis, acyclic diene metathesis polymerization, ring-opening metathesis, ring-opening metathesis polymerization, ring-closing metathesis, asymmetric ring-closing metathesis, and ene-yne metathesis.

3.2.1 Cross-metathesis (CM)

Cross-metathesis can be described as the reaction between two acyclic alkenes to form two new alkene products (Figure 3.3). Selectivity during this type of metathesis reaction is of great importance as self-metathesis may also occur. Solvent, temperature, catalyst type, and concentration have a major effect on the outcome of these reactions and have to be taken into consideration when planning these reactions.

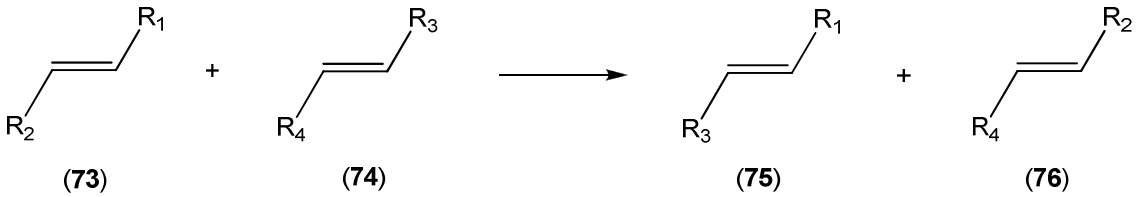

Figure 3.3: Example of a cross-metathesis reaction.

3.2.2 Self-metathesis (SM)

Self-metathesis, also known as homo-metathesis, is a form of metathesis where an unsymmetrical acyclic alkene reacts with itself to form two new alkene products. This type of metathesis can be either productive (Figure 3.4)[8] or non-productive (Figure 3.5).[8]

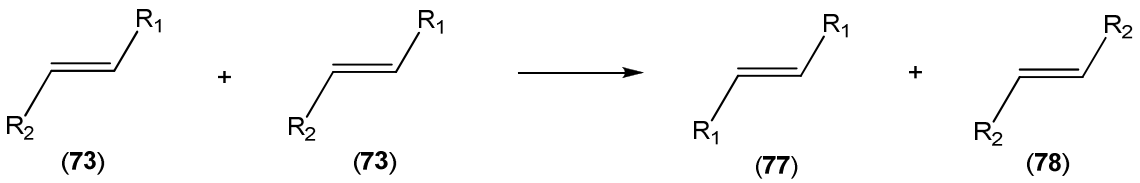

Figure 3.4: Example of a productive self-metathesis reaction.

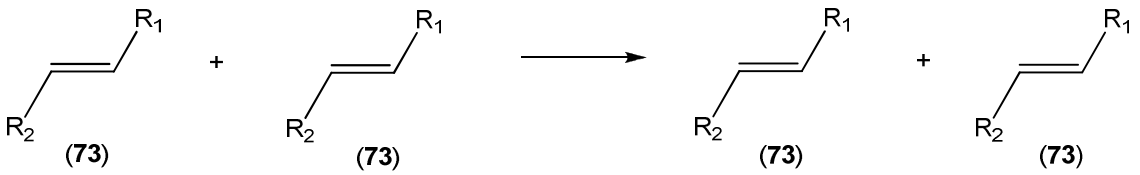

Figure 3.5: Example of a non-productive self-metathesis reaction.

3.2.3 Acyclic diene metathesis polymerization (ADMET)

Acyclic diene metathesis polymerization can be viewed as polymerization of a linear diene molecule through metathesis leading to a longer olefinic polymer (Figure 3.6).

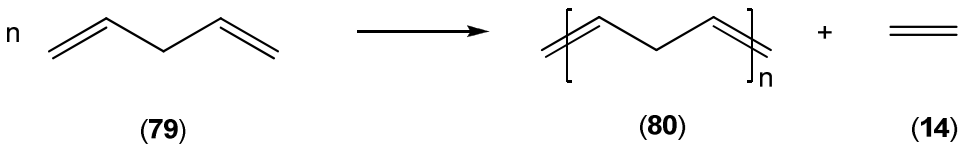

Figure 3.6: Example of an acyclic diene metathesis polymerization reaction.

3.2.4 Ring-opening metathesis (ROM)

Ring-opening metathesis describes the reaction in which a cyclic olefin reacts with a short chain alkene to form an acyclic diene as product (Figure 3.7).

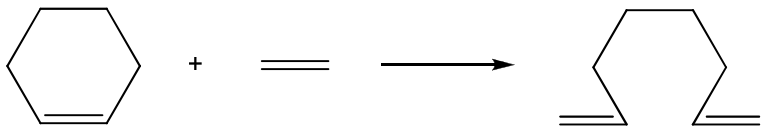

(**81**) (**14**) (**82**)

Figure 3.7: Example of a ring-opening metathesis reaction.

3.2.5 Ring-opening metathesis polymerization (ROMP)

Ring-opening metathesis polymerization is the opening of a cyclic molecule by a self-metathesis reaction to yield a long chain olefinic polymer (Figure 3.8).

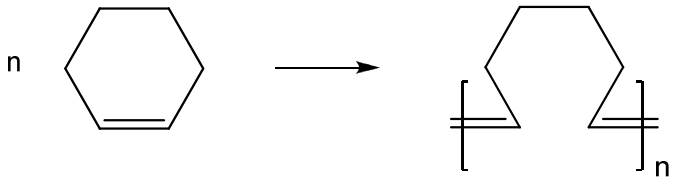

(**81**) (**83**)

Figure 3.8: Example of a ring-opening metathesis polymerization reaction.

3.2.6 Ring-closing metathesis (RCM)

Ring-closing metathesis is the opposite of ROM and consists of the self-condensation of a diene to form a cyclic olefin with ethene as by-product (Figure 3.9).

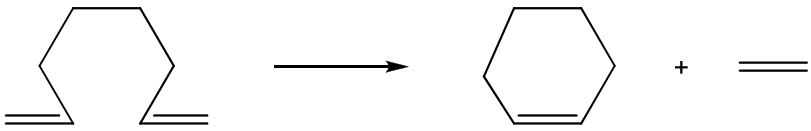

(**82**) (**81**) (**14**)

Figure 3.9: Example of a ring-closing metathesis reaction.

3.2.7 Asymmetric ring-closing metathesis (ARCM)

Asymmetric ring-closing metathesis resembles RCM with the only difference being that the by-product is a short chain alkene instead of ethene (Figure 3.10).

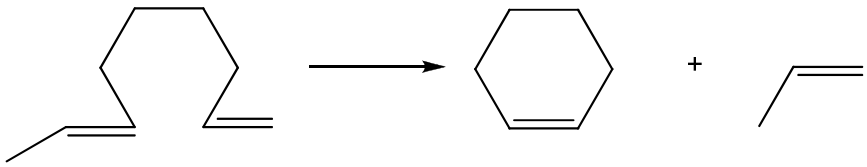

(**84**) (**81**) (**54**)

Figure 3.10: Example of an asymetric ring-closing metathesis reaction.

3.2.8 Ene-yne metathesis

Ene-yne metathesis comprises the formation of a cyclic olefin with a double bond containing side chain through self-reaction of an α,ω-enyn (Figure 3.11).

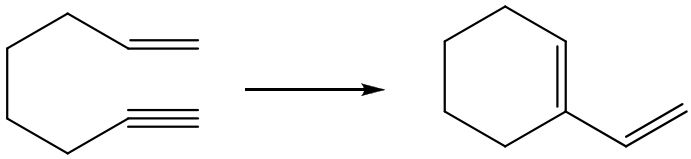

(**85**) (**86**)

Figure 3.11: Example of an ene-yne metathesis reaction.

One has to note that all metathesis reactions are equilibria reactions, due to the fact that all products are alkenes. Keeping this in mind, the reactions can be shifted to favor the desired product by removal of one of the products, usually a low boiling alkene like ethylene or propylene.

3.3 Catalyst development

3.3.1 Early investigations

Although the synthetic potential of the metathesis reaction was realized early on, development of useful catalyst systems did not take off until the mid 1970's. One of these early pioneers for metathesis reaction was Ernst Fischer. In 1964, Fisher and Maasböl,[9] prepared the first active metal carbene catalyst. This metallocarbene was prepared from tungsten hexacarbonyl (**87**) with phenyl lithium (**88**) to form a lithium acyl pentacarbonyl tungstenate complex (**89**). This complex (**89**) was then acidified and methylated with diazomethane to form active complex (**91**) (Figure 3.12).[10,11]

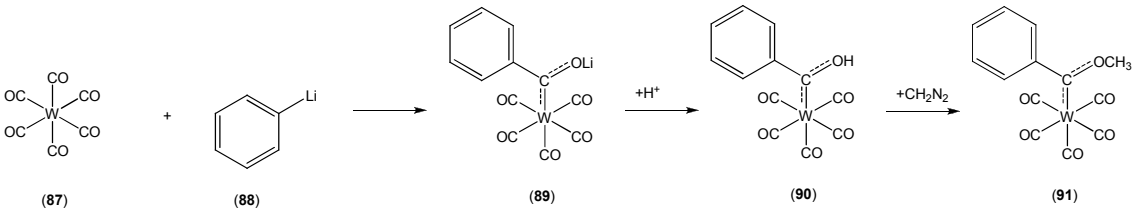

Figure 3.12: Preparation of first reported active Tungsten metal carbene complex.

Other early work around the development of catalysts covered a wide variety of metals such as Mo, Ru, W, Re, Os, Ir, Ti, V, Cr, Co, Nb, Rh, and Ta.[5,12] Progress was slow and many systems failed with regard to turn-over numbers, substrate selectivity, catalyst stability, and compatibility with/towards other functional groups. In 1973, Fischer *et al.*[13] reported the first metal-carbon triple bond complex (**92**) with tungsten metal centers being the more stable complexes (Figure 3.13).

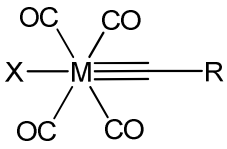

(**92**)

Figure 3.13: First carbyne complexes (X =Cl, Br, I, M=Cr, Mo, W, R=CH_3, C_6H_5) as prepared by Fischer *et al*.[13]

3.3.2 Development of the Schrock catalyst

In 1974, Schrock[14] isolated the first stable metallocarbene, $Ta[CH_2C(CH_3)_3]_3[CHC(CH_3)_3]$, but it was not until the 1980's when Schrock *et al.*[15] prepared a well-defined tungsten complex (**96**) (Figure 3.14) that could be used for the metathesis reaction of 2-pentene (Figure 3.15) in the presence of $AlCl_3$, that noteworthy progress was made from a synthetic point of view. With turn-over numbers of 50 in 24 hours, this catalyst showed a vast improvement over previous reagents.

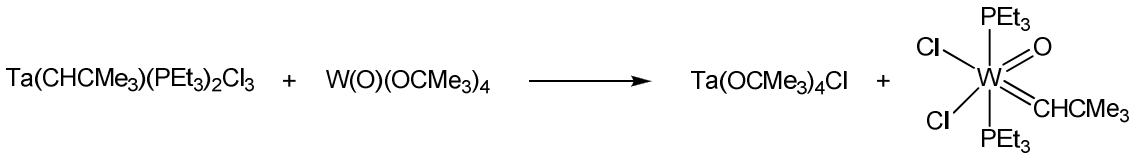

(**93**) (**94**) (**95**) (**96**)

Figure 3.14: Preparation of tungsten complex (**96**).

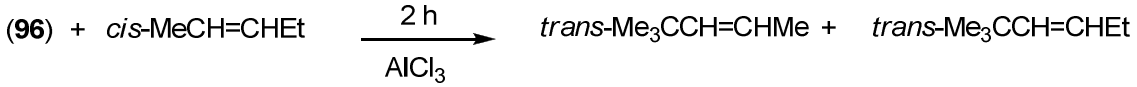

(**97**) (**98**) (**99**)

[i]Figure 3.15: Cross-metathesis reaction with complex (**96**).

---

[i]The original paper depicts the reaction as:

(**97**) (**100**) (**101**)

But there is a clear mistake as the products formed (**100** and **101**) are not possible.

In an effort to improve on catalyst activity, Schrock *et al.*[15] decided to open up another co-ordination site on the tungsten and therefore removed one of the PEt_3 ligands from the complex (Figure 3.16). Although this did not lead to a dramatic improvement in metathesis activity, it resulted in a catalyst that was active in the absence of Lewis acid activation.

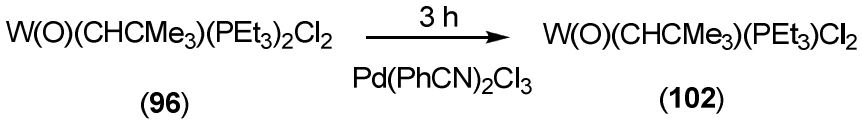

Figure 3.16: Preparation of tungsten complex (**102**).

Through continued investigations, the Schrock group was set out to design the ideal Tungsten metathesis catalyst.

The oxo ligand was undesired as it was known to encourage a bimolecular decomposition reaction.[16] In an attempt to remove the oxo ligand, Schrock *et al.*[15,16] reacted a tantalum alkylidene ligand (**103**) (L = PEt_3 *etc*.) with a tungsten ligand (**104**), anticipating a "Wittig-like" reaction to give [W(CH*t*Bu)(O*t*Bu)$_4$], but obtaining a tungsten oxo alkylidine complex (**105**) instead (Figure 3.17).

This compound proved to catalyze metathesis reactions of both terminal and internal alkenes well, but only in the presence of $AlCl_3$.

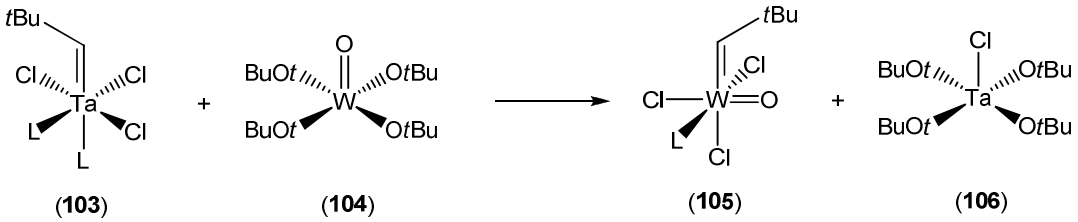

Figure 3.17: Formation of a tungsten oxo neopentylidene complex (**105**).

It was proposed[16] that the $AlCl_3$ removes either a Cl or a phosphine ligand from the metal center, thus creating an empty coordination site.

A four-coordinate alkylidene metal species with bulky covalently bound ligands was believed to be the most likely isolable, but reactive, species. Based on their previous findings,[17] it was decided that a neopentylidene ligand and two alkoxide ligands need to be included in this species. The oxo ligand was replaced by a bulky imino group, as it had isoelectronic properties to the oxo group, but with the advantage of steric bulk. With all of this in mind, a stable tungsten imido alkylidine bisalkoxide complex was designed (Figure 3.18).[16]

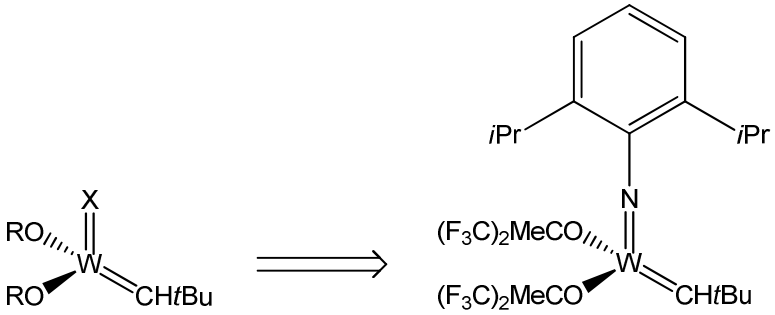

(**107**) (**108**)

Figure 3.18: Design of a stable Tungsten complex.

After preparation of (**108**) and similar alkoxide derivative complexes, it was clear that these complexes catalyzed olefin metathesis in the expected manner, with activities correlating to the electron withdrawing capability of the alkoxides, hexafluoro-*tert*-butoxide being the most active. Replacing the metal center with molybdenum, as the weaker metal-ligand bonds were considered to enable the intermediate metallacyclobutane to lose an olefin more readily, and replacing the neopentylidene $Me_3C(H)=$ group with the cheaper neophylidene $Me_2PhC(H)=$ analogue, led to the formation of what is known today as Schrock's catalyst[1,16,18,19] (**109**) (Figure 3.19). This catalyst displayed high activity, reacting with both terminal and internal alkenes. Being highly oxophilic, the molybdenum metal centre renders this catalyst, similar to others based on early transition metals, highly sensitive to oxygen and moisture, though.[6] Complex (**109**) furthermore has limited functional group tolerance and is incompatible with aldehydes and alcohols, for example (Table 3.1, *vide infra*).[6]

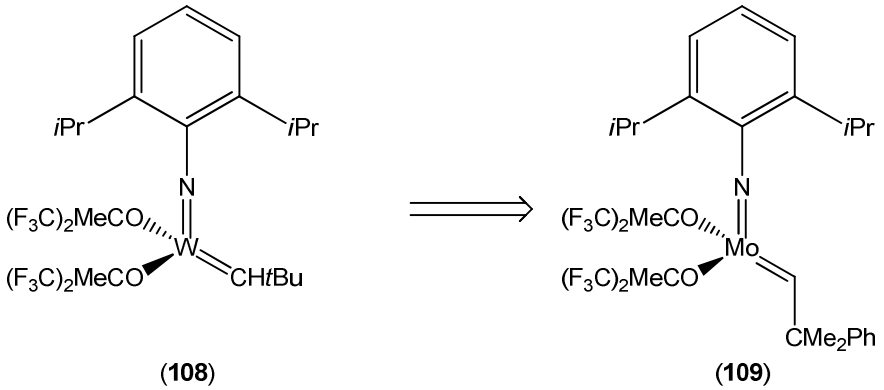

Figure 3.19: Alterations for the preparation of Schrock catalyst.

3.3.3 Development of the Grubbs catalysts

While Schrock *et al*. were developing tungsten and molybdenum based catalysts, Grubbs became active in the field as well and developed a ruthenium based metathesis catalyst (**112**) (Figure 3.20).[20,21,22] This compound showed some stability in air and demonstrated higher selectivity, but lower reactivity when compared to the Mo catalysts.

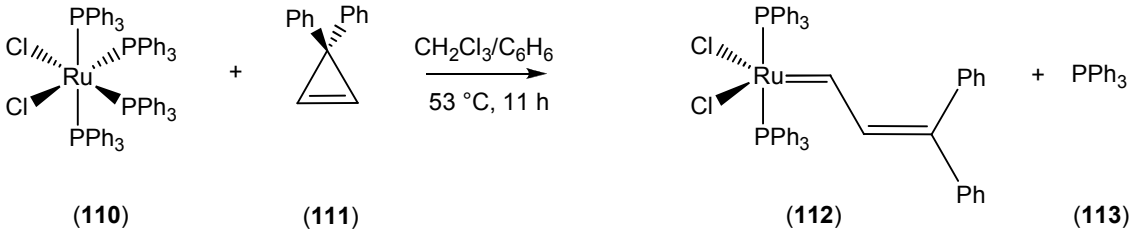

Figure 3.20: Preparation of Grubbs first generation-like catalyst.

An investigation to increase the reactivity of the catalyst[23] led to the exchange of one of the triphenylphosphine ligands with a tricyclohexylphoshine ligand (Figure 3.21).

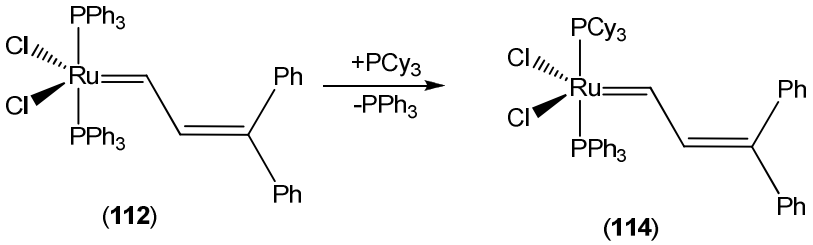

(**112**) (**114**)

Figure 3.21: Preparation of the first well-defined Ru carbene catalyst.

This catalyst preparation route however was not the ideal as it utilized unstable reagents, required large solvent quantities and involved an additional ligand substitution step. Alternative routes[24] for the preparation of Grubbs first generation-like catalysts were thus investigated. In this process a suitable ruthenium hydride starting material with the desired number of phosphines already attached to the metal, like $Ru(H)(H_2)Cl(PCy_3)_2$ (**115**), was utilized as starting material.

This ruthenium starting material could now undergo an insertion-elimination reaction with propargyl chlorides (Figure 3.22) to produce the desired metal complex[6] (**118**) in a one pot procedure in high yields (95%). Catalyst (**118**) proved to be tolerant of trifluoroacetyl and *t*-butoxycarbonyl protecting groups and remained active in the presence of water, alcohols and acids.[6]

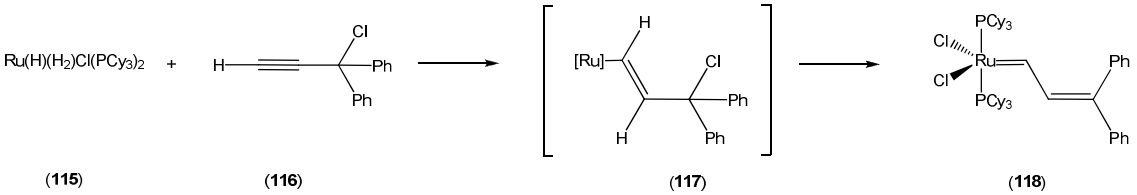

(**115**) (**116**) (**117**) (**118**)

Figure 3.22: Propargyl chloride insertion-elimination reaction.

Since this reaction was difficult to run on a large scale and taking into account the high demand for this catalyst, further studies[1,18,25,26] led to the development

of what became known as the Grubbs 1st generation catalyst (**122**) (Figure 3.23).

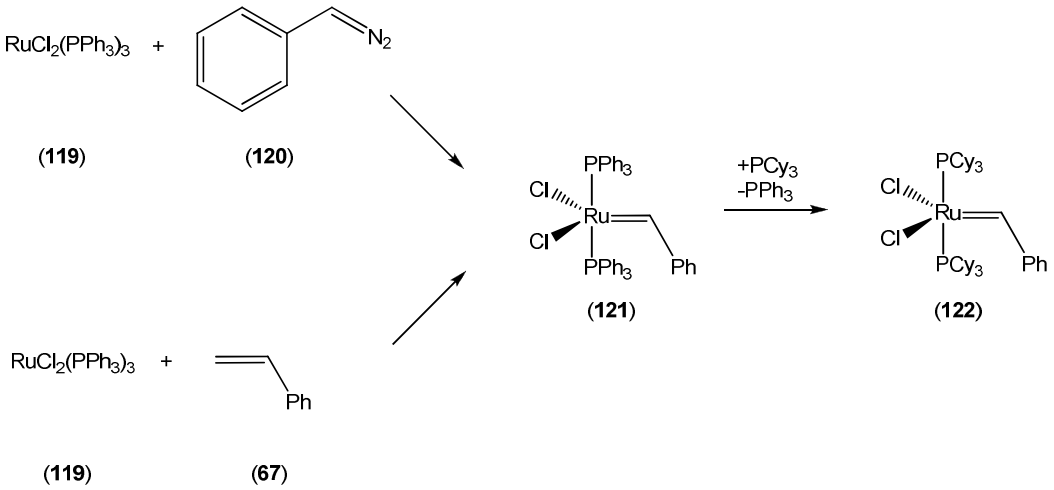

Figure 3.23: Preparation of Grubbs first generation catalyst.

While the Grubbs 1st generation catalyst (**122**) proved to be highly efficient in ROMP, RCM, CM, and ene-yne metathesis reactions, it did not perform that well with highly substituted or sterically hindered substrates in RCM and CM reactions or CM reactions involving substrates with electron-withdrawing functional groups. It was robust, though, and tolerant of water, oxygen and a variety of polar functional groups (excluding amines and nitriles in basic media).[26,27,28,29]

Ruthenium proved to be an excellent choice for a metathesis catalyst as it is more reactive towards carbon-carbon double bonds than to most other functional groups (Table 3.1) and therefore more versatile than catalysts based on titanium, tungsten or molybdenum.[6]

Table 3.1: Reactivity of functional groups toward selected metal catalysts.[6]

Titanium	Tungsten	Molybdenum	Ruthenium
Acids	Acids	Acids	**Olefins**
Alcohols, Water	Alcohols, Water	Alcohols, Water	Acids
Aldehydes	Aldehydes	Aldehydes	Alcohols, Water
Ketones	Ketones	**Olefins**	Aldehydes
Esters, Amides	**Olefins**	Ketones	Ketones
Olefins	Esters, Amides	Esters, Amides	Esters, Amides

↑ Increasing Reactivity

A subsequent series of experiments[30,31,32] led to the development of the Grubbs 2nd generation catalyst (**125**), in which one of the phospine groups (of Grubbs 1 (**122**)) was replaced by a stronger σ-donating NHC (*N*-heterocyclic carbene) ligand (Figure 3.24). This led to a catalyst that was found to be very active and thermally stable.[29] The increased stability of the Grubbs 2nd generation catalyst[26] (**125**), as this complex was called, could be attributed to a stronger bond between the metal center and the NHC carbene in comparison to PCy_3.[33]

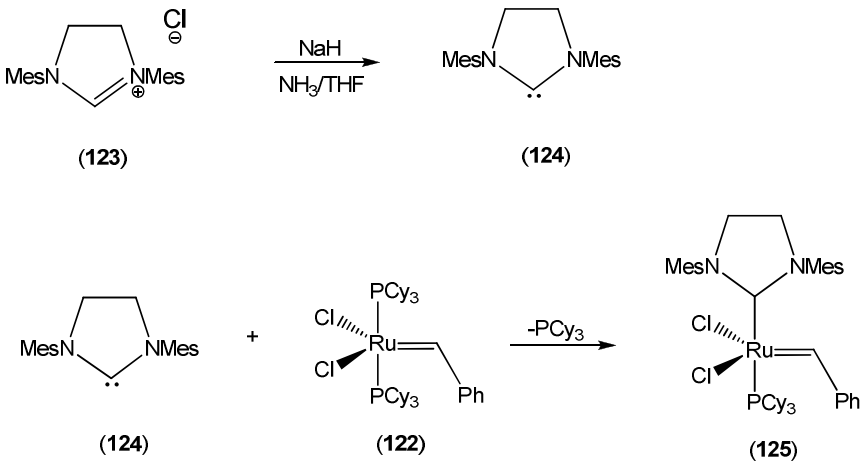

Mes = 2,4,6-trimethylphenyl

Figure 3.24: Preparation of Grubbs second generation catalyst.

The stability of the catalyst is further enhanced by π–stacking[34] between the phenyl ring of the carbene and one of the phenyl groups on the NHC (Figure 3.25).

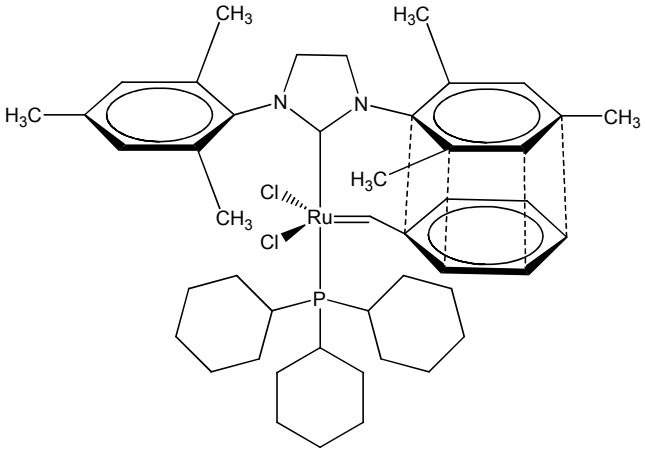

(**125**)

Figure 3.25: Illustration of π–stacking within Grubbs 2nd generation catalyst.

While the Grubbs 2nd generation catalyst (**125**) proved to be more stable when compared to Grubbs 1st generation (**122**), Wakamatsu and Blechert[35,36] proved that that the stability of the catalyst is indirectly proportional to reaction time.

3.3.4 Catalyst variations

In an attempt to improve metathesis catalysts, Hoveyda *et al.*, started investigating the various available catalysts. They first turned their focus to the Mo centered Schrock catalyst.[37,38] Hoveyda *et al*. figured by replacing the two alkoxy ligands with a chiral biphenol, control of the stereochemistry can be maintained. The produced catalyst, the Hoveyda-Schrock catalyst (**126**), proved to be an efficient ARCM catalyst that yielded products enantioselectively (Figure 3.26).

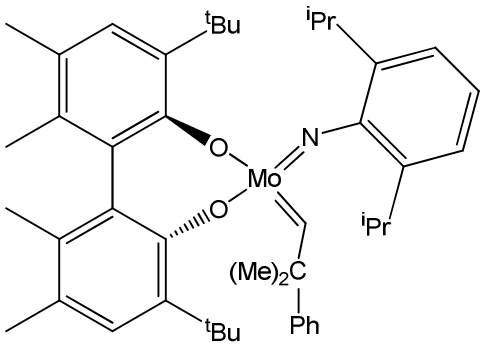

(**126**)

Figure 3.26: Hoveyda-Schrock catalyst.

Turning their focus to the Grubbs catalysts, Hoveyda *et al.*,[39] also embarked on altering the complex ligands, as with the Schrock catalyst, to improve these catalysts. They found that the replacement of one of the PCy_3 ligands of the Grubbs 1st generation catalyst with a chelating benzylidene ether ligand rendered a catalyst that was exceptionally moisture and air stable[39]. This discovery led to the known Hoveyda-Grubbs 1st generation catalyst (**127**). In an attempt to improve on the Grubbs 2nd generation catalyst, Hoveyda *et al*.[40] replaced the PCy_3 ligand of the Grubbs 2nd generation catalyst with this chelating benzylidene ligand[40]. The resulting catalyst, now known as the Hoveyda-Grubbs 2nd generation catalyst (**128**), not only was more stable than the Grubbs alternative, but also showed higher reactivity towards electron deficient substrates, (*i.e*. alkenes conjugated to -CN, $-SO_2Ph$)[41] (Figure 3.27).

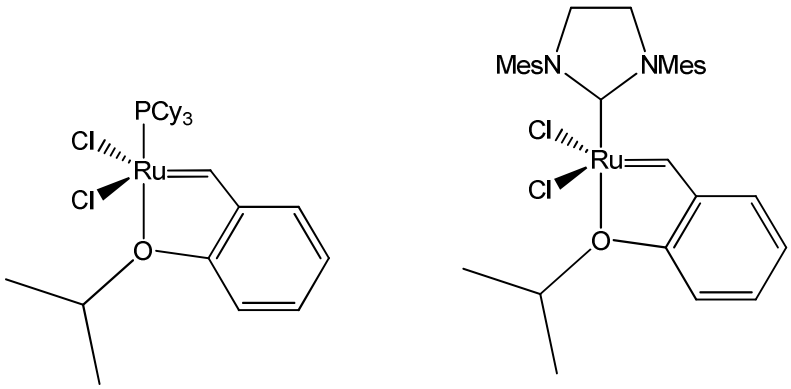

(**127**) (**128**)

Figure 3.27: Hoveyda-Grubbs 1st and 2nd generation catalysts.

Dias *et al.*[42] modified these catalysts by synthesizing bimetallic catalysts (Figure 3.28). These catalysts were stable in air in their solid state and both (**129**) and (**130**) were stable for days in a DCM solution under an inert atmosphere. It was further found that bimetallic catalysts (**129**), (**130**) and (**131**) are able to perform RCM, CM, and ROMP. The ROMP of 1,5-cyclooctadiene (COD) catalyzed by Ru-Ru catalyst (**129**) proceeded at rates 20 times faster than when catalyzed by (**112**) and 2.4 times faster than with (**122**) (Grubbs I), whereas the osmium-rhodium (**130**) and rhodium-ruthenium (**131**) catalysts increased the respective reaction rates relative to (**112**) by 40 and 80 times, and 2.9 and 6.1 times relative to (**122**).

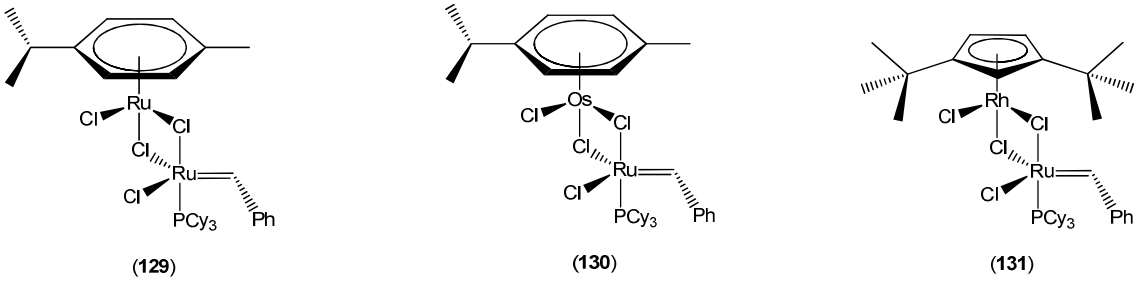

Figure 3.28: Dias *et al*.'s bimetallic modified metathesis catalysts.

At this point in time, two other research groups, namely Blechert *et al*.[35,36] and Bujok *et al.*[42,43], joined the catalyst development team. Blechert *et al*. altered the Hoveyda-Grubbs 2nd generation catalyst by replacing the chelating ligand with an even more sterically demanding chelating ligand (Figure 3.29) whereas Bujok *et al*. researched the effect of electron withdrawing groups situated para to the alkoxy groups (Figure 3.30). Both of these groups' efforts led to a faster initiation rate.

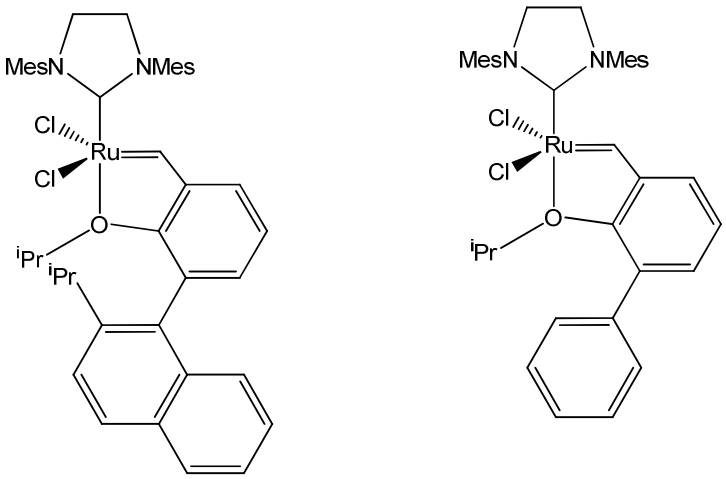

(**132**) (**133**)

Figure 3.29: Blechert *et al*.'s metathesis catalyst modifications.

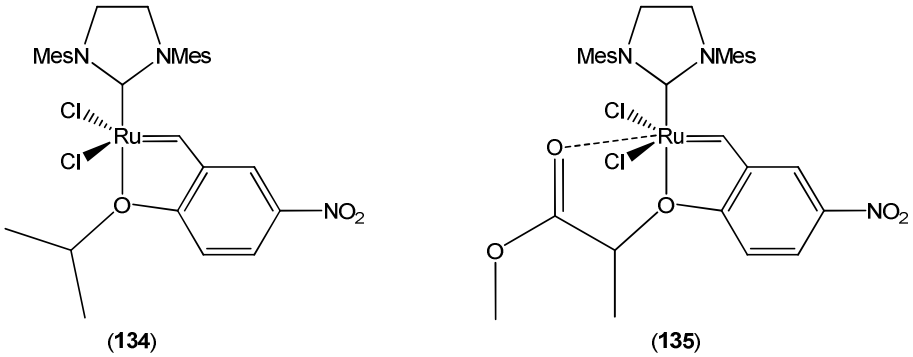

(**134**) (**135**)

Figure 3.30: Bujok *et al*.'s metathesis catalyst modifications.

Z-selectivity however posed a great drawback as the majority of catalysts favor the thermodynamically more stable *E*-isomer. Schrock and Hoveyda[44,45,46] therefore focused their investigations on the preparation of Z-selective metathesis catalysts (Figure 3.31).[44,45,46,47]

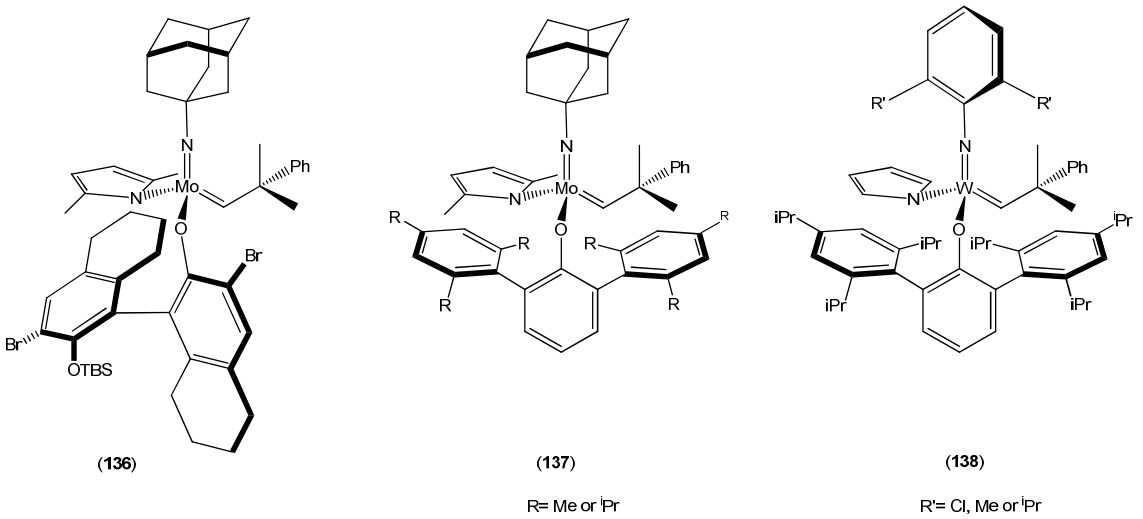

Figure 3.31: Modified Hoveyda-Schrock catalysts for Z-selective metathesis.[44,45,46,47]

Building on the results obtained from Schrock and Hoveyda, Keitz *et al*.[48] attempted to prepare a catalyst that was even more reactive. In their attempts to do so, catalysts (**139 - 145**) were created and studied (Figure 3.32).

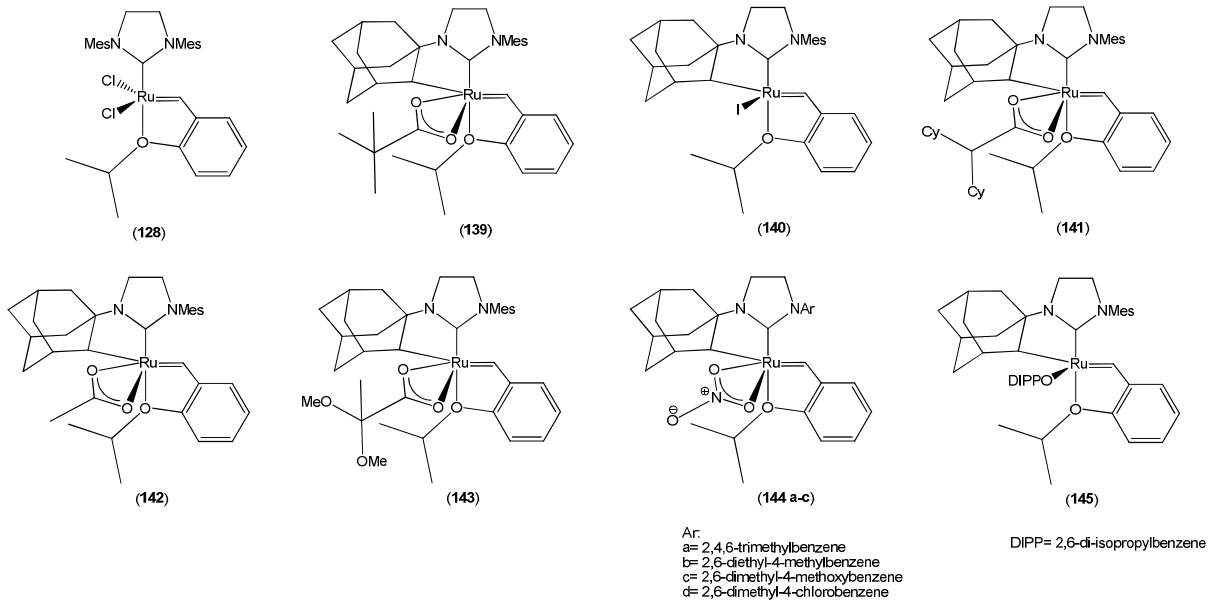

Figure 3.32: Keitz *et al*.'s inproved metathesis catalysts.

Compared to the Hoveyda-Grubbs second generation catalyst (**128**), the catalysts with bidentate ligands (**139, 141 - 144**) exhibited similar initiation rates,

whereas the monodentate analogues (**140** and **145)** initiated slower. TON of up to 1000 were reached in *Z*-selective homo- and cross-metathesis reactions.[38]

3.4 Catalyst types

It was clear at this point that two main types of metathesis catalysts were developed,[11,49,50] namely the Fisher- and Schrock-type carbenes.

3.4.1 Fischer-type catalysts

Fisher-type[50] carbenes are characterized by a low oxidation state transition metal, (e.g. W(0), Fe(0), Mo(0), Cr(0)) and an electrophilic carbene carbon (empty p orbital) typically bearing O, N or S substituents (X in Figure 3.33) capable of π-donation to the carbene *p*-orbital. The metal-carbon bond has partial double bond character with carbene-metal σ-donation as well as metal-carbene π-back donation (Figure 3.33). The π-electrons are polarized toward the metal and the electrophilic carbene carbon thus susceptible to nucleophilic attack. The more electron donating the carbene group becomes, the more electron-rich the metal center becomes, resulting in stronger back-bonding and thus stronger M=C bonds.

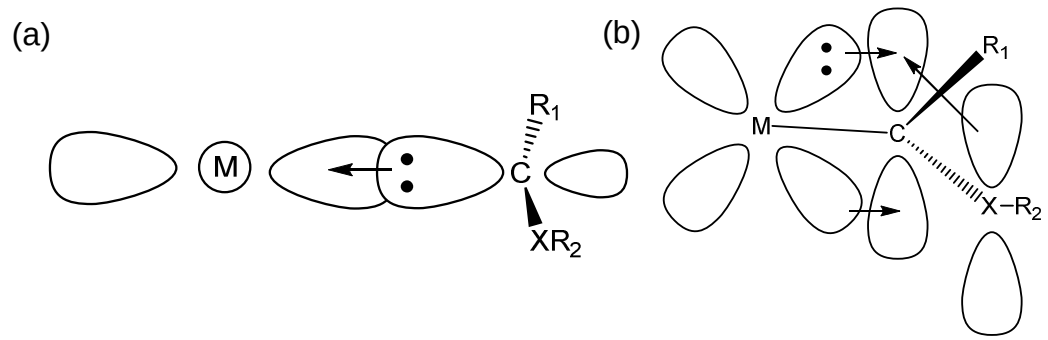

(**146**) (**147**) (**148**)

Figure 3.33: σ- (a) and π-bonding (b) between the metal center and the carbene in Fisher-type carbenes.

3.4.2 Schrock-type catalysts

Schrock-type carbenes[50] typically are nucleophilic, with the carbenoid carbon (with alkyl or hydrogen substituents, but not π-donors) bonded to a high oxidation state (d^0) early-transition metal such as tantalum(V) or titanium(IV). The metal-carbon bond is a true double bond with covalent character, formed between two triplet fragments (Figure 3.34), and the π-electrons are evenly distributed between the carbene carbon and metal.

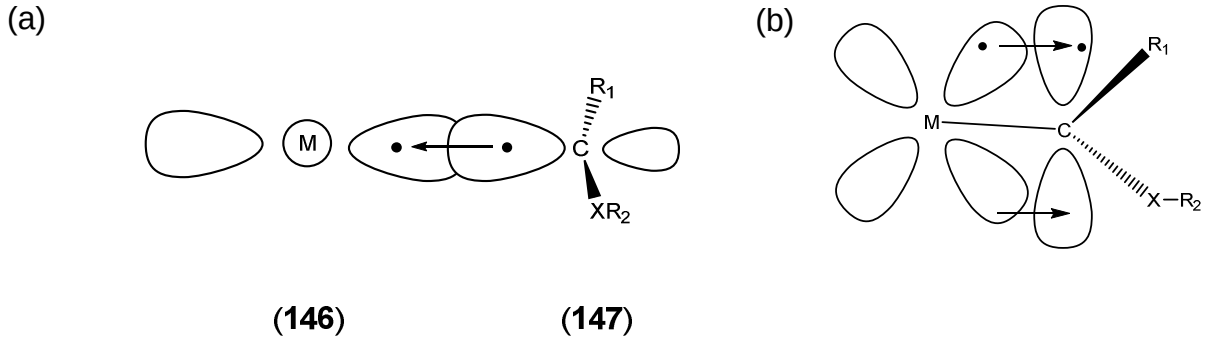

(**146**) (**147**)

Figure 3.34: σ- (a) and π-bonding (b) between the metal center and the carbene in Schrock-type carbenes.

3.5 Mechanisms

3.5.1 Metathesis mechanism

Since the very early stages of the discovery of the metathesis reaction, two major pathways for the formation of the products were being considered. In the "pair-wise" mechanism, it was postulated[4,51,52,53] that two molecules of the starting alkene would simultaneously react with the metal by forming a tetramethylene (**150**) - (Figure 3.35) or cyclobutane intermediate (**153**) (Figure 3.36).

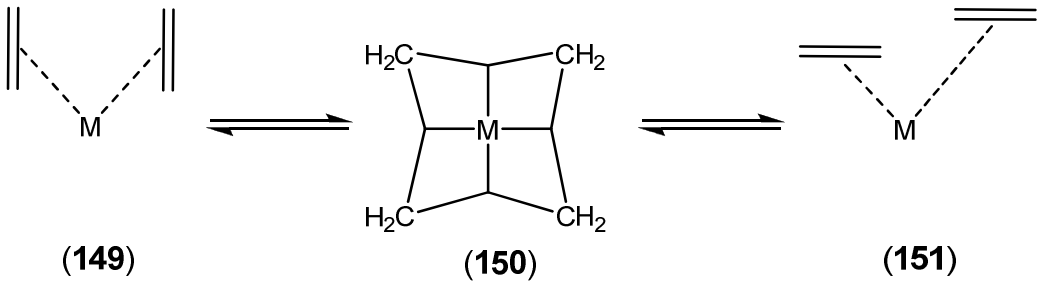

Figure 3.35: Proposed tetramethylene intermediate.

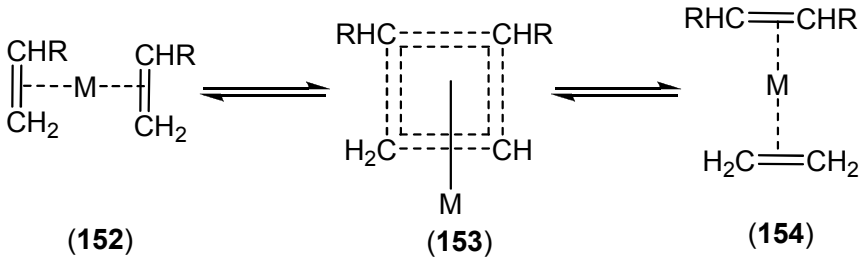

Figure 3.36: Proposed cyclobutane intermediate.

Chauvin,[54,55] however, proposed a "step-wise" metal carbene-metallacyclobutane mechanism where the metal carbene catalyst would first react with one alkene to form a four-member ring metallacycle (metallacyclobutane). This ring can open either reversibly or in a different way to form a new metal carbene available to react with a second alkene. The newly formed metallacyclobutane similarly can open to form a metal carbene and alkene product. (Figure 3.37).

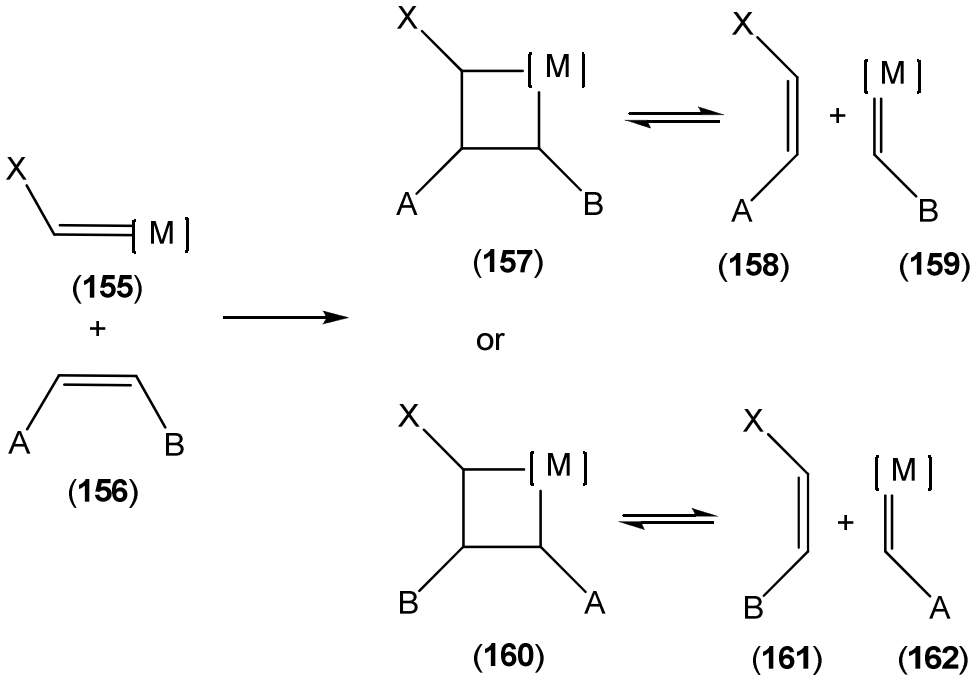

Figure 3.37: Condensed version of Chauvin's proposed metathesis mechanism.

Although Chauvin's proposal initially received very little support, experimental results[56] from the reaction between cyclopentene (**71**) and 2-pentene (**68**) (Figure 3.38) gave credence to the "step-wise" - vs the "pair-wise" mechanistic route, since a product distribution of 1:2:1 was found. Additional support for the "step-wise" mechanism came from the work of Schrock and Kress[57,58,59,60] who obtained NMR data suggesting the formation of a metallocyclobutadiene during *alkyne* metathesis.[16] This observation finally discredited the "pair-wise" mechanism and it is now generally accepted that metathesis reactions follow a "step-wise" pathway with a metallacyclobutane entity as reactive intermediate.

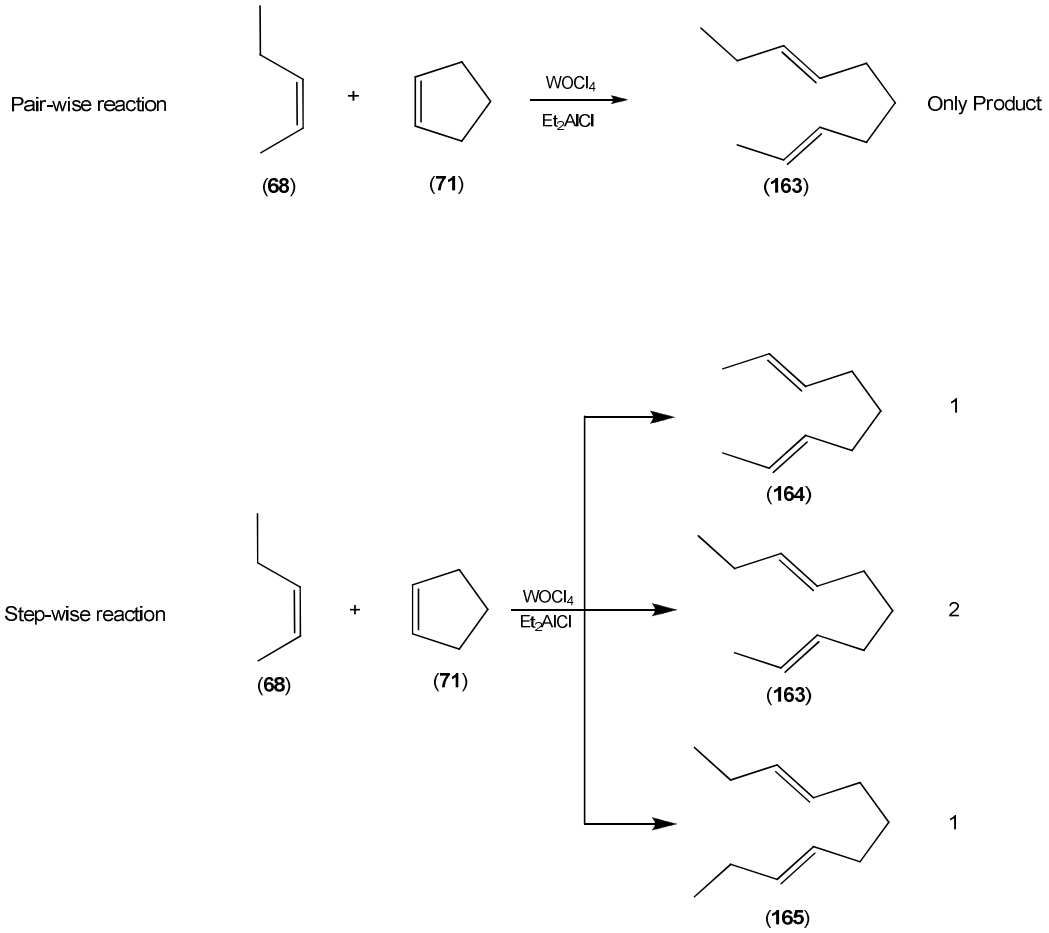

Figure 3.38: Cross-metathesis of 2-pentene with cyclopentene.

In order to better understand the the mechanism of metathesis catalysts, Grubbs focused his studies on active metathesis biscyclopentadienyl-titanium complexes. Through the utilization of labelling studies[61], it was determined that the reaction does proceed through the carbene intermediate and that the stable resting state of the catalyst is the titanacyclobutane (Figure 3.39).

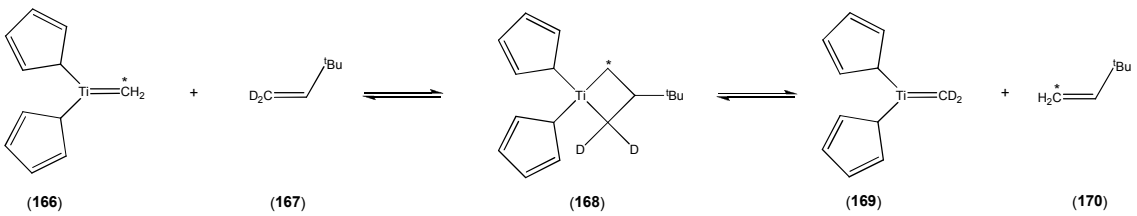

Figure 3.39: Grubbs's titanacyclobutane catalyst mechanistic study.

It was consequently accepted that a metallacyclobutane also is the key intermediate in ruthenium based metathesis reactions. Grubbs therefore proposed the now generally accepted mechanism depicted in Figure 3.40 for ruthenium based metathesis reactions.

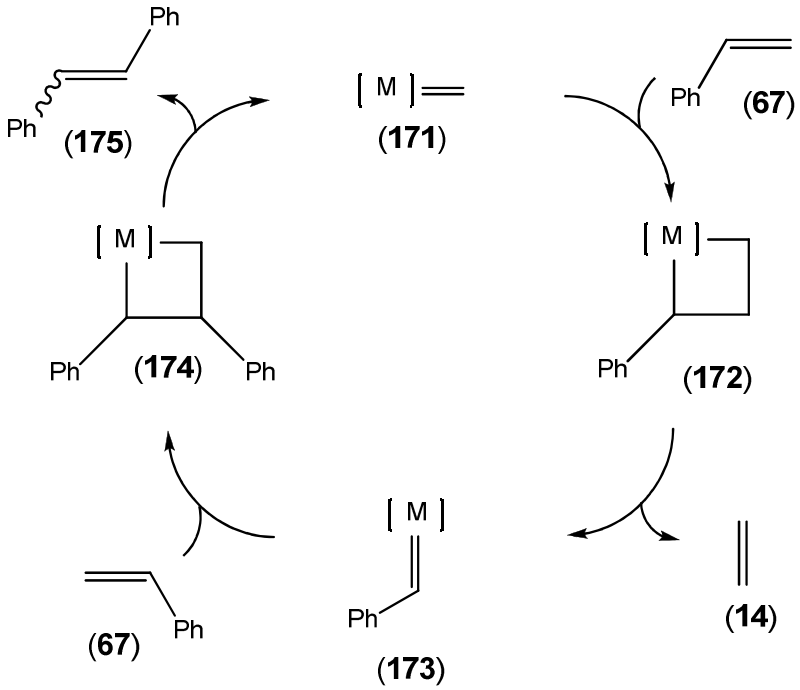

Figure 3.40: Mechanistic cycle of Grubbs catalysts.

3.5.2 Catalyst deactivation mechanisms

As previously mentioned, metathesis catalysts, like many other early transition metal based catalysts, are readily deactivated by functionalized impurities (oxygenates, etc.) in the reaction mixture or functional groups in the substrate molecule itself. For this reason, high catalyst loads or continued addition of the catalyst is needed for optimal turn-over output during metathesis reactions. Catalysts are deactivated/decomposed[62] by compounds like alcohols, oxygen, and water (Figure 3.41) as well as carbonyl compounds (Figure 3.42).

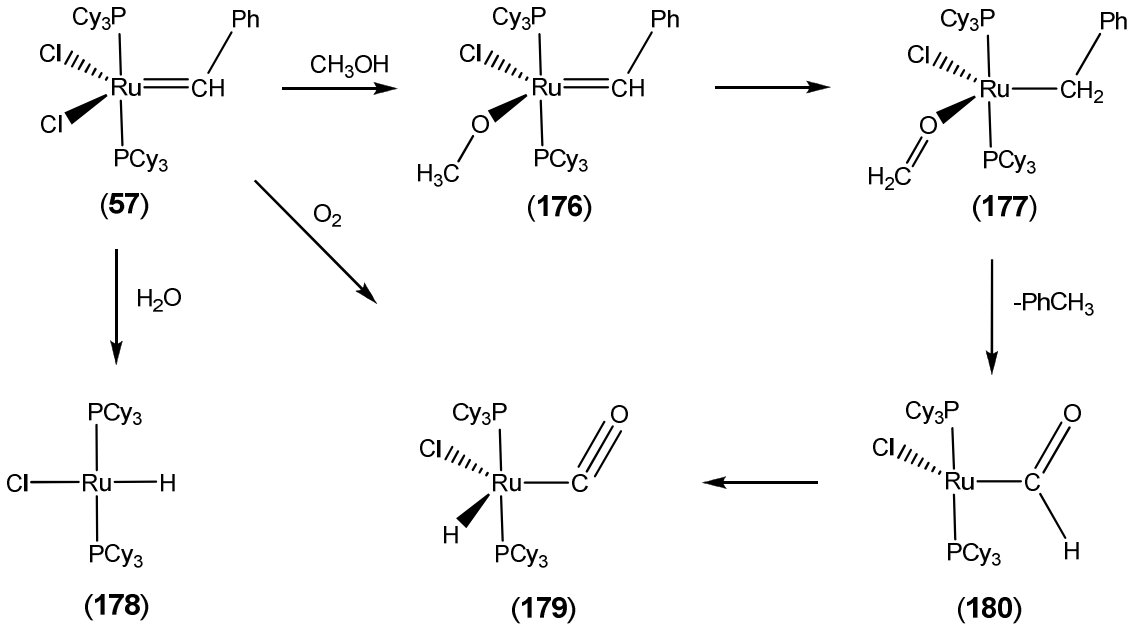

Figure 3.41: Catalyst deactivation by alcohol, oxygen and water.

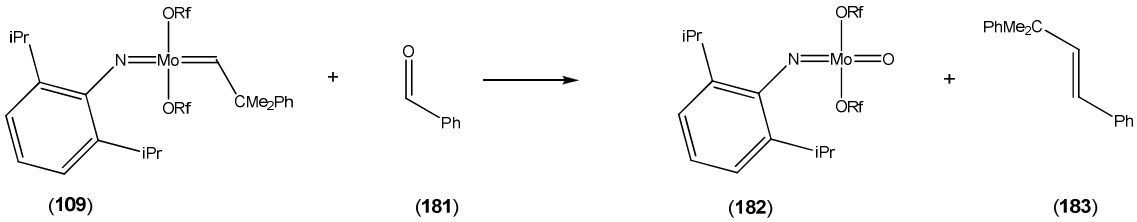

Figure 3.42: Catalyst deactivation by carbonyl compounds.

While oxygenated impurities can be removed from the starting material in reactions where true catalytic activity is required and especially Grubbs 2nd generation catalyst (**125**) shows good tolerance towards alcohol and ketone functional groups in the substrate, a more serious limitation is found in the inherent decomposition of the catalyst by β-hydride elimination. In an excellent piece of work, Janse van Rensburg *et al*.[63] studied the loss of catalyst activity during ethylene metathesis. DFT calculations, together with the experimental observation that propene is formed during the metathesis of ethene (Figure 3.43), was applied to explain how β-hydride transfer could account for the loss

in activity observed for many ruthenium based catalysts like the Grubbs 1st generation catalyst (**122**) (Figure 3.44).

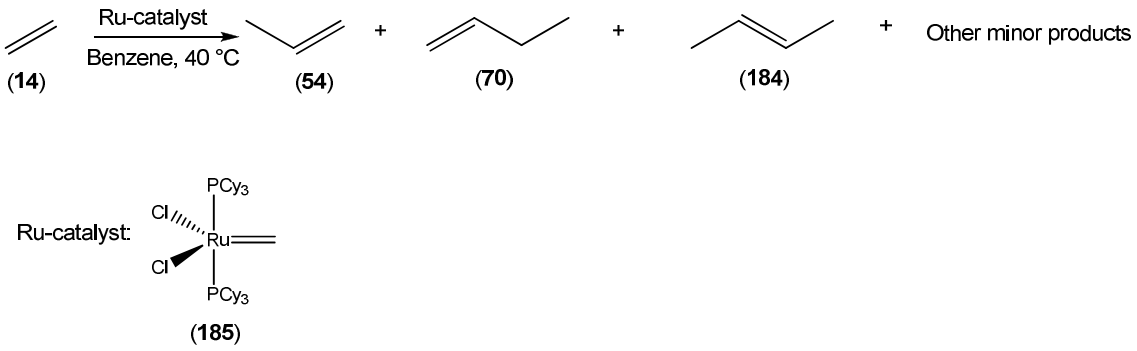

Figure 3.43: Experimental observation to prove β-hydride elimination.

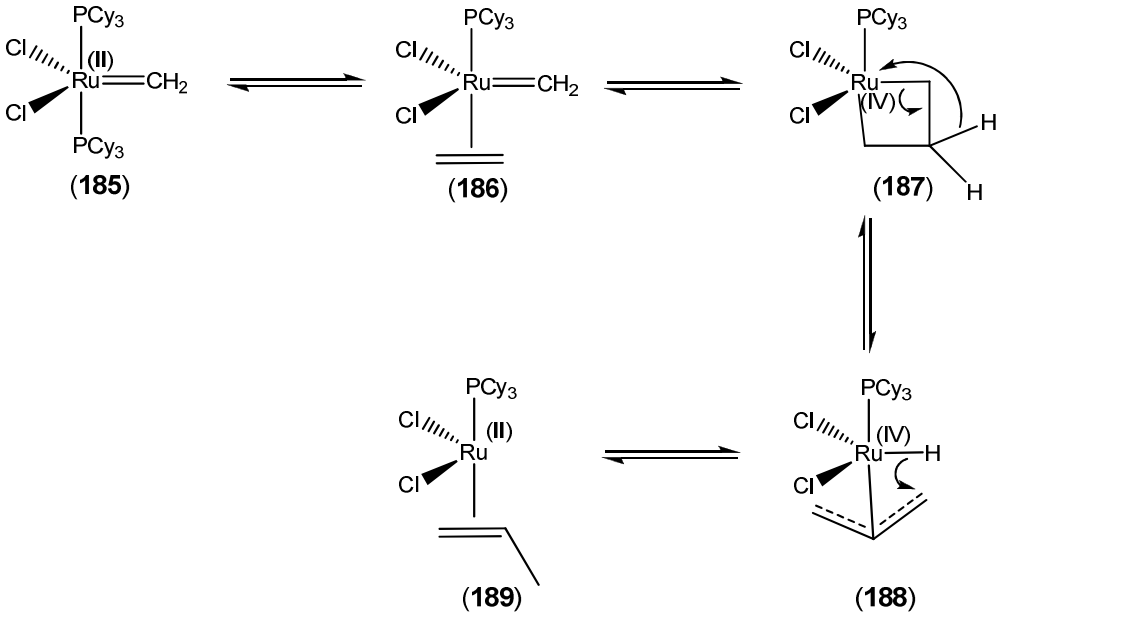

Figure 3.44: Proposed β-hydride elimination intermediates.

3.6 Application of metathesis

In addition to metathesis reactions, various other alkene-forming procedures (Figure 3.45)[64] have been developed, but these reactions require synthetic investment into activating group (halides and triflates) containing starting materials or the masking of other functional groups (aldehydes and ketones).

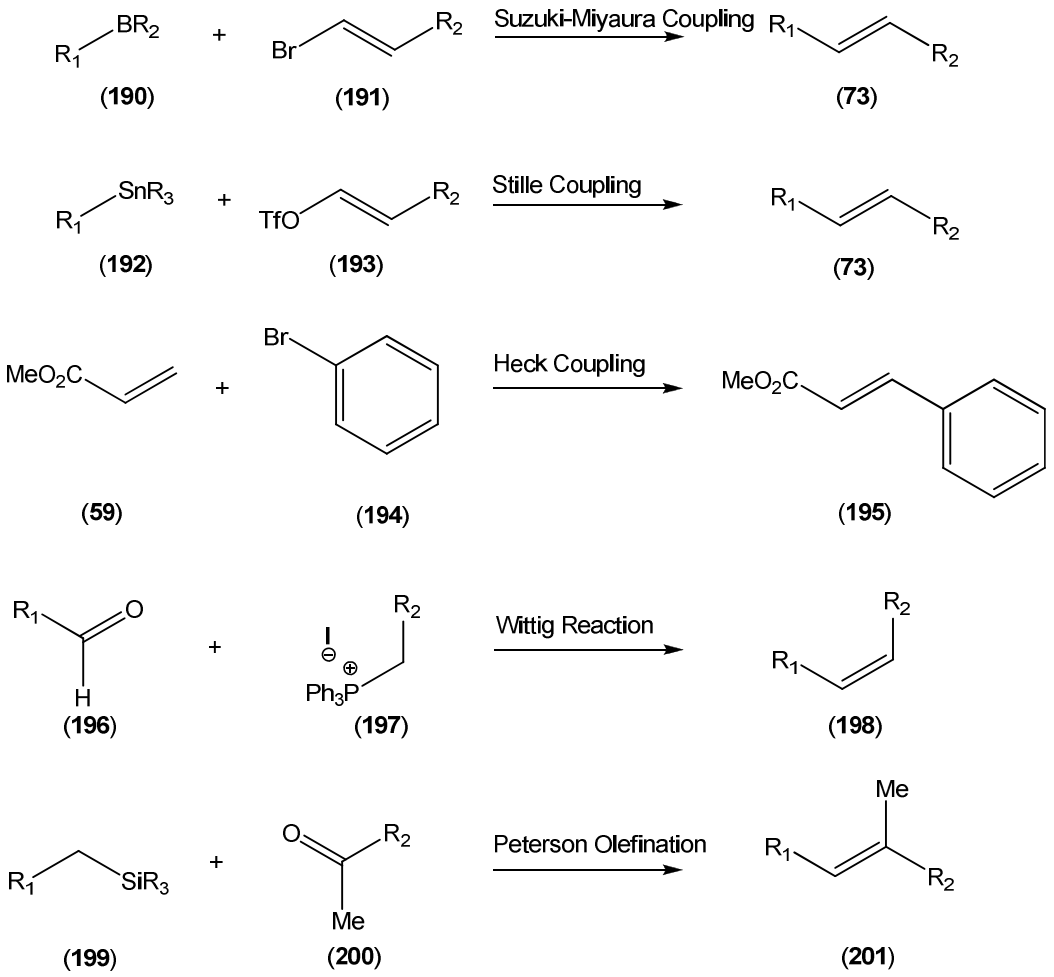

Figure 3.45: Alkene forming procedures.

In the case of metathesis reactions, the double bond itself is the reactive functional group, making it a much more desirable reaction. Metathesis is established as a field of immense importance in synthetic chemistry, especially in the bioorganic and pharmaceutical fields, as demonstrated by the following examples.

3.6.1 Synthesis of tsetse fly attractants[65]

Being the main vector of African sleeping sickness (trypanosomiasis), tsetse flies pose a great problem in the sub-Saharan Africa region. It is thus a priority to control this fly population. One of the methods used is to employ traps with known tsetse fly attractants, 3-ethylphenol (**202**) and 3-propylphenol (**203**), (Figure 3.46).

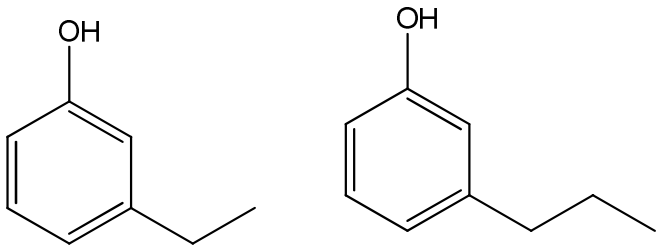

(**202**) (**203**)

Figure 3.46: Structures of 3-ethylphenol and 3-propylphenol.

One of the synthetic routes (Figure 3.47) for the preparation of these compounds are to start off with cashew nut shell liquid (CNSL), a by-product of cashew nut processing, and to separate the acids (**204-207**) from other compounds *via* $Ca(OH)_2$ precipitation, followed by acidification. Ethenolysis can then be employed with the Hoveyda-Grubbs 1st generation catalyst (**122**). Crack distillation (120 ˚C, 10^{-2} mbar) accompanied by decarboxylation of the metathesis product render the decarboxylated 3-(non-8-enyl)phenol (**209**) product quantitatively.

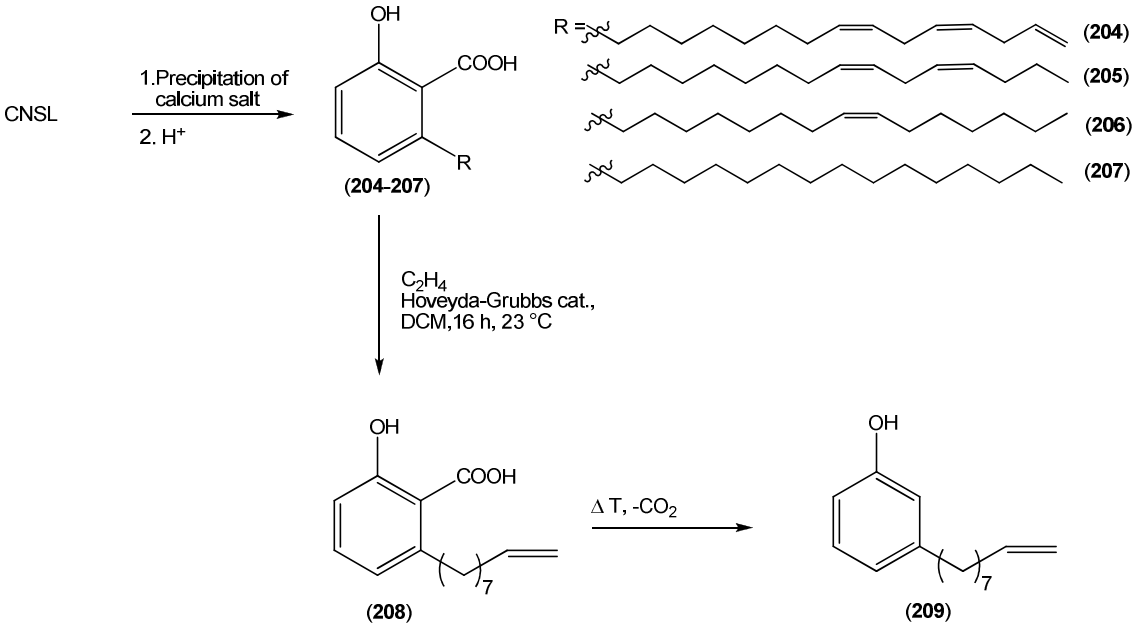

Figure 3.47: Synthesis of 3-(non-8-enyl)phenol from CNSL.

When 3-(non-8-enyl)phenol (**209**) is subjected to isomerizing ethenolysis conditions, using $[Pd(\mu\text{-}Br)(^tBu_3P)]_2$ and a Hoveyda-Grubbs type catalyst (**214**), the chain length is shortened stepwise to give a mixture of (**210**) and (**211**) in a 1:1.3 ratio. Hydrogenation of this mixture finally produces (**212**) and (**213**) (Figure 3.48).

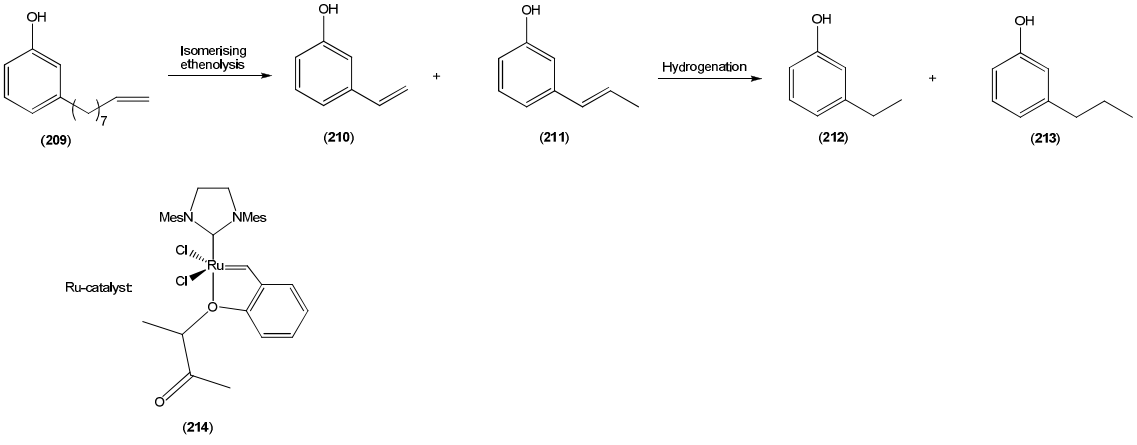

Figure 3.48: Utilization of metathesis and hydrogenation reactions for the preparation of tsetse fly attractant precursors.

Selective synthesis of either product can also be obtained by introducing an additional butenolysis step. After the isomerising ethenolysis, the reaction mixture gets purged with 2-butene and stirred. This produces (**211**) in a 92% yield. Hydrogenation of (**211**) then produces the (**213**) only. Similarly, (**212**) can be produced by replacing 2-butene with ethene and then performing hydrogenation (Figure 3.49).

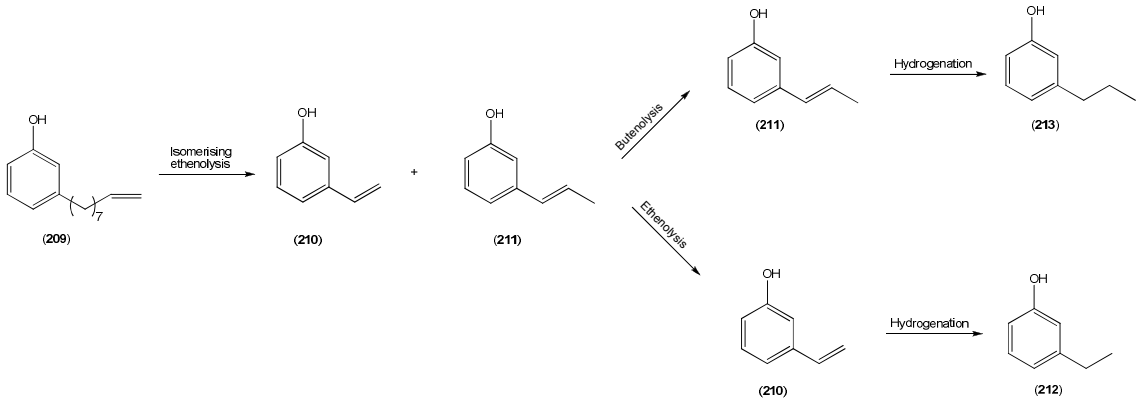

Figure 3.49: Synthetic route for the preparation of 3-propylphenol and 3-ethylphenol.

3.6.2 Synthesis of bicyclic hybrid sugar glycosidase inhibitors[66]

Glycosidase inhibitors are known for their therapeutic potential as drugs for a variety of diseases, including diabetes, cancer, viral infections and metabolic disorders. In an effort to synthesize more active inhibitors, various studies are being conducted to synthesize new kinds of hybrid glycosidase inhibitors from powerful inhibitory active molecules. These hybrid molecules' inhibitory activities are then tested and compared to other naturally found and synthetically prepared inhibitors. Ansari *et al*. are one of the groups investigating the potential in inhibitor designs, focusing on oxa-aza, oxa-oxa and oxa-carbasugar hybrid molecules. Starting with C-2 acetoxy glucal (**215**), key steps of their synthetic route include Ferrier rearrangement,[67,68] Grignard addition and ring-closing metathesis (Figures 3.50 and 3.51).

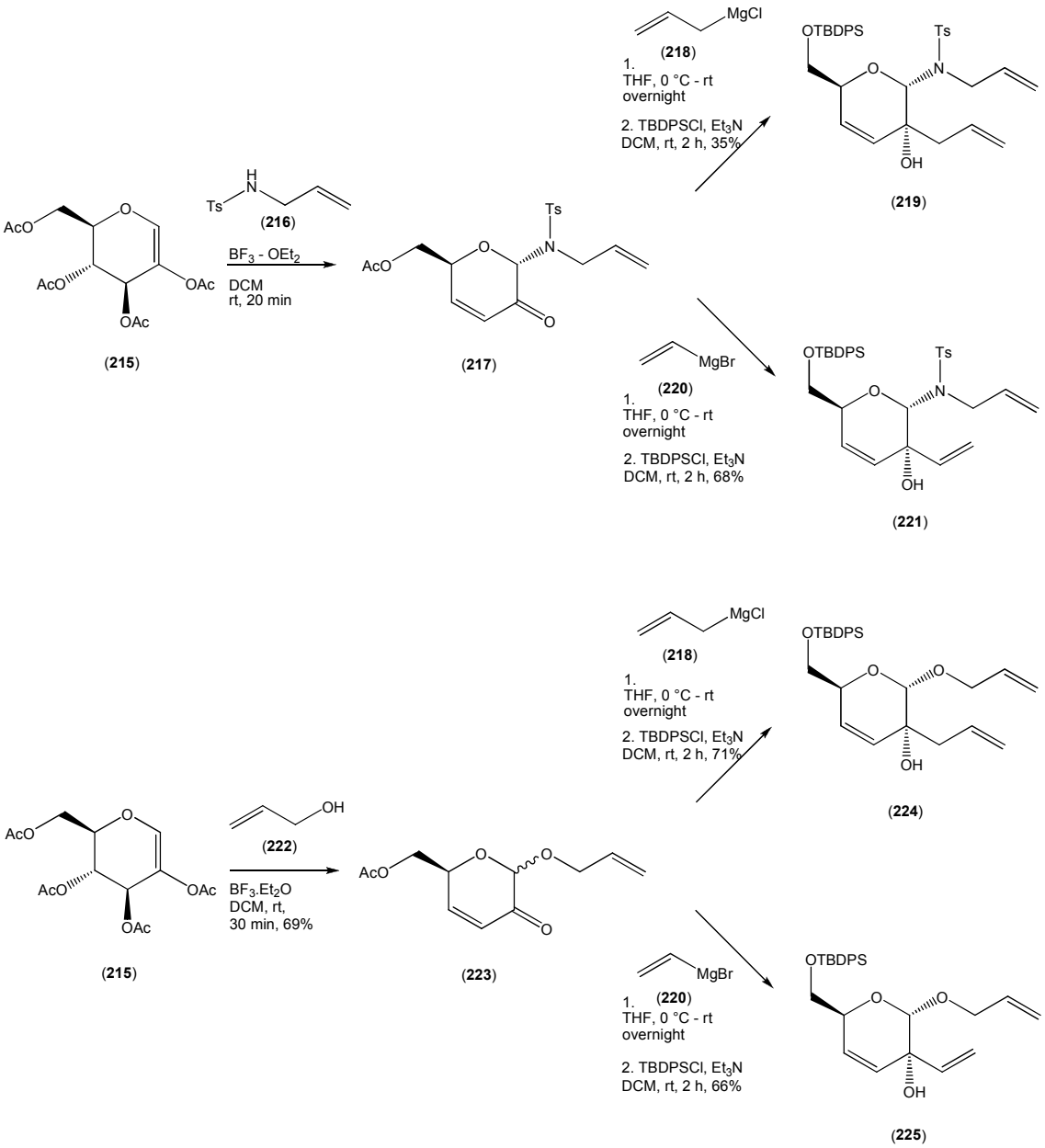

Figure 3.50: Preparation of metathesis precursors for glycosidase.

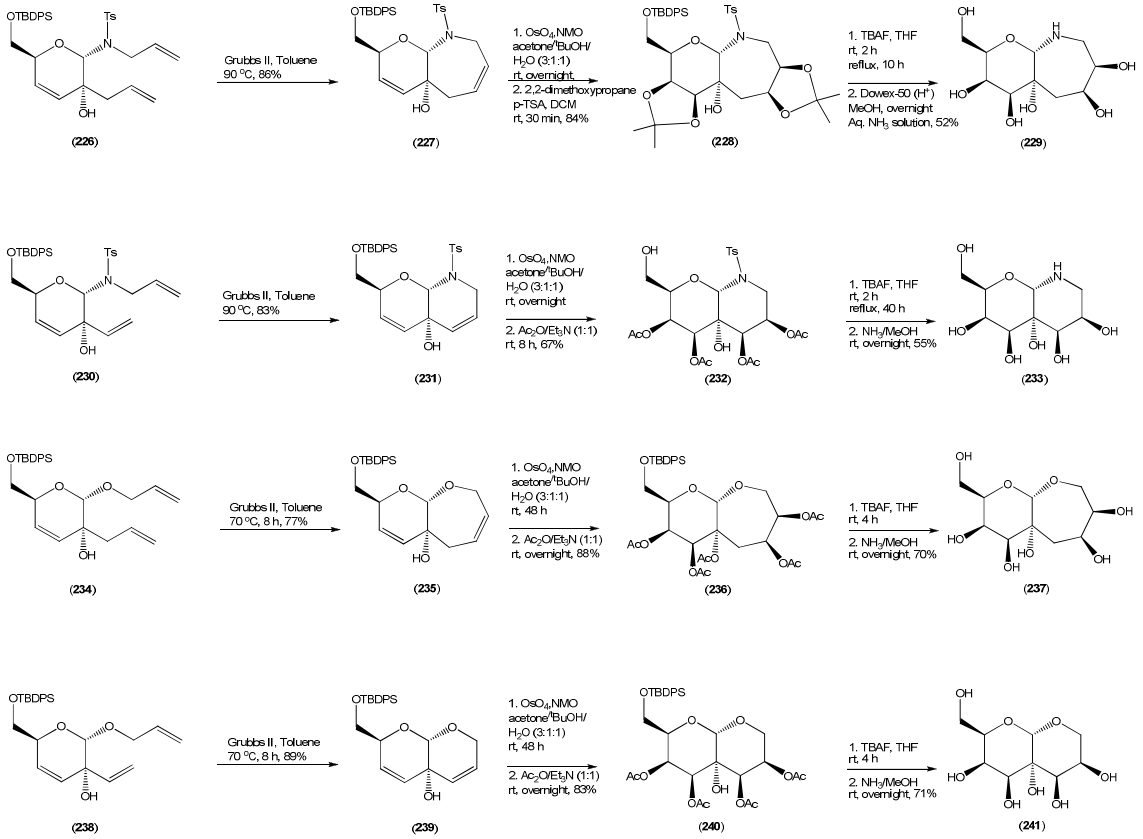

Figure 3.51: Preparation of glycosidase inhibitors.

3.7.3 Synthesis of vicinal diketose precursors, diulose[69]

Diketoses are common intermediates in Maillard reactions, complex sugar and amino acid pathways, determining the colour and flavour of food. Diketoses are versatile synthons in carbohydrate chemistry and can possibly be exploited to combat type II diabetes. Menzel and Ziegler prepared two of these diketose precursors, D (**244**) and L (**247**), by first employing oxidative cleavage of the thioacetal by I_2- acetone,[70] to afford the corresponding open-chain arabinose derivative, and then making use of Wittig olefination (Figure 3.52).

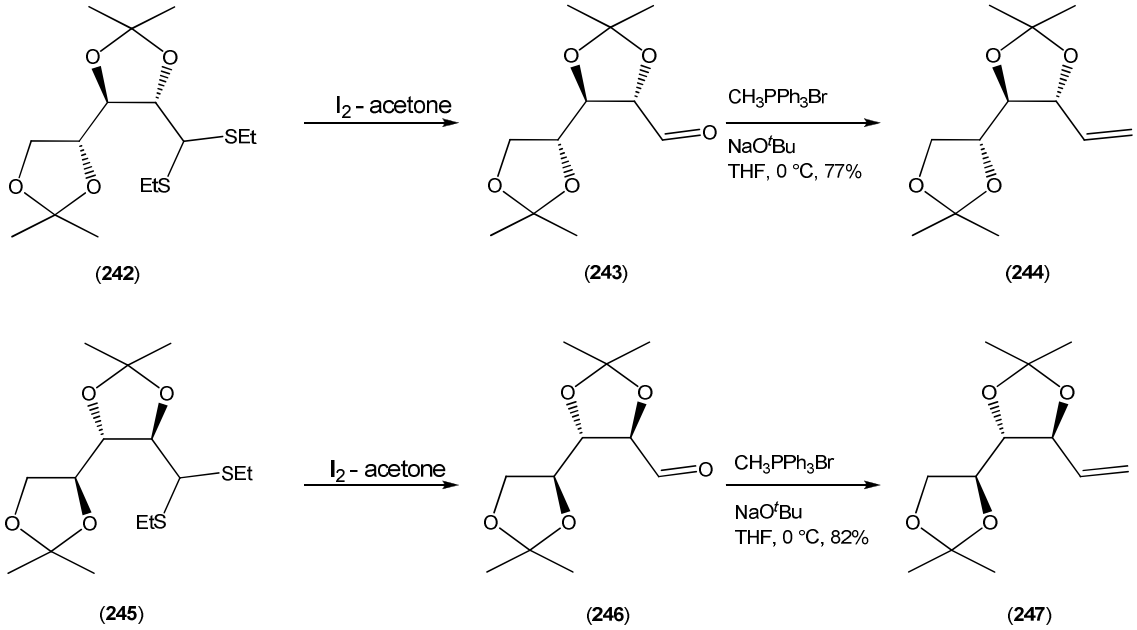

Figure 3.52: Preparation of metathesis precursors for diketose synthesis.

Self-metathesis of (**244**) using Hoveyda-Grubbs 2nd generation catalyst (**128**) yielded 91% of the desired enitol (**248**) whereas cross-metathesis of (**244**) with (**247**) yielded a 3:1 mixture of the desired DL enantiomer (**249**), in a 59% yield, and a racemic mixture of DD and LL enantiomers (Figure 3.53).

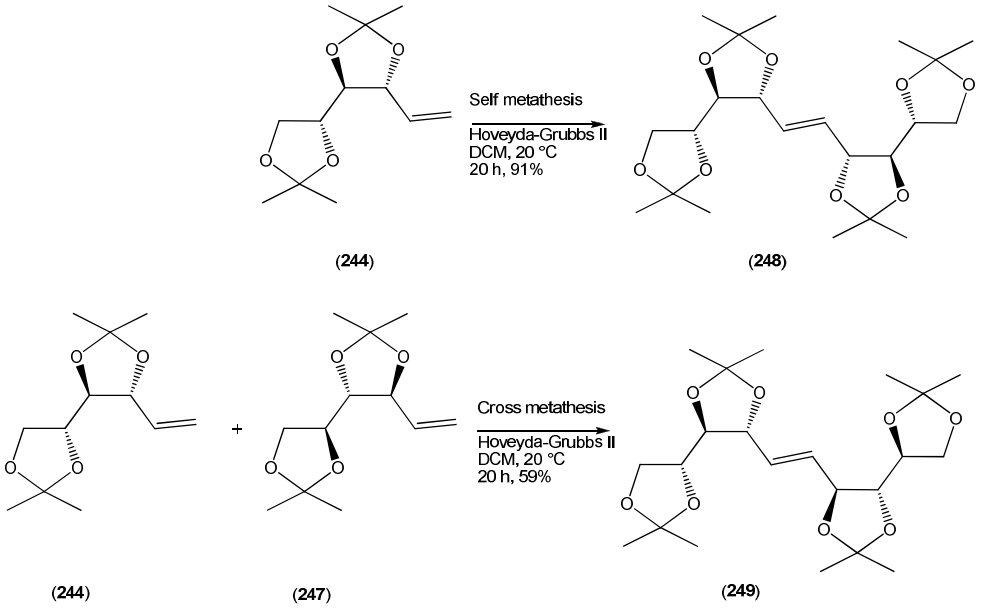

Figure 3.53: Metathesis reactions for the formation of diketose precursor.

Selective dihydroxylation of these metathesis products using OsO_4 and *N*-methylmorpholine *N*-oxide (NMO), followed by modified Swern oxidation and finally deprotection using TFA, led to the formation of the desired diuloses (**252** and **256**) (Figure 3.54).

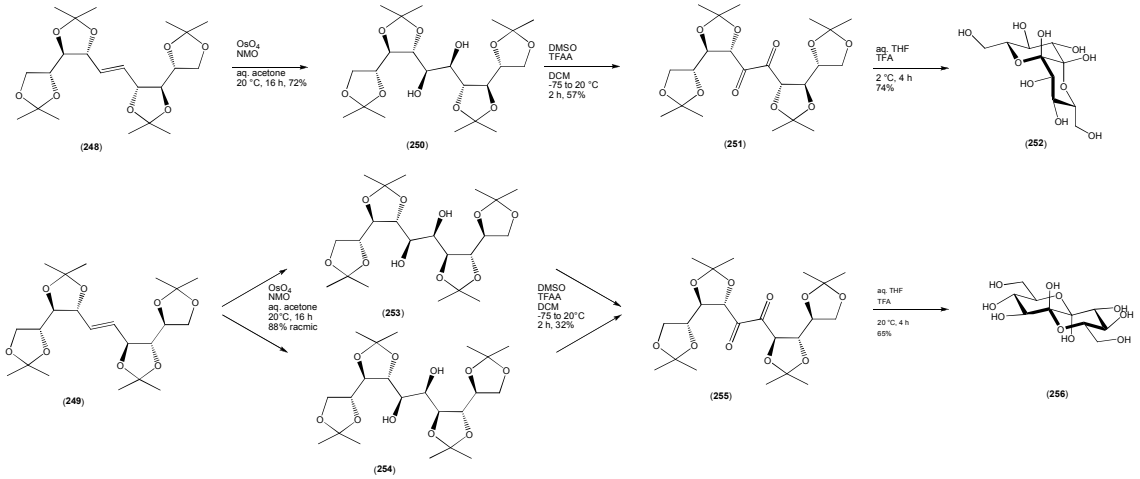

Figure 3.54: Continuation of synthetic route for diketoses formation.

References

[1]Astruc, D. *New J. Chem*. **2005**, *29* , 42 – 56.

[2] Eleutrio, H.S. US Patent 3074918, 1963.

[3] Banks, R. L.; Bailey, G. C. *Ind. Eng. Chem. Prod. Ras. Dev.* **1964**, *3*, 170 – 173.

[4] Chauvin, Y. *Chem. Int. Ed.* **2006**, *45*, 3740 – 3765.

[5] Singh, O. M. *J. Sci. Ind. Res*. **2006**, *65*, 957 – 965.

[6] Trnka, T. M.; Grubbs, R. H. *Acc. Chem. Res*. **2001**, *34*, 18 – 29.

[7] Grubbs, R. H., *Handbook of Metathesis*, Wiley-VCH, **2003**; Vol. 2, pp 5, 128, 151, 176, 205, 238, 246.

[8] Ivan, K. J.; Mol, J. C., *Olefin Metathesis and Metathesis Polymerization*, Academic Press, **1997**; pp 1 – 2.

[9] Fischer, E. O.; Maasböl, A., *Angew. Chem*. **1964**, *76*, 645.

[10] Schrock, R. R.; Hoveyda, A. H. *Angew. Chem. Int. Ed*. **2003**, *42*, 4592 – 4633

[11] de Frémont, P.; Marion, N.; Nolan, S. P. *Coord. Chem. Rev*. **2009**, *253*, 862 – 892.

[12] Grubbs, R.H. and Trinka, T.M. *Acc. Chem. Res*. **2001**, *34*, 18 – 29.

[13] Fischer, E. O.; Kreis, G.; Kreoter, C. G.; Müller, J.; Huttner, G.; Lorenz, H. *Angew. Chem. Int. Ed*. **1973**, *12*, 564 – 565.

[14] Schrock, R. R., *J. Am. Chem. Soc.* **1974**, 6796 – 6797.

[15] Schrock, R. R.; Wengrovius, J. H.; Churchhill, M. R.; Missert, J. R.; Youngs, W. J. *J. Am. Chem. Soc.* **1980**, *102*, 4515 – 4516.

[16] Shrock, R.R. *Angew. Chem. Int. Ed*. **2006**. *45*, 3748 – 3759

[17] Rocklage, S. M.; Fellmann, J. D.; Rupprecht, G. A.; Messerle, L. W.; Schrock, R. R. *J. Am. Chem. Soc*. **1981**, *103*, 1440 – 1447.

[18] Miller, B. J. M.Sc. thesis, University of the Free State, Bloemfontein, SA, 2010.

[19] Schrock, R. R.; Murdzek, J. S.; Bazan, G. C.; Robbins, J.; DiMare, M.; O'Regan, M. *J. Am. Chem. Soc*. **1990**, *112*, 3875 – 3886.

[20] Nguyen, S. T.; Johnson, L. K.; Grubbs, R.H. *J. Am. Chem. Soc.* **1992**, *114*, 3974 – 3975.

[21] Wu, Z.; Nguyen, S. T.; Grubbs, R. H.; Ziller, J. W. *J. Am. Chem. Soc.* **1995**, *117*, 5503 – 5511.

[22] Novak, B. M.; Grubbs, R. H. *J. Am. Chem. Soc.* **1988**, *110*, 7452 – 7453.

[23] Grubbs, R. H. *Angew. Chem. Int. Ed.* **2006**, *45*, 3760 – 3765

[24] Wilhelm, T. E.; Belderrain, T. R.; Brown, S. N.; Grubbs, R. H. *Organometallics* **1997**, *16*, 3867 – 3869.

[25] Schwab, P.; Grubbs, R. H.; Ziller, J. W. *J. Am. Chem. Soc.* **1996**, *118*, 100 – 110.

[26] Grubbs, R. H.; Trnka, T. M. *Acc. Chem. Res*. **2001**, *34*, 18 – 29.

[27] Wolf, J.; Stüer, W.; Grünwald, C.; Werner, H.; Schab, P.; Schulz, M. *Angew. Chem. Int. Ed.* **1998**, 37, 1124 – 1126.

[28] Blecher, S; Schuster, M. *Angew. Chem. Int. Ed. Engl*. **1997**, 36, 2036 – 2056.

[29] Cossy, J. *Synthesis of saturated oxygenated heterocycles II*, Springer, **2014**, pp. 323-324.

[30] Huang, J.; Stevens, E. D.; Nolan, S. P.; Petersen, J. L. *J. Am. Chem. Soc.* **1999**, *121*, 2674 – 2678.

[31] Scholl, M.; Trnka, T. M.; Morgan, J. P.; Grubbs, R. H. *Tetrahedron Lett.* **1999**, *40*, 2247 – 2250.

[32] Huang, J.; Schanz, H.-J.; Stevens, E. D.; Nolan, S.P. *Organometallics* **1999**, 2370 – 2375.

[33] Lummiss, J. A. M.; Highman, C. S.; Fyson, D. L.; McDonald, R.; Fogg, D. E. *Chem. Sci*. **2015**, *6*, 6739 – 6746.

[34] Ledoux, N.; Allaert, B.; Pattyn, S.; Vander Mierde, H.; Vercaement, C.; Verpoort, F. *Chem. Eur. J.* **2006**, *12*, 4654 – 4661.

[35] Wakamatsu, H.; Blechert, S. *Angew. Chem. Int. Ed.* **2002**, *41*, 794 – 796.

[36] Wakamatsu, H.; Blechert, S. *Angew. Chem. Int. Ed.* **2002**, *41*, 2403 – 2405.

[37] La, D. S.; Alexander, J. B.; Cefalo, D. R.; Graf, D. D., Hoveyda, A. H.; Schrock, R. R. *J. Am. Chem. Soc*. **1998**, *120*, 9720 – 9721.

[38] Alexander, J. B; La, D. S.; Cefalo, D. R.; Hoveyda, A. H. Schrock, R. R. *J. Am. Chem. Soc*. **1998**, *120*, 4041 – 4042.

[39] Kingsbury, J. S.; Harrity, J. P. A., Bonitatebus, P. J.; Hoveyda, A. H. *J. Am. Chem. Soc.* **1999**, *121*, 791 – 799.

[40] Garber, S. B.; Kingsbury, J. S.; Gray, B. L.; Hoveyda, A. H. *J. Am. Chem. Soc.* **2000**, *122*, 8168 – 8179.

[41] Michrowska, A.; Bujok, R.; Harutyunyan, S.; Sashuk, V.; Dolgonos, G.; Grela, K. *J. Am. Chem. Soc*. **2004**, *126*, 9318 – 9325.

[42] Dias, E. L.; Grubbs, R. H. *Organometallics* **1998**, *17*, 2758 – 2767.

[43] Bieneik, M.; Bujok, R.; Cabaj, M.; Lugan, N.; Lavigne, G.; Arlt, D.; Grela, K. *J. Am. Chem. Soc*. **2006**, *128*, 13652 – 13653.

[44] Flook, M. M.; Jiang, A. J.; Schrock, R. R.; Muller, P.; Hoveyda, A. M. *J. Am. Chem. Soc*. **2009**, *131*, 7962 – 7963.

[45] Jiang, A. J.; Zhao, Y.; Schrock, R. R.; Hoveyda, A. M. *J. Am. Chem. Soc*. **2009**, *131*, 16630 – 16631.

[46] Marinescu, S. C.; Schrock, R. R.; Muller, P.; Takase, M. K.; Hoveyda, A. H. *Organometallics*, **2011**, *30*, 1780 – 1782.

[47] Ibrahem, I.; Schrock, R. R.; Hoveyda, A. H. J. Am. Chem. Soc. 2009, 131, 3844 – 3845.

[48] Keitz, B. K.; Endo, K; Patel, P. R.; Herbert, M. B.; Grubbs, R. H. *J. Am. Chem. Soc***. 2012**, *134*, 693 – 699.

[49] Grubbs, R. H., *Handbook of Metathesis*, Wiley-VCH, **2003**; Vol. 1, pp 47 – 57.

[50] Garrison, J. C.; Youngs, W. J. *Chem. Rev.* **2005**, *105*, 3978 – 4008.

[51] Grubbs, R. H.; Brunck, T. K. *J. Am. Chem. Soc.* **1972**, *94*, 2538 – 2540.

[52] Lewandos, G. S.; Pettit, R. *J. Am. Chem. Soc.* **1971**, *93*, 7087 – 7088.

[53] Calderon, N.; Ofstead, E. A.; Ward. J. P.; Judy. W. A.; Scott. K.W. *J. Am. Chem. Soc.* **1968**, *90*, 4133 – 4140.

[54] Elevance: Metathesis. http://www.elevance.com/technology/metathesis (accessed: Mar 15, 2014)

[55] Casey, C. P. *J. Chem. Educ*. **2006**, *83*, 192 – 195.

[56] Katz, T. J.; McGinnis, J. *J. Am. Chem. Soc.* **1975**, *97*, 1592 – 1594.

[57] Kress, J.; Wesolek, M.; Osborn, J. A. *J. Chem. Soc. Chem. Commun.* **1982**, 514 – 516.

[58] Kress, J., Osborn, J. A., Greene, R. M. E., Ivin, K. J.; Rooney, J. J. *J. Chem. Soc. Chem. Commun.* **1985**, 874 – 876.

[59] Kress, J.; Osborn, J. A.; Greene, R. M. E.; Ivin, K. J.; Rooney, J. J. *J. Am. Chem. Soc.* **1987**, *109*, 899 – 901.

[60] Kress, J.; Osborn, J. A.; Amir-Ebrahimi, V.; Ivin, K. J.; Rooney, J. J. *J. Chem. Soc. Chem. Commun.* **1988**, 1164 – 1166.

[61] Van Leeuwen, P. W. N. M. in *Homogeneous Catalysis,* Kluwer Academic Publishers: London, **2004**; Vol. 1, p. 342.

[62] Van Leeuwen, P. W. N. M. in *Homogeneous Catalysis,* Kluwer Academic Publishers: London, **2004**; Vol. 1, pp. 350 – 352.

[63] Janse van Rensburg, W.; Steynberg, P. J.; Meyer, W. H.; Kirk, M. M.; Forman, G. S. *J. Am. Chem. Sos.* **2004**, *126*, 14332 – 14333.

[64] Grubbs, R. H. *Handbook of Metathesis*, Wiley-VCH, **2003**; Vol. 2, pp 246 – 247.

[65] Baader, A.; Podsiadly, P. E.; Cole-Hamilton, D. J.; Goossen, L. J., *Green Chem*. **2014**, *16*, 4885 – 4890.

[66] Ansari, A. A.; Rajasekaran, P.; Khan, M. M.; Vankar, Y. D. *J. Org. Chem*. **2014**, *79*, 1690 – 1699.

[67] Ichikawa, Y.; Hirata, K.; Ohbayashi, M.; Isobe, M. *Chem. Eur. J.* **2004**, *10*, 3241 – 3251.

[68] Ding, F.; William, R.; Liu, X.-W. *J. Org. Chem*. **2013**, *78*, 1293 – 1299.

[69] Menzel, M.; Ziegler, T. *Eur. J. Org. Chem*. **2014**, *34*, 7658 – 7663.

[70] Sun, J.; Dong, Y.; Cao, L.; Wang, X; Wang, W.; Hu, Y. *J. Org. Chem.*, **2004**, *69*, 8932 – 8934.

RESULTS & DISCUSSION

Chapter 4

Results and Discussion

4.1 Introduction

Due to their UV absorption properties (*cf*. Chapter 2.5), cinnamates and especially OMC [2-ethylhexyl (*E*)-3-(4-methoxyphenyl)acrylate] (**7**), are widely used in the cosmetic industry as blockers of UV-rays and therefore sun protecting agents. Manufacturing processes for the preparation of OMC, however, are hampered by multiple synthetic steps, high temperatures, tedious work-up procedures, halogenated by-products, low atom economy and patented procedures.[1,2,3]

Since the OMC molecule (**7**) contains a double bond, it was envisaged that it could be prepared through metathesis based methodology from *p*-methoxystyrene [1-methoxy-4-vinylbenzene] (**257**) and 2-ethylhexylacrylate (**2**) (Figure 4.1). While both starting materials are available commercially, it is known that styrenes are prone to polymerization,[4] which may lead to low yields and/or separation difficulties at the end of the synthesis. The propene equivalent of 4-methoxystyrene (**257**), *trans*-anethole [(*E*)-1-methoxy-4-(prop-1-enyl)benzene] (**11**), however, does not polymerize that easily and can be regarded as a substituted styrene that would just lose ethylene instead of a C-1 unit during the metathesis reaction. Since *trans*-anethole (**11**) also is considerably cheaper than 4-methoxystyrene (**257**) (±R 460 / kg *vs* ±R 157300 / kg[i]), it was decided to utilize this compound rather than the styrene equivalent as building block in the synthesis of OMC.

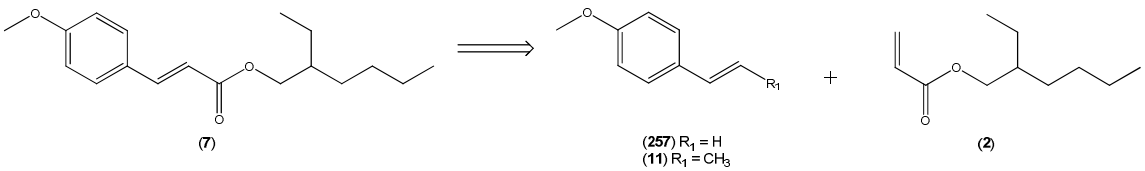

Figure 4.1 Proposed retrosynthesis of OMC (**7**).

[i] Prices calculated from the cheapest and largest sample size available from Sigma-Aldrich on Dec 08, 2015.

Although the preparation of OMC by a metathesis protocol seemed straightforward, it must be kept in mind that all cross-metathesis reactions are accompanied by some degree of homo-metathesis of the two reactants (*cf*. paragraph 3.2.2). These unwanted side reactions is usually limited by adding one of the starting materials to the reaction mixture in excess, thus minimizing the statistical change for a homo-metathesis reaction between two molecules of the other (more expensive) reactant. It must also be kept in mind that product formation might be compromised by secondary metathesis reactions in which the desired product may react further to unwanted side-products.

4.2 Attempts to optimize the metathesis reaction

Unsubstituted *trans*-β-methylstyrene [(*E*)-prop-1-enylbenzene] (**69**) and methyl acrylate (**59**) were used as model substrates for the optimization of the metathesis reaction, starting with the procedure reported by Miller,[5] i.e. refluxing *trans*-β-methylstyrene (**69**) and methyl acrylate (**59**), in a 1:2 ratio, in DCM (10 mL) with Grubbs second generation catalyst (*ca* 5 mol %) (Figure 4.2).

Soon after the DCM started refluxing, the formation of a precipitate was observed. Since only *trans*-β-methylstyrene (**69**) and a product could be observed by TLC, the reaction was allowed to continue until all the starting material was consumed before the product (precipitate) was isolated by filtration and characterised as *trans*-stilbene (**258**). Apart from the expected aromatic protons in the ^{1}H NMR spectrum (Plate 1a), the only other resonance observed was a singlet at δ7.14 ppm (integrating for two protons) that was ascribed to the double bond protons of stilbene. The NMR-data and melting point (123.6 °C) corresponded to those reported for the *trans*-isomer of stilbene.[6] The ^{13}C NMR spectrum showed the expected resonances, which were allocated by means of HSQC and HMBC, i.e. δ (ppm) 137.5 (C-1), 128.8 (C-3, C-5 and C<u>H</u>=C<u>H</u>), 127.8 (C-4), 126.7 (C-2, C-6). C-1 (δ 137.5 ppm) showed long distance coupling to H-3, H-5 (δ 7.39 ppm) and an olefinic proton (δ 7.14 ppm). MS [*m/z* (EI) 180 (M^+, 100)] served as further confirmation of this product being stilbene. The filtrate contained only dissolved stilbene and no cinnamate product. Thus, using these reaction conditions, only homo-metathesis occurred to form *trans*-stilbene

(**258**) in quantitative yield (>99%) (Table 4.1, entry 1). While *trans*-stilbene (**258**) can be formed through secondary metathesis of the cinnamate (**195**) as well as homo-metathesis of the styrene derivatives (**69**) and (**67**), and stilbene (**258**) can be regarded as the thermodynamic sink for the reaction,[5] the fact that no other product were observed pointed towards the stilbene (**258**) originating from β-methylstyrene (**69**) self-metathesis.

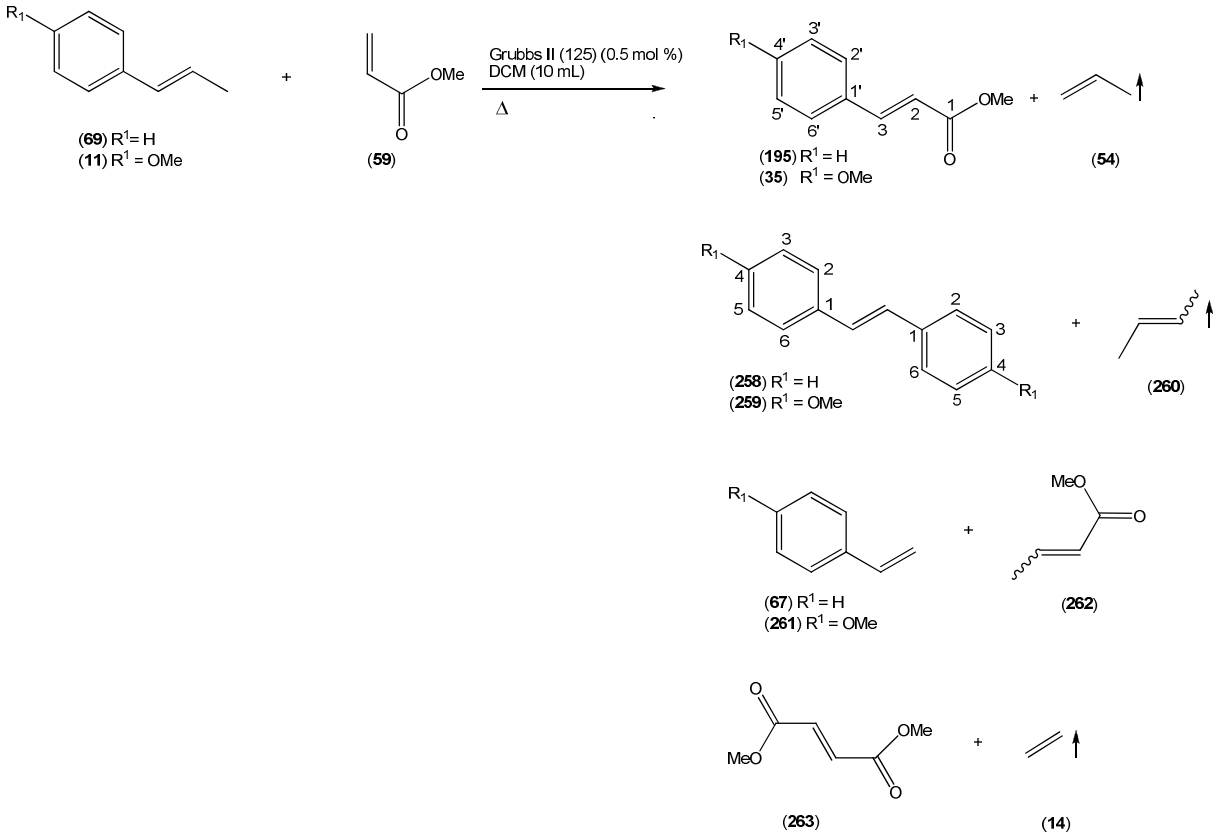

Figure 4.2: Metathesis of *trans*-β-methylstyrenes (**69**) and (**11**) with methyl acrylate (**59**).

In an effort to decrease self-metathesis in favour of the cross-metathesis reaction, the reaction was repeated and the temperature lowered to 25 °C and eventually 10 °C. *Trans*-stilbene (**258**), however, remained the only product in almost quantitative yield. Although stilbene (**258**) formation was detected right from the onset of the reaction, the reaction was repeated and the mixture analysed (TLC) for cinnamate formation in 5 minute intervals, but no indication of the desired product could be found.

Since it is known that the polarity of the solvent could have an effect on the outcome of metathesis reactions,[7,8,9] it was decided to repeat the reaction in THF, toluene and under neat conditions at 40 °C. These changes, however, did not have any effect on the outcome of the reactions as once again only the self-metathesis product, *trans*-stilbene (**258**), was formed in quantitative yield.

As a last attempt to force the reaction towards the wanted cross-metathesis, it was decided to repeat the reaction in DCM, but to change the ratio of the reactants (**69** : **59)** from 1:5, to 1:1 and finally to 5:1, respectively. *trans*-Stilbene (**258**), however, was still formed in 97 to >99 % yield.

When the reaction was conducted under standard conditions with *trans*-anethole (**11**), the *trans*-β-methylstyrene (**69**) analogue with an electron-donating *p*-methoxy group (Figure 4.2), the only product formed was once again the homo-metathesis product, in this case *trans*-4,4'-dimethoxystilbene (**259**) (>99%) (Table 4.1, entry 2). ^{1}H NMR spectrum analysis (Plate 2a) showed the expected AA'BB' aromatic resonances system [δ (ppm) 7.43 (4H, d, *J* = 8.8 Hz, H-2,6) and 6.89 (4H, d, *J* = 8.8 Hz, H-3,5)], a singlet at δ 6.93 ppm corresponding to the double bond resonance, and a singlet at δ 3.83 ppm, integrating for 6 protons, which was allocated to be the two *p*-methoxy groups. The NMR-data were similar to those previously reported.[6] Ambigious resonances were allocated by means of HSQC and HMBC. C-4 (δ 159.2 ppm) showed long-distance coupling in the HMBC experiment with the methoxy hydrogens (δ 3.83 ppm) as well as H-2 and H-6 (δ 7.43 ppm), whereas C-1 (δ 130.6 ppm) showed an interaction with H-3 and H-5 (δ 6.89 ppm) as well as an olefinic hydrogen (δ 126.3 ppm). MS gave the expected mass for the molecular ion of 4,4'-dimethoxystilbene [*m/z* (EI) 240 (M^+, 100)].

4.3 Cresol as additive to Grubbs II catalyst

Since Forman and co-workers [10, 11] found a significant enhancement in cross-metathesis when cresol was added to a methyl acrylate (**59**) - 1-decene (**264**) reaction with Grubbs II catalyst (**125**) (Figure 4.3), the effect of the addition of *p*-

cresol (**266**) as co-catalyst when applied to the substrates in the current study, was investigated.

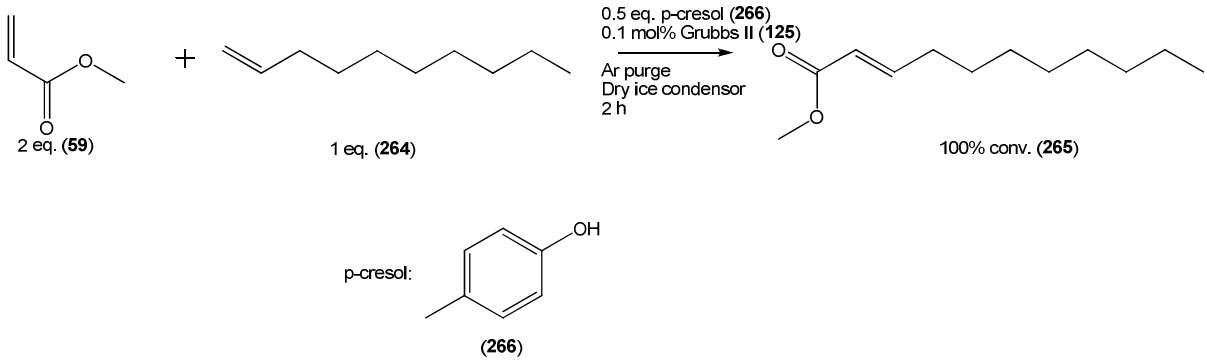

Figure 4.3: Metathesis reaction of methyl acrylate (**59**) and 1-decene (**264**) as proposed by Forman *et al*.[10, 11]

4.3.1 Metathesis reaction of trans-β-methylstyrene (69) and methyl acrylate (59)

In order to remove the volatile metathesis products that can potentially be formed, i.e. propene, but-1-ene and ethene (Figure 4.2), from the reaction mixture, it was also decided to purge the reaction mixture with dry Argon. Since the low boiling methyl acrylate (**59**) could also be stripped from the mixture in this way, a -20 ˚C condenser was added to the reaction set-up and the reaction between *trans*-β-methylstyrene (**69**) and methyl acrylate (**59**) repeated in refluxing DCM with Grubbs II catalyst (0.5 mol %) and *p*-cresol (0.25 eq.) (Table 4.1).

Finally the cross-metathesis product, methyl cinnamate (**195**), was obtained in 38 % yield (Table 4.1, entry 3). The structure of the product was confirmed by ^{1}H NMR (Plate 3a), with five aromatic proton signals being observed [δ 7.52 – 7.50 (2H, m, H-2', H-6'), 7.37 – 7.36 (3H, m, H-3', H-4', H-5')], two double bond doublets found at δ 7.70 and 6.44 ppm respectively, and a singlet, integrating for 3 protons, being displayed in the methoxy region. The coupling constant of the olefinic carbons (J = 16.0 Hz) confirmed the (*E*)-geometry of the product. IR (ν_{max} 1712 cm^{-1}) and ^{13}C NMR confirmed the presence of a carbonyl group, with this carbon (δ 167.4 ppm) showing long distance coupling with the β-hydrogen [δ 7.70 (1H, d, J = 16.0 Hz)] as well as the methoxy hydrogens (δ 3.79 ppm) in an HMBC experiment. MS confirmed

the presence of the molecular ion of the desired cinnamate (**195**) [*m/z* (EI) 162 (M^+, 53)]. *Trans*-stilbene (**258**) was also formed in 18% yield.

Table 4.1 Metathesis of β-methylstyrenes and α,β-unsaturated carbonyl compounds catalysed by Grubbs II catalyst (0.5 mol%)[a]

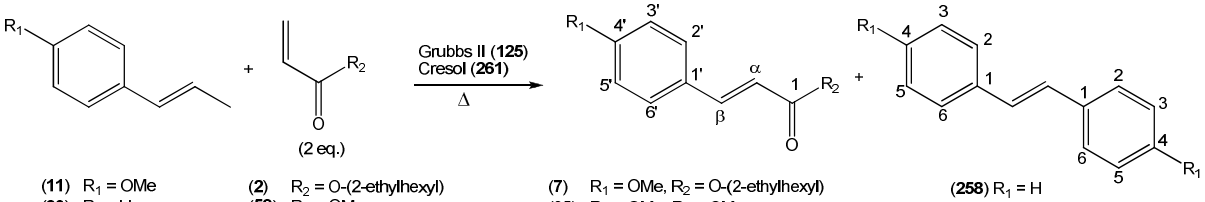

(**11**) R_1 = OMe
(**69**) R_1 = H
(**271**) R_1 = OTf

(**2**) R_2 = O-(2-ethylhexyl)
(**59**) R_2 = OMe
(**273**) R_2 = H
(**274**) R_2 = Me
(**275**) R_2 = O_nBu

(**7**) R_1 = OMe, R_2 = O-(2-ethylhexyl)
(**35**) R_1 = OMe, R_2 = OMe
(**195**) R_1 = H, R_2 = OMe
(**273**) R_1 = OTf, R_2 = OMe
(**276**) R_1 = H, R_2 = H
(**277**) R_1 = H, R_2 = Me
(**278**) R_1 = H, R_2 = O_nBu
(**279**) R_1 = OMe, R_2 = H
(**280**) R_1 = OMe, R_2 = Me
(**281**) R_1 = OMe, R_2 = O_nBu
(**282**) R_1 = H, R_2 = O-(2-ethylhexyl)

(**258**) R_1 = H
(**259**) R_1 = OMe
(**272**) R_1 = OTf

Entry	Reactants		Substituents		Products			
			R 1	R 2	CM	Yield (%)	SM	Yield (%)
1[b]	(**69**)	(**59**)	H	OMe	-	-	(**258**)	>99
2[b]	(**11**)	(**59**)	OMe	OMe	-	-	(**259**)	>99
3	(**69**)	(**59**)	H	OMe	(**195**)	38	(**258**)	18
4	(**11**)	(**59**)	OMe	OMe	(**35**)	36	(**259**)	50
5	(**271**)	(**59**)	OTf	OMe	(**273**)	43	(**272**)	4
6	(**69**)	(**275**)	H	OBu	(**278**)	55	(**258**)	18
7	(**11**)	(**275**)	OMe	OBu	(**281**)	41	(**259**)	36
8	(**69**)	(**274**)	H	Me	(**277**)	34	(**258**)	38
9	(**11**)	(**274**)	OMe	Me	(**280**)	32	(**259**)	27
10	(**69**)	(**273**)	H	H	(**276**)	trace	(**258**)	58
11	(**11**)	(**273**)	OMe	H	(**279**)	trace	(**259**)	52
12	(**69**)	(**2**)	H	O-(2-ethylhexyl)	(**282**)	64	(**258**)	6
13	(**11**)	(**2**)	OMe	O-(2-ethylhexyl)	(**7**)	47	(**259**)	32

[a]Reaction conditions: **A** (1.5 mmol) and **B** (2 eq.) were refluxed in dry dichloromethane (10 mL) in the presence of Grubbs II catalyst (5 mol%) and *p*-cresol (0.25 eq.) while purged with Ar. A dry ice condenser (-20 °C) was used.

[b]No *p*-cresol was added.

4.3.2 Effect of the electronic properties of the β-methylstyrene on the cross-metathesis reaction

In order to establish the effect, if any, of an electron-donating vs an electron-withdrawing β-methylstyrene substituent on the metathesis reaction, it was decided to repeat the reaction with *trans*-anethole (**11**) and 4-(prop-1-enyl)phenyl trifluoromethanesulfonate (**271**), respectively.

The triflate substituted β-methylstyrene (**271**), is not commercially available and had to be synthesized (Figure 4.4). This was achieved by reacting 4-hydroxypropiophenone (**267**) with trifluoromethanesulfonic anhydride (**269**) and DMAP in dry DCM to form 4-propionylphenyl trifluoromethanesulfonate[12] (**268**). The ^{1}H NMR spectrum (Plate 11a) confirmed the presence of all the expected protons: the aromatic protons resonating as an AA'BB' system at δ 8.02 and δ 7.33 ppm along with a methylene quartet at δ 2.97 ppm and a methyl triplet at δ 1.18 ppm. It was also apparent that the triflate group was present according to the ^{19}F NMR spectrum (δ -75.83 ppm) and the characteristic quartet carbon resonance at δ 118.7 ppm in the ^{13}C NMR spectrum (Plate 11b). HRMS furthermore confirmed the presence of the expected molecular ion (AP+) (*m/z*) calcd for $C_{10}H_{10}O_4F_3S$ $[M]^+$ 283.0252, found 283.0256).

Reduction of the formed ketone (**268**) to the corresponding alcohol (**270**) was then achieved by reaction with $NaBH_4$ in THF : ethanol (1:1, v/v). The ^{13}C NMR spectrum (Plate 12b) confirmed the presence of the triflate group as a quartet at δ 118.9 ppm ($-CF_3$) together with the ^{19}F NMR spectrum (δ -75.95 ppm) (Plate 12f). All the expected proton signals were observed by ^{1}H NMR (Plate 12a), including a broad triplet at δ 4.63 ppm (*J* = 6.5Hz, 1H) corresponding to the α-hydrogen of the alcohol (H-1'). The $-CH_2$ and $-CH_3$ moieties were also clearly visible as a multiplet and a triplet at δ 1.81 – 1.69 and 0.91 ppm, respectively, whereas the –OH group resonates as a doublet at δ 1.17 ppm (*J* = 6.2 Hz). HMBC correlation of H-1 (δ 4.63 ppm, 1H, t, *J* = 6.5 Hz) with C-2' and C-6' (δ 127.9 ppm), allowed allocation of the corresponding H-2' and H-6' resonances (δ 7.41, 2H, d, *J* = 8.7 Hz) by HSQC,

whereas long distance HMBC correlation of C-1' (δ 145.3 ppm) with H-3' and H-5' (δ 7.24, 2H, d, *J* = 8.7 Hz) as well as H-2 (δ 1.81 – 1.69, 2H, m) confirmed the distinction between the resonances of H-2' and H-6' (δ 7.41 ppm) and H-3' and H-5' (δ 7.24 ppm). The expected molecular ion was detected by HRMS [(ES-) (*m/z*) calcd for $C_{10}H_{12}O_4F_3S$ $[M]^+$ 283.0252, found 283.0255].

4-(1-Hydroxypropyl)phenyl trifluoromethanesulfonate (**270**) was subsequently subjected to treatment with anhydrous $CuSO_4$ in refluxing hexane to eliminate water and form the desired (*E*)-4-(prop-1-en-1-yl)phenyl trifluoromethanesulfonate (**271**) in 60% yield and 42% overall yield (Figure 4.4). The ^{1}H NMR spectrum (Plate 13a) supported the structure allocated with resonances of the AA'BB' aromatic system as two doublets, δ 7.37 and 7.18 ppm (*J* = 8.80 Hz), double bond resonances at δ 6.39 (1H, br d, *J* = 15.8 Hz, H-1) and δ 6.29 – 6.23 (1H, m, H-2), as well as δ 1.90 (3H, m) corresponding to the terminal methyl group. HMBC and HSQC once again facilitated the distinction between the resonances of the AA'BB' system as C-1' (δ 138.5 ppm) showed an HMBC correlation with H-3' and H-5' (δ7.18 ppm, 2H, d, *J* = 8.6 Hz). The ^{13}C NMR (Plate 13b) and ^{19}F NMR (δ -75.85 ppm) spectrums confirmed the presence of CF_3 and thus the triflate group, whereas the expected molecular ion was observed by GC-MS *m/z* (EI) 266 (M^+, 19). The (*E*)-geometry of the double bond was confirmed by the coupling constant of H-1 (*J* = 15.8 Hz).

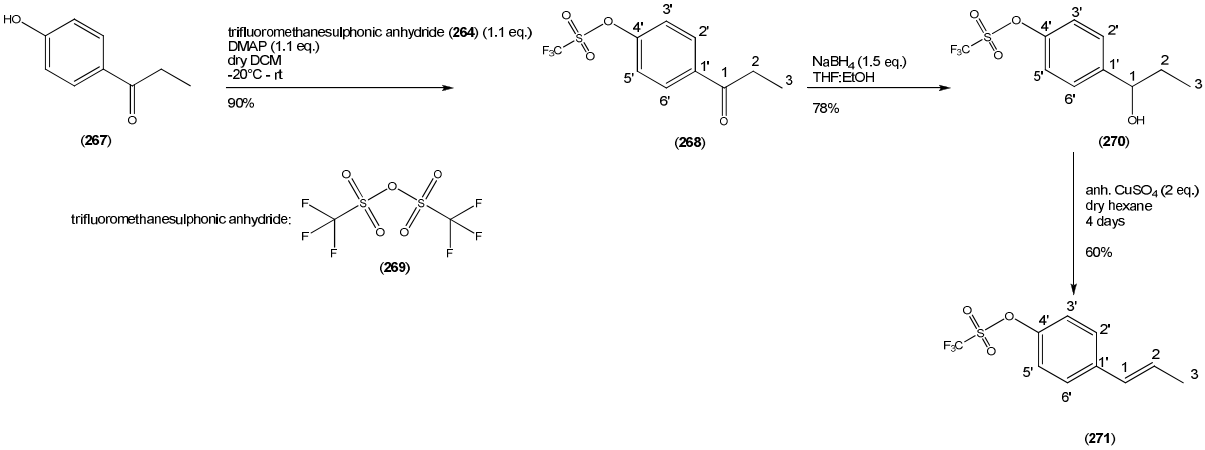

Figure 4.4: Preparation of 4-(prop-1-enyl)phenyl trifluoromethanesulfonate (**271**).

With β-methylstyrenes with electron-withdrawing (*E*)-4-(prop-1-enyl)phenyl trifluoromethanesulfonate (**271**) as well as electron-donating substituents [*trans*-anethole (**11**)] now available, the effect of the electronic properties of β-methylstyrenes on the metathesis reaction with Grubbs II catalyst in the presence of *p*-cresol could be investigated (Table 4.1).

Firstly, *trans*-anethole (**11**) was allowed to react with methyl acrylate (**59**), under the same conditions as the unsubstituted analogue. Two products were observed for this reaction, namely *trans*-4,4'-dimethoxystilbene (**259**) (*vide supra*, par. 4.2) and methyl (*E*)-*p*-methoxycinnamate (**35**) in 50% and 36% yields, respectively (Table 4.1, entry 4). The ^{1}H NMR spectrum of methyl (*E*)-*p*-methoxycinnamate (**35**) (Plate 7a) gave the expected doublets of the AA'BB' system in the aromatic region [δ 7.45 (2H, d, *J* = 8.8 Hz, H-2',6'), 6.88 (2H, d, *J* = 8.8 Hz, H-3',5')], two olefinic doublets at δ 7.63 and 6.29 ppm and two methoxy signals at δ 3.80 and 3.77 ppm. The coupling constant of 16.0 Hz for the olefinic protons confirmed (**35**) to be the (*E*)-isomer. Both IR (ν_{max} 1712 cm^{-1}) and ^{13}C NMR (δ 167.8 ppm) confirmed the presence of a carbonyl group. HMBC confirmed long distance coupling of the carbonyl carbon (δ 167.8 ppm) with the ester methoxy hydrogens (δ 3.77 ppm) and olefinic β-hydrogen (δ 7.63 ppm), whereas C-4' showed long-distance interaction with the aromatic methoxy group (δ 3.80 ppm) as well as H-2' and H-6' (δ 7.45 ppm). The physical data obtained, corresponded with those published by Tan *et al*.[13] and mass spectroscopy confirmed the structure with the presence of the expected molecular ion [*m/z* (EI) 192 (M^{+}, 61)].

For the triflate reaction, (*E*)-4-(prop-1-enyl)phenyl trifluoromethanesulfonate (**271**) and methyl acrylate (**59**) was added to a solution of *p*-cresol (**266**) and Grubbs II catalyst (**125**) in dry DCM under an Ar atmosphere according to the procedure used in par. 4.3.1. This reaction also yielded both the self-metathesis stilbene product and the cross-metathesis cinnamate product in 4% and 43% yields, respectively, but with increased selectivity towards cross-metathesis (Table 4.1, entry 5). The ^{1}H NMR spectrum (Plate 14a) of (*E*)-4,4'-bis(trifluoromethanesulfonyloxy)stilbene (**272**) showed the aromatic proton resonances as two doublets (δ 7.58 and 7.29 ppm; *J* =

8.8 Hz) and a double bond singlet at δ 7.09 ppm. C-4 (δ 149.1 ppm) showed long distance correlation with H-2 and H-6 (δ 7.58, 4H, d, *J* = 8.8 Hz) in an HMBC experiment, whereas C-1 (δ 137.2 ppm) correlated with H-3 and H-5 (δ 7.29, 4H, d, *J* = 8.8 Hz) as well as the double bond (δ 7.09 ppm, 2H, s). The $-CF_3$ resonance was observed at δ -75.91 ppm in the ^{13}C NMR and δ -75.91 ppm in the ^{19}F NMR spectra, respectively. *m/z* (EI) 477 (M^+, 6) confirmed the presence of the protonated molecular ion and supports the structure of this novel product.

In the ^{1}H NMR spectrum of methyl (*E*)-3-(4-(trifluoromethylsulfonyloxy)phenyl) acrylate (**273**) (Plate 15a), five signals can clearly be seen, namely two AA'BB' doublets in the aromatic region (δ 7.59 and 7.9 ppm, *J* = 8.7 Hz), two double bond doublets at δ 7.66 and 6.44 ppm with a coupling constant of 16 Hz, which indicates (*E*)-regiochemistry, and a methoxy singlet at δ 3.81 ppm. C-1' (δ 134.9 ppm) showed long distance coupling with H-3' and H-5' (δ 7.29, 2H, d, *J* = 8.7 Hz) as well as H-2 (δ 6.44, 1H, d, *J* = 16.0 Hz) in an HMBC experiment, whereas C-3 (δ 142.5 ppm) coupled with H-2' and H-6' (δ 7.59, 2H, d, *J* = 8.7 Hz). The quartet at δ 118.8 ppm in the ^{13}C NMR spectrum and the ^{19}F -signal at δ -75.87 ppm confirmed that the triflate group was still attached. IR [(neat, cm^{-1}) ν_{max} 1718 (CO)] and a carbon resonance at δ 166.9 ppm (C-1), showing long-distance coupling with the β-hydrogen [δ 7.66, 1H, d, *J* = 16.0 Hz, H-3] as well as the ester methoxy group (δ 3.81 ppm) in an HMBC experiment, confirmed the presence of a carbonyl group. The expected molecular ion was observed by GC-MS *m/z* (EI) 310 (M^+, 43) in support of the formation of methyl 3-(4-trifluoromethylsulfonyloxy)phenyl)acrylate (**273**).

The results obtained indicate that the electron-donating methoxy group in the *para* position of the β-methylstyrene aryl ring (**11**) doesn't have a significant effect on cross-metathesis and causes only a slight decrease in the yield of the cross-metathesis product when compared to the unsubstituted β-methylstyrene (**69**) [36 vs 38 % yield of (**35**) and (**195**), respectively; Table 4.1, entries 4 and 3], while an electron-withdrawing group in the *para* position of the β-methylstyrene aryl ring (**271**) enhances the cross-metathesis reaction [43 *vs* 38% yield of (**273**) and (**195**), Table 4.1, entries 5 and 3] to form the corresponding methyl 3-arylacrylate [43 *vs* 38% yield of (**273**) and (**195**); Table 4.1, entries 5 and 3].

Homo-metathesis to the stilbene products follows the opposite trend. An electron-donating methoxy group in the *para* position enhances self-metathesis [50 *vs* 18% of (**259**) and (**258**), respectively; Table 4.1, entries 4 and 3], whereas an electron-withdrawing triflate group suppresses self-metathesis [4 v*s* 18% yield of (**272**) and (**258**); Table 4.1, entries 5 and 3].

Though no other products derived from the β-methylstyrenes could be isolated, it is plausible that the corresponding styrene and methyl butanoate could also have formed in the alternative cross-metathesis reaction between the propylidene carbene (originating from home-metathesis of the β-methylstyrene) and methyl acrylate (**59**) (Figure 4.2). Polystyrene formed from the styrene (*vide supra*, par. 4.1) would be expected to remain at the origin during TLC and PLC (Hexane:Acetone 8:2, v/v) separation.

It may therefore be concluded that, under the prevailing reaction conditions, electron poor double bonds of β-methylstyrenes favour cross-metathesis with acrylates, whereas electron rich double bonds favour homo-metathesis of β-methylstyrenes.

4.3.3 Effect of the α,β-unsaturated compound on the selectivity and rate of the reaction

With the effect of electron-donating and electron-withdrawing substituents on the styrene reactant determined, attention was turned towards the influence of the α,β-unsaturated carbonyl compound on the outcome of the cross-metathesis reaction in the presence of *p*-cresol (**266**). In order to assess the steric effect of a more bulky ester on the reaction, *n*-butyl acrylate (**275**) was included in the series of substrates, while the effect, if any, of an alkyl (ketone) or hydrogen (aldehyde) attached to the carbonyl group was to be evaluated by subjecting methylvinylketone (3-buten-2-one) (**274**) and acrolein (**273**) to the reaction conditions (Table 4.1).

Firstly in order to determine the effect of a longer chain acrylate on metathesis reactions, *n*-butyl acrylate (**275**) was reacted with the commercially available *trans*-β-

methylstyrene (**69**) and *trans*-anethole (**11**). The reaction between *n*-butyl acrylate (**275**) and *trans*-β-methylstyrene (**69**) yielded the self-metathesis product, *trans*-stilbene (**258**), in 18% yield (*cf*. par. 4.2) together with the cross-metathesis product, butyl cinnamate (**278**), in 55% yield (Table 4.1, entry 6). The ^{1}H NMR spectrum (Plate 4a) showed two multiplets in the aromatic region, one integrating for two and the other for three protons [δ 7.42 – 7.36 (2H, m, H-2',6'), 7.25 – 7.21 (3H, m, H-3',4',5')], two doublets at δ 7.57 and 6.33 ppm with a coupling constant of 16 Hz, thus confirming a double bond with (*E*)-geometry, a triplet for the -OCH_2- group at δ 4.09 ppm (2H, t, *J* = 6.7 Hz, H-1''), two methylene multiplets [δ (ppm) 1.59 – 1.55 (2H, m, H-2''), 1.35 – 1.29 (2H, m, H-3'')] and a methyl triplet at δ 0.85 ppm (3H, t, *J* = 7.4 Hz, H-4''). As before, the presence of a carbonyl group was confirmed by a carbon resonance at δ 167.0 ppm in the ^{13}C NMR spectrum (plate 4b) and the relevant long-distance interactions thereof [δ (ppm) 7.57 (β-H) and 4.09 (H-1'')] in an HMBC experiment, as well as IR [(neat, cm^{-1}) ν_{max} 1709 (CO)]. Finally, MS confirmed the presence of the molecular ion of this cinnamate [*m/z* (EI) 204 (M^+, 13)].

The reaction between *n*-butyl acrylate (**275**) and *trans*-anethole (**11**) also yielded two products, namely *trans*-4,4'-dimethoxystilbene (**259**) (*cf*. par. 4.2) and butyl (*E*)-*p*-methoxycinnamate (**281**) in 36% and 41% yields respectively. The ^{1}H NMR spectrum of butyl (*E*)-*p*-methoxycinnamate (Plate 8a) confirmed the structure of the product as (**281**) by the presence of an AA'BB' aromatic system [δ 7.45 (2H, d, *J* = 8.7 Hz, H-3',5'), 6.87 (2H, d, *J* = 8.7 Hz, H-2',6')], a double bond with (*E*)-geometry [δ 7.62 (1H, d, *J* = 16.0 Hz, H-β) and 6.29 (1H, d, *J* = 16.0 Hz, H-α)] which also shows long-distance coupling to the carbonyl carbon (δ 167.4 ppm) in an HMBC experiment, a methoxy singlet at δ 3.80 ppm and the *O*-butyl resonances [δ 4.18 (2H, t, *J* = 6.7 Hz, H-1"), 1.71 – 1.61 (2H, m, H-2"), 1.46 – 1.36 (2H, m, H-3"), 0.95 (3H, t, *J* = 7.4 Hz, H-4")]. IR showed the stretching frequency of a carbonyl at ν_{max} 1707 cm^{-1}, whereas the observation of the molecular ion of butyl (*E*)-*p*-methoxycinnamate (**281**) by MS [*m/z* (EI) 234 (M^+, 28)] supported the allocated structure.

Having established that cross-metathesis of β-methylstyrenes with α,β-unsatured esters (acrylates) is possible, the study was extended to the α,β-unsatured ketone, methylvinylketone (**274**). Both β-methylstyrene (**69**) and *trans*-anethole (**11**) formed the respective stilbene homo-metathesis products (**258** and **259** in 38 and 27% yield, respectively) together with the phenylbutenone cross-metathesis products (**277** and **280** in 34 and 32% yield, respectively) with methylvinylketone (**274**) (Table 4.1, entries 8 and 9). The ^{1}H NMR spectrum of (*E*)-4-phenylbut-3-en-2-one (**277**) displayed signals as expected for five aromatic protons and a double bond with the (*E*)-geometry [δ (ppm) 7.51 (3H, m, H-β, H-2',6'), 7.39 (3H, m, H-3',4',5'), 6.71 (1H, d, *J* = 16.3 Hz, H-α)], together with a methyl singlet at δ 2.37 ppm (Plate 6a). ^{13}C NMR (δ 198.55 ppm) and IR (ν_{max} 1667 cm^{-1}) supported the presence of a carbonyl group, whereas MS confirmed the expected mass [HRMS (AP+) (*m/z*) calcd for $C_{10}H_{10}O$ $[M]^+$ 146.0732, found 146. 0728].

The structure of (*E*)-4-(4-methoxyphenyl)but-3-en-2-one (**280**) was corroborated by an AA'BB' and (*E*)-alkene resonances in the ^{1}H NMR spectrum [δ (ppm) δ 7.37 (3H, m, H-β, H-2',6'), 6.89 (2H, d, *J* = 8.7 Hz, H-3',5'), 6.58 (1H, d, *J* = 16.2 Hz, H-α) (Plate 9a), together with methoxy and methyl singlets at δ 3.81 and 2.33 ppm, respectively. C-4' (δ 161.6 ppm) showed long distance coupling with the methoxy hydrogens (δ 3.81 ppm) as well as H-2' and H-6' (δ 7.37 ppm) in an HMBC experiment, whereas the carbonyl carbon (δ 198.4 ppm) showed interaction with the double bonded hydrogen β to it (δ 7.37 ppm). IR displayed a carbonyl stretching frequency (ν_{max} 1660 cm^{-1}) and HRMS the expected molecular ion [(AP+) (*m/z*) calcd for $C_{11}H_{12}O_2$ $[M]^+$ 176.0789, found 176.0790] .

The last part of this investigation was to subject the α,β-unsaturated aldehyde, acrolein (**273**) to these conditions with each of the two methylstyrene derivatives (**11**) and (**69**). Results, however were not promising as only the self-metathesis products, *trans*-stilbene (**258**) (58%) and *trans*-4,4'-dimethoxystilbene (**259**) (52%) (par. 4.2) could be isolated (Table 4.1, entries 10 and 11). GC-MS did however show peaks with corresponding *m/z* values similar to those expected for the molecular ions of cinnamaldehyde (**276**) [*m/z* 132 (M^+, 10)] and (*E*)-4-methoxycinnamaldehyde (**279**) [*m/z* 162 (M^+, 99)] in the crude reaction mixtures, but only in trace amounts.

These results clearly indicate that more steric hindrance in the ester (^{n}Butyl *vs* Me) lead to improved yields of the cross-metathesis product (55 and 41% *vs* 38 and 36%; Table 4.1, entries 6 and 7 vs entries 3 and 4) with β-methylstyrenes, while it also became evident that esters are superior cross-metathesis substrates over ketones (38 and 36% *vs* 34 and 32%; Table 4.1, entries 3 and 4 vs 8 and 9) under the prevailing reaction conditions. The failure of the aldehyde acrolein (**273**) to give more than trace amounts of the cross-metathesis products (<5%, GC; Table 4.1, entries 10 and 11) is probably explicable in terms of acrolein's high propensity towards polymerization.[14]

4.3.4 Preparation of OMC (7) and related 2-ethylhexyl esters

Encouraged by the fact that sterically more demanding esters gave better yields in the cross-metathesis reaction, the investigation was extended to the synthesis of 2-ethylhexyl cinnamate (**282**) and OMC (**7**). 2-Ethylhexyl acrylate (**2**) was therefore subjected to the metathesis reaction conditions with *trans*-β-methylstyrene (**69**) and *trans*-anethole (**11**), respectively, to give the desired 2-ethylhexyl cinnamate (**282**) and OMC (**7**) in 64 and 47% yield (Table 4.1, entries 12 and 13) together with the respective stilbenes (**258)** and (**259)** in 6% and 32% yields, respectively (*cf*. par. 4.2).

^{1}H NMR analysis of (**282**) (Plate 5a) confirmed the presence of five aromatic protons with resonances at δ (ppm) 7.55 – 7.51 (2H, m, H-2',6') and 7.40 – 7.35 (3H, m, H-3',4',5'), a double bond with (*E*)-geometry [δ 7.68 (1H, d, *J* = 16.0 Hz, H-β) and 6.45 (1H, d, *J* = 16.0 Hz, H-α) and a 2-ethylhexyl group [δ (ppm) 4.17 – 4.09 (2H, m, H-1''), 1.69 – 1.61 (1H, m, H-2''), 1.47 – 1.29 (8H, m, H-3'',4'',5'',1'''), 0.94 – 0.89 (6H, m, H-6'',2''')]. The ^{13}C NMR spectrum (δ 167.3 ppm) and IR (ν_{max} 1712 cm^{-1}) supported the presence of the carbonyl group, whereas HRMS revealed the presence of the molecular ion of 2-ethylhexyl cinnamate (**282**) [(AP+) (*m/z*) calcd for $C_{17}H_{24}O_2$ $[M]^+$ 260.1799, found 260.1801].

The structure of OMC [2-ethylhexyl *p*-methoxycinnamate] (**7**) was corroborated in a similar way by the ^{1}H NMR spectrum (Plate 9a) indicating the presence of an AA'BB'

system [δ (ppm) 7.45 (2H, d, *J* = 8.7 Hz, H-2',6'), 6.87 (2H, d, *J* = 8.7 Hz, H3',5')], a double bond with (*E*)-geometry [δ (ppm) 7.62 (1H, d, *J* = 16.0 Hz, H-β), 6.30 (1H, d, *J* = 16.0 Hz, H-α)], an 2-ethylhexyl group [δ (ppm) 4.09 (1H, m, H-1''), 1.67 – 1.58 (1H, m, H-2''), 1.47 – 1.24 (8H, m, H-3'',4'',5''.1'''), 0.94 – 0.86 (6H, m, H-6'',2''') and a methoxy group [δ 3.79 ppm (3H, s, -OC$\underline{H_3}$)]. A carbonyl group is present was present according to the ^{13}C NMR spectrum (δ 167.5 ppm) and IR (ν_{max} 1706 cm^{-1}). HRMS confirmed the presence of the molecular ion of OMC (**7**) [*m/z* (EI) 290 (M^+, 8)].

Yields of the cross-metathesis product once again increased with increasing steric bulk of the ester, ranging from 38 to 55 and 64% for the reactions of the methyl (**59**), butyl (**275**) and 2-ethylhexyl acrylate (**2**) with *trans*-β-methylstyrene (**69**) (Table 4.1, entries 3, 6 and 12) and 36 to 41 to 47% for these acrylates with anethole (**11**) (Table 4.1, entries 4, 7 and 13). Homo-metathesis yields ranged from 18 to 6% with *trans*-β-methylstyrene (**69**) (Table 4.1, entries 3, 6 and 12) and 50 to 36 and 32% with anethole (**11**) (Table 4.1, entries 4, 7 and 13), confirming a trend of decreased homo-metathesis with increased steric bulk of the ester.

Metathesis catalysed by Grubbs II catalyst (**125**) with *p*-cresol (**266**) as additive thus offers a catalytic and mild one-step method for the synthesis of OMC (**7**) in 47 % yield, though not selective yet as stilbene (**259**) concurrently formed in 32% yield. As the preference for cross versus homo-metathesis has been demonstrated to be a function of the electronic properties of the β-methylstyrene with this catalyst system, it might be necessary to expand the study to other catalysts in future.

4.4 Literature mechanism of the reaction and effect of cresol addition to the catalyst

During an investigation into the Grubbs II catalysed homo-metathesis of alkene substrates, Forman *et al.*[10,11] found that these reactions could be enhanced by the simple addition of phenol and that very low quantities of unwanted by-products were formed in comparison with reactions in the absence of phenol. These workers also found that the efficiency of cross-metathesis reactions between methyl acrylate and 1-decene (*cf*. Figure 4.3) catalysed by Grubbs II catalyst were significantly increased by addition of phenol and *p*-cresol to the reaction mixture. Careful kinetic investigations backed up by molecular modelling studies allowed these researchers to identify and propose several mechanistic steps in the catalytic cycle of these reactions (Figure 4.5).

Through molecular modelling calculations and extensive NMR work, Forman *et al*.[10,11] found that phenol addition to the Grubbs type catalysts results in the formation of Ph-OH···Cl-Ru complexes (**284**) in which the ruthenium-bound chloride acts as hydrogen bond acceptor to the acidic phenoxy proton. These workers further concluded that although the addition of phenol, slows down dissociation of the phosphine ligand from the Grubbs catalyst to afford the 14 electron intermediate (**285**) required for the metathesis reaction, phenol also interacts with the free phosphine ligand forming a species of the type $(PhOH)_nPCy_3$ (**286**); thus sequestering dissociated phosphine form the reaction mixture. This leads to an increase in the concentration of the 14 electron intermediate (**285**) and thus enhanced reaction rates with the olefin substrate. Phenol addition, furthermore, increases the electrophilic character of the carbene carbon while it also stabilises the 14 electron intermediate (**287**) through the formation of a hemilabile phenoxy-ruthenium interaction (**288**). The addition of phenols to metathesis reactions therefore leads to a profound increase in catalyst lifetime, while at the same time increasing the overall turnover numbers observed for these reactions.

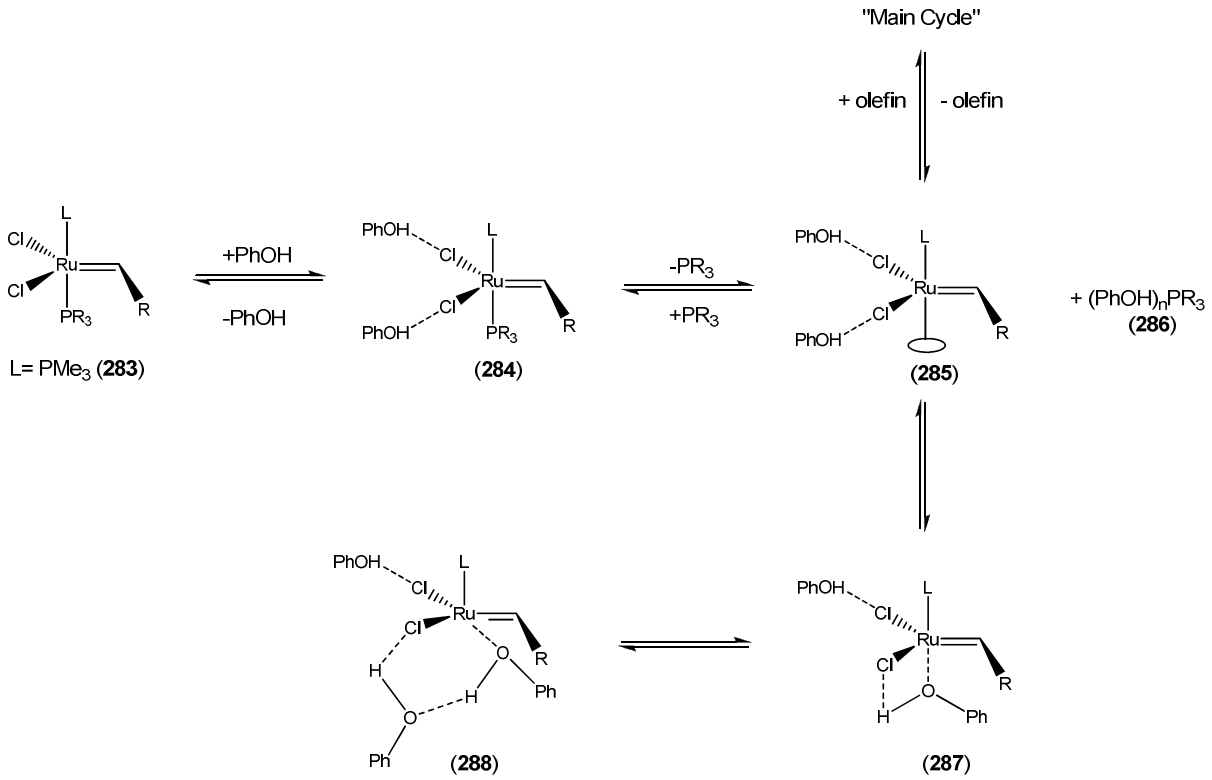

Figure 4.5: Proposed mechanism for the phenol assisted Grubbs II catalysed metathesis reaction of alkenes.

Although Foreman and co-workers[10,11] executed an intensive investigation into the effect of phenol addition to the active catalytic species involved in these metathesis reactions, they failed to come up with answers as to why the addition of cresol, for example, would lead to enhanced cross-metathesis products being formed when different alkene substrates are subjected to the reaction. In an attempt to come up with an explanation as to why and how cresol influences the catalytic cycle of Grubbs 2nd generation catalyst during metathesis reactions in favour of CM products, an NMR study to identify and confirm the different intermediates in the catalytic cycle with and without the presence of cresol, was embarked upon.

4.5 NMR analysis of the possible effect of *p*-cresol addition on the Grubbs II catalyst and reaction sequence

In order to be able to look at the differences in catalyst structure and reactivity with and without cresol, it was first required to identify and allocate all the proton, carbon and phosphorus resonances within the Grubbs second generation catalyst (Figure

4.6) itself. Though the Grubbs II catalyst is well defined,[15,16,17] no literature was found where the peaks were completely assigned.

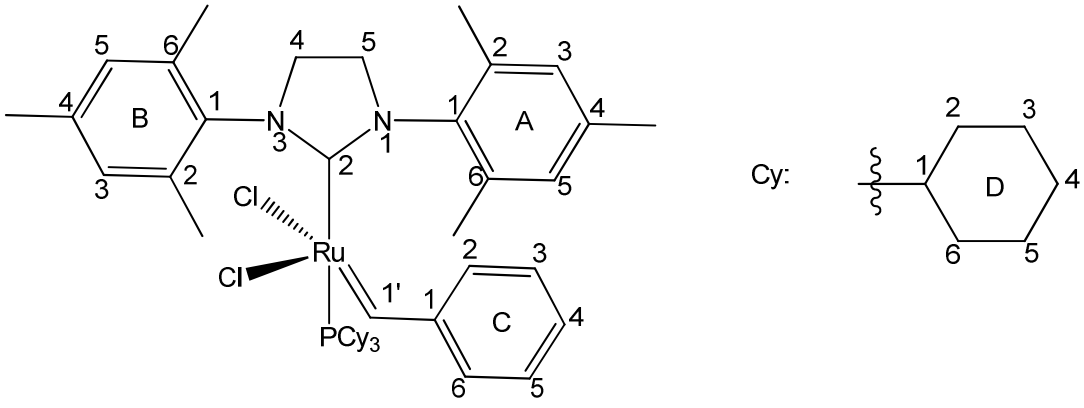

Figure 4.6: Grubbs second generation catalyst.

4.5.1 ^{1}H NMR

The aliphatic region of the ^{1}H NMR spectrum (Plate 16a, Figures 4.7 and 4.8; Table 4.2) of the Grubbs II catalyst (in $CDCl_3$ at room temperature) displayed two broad multiplets at δ 0.70 – 1.17 and 1.17 – 1.63 ppm (both integrating for 15 protons), a broad doublet of doublets at δ 2.19 ppm (3 protons), as well as two sharp singlets at δ 1.90 and 2.31 ppm and four very broad singlets (δ 2.04, 2.52, 2.57 and 2.76 ppm), each integrating for three protons. The broad multiplets could be allocated to the equatorial and axial protons [H-2-6 (D)] respectively of the three cyclohexyl rings attached to the phosphorous atom, while the doublet of doublets originated from the three methine protons [H-1 (D)]-of the cyclohexyl groups. These peaks sharpened somewhat when the spectrum was obtained at 60 °C (Plate 16a_2, Figure 4.9), whereas the methine resonance broadened at -40 °C (Plate 16a_3, Figure 4.10). As expected, small changes in chemical shifts were observed at the different temperatures (Figures 4.8 – 4.21; Table 4.2).

Although the sharp and broad singlets clearly resembled aromatic methyl groups in their chemical shift positions, only four methyl resonances were expected from the

mesityl rings if these rings were in a position that would allow free rotation. Since six signals were observed and taking into account that four of those were broadened, it could be concluded that the mesityl rings were under conditions of severely restricted rotation at 20 °C. The sharp resonances at δ 1.90 and 2.31 ppm could therefore be allocated to the methyl groups in the 4-positions of the mesityl rings, while the broad signals originated from the four *ortho*-methyl groups which, due to restricted rotation, were non-equivalent. Additional proof of restricted rotation being the cause of these methyl resonances showing up as four broad singlets came from the spectrum that was taken up at 60 °C where the four signals collapsed into two broad singlets at δ 2.59 and 2.23 ppm, each integrating for six hydrogens (Figure 4.9). Six sharp singlets (δ 1.90, 2.03, 2.31, 2.52, 2.57, 2.77 ppm) were obtained at -40 °C for these methyl groups (Figure 4.10, Table 4.2).

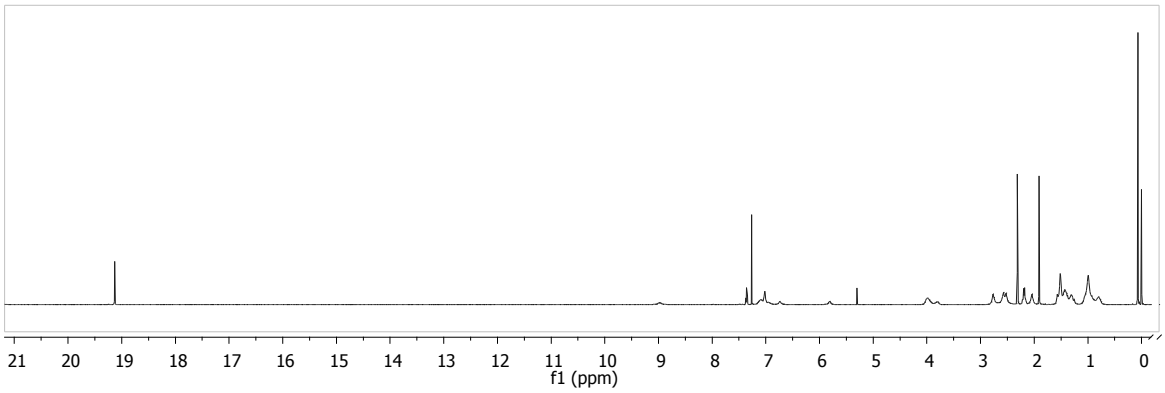

Figure 4.7: ^{1}H NMR spectrum of the Grubbs II catalyst in $CDCl_3$ at room temperature.

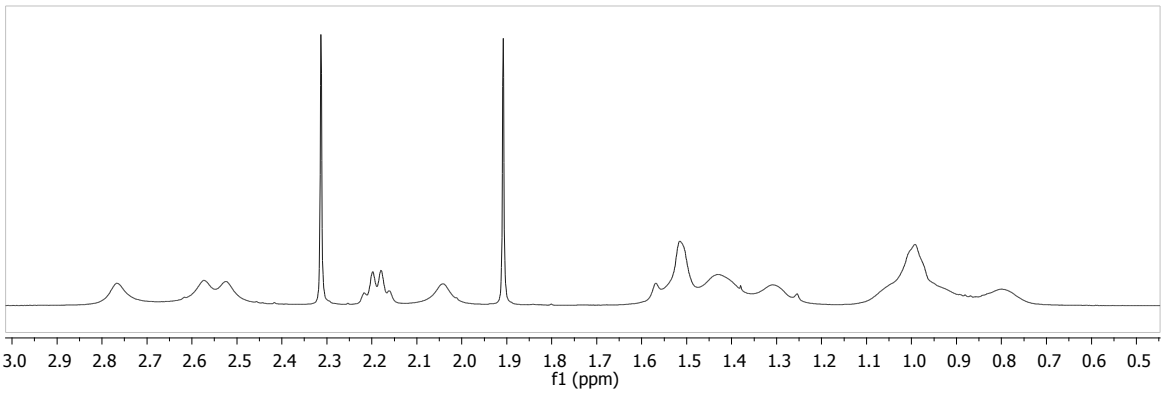

Figure 4.8: Aliphatic region of the ^{1}H NMR spectrum of the Grubbs II catalyst at room temperature.

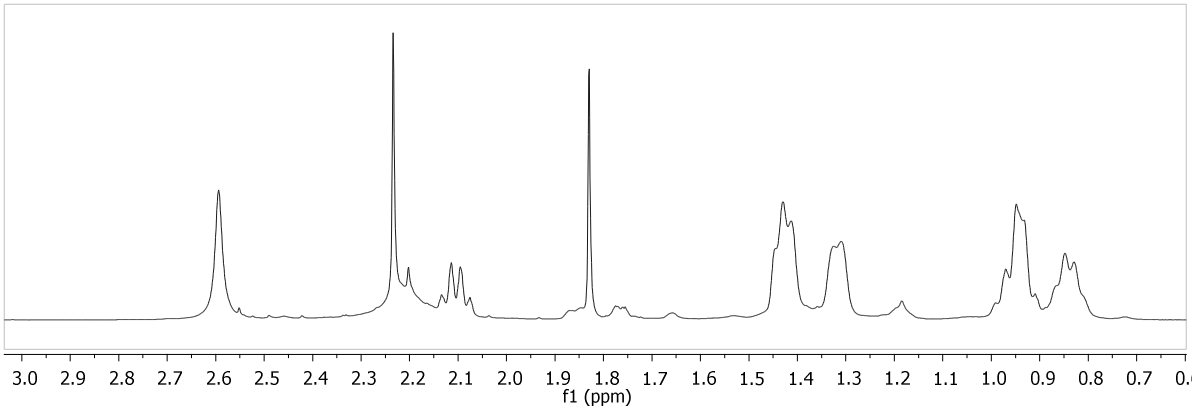

Figure 4.9: Aliphatic region of the ^{1}H NMR spectrum of the Grubbs II catalyst at 60 ˚C.

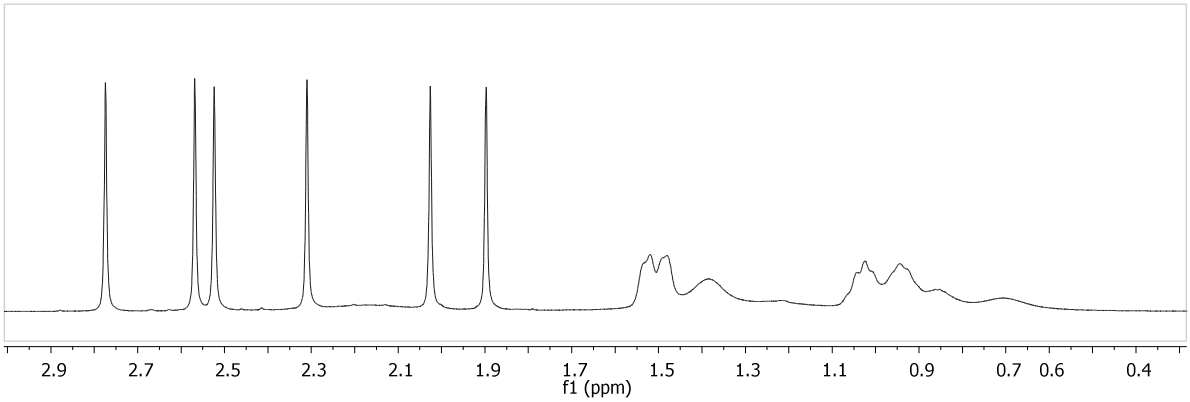

Figure 4.10: Aliphatic region of the ^{1}H NMR spectrum of the Grubbs II catalyst at -40 ˚C.

The heterocyclic region of the spectrum (Figures 4.7 and 4.11) displayed two broad singlets at δ 3.80 (1H) and 3.97 (3H) ppm. While it was obvious that these signals should be attributable to the two CH_2 groups (H-4,5) of the nitrogen containing ring, the integral ratio and unsymmetrical appearance of the resonances were somewhat unexpected. The spectrum obtained at 60 °C [Figure 4.11(b)], however, displayed the expected two triplets (each integrating for two protons), again indicating severely restricted rotation to be present in the catalyst molecule in solution at room temperature. The -40 °C spectrum [Figure 4.11(c)] resembles the room temperature one with the exception that the resonance at δ 3.82 ppm now clearly exists as a ddd integrating for one proton, while the remaining three protons appears as a multiplet at δ 3.91 – 4.08 ppm. NOE association (-40 °C) (Plate $16h_3$), between the methyl singlets at δ 2.03 [2-Me (A)] and 2.52 [6-Me (A)] ppm (*vide infra*) and the proton at δ 3.82 indicated this resonance to be associated with H-5(a), while a clear NOE

between the multiplet at δ 3.91 – 4.08 ppm and methyl resonances at δ 2.77 and 2.52 ppm confirmed two of these hydrogens to be at C-4.

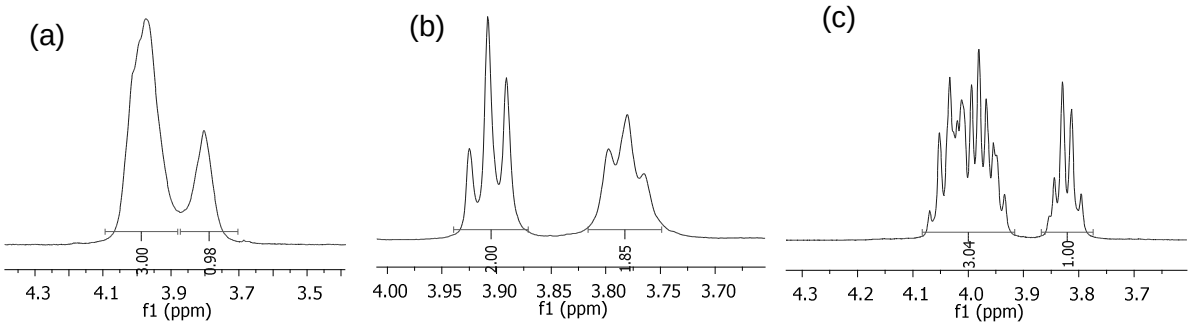

Figure 4.11: Heterocyclic region of the ^{1}H NMR spectrum of the Grubbs II catalyst in $CDCl_3$ at (a) rt., (b) 60°C and (c) -40°C.

The presence of the methyl carbene in the structure was confirmed by a resonance at δ 19.12 ppm integrating for one proton (H-1') at room temperature; the chemical shift of which was in good agreement with literature values.[15]

While integrating for the correct number of protons (9), the aromatic region of the room temperature ^{1}H NMR spectrum (Figures 4.7 and 4.12), apart from a single one-proton multiplet at δ 7.37 – 7.34 ppm, displayed an array of broad singlets and multiplets. Since H-4 (C) would be the only hydrogen not affected by slow rotation of the aromatic ring, this resonance (at δ 7.37 – 7.34 ppm) could be assigned to H-4 (C). The low temperature (-40 °C) ^{1}H NMR spectrum (Figure 4.13) where the molecule was "frozen" in its low energy conformation, however, led to this region of the spectrum to become well defined allowing for the allocation of all the observed resonances (Table 4.2). The four singlet resonances at δ 7.08, 7.03, 6.75 and 5.77 ppm, each integrating for 1 proton, clearly belonged to rings A and B, as was evident from the fact that an NOE effect from the methyl group at δ 1.90 ppm and the protons at δ 5.77 and 6.75 ppm as well as the methyl group at δ 2.31 ppm and the singlets at δ 7.03 and 7.08 ppm were clearly visible in the low temp. NOESY spectrum (Figure 4.14, Plate $16h_3$). The resonances at δ 5.77 and 6.75 ppm could therefore be allocated to H-3,5 of the A or B rings with the other two (δ 7.03 and 7.08

ppm) to the analogous protons of the other mesityl ring, whereas the methyl resonances (δ 1.90 and 2.31 ppm) correspond to the respective 4-methyl substituents of rings A and B. The absence of any coupling between the two sets of non-equivalent *meta*-protons is currently inexplicable. Finally, due to the resonance at δ 5.77 showing NOE correlation to two methyl groups at δ 1.90 and 2.03 ppm and δ 7.08 ppm similarly to methyl groups at δ 2.31 and 2.77 ppm, it could be concluded that H-3 (A) and H-3 (B) could be assigned to the signals at δ 5.77 and δ 7.08 ppm, respectively, if δ 2.03 and 2.77 are assigned to the respective 2-methyl substituents.

The remaining aromatic resonances, i.e. two broad doublets at δ 8.87 (J = 7.84 Hz) and 6.89 ppm (J = 7.57 Hz) along with three multiplets at δ 7.39 – 7.35, 7.18 – 7.14 and 7.09 – 7.04 ppm, all integrating for 1 proton each, clearly belonged to the C-ring. Since *meta*-coupling is again not observed, the two doublets (at δ 8.87 and 6.89 ppm) could be assigned to H-2 and H-6 of the C-ring and the resonance at δ 7.39 – 7.35, as already indicated, to H-4 (C). The residual doublets of doublets could therefore be accounted for by H-3 and 5 (C).

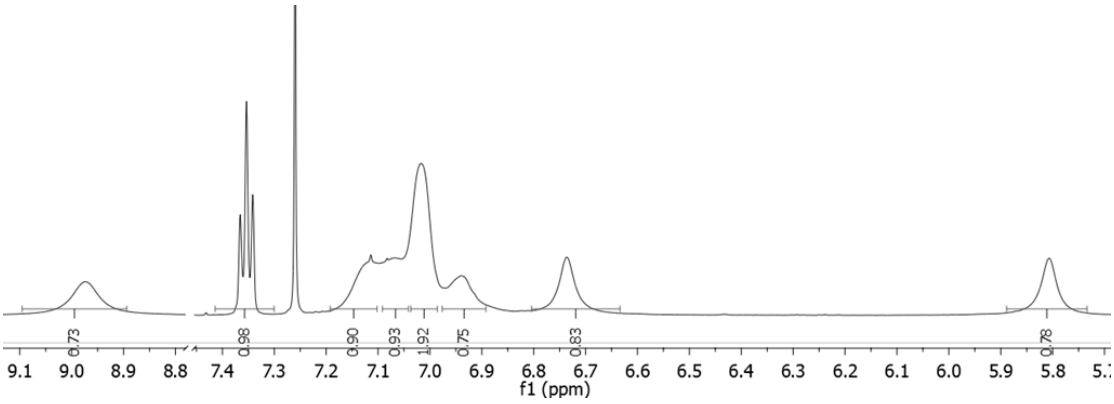

Figure 4.12: Aromatic region of the ^{1}H NMR spectrum of the Grubbs II catalyst at room temperature.

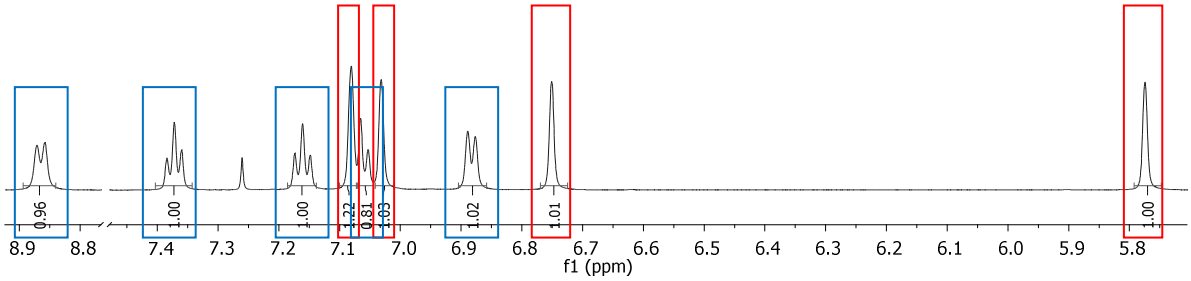

Figure 4.13: Aromatic region of the ^{1}H NMR spectrum of the Grubbs II catalyst at -40 °C.

Since the carbene proton (δ 18.94 ppm) showed clear NOE association with the doublet at δ 6.89 ppm in the low temperature NOESY spectrum (Plate 16h$_3$, Figure 4.14) and this resonance showed association with the resonance at δ 7.09 – 7.04 ppm in the NOESY spectrum, the resonances at δ 6.89 and 7.09 – 7.04 ppm could be assigned to H-6 and 5 (C) respectively. As the multiplet at δ 7.39 – 7.35 ppm has already been allocated to H-4(C), the remaining multiplet (δ 7.18 – 7.14 ppm) could be assigned to H-3 (C). This allocation of resonances was confirmed by the multiplet at δ 7.39 – 7.35 showing NOE associations to both the resonances at δ 7.09 – 7.04 ppm and δ 7.18 – 7.14 ppm, while the fact that the multiplet at δ 7.18 – 7.14 showed association with the doublet at δ 8.87 ppm resulted in the fact that this resonance could be assigned to H-2 (C), as expected.

Finally, NOE association between the carbene proton (at δ 18.94 ppm) and 6-CH$_3$ (A) (at δ 2.52 ppm) in the low temp. NOESY spectrum (Plate 16h$_3$) as well as between H-2 (δ 8.87 ppm) and H-3 (C) (δ 7.18 – 7.14 ppm) and the methyl at δ 2.03 ppm [2-CH$_3$ (A)] indicated these protons to be in close proximity to each other, thus leading to the conclusion that the A and C-rings are in a π-stacking arrangement with regard to each other (Figure 4.14). The assignment of protons to ^{1}H NMR resonances as indicated here were in good agreement with the findings of Gallagher *et al*.[17] who reported on the NMR spectrum of the Grubbs II catalyst at -50 °C.

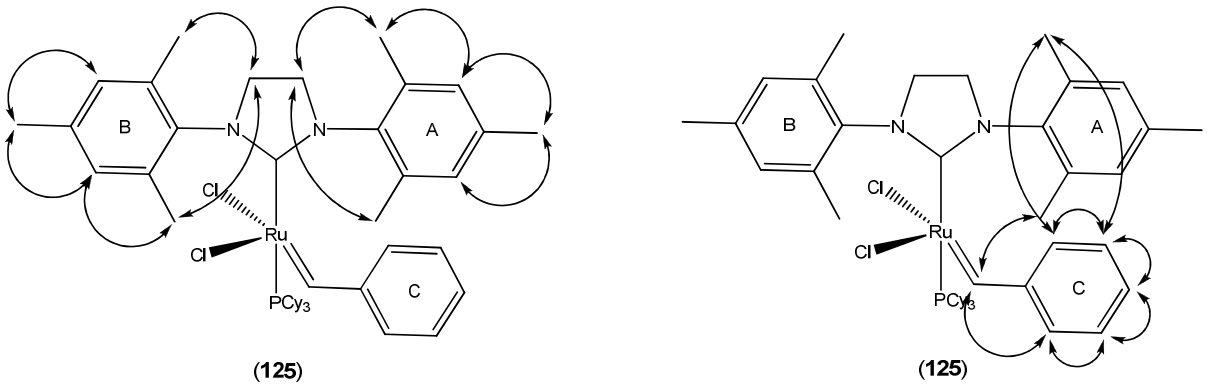

Figure 4.14: Illustration of NOE associations of Grubbs II catalyst.

4.5.2 ^{13}C NMR

With all the proton resonances assigned, attention was turned towards assigning the resonances in the ^{13}C NMR spectrum (Figures 4.15 – 4.17) of the Grubbs catalyst to the appropriate carbon atoms.

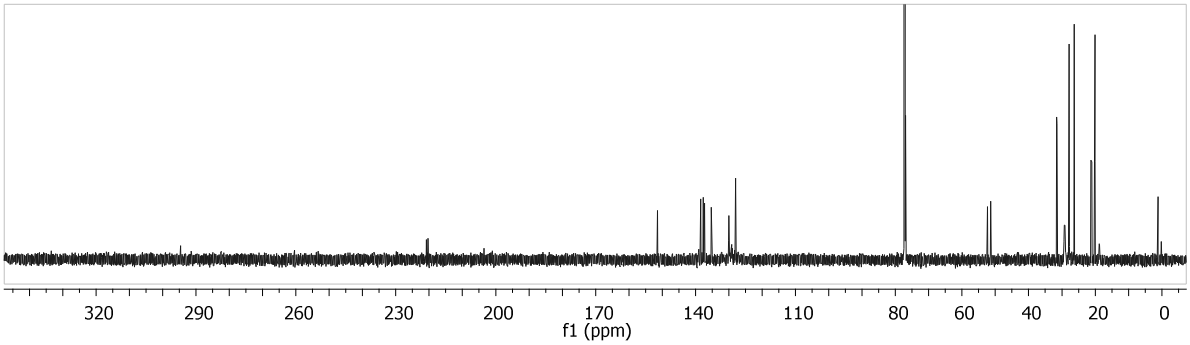

Figure 4.15: ^{13}C NMR spectrum of the Grubbs II catalyst at rt.

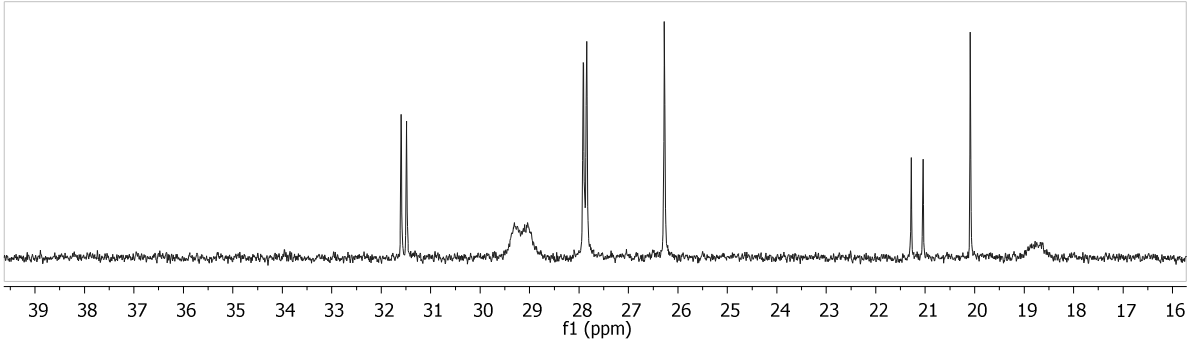

Figure 4.16: Aliphatic region of the ^{13}C NMR spectrum of the Grubbs II catalyst at rt.

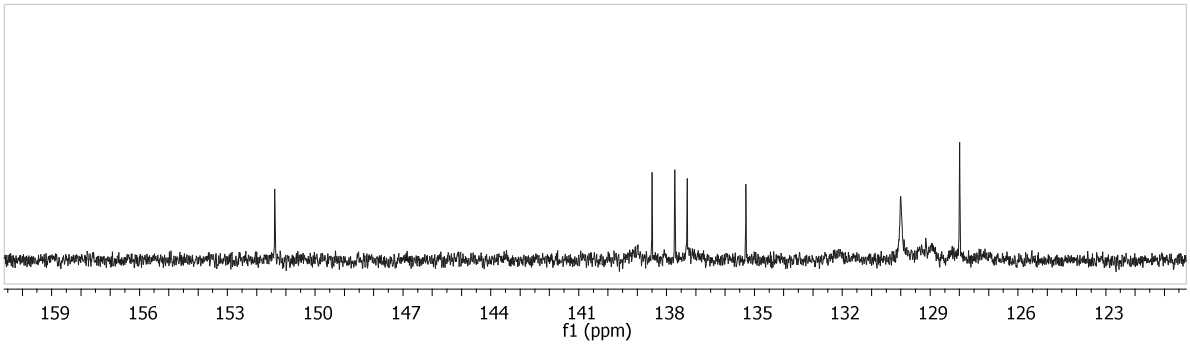

Figure 4.17: Aromatic region of the ^{13}C NMR spectrum of the Grubbs II catalyst at rt.

From the spectra at room temperature indicated above (Figures 4.16 and 4.17), it was clear that resonances could only be assigned with confidence to carbons in the alkyl region of the spectrum (δ 25 – 30 ppm). Keeping in mind that coupling with the phosphorous would lead to carbons 1, 2, and 3 of the cyclohexyl groups to appear as doublet resonances and through application of the HSQC technique, the doublets at δ 29.2 (3C, *J* = 40.4 Hz), 31.5 (6C, *J* = 16.6 Hz), and 27.9 (6C, *J* = 9.9 Hz) could be assigned to H-1 (D), H-2,6 (D) and H-3,5 (D) of the cyclohexyl groups, respectively, while the singlet at δ 26.1 ppm (3C) originated from C-4 (D) (Figure 4.16).

The interpretability of the rest of the spectrum was seriously hampered by restricted rotation and the fact that many resonances were broadened and/or so small that it could not be allocated with confidence (Figures 4.16 and 4.17). While the spectrum at -40 °C (Figure 4.18) once again looked much better, it still displayed quite a number of small peaks, which could either belong to the spectrum or be due to impurities, and it was therefore decided to obtain an integratable carbon spectrum at room temperature to be able to determine whether all the resonances actually are originating from the pure catalyst (Figure 4.19). At this temperature, the four singlet carbon signals in the aromatic alkyl region (Figure 4.20) (δ 18.4, 19.0, 21.0, and 21.3 ppm) integrating for one carbon each, could be assigned to the methyl groups of the A-ring [δ 18.6, (6-Me), 18.9, (2-Me) and 21.0, (4-Me)] and the *p*-methyl of the B-ring (δ 21.3 ppm) using the HSQC technique, while the remaining singlet at δ 20.1 ppm, integrating for 2 carbons, could be allocated to the 2 and 6 methyl groups of the B-ring.

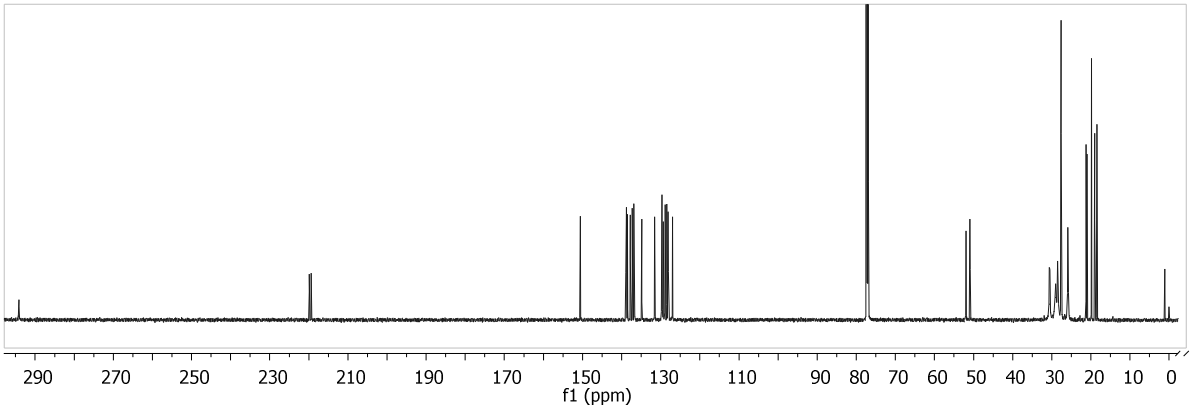

Figure 4.18: ^{13}C NMR spectrum of the Grubbs II catalyst at -40 °C.

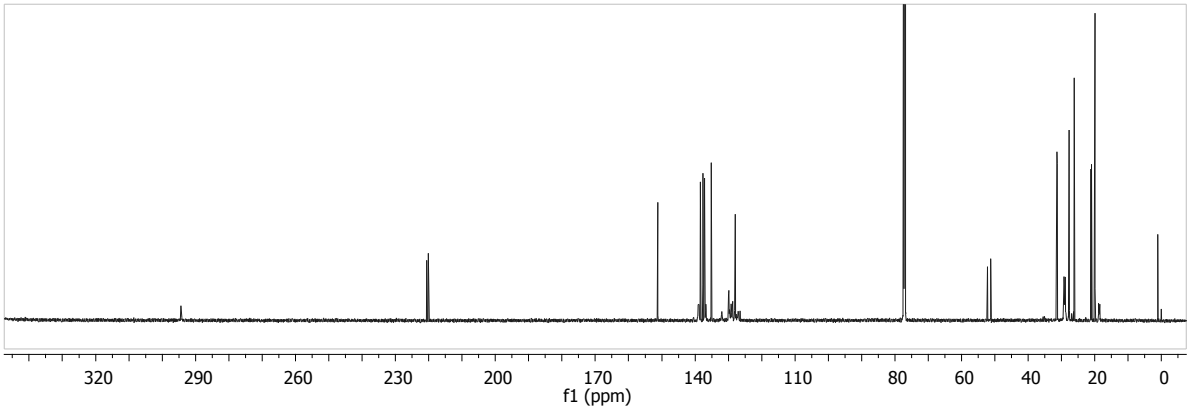

Figure 4.19: Integratable ^{13}C NMR spectrum of the Grubbs II catalyst at rt.

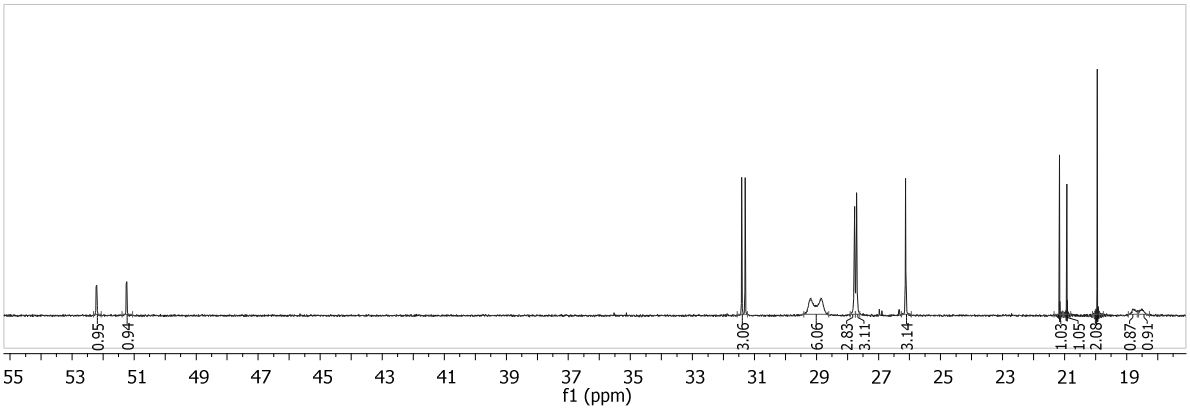

Figure 4.20: Aliphatic region of the integratable ^{13}C NMR spectrum of the Grubbs II catalyst at rt.

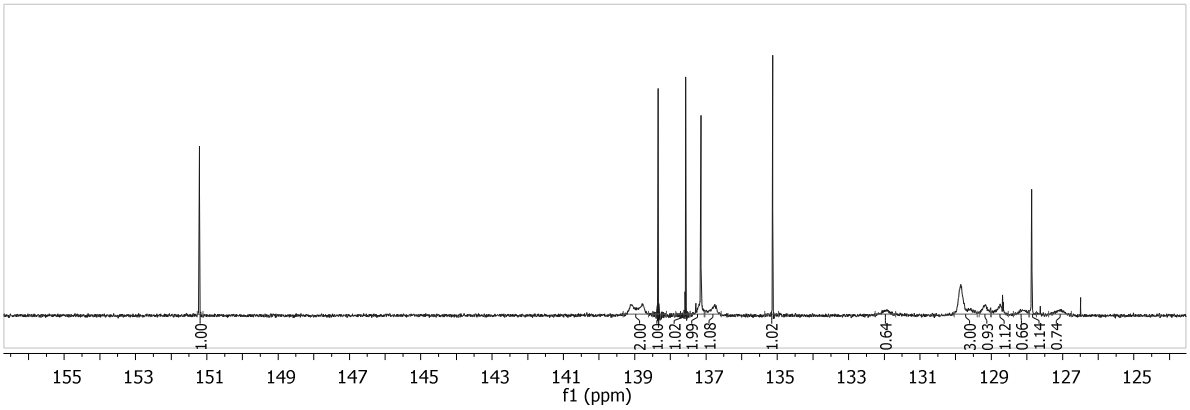

Figure 4.21: Aromatic region of the integratable ^{13}C NMR spectrum of the Grubbs II catalyst at rt.

Careful study of the HSQC yields an interesting observation regarding the ^{13}C imidazolidine methylene signals (C-4 and C-5) at δ 52.3 and 51.4 ppm. The carbon signal at δ 51.4 ppm correlated only to the corresponding imidazolidine methylene proton resonance at δ 3.97 ppm in the room temperature spectrum (Plate 16c), whereas the δ 52.3 ppm carbon correlated with both proton signals (at δ 3.97 and 3.80 ppm), proving that one of the methylene protons are indeed experiencing signal different chemical environment than the other three. The resonance at δ 52.3 ppm could therefore be allocated to C-5 through HSQC association with H-5(a) (δ 3.80 ppm).

The low field area of the ^{13}C NMR spectrum (Figure 4.19) exhibited two resonances at δ 220.5 (d, J = 77.4 Hz) and 294.4 ppm, each integrating for one carbon, which could be allocated to the two carbene carbons present in the catalyst molecule. Since strong phosphorous coupling was observed to the carbon appearing at δ 220.5 ppm, this resonance could be allocated to the imidazolidine-carbene carbon, and the other signal (δ 294.4 ppm) to the methyl carbene attached to the ruthenium. The fact that one carbene carbon shows coupling with phosphorous and the other one no or very small coupling, is probably explicable in terms of the imidazolidine-carbene carbon being in the *trans* position with regard to the P and the methyl carbene at a 90° angle. This observation can be explained using Karplus diagrams where it is known that the J-coupling is the largest for dihedral angles of 0° and 180° and around zero at 90° angles. Although *cis*/*trans* isomers in metal complexes does not possess dihedral angles it can be assumed that the same principle applies here and

that for *cis*-complexes the coupling constant will approach 0 and for the *trans*-analogues large coupling constants will be observed.[18]

The aromatic region of the ^{13}C NMR spectrum at -40 °C (Figure 4.21) displayed the expected 18 resonances (δ 127.0, 128.1, 128.2, 128.5, 128.9, 129.3, 129.7, 129.8, 131.6, 134.9, 136.7, 136.9, 137.3, 137.8, 138.5, 138.8, 138.9, and 150.6 ppm) all integrating for one carbon each, of which 9 (δ 134.9, 136.7, 136.9, 137.3, 137.8, 138.5, 138.8, 138.9, and 150.6 ppm) were not associated with hydrogen atoms in the HSQC correlated spectrum. HSQC correlation of the protons at δ 5.77 and 6.75 ppm [H-3,5 (A)] as well as those at δ 7.08 and 7.03 ppm [H-3,5 (B)] with the carbons at δ 128.9, 128.5, 129.8, and 127.0 ppm allowed for the mesityl carbons, C-3,5 (A) and C-3,5 (B) respectively, to be assigned to these resonances. Simmilarly, due to HSQC correlation between the C-ring protons, H-2, 3, 4, 5 and 6 (at δ 8.87, 7.16, 7.37, 7.07 and 6.89 ppm) and the signals at δ 131.6, 128.2, 128.1, 129.7 and 129.3 ppmin the carbon spectrum, these resonances could be assigned to carbons 2 to 6 of the C-ring.

The quaternary aromatic carbons [C-1, 2, 4, and 6 (A); C-1, 2, 4, and 6 (B) and C-1 (C)] in the spectrum were assigned to the resonances at δ 134.9, 136.7, 136.9, 137.3, 137.8, 138.5, 138.8, 138.9, and 150.6 ppm in the spectrum in the following way: Due to it appearing as a doublet with small coupling (4.18 Hz) to the phosphorous atom, the doublet at δ 150.6 ppm could be allocated to C-1 of the C-ring. Although it seems strange that the carbene carbon next to C-1 (C) did not show any, or very small coupling to the phosphorous, instances where ^{2}J (P,C) coupling are smaller than ^{3}J (P,C) coupling have been reported in the literature.[19,20] The *para* carbons in rings A and B [C-4 (A) and C-4 (B)] could be assigned to the singlets at δ 137.8 and 138.5 ppm respectively due to HMBC correlations with the methyl groups in the 2-positions (δ 1.90 and 2.31 ppm). Lastly, the six singlets at δ 134.9, 136.7, 136.9, 137.3, 138.8, and 138.9 ppm, all integrating for 1 carbon each, should belong to the remaining quaternary carbons of the mesityl rings [C-1,2 and 6 (A) and C-1,2 and 6 (B)], but because of no correlations between any protons and these carbons observable in the HMBC spectrum, these resonances could not be assigned to specific carbons.

A summary of the ^{1}H and ^{13}C chemical shift values and assignment of resonances to carbons and protons for Grubbs second generation catalyst at -40 °C and room temperature is reflected in Table 4.2.

Table 4.2: ^{1}H and ^{13}C allocation for Grubbs II catalyst.

		-40°C		Room Temperature	
	Position	^{1}H δ (ppm)	^{13}C δ (ppm)	^{1}H δ (ppm)	^{13}C δ (ppm)
	2	-	219.6 (d, J = 77.3 Hz)	-	220.5 (d, J = 77.4 Hz)
	4	4.08-3.91 (m)	52.0 (s)	3.97 (bs)	52.3 (d, J = 3.4 Hz)
	5	3.82 [ddd, H-(a, J = 18.27 Hz, 17.27 Hz, 6.95 Hz)] and 3.91 - 4.08 [m, H-(b)]	50.9 (s)	3.80 (bs) and 3.97 (bs)	51.4 (d, J = 1.74 Hz)
	1'	18.94 (s)	294.1 (s)	19.12 (s)	294.4 (s)
Ring A	1	-	137.3 (s) or 134.9 (s)	-	137.3 (s) or 135.3 (s)
	2&6	-	138.8 (s) and 138.9 (s) or 136.7 (s) and 136.9	-	139.0 (bs) and 139.2 (bs) or 136.9 (bs) and 137.2 (s)
	3	5.77 (s)	128.9 (s)	5.81 (s)	129.3 (bs)
	4	-	137.8 (s)	-	137.7 (s)
	5	6.75 (s)	128.5 (s)	6.74 (s)	128.9 (bs)
	2-Me	2.03 (s)	19.0 (s)	2.04 (s)	18.9 (s)
	4-Me	1.90 (s)	21.0 (s)	1.90 (s)	21.0 (s)
	6-Me	2.52 (s)	18.4 (s)	2.52 (s)	18.6 (s)
Ring B	1	-	134.9 (s) or 137.3 (s)	-	135.3 (s) or 137.3 (s)
	2&6	-	136.7 (s) and 136.9 (s) or 138.8 (s) and 138.9 (s)	-	136.9 (bs) and 137.3 (s) or 139.0 (bs) and 139.2 (bs)
	3	7.08 (s)	129.8 (s)	7.07 (bs)	130.0 (bs)
	4	-	138.5 (s)	-	138.4 (s)
	5	7.03 (s)	127.0 (s)	7.02 (bs)	127.2 (bs)
	2-Me	2.77 (s)	19.8 (s)	2.76 (s)	20.1 (s)
	4-Me	2.31 (s)	21.3 (s)	2.31 (s)	21.3 (s)
	6-Me	2.57 (s)	19.8 (s)	2.57 (s)	20.1 (s)
Ring C	1	-	150.6 (s)	-	151.3 (d, J = 4.2 Hz)
	2	8.87 (d, J = 7.84Hz)	131.6 (s)	8.97 (s)	132.0 (bs)
	3	7.18 - 7.14 (m)	128.2 (s)	7.16 - 6.91 (m)	128.2 (bs)
	4	7.39 - 7.35 (m)	128.1 (s)	7.37 - 7.34 (m)	128.0 (s)
	5	7.09 - 7.04 (m)	129.7 (s)	7.16 - 6.91 (m)	130.0 (bs)
	6	6.89 (d, J = 7.57 Hz)	129.3 (s)	7.16 - 6.91 (m)	129.8 (bs)
Ring D	1	2.25 - 2.07 (m)	30.6 (bs)	2.23 - 2.14 (m)	29.2 (d, J = 40.4 Hz)
	2&6	0.51 - 1.11 (m)	28.8 (d, J = 85.8 Hz)	0.70 - 1.17 (m)	31.5 (d, J = 16.6 Hz)
	3&5	&	27.6 (t, J = 9.2 Hz)	&	27.9 (d, J = 9.9 Hz)
	4	1.11 - 1.67 (m)	25.9 (s)	1.17 - 1.63 (m)	26.3 (s)

4.5.3 ^{31}P NMR

In order to identify the effect cresol would have on the mechanism of the metathesis reaction and/or the reagents, ^{31}P NMR spectra were obtained after systematic addition of these reagents to Grubbs second generation catalyst (Figure 4.6) in $CDCl_3$. Firstly, the effect of cresol addition (2 eq.) to Grubbs catalyst was determined and it was found that apart from two very small resonances appearing at δ 55.6 and 40.7 ppm, the P-resonance of the catalyst remained unchanged at δ 28.9 ppm. Although Forman *et al*.[11] postulated phenol to form hydrogen bonding complexes with the chlorides in the catalyst (**284**) and to facilitate dissociation of the phosphine

from the catalyst, no appreciable quantities of free tricyclohexylphosphine or tricyclohexylphosphine-cresol complex (**286**), as indicated in Figure 4.5, could be observed. Despite their postulation with regard to the dissociation of the catalyst to the four coordinated ruthenium species (**285**) and the phosphine-phenol complex (**283**), this phenomenon was also reported by Forman *et al.*[11] The fact that *p*-cresol, however, does form a complex, most probably with the catalyst, was evident from a downfield shift (from δ 6.73 to 6.81 ppm) of the *p*-cresol H-2,6 resonance in the proton spectrum of the *p*-cresol-catalyst mixture (Figure 4.22).

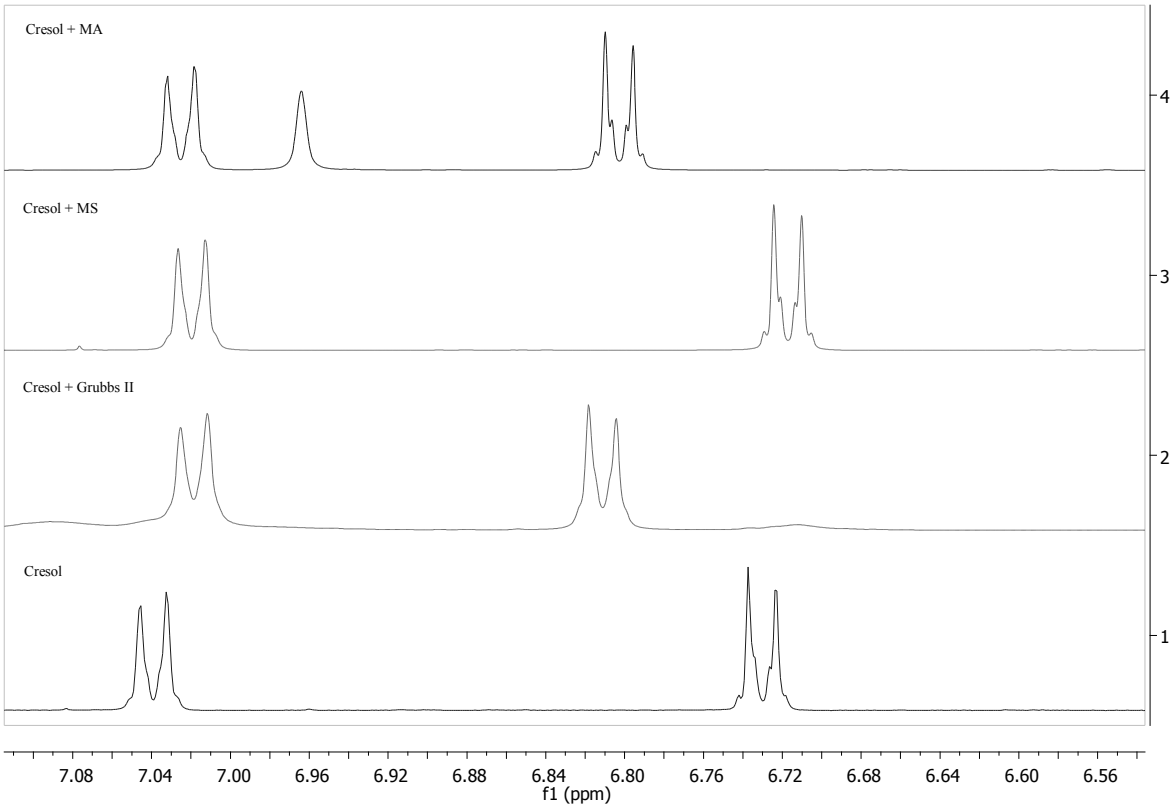

Figure 4.22: ^{1}H spectra of the aromatic protons of *p*-cresol.

Since the dissociation of the phosphine from the catalyst was postulated to be an equilibrium process and the formation of the *p*-cresol-phosphine complex could also be equilibrium limited, it was at this stage decided to look at the ^{31}P NMR spectra of mixtures of *p*-cresol and tricyclohexylphosphine in order to determine the chemical shift of the phosphorous in the equilibrium mixtures. The ^{13}P NMR spectrum of 'pure' tricyclohexylphosphine (Figure 4.23) obtained from Sigma-Aldrich, however, contained three resonances (δ 11.2, 50.8 and 57.6 ppm). By comparing the

spectrum with that of tricyclohexylphosphine oxide (Figure 4.23) as well as published values, it was possible to assign the resonances at δ 11.2 and 50.8 ppm to the phosphine[21,22] and phosphine oxide,[22,23] respectively, while the signal at δ 57.6 ppm probably is some impurity from the preparation process. When *p*-cresol (1 and 2 eq.) was added to the solution, the tricyclohexylphosphine signal shifted to δ 33.2 ppm, while the phosphine oxide resonance moved downfield to δ 53.6 ppm (Figures 4.23 and 4.24). In order to confirm the position of these signals as being protonated phosphine and phosphine oxide, respectively, triflic acid (2 eq.) was added to these compounds before NMR analysis and it was found that the resonance at δ 33.2 ppm indeed originates from protonated tricyclohexylphosphine (Lit.[24]: δ 32.7 ppm). The resonance for fully protonated phosphine oxide, however, appears at δ 86.5 ppm (Figure 4.25), indicating cresol to be too weak an acid to fully protonate tricyclohexylphosphine oxide, but only leading to the formation of a hydrogen bonding complex between the oxide and the cresol. Again, impurities present in the commercially available tricyclohexylphosphine oxide renders assignment of these resonances to the appropriate species ambiguous.

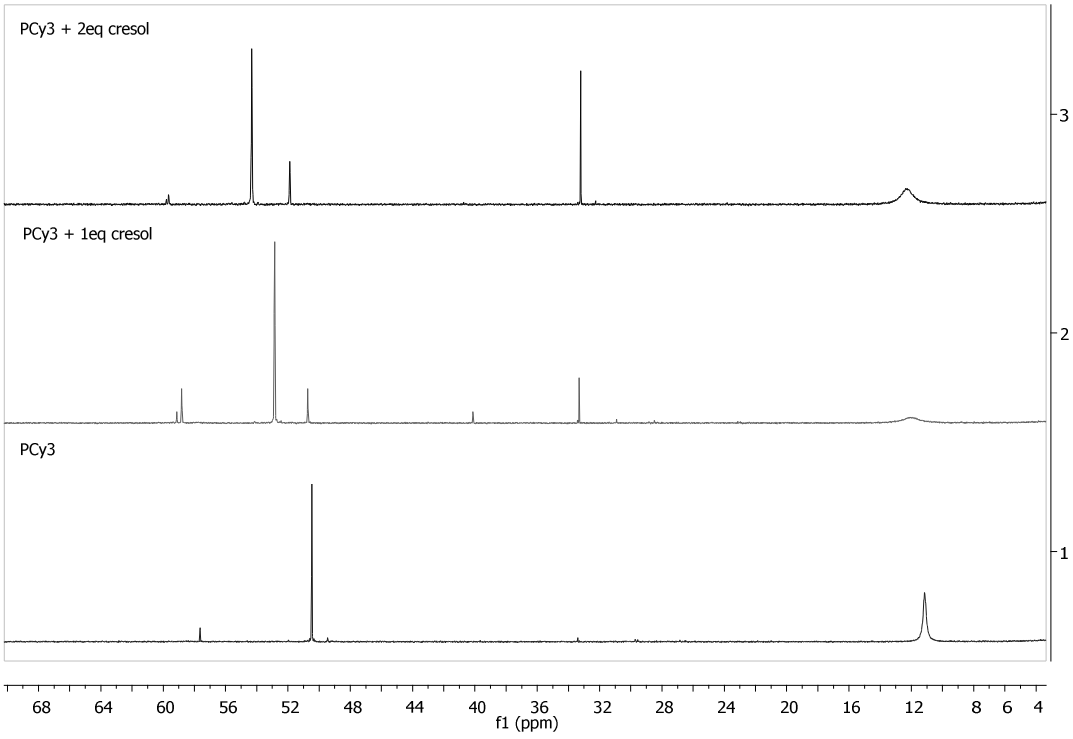

Figure 4.23: ^{31}P spectrums of tricyclohexylphosphine with cresol.

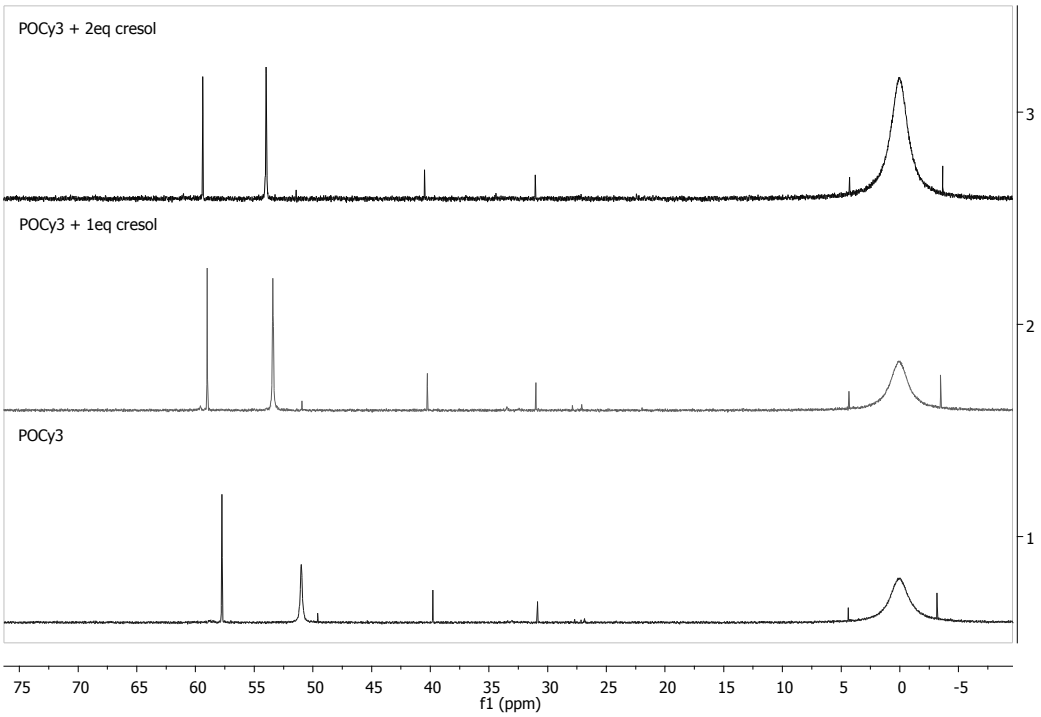

Figure 4.24: ^{31}P spectrums of tricyclohexylphosphine oxide with cresol.

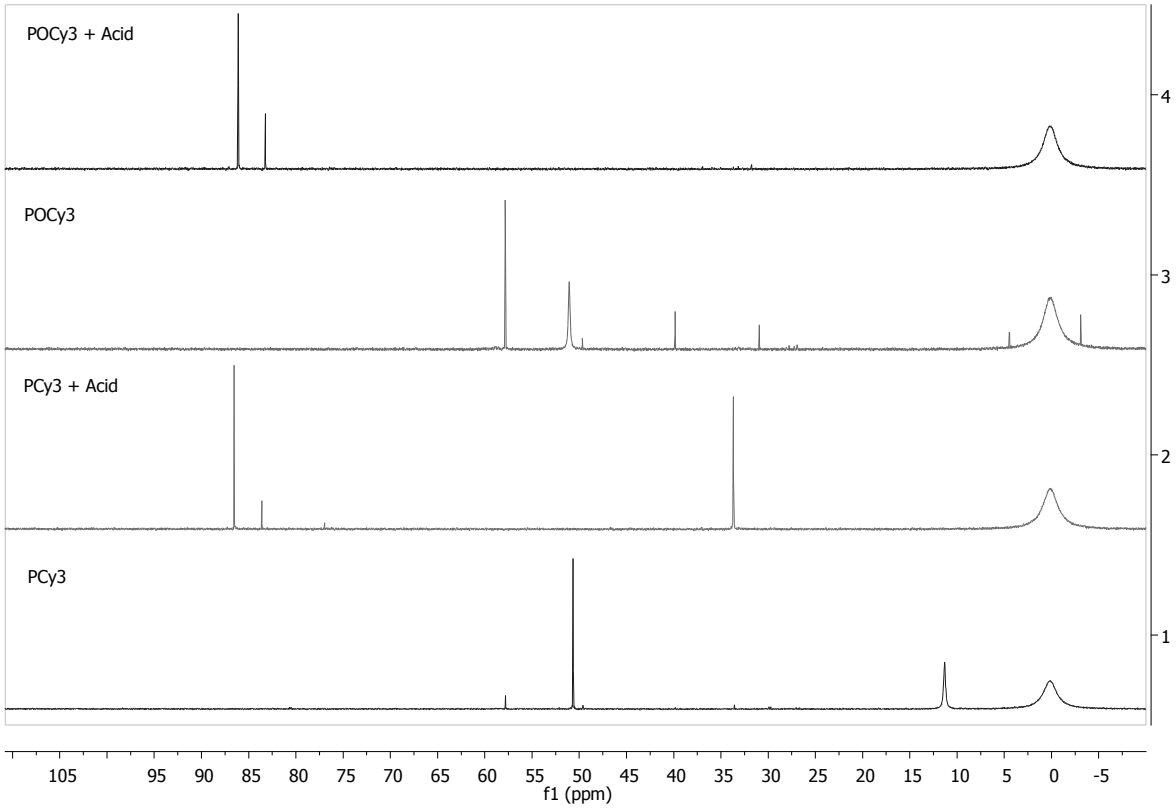

Figure 4.25: ^{31}P spectrums of tricyclohexylphosphine and tricyclohexylphosphine oxide with and without triflic acid.

With the positions of the phosphorous resonances in tricyclohexylphosphine and tricyclohexylphosphine oxide in the presence of cresol determined, attention was paid to the interaction of the Grubbs II catalyst (**125**) and the reactants (methyl acrylate (**59**) and β-methylstyrene (**69**)) in the cross-metathesis reaction with and without cresol (**266**) being added. As baseline case, a solution of Grubbs II catalyst (**125**) (1 mole) and β-methylstyrene (**69**) (2 moles) in DCM (10 mL) was therefore stirred at 40°C for 1 hour, whilst argon was bubbled through the solution. The solution was then concentrated until all the DCM was removed, 0.6 mL $CDCl_3$ added and the sample analysed by NMR. Apart from the expected P-resonance of the catalyst (at δ 28.9 ppm), the ^{31}P NMR spectrum (Figure 4.26) also showed a resonance at δ 27.5 ppm, which could possibly be allocated to the phosphorous in the Grubbs catalyst where the benzyl carbene has been replaced by an ethyl carbene; the catalyst residue after formation of the stilbene (*cf*. 4.6). ^{1}H and ^{13}C NMR confirms the formation of the new carbene as a quartet at δ 18.53 (J = 5.3 Hz) ppm and a singlet at δ 315.2 ppm respectively, were observed in the relevant NMR spectra (Plates 31a and 31b) of the reaction mixture. The fact that the resonance at δ 27.5 ppm in the ^{31}P NMR spectrum actually originates from the ruthenium complex containing an ethyl carbene was confirmed by the carbene proton (at δ 18.53 ppm) correlating with the phosphorous in the ^{1}H-^{31}P HMBC spectrum. When *p*-cresol (**266**) (4 moles) was added to a similar reaction mixture, no changes in the chemical shift of these ^{31}P, ^{1}H and ^{13}C resonances were observed, though the homo-metathesis reaction of the methylstyrene (**69**) was slowed down by the addition of the cresol.

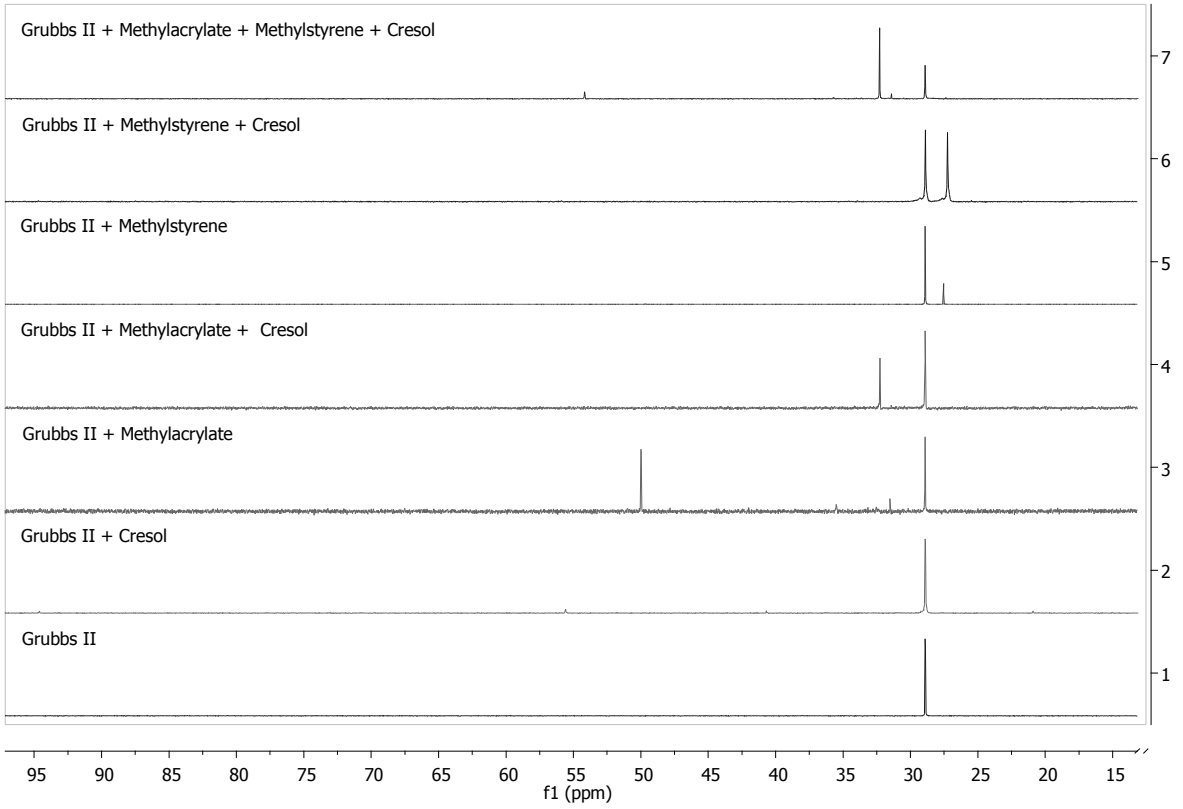

Figure 4.26: Overlayed ^{31}P spectra of reagents and reaction mixtures.

Secondly, the reaction of Grubbs II catalyst (**125**) with methyl acrylate (**59**) was investigated without cresol (**266**) being added and in the presence of 2 eq. of cresol (**266**), with regard to the methyl acrylate (**59**). In the absence of cresol (**266**), the ^{31}P NMR (Figure 4.26) showed, apart from the resonances belonging to the phosphine in the catalyst (δ 28.9) and phosphine oxide (δ 50.8), another signal at δ 31.5. Since no product formation could be found at all, careful analysis of the reported literature indicated this resonance could be coming from 1,4-addition of the tricyclohexylphosphine liberated from the catalyst to the acrylate, thus leading to the zwitterionic phosphonium compounds (**290** and **291**) (Figure 4.27).[9] When the reaction was left for 2.5 hours before NMR analysis, it was found that the resonance at δ 31.5 ppm almost disappeared and, apart from the phosphine oxide signal (δ 50.8 ppm), four new P-resonances (δ 35.5, 32.5, 32.4, and 32.3 ppm) were observed. Since Lummiss *et al.*[25] and Bailey and Fogg[26] found that several oligomeric products like (**292** and **293**) could be formed through reaction of the zwitterionic phosphonium compound (**291**) with more acrylate molecules (**59**), these phosphorous resonances

could be indicative of the formation of such compounds, which could exist as either the anionic or protonated forms, after prolonged reaction times. The existence of products like (**292, 293** and **296**) in the reaction mixture was confirmed by MALDI - TOF MS analysis where the molecular ion of *m/z* 453 was found.

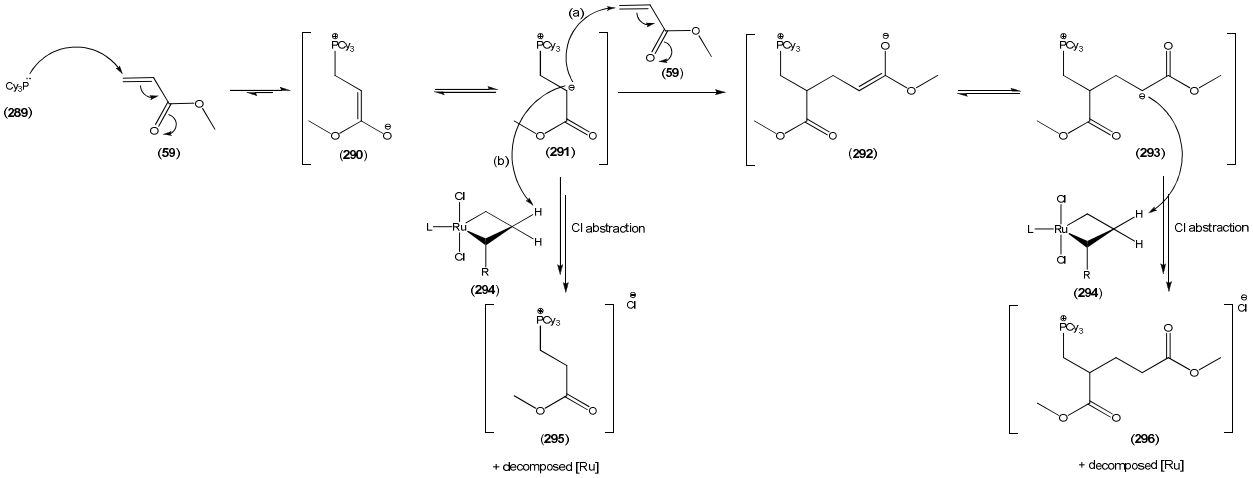

Figure 4.27: Zwitterionic phosphonium compound formation via 1,4-addition of tricyclohexylphosphine (**289**) and methyl acrylate (**59**).

The resonance at δ 35.5 ppm in the ^{31}P spectrum (Figure 4.32) obtained after 2.5 hours, could probably be assigned to the methylidene carbene ruthenium species (**297**) as Lummiss *et al.*[8] reported this compound to have a phosphorous signal at δ 37.1 ppm (NMR in C_6D_6). The formation of the methylidene carbene (**297**) (Figure 4.28) was confirmed by an additional carbene resonance at δ 17.76 ppm in the ^{1}H spectrum of the reaction mixture (Figures 4.29 and 4.31) and is explicable in terms of a very slow reaction between the Grubbs II catalyst and the acrylate.

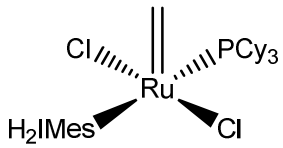

(**297**)

Figure 4.28: Structure of methylidene carbene ruthenium species (**297**)

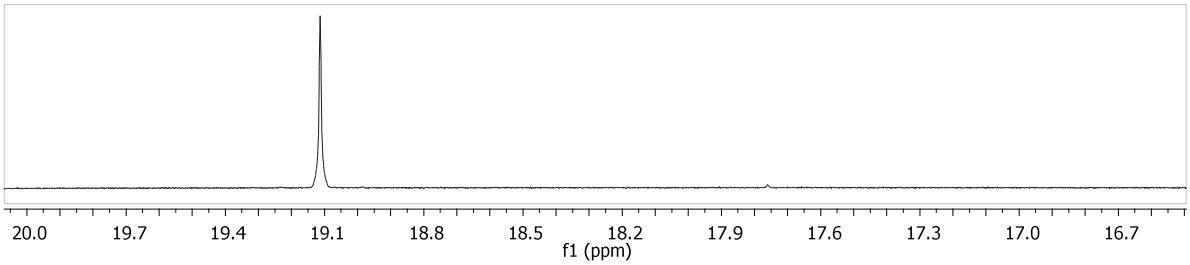

Figure 4.29: Carbene region of the ^{1}H NMR spectrum of the Grubbs II (**125**), in the presence of methyl acrylate (**59**), after 1 hour.

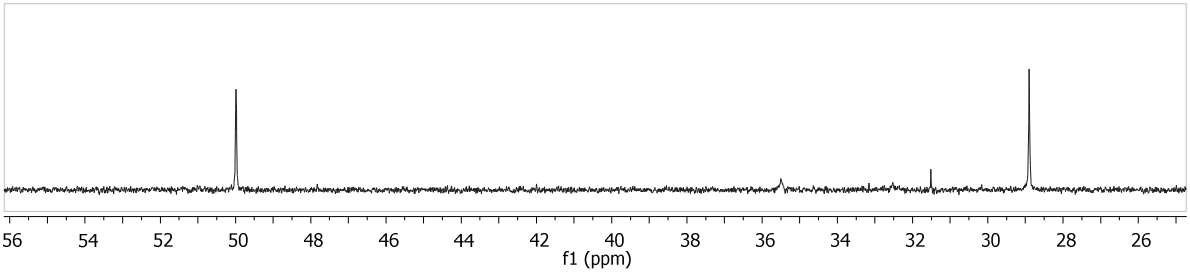

Figure 4.30: ^{31}P spectrum of the Grubbs II (**125**), in the presence of methyl acrylate (**59**), after 1 hour.

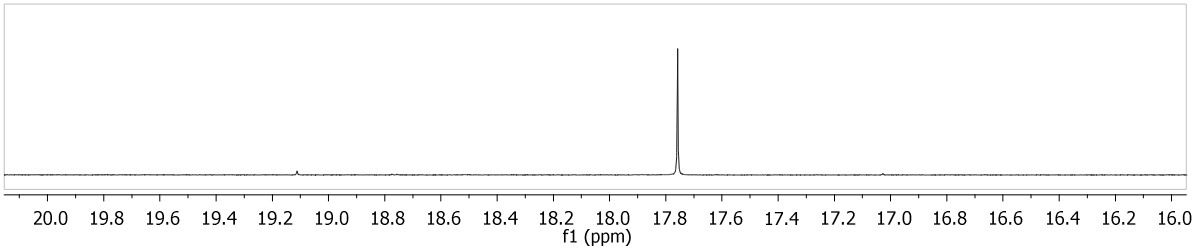

Figure 4.31: Carbene region of the ^{1}H NMR spectrum of the Grubbs II (**125**), in the presence of methyl acrylate (**59**), after 2.5 hours.

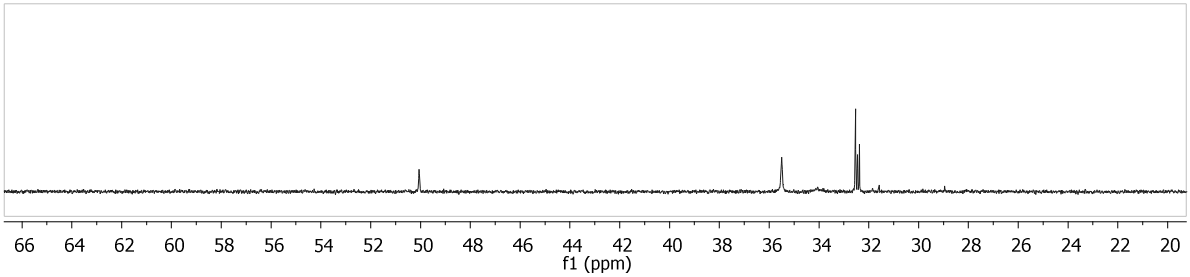

Figure 4.32: ^{31}P spectrum of the Grubbs II (**125**), in the presence of methyl acrylate (**59**), after 2.5 hours.

When the reaction between the acrylate and Grubbs II catalyst was repeated in the presence of cresol (2 eq. with regards to the methyl acrylate) and the reaction

mixture analysed by ^{31}P NMR after 1 hour as described before, the Grubbs II phosphine resonance (δ 28.9 ppm) was accompanied by an additional signal at δ 32.3 ppm. Since it was already established that the zwitterionic phosphonium compound (**295**) could be formed through interaction between the 'liberated' tricyclohexylphosphine and the acrylate, this resonance probably originated from the protonated form of the anion (**290** and **291**) (Figure 4.27), which was confirmed by a molecular ion at *m/z* 367 in the MALDI-TOF MS.

To investigate and confirm the possibility that compounds like $[PCy_3(CH_2)_2CO_2Me]Cl$ (**295**) or its anion (**290** and **291**) could be responsible for the observed P resonances, in the reaction of the Grubbs catalyst with methyl acrylate in the presence or absence of cresol, the P-salts (**295**) and/or (**296**) was synthesized by stirring PCy_3 (1 mole), methyl acrylate (**59**) (1 mole) and LiCl (1 mole) in DCM (5 mL) at room temperature with and without added cresol for 4 hours. After completion of the reactions, the mixtures were concentrated until all the DCM was removed, $CDCl_3$ (0.6 mL) added and the ^{31}P NMRs obtained. Once again the expected phosphine oxide signal was accompanied by two new resonances δ 32.3 and 31.7 ppm in both reaction mixtures. Although both resonances were present in both reactions, the cresol had an effect on the ratio of the two "P-salt" signals in the reaction mixtures in that it changed from 0.5:1 (δ 32.3 ppm : δ 31.7 ppm) to 1.5:1 with the addition of the cresol. Although the formation of the protonated salt (**295**) would require a source of protons, which would not be readily available in the absence of cresol, Bailey and Fogg[9] also reported the formation of this compound when no external proton source was available and explained it in terms of hydrogen abstraction from the metallacyclobutane (**294**) formed during the metathesis reaction (*cf*. 4.6). Since this could not be the case in the current investigation, another source of protons, the origin of which is not clear at the moment, must be available for the formation of the protonated 1,4-addition product (**292**).

Finally, the CM reaction between β-methylstyrene (**69**) and methyl acrylate (**59**) (1 : 1) in the presence of cresol (**266**) (2 eq.) was followed over 60 minutes by ^{31}P NMR (Figure 4.26) and the following species could be identified in the reaction mixture:

The tricyclohexylphosphine oxide-cresol complex at δ 54.2 ppm, the protonated 1,4-addition product (**295**) at δ 32.3 ppm, the anion of the 1,4-addition product (**290** or **291**) at δ 31.4 ppm, and the tricyclohexylphosphine (**289**) of the Grubbs II catalyst (**125**) (δ 28.9 ppm) While it was hoped that the formation and identification of other phosphorous species might shed some light on the mechanism of the reaction and how cresol addition would influence the reaction to enhance the formation of the cross-metathesis product (**195**) over the homo-metathesis one (**258**), the results were inconclusive as to the mechanism of the metathesis reaction and only indicated that some dissociation of the tricyclohexylphosphine (**289**) from the catalyst indeed occurs and that it prefers to react with the acrylate rather than form a complex with the cresol as was postulated by Forman *et al*.[1] This result confirms the conclusion of Bailey and Fogg[9] that during the metathesis reaction over the Grubbs II catalyst (**125**), the phosphine ligand (**289**) dissociates from the metal centre and has a tendency to react with the acrylate (**59**) to form a phosphonium zwitterion salt (**295** and/or **296**) that could be protonated if a source of hydrogen ions is present in the reaction mixture.

4.6 Possible mechanism to explain the enhanced formation of the cross-metathesis products

Since the ^{13}P NMR investigation did not shed any light on the influence of cresol on the metathesis reaction, the question remained as to how the addition of cresol could enhance the cross-metathesis process over homo-metathesis. From the results obtained during the current investigation it is clear that in the absence of cresol, the styrene analogues are way more reactive towards the Grubbs II catalyst than the acrylate (*cf* Paragraph 4.2); which is evident from the fact that only the homo-metathesis product from the styrene is formed when a mixture of acrylate and styrene is subjected to the reaction. If the styrene substrates are prone to homo-metathesis, it means that the first step in the catalytic cycle would be the regeneration of the benzylidene carbene ruthenium complex (**298**), which then reacts with another styrene molecule (**69**) to form the stilbene product (**258**) (Figure 4.33). Benzylidene carbene ruthenium complex (**298**) may alternatively react with acrylate (**125**) (in the presence of cresol) to form the cinnamate (**305**) (Figure 4.34). If the

ethylidene or methylidene carbene moieties (**300**) or (**303**) would not react with a styrene molecule, but rather with an acrylate entity (**125**) (Figure 4.35), the catalytic cycle should be completed by the formation of either the cinnamate product (**305**) or the acrylate homo-metathesis product (**309**). The fact that acrylate homo-metathesis is never observed, points towards acrylate being such a lousy reactant in the metathesis reaction with Grubbs II catalyst that the catalytic cycle as depicted in Figure 4.35 is never followed.

From the results in paragraph 4.3.2 (Table 4.1) it also is clear that the more electron rich the styrene becomes, the higher the tendency towards homo-metathesis, so it could be concluded that the Grubbs II catalyst shows a preference towards reaction with electron rich substrates.

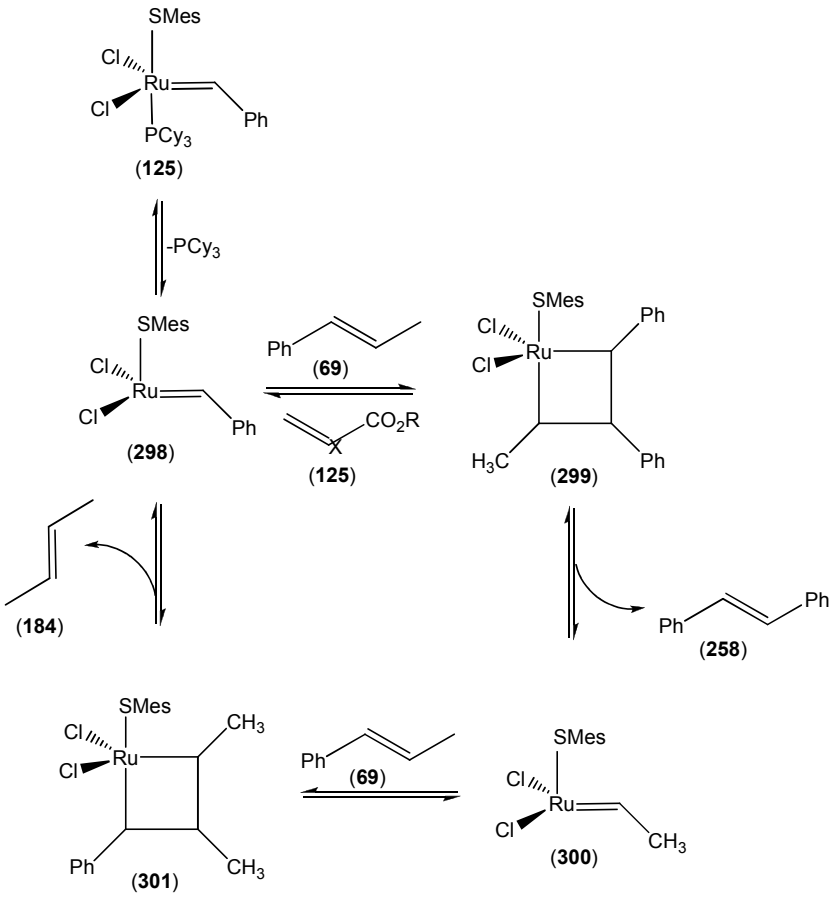

Figure 4.33: Catalytic cycle for the metathesis reaction between β-methylstyrene (**69**) and acrylate (**125**) with and without cresol (**266**).

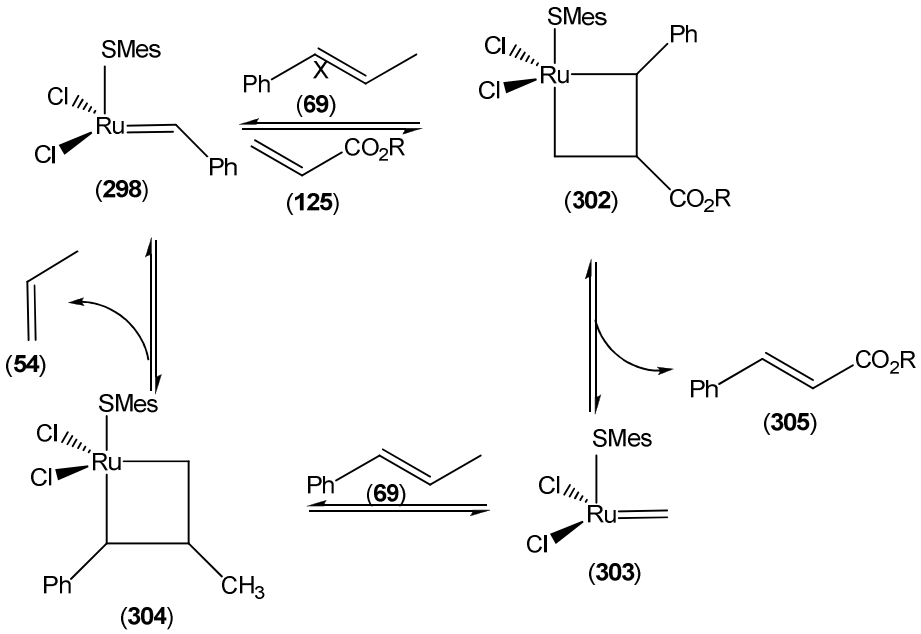

Figure 4.34: Mechanism of the metathesis reaction between β-methylstyrene (**69**) and acrylate (**125**) with cresol (**266**).

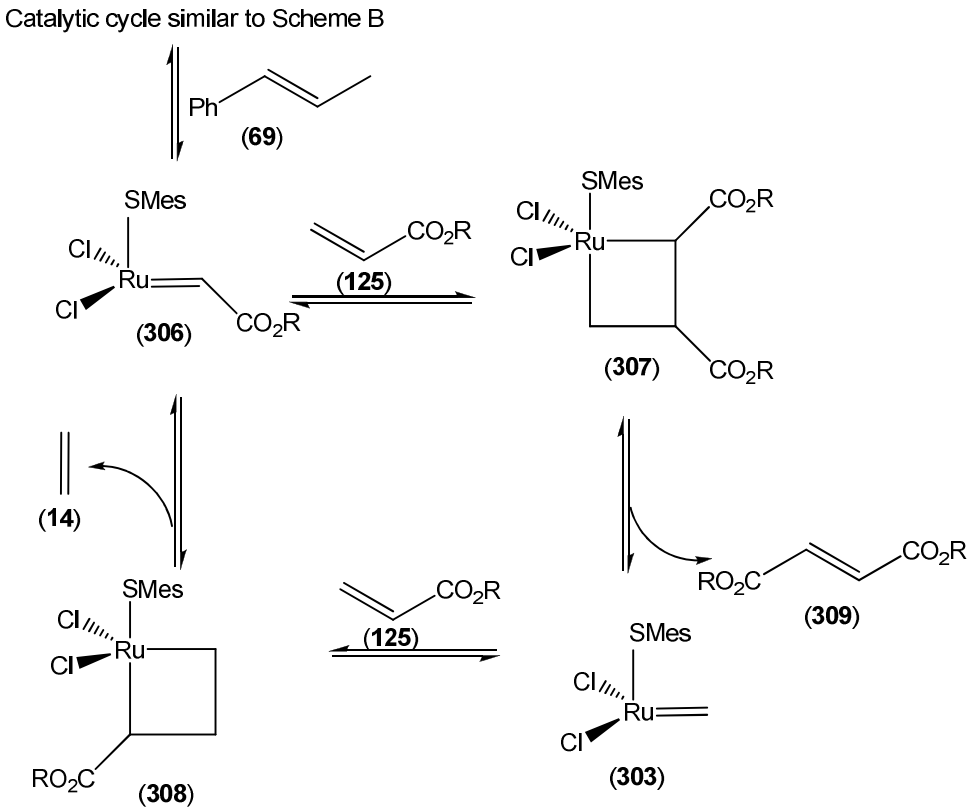

Figure 4.35: Catalytic cycle for acrylate (**125**) homo-metathesis.

Forman *et al.*[11] proposed the addition of phenols to stabilize the Grubbs II catalyst by slowing down the dissociation of the tricyclohexylphosphine from the metal and once dissociated, prevents the phosphine from binding to the metal again (Figure 4.5). This explanation, however, does not allow for the fact that the more reactive styrene analogue becomes less reactive than the acrylate moiety when cresol is added to the reaction mixture, i.e. either the ethylidene or methylidene carbenes [(**300**) or (**303**)] in Figures 4.33 and 4.34 would rather react with the acrylate (**125**) (as depicted in Figure 4.35) than the styrene (**69**) in the presence of cresol. If the relative reactivity of the reactants (styrene analogues and/or acrylates) is to be influenced by cresol addition, some interaction between the styrene and/or the acrylate and cresol should exist. Virtually no difference in the chemical shift values of the aromatic protons of cresol were, however, observed when the ^{1}H NMR of a mixture of *p*-cresol (**266**) and β-methylstyrene (**69**) was compared to that of pure *p*-cresol (**266**) (Figure 4.22). With acrylate on the other hand, the chemical shift of the aromatic proton resonances of the cresol moved from δ 7.04 and 6.73 ppm to δ 7.03 and 6.80 ppm, indicating some proton donating interaction between the cresol and the acrylate. The protonation of acrylate by cresol was confirmed by the formation of the protonated 1,4-addition product of tricyclohexylphosphine and acrylate (*cf* paragraph 4.5.3). Since protonation or formation of a hydrogen-bonding complex between cresol and the acrylate would have an electron-withdrawing effect on the acrylate, this interaction would render the acrylate even more electron deficient and thus less reactive towards metathesis with the Grubbs II catalyst. There is therefore no chance that the ethylidene or methylidene carbene complexes (**300**) and (**303**) could preferentially react with the acrylate in the presence of the β-methylstyrene. The observed enhancement of cross-metathesis over homo-metathesis of β-methylstyrene on addition of cresol to the reaction mixture, must therefore lie in another aspect of the reaction.

The possibility of a secondary metathesis reaction between the stilbene (**258**), formed as primary metathesis product, and methyl acrylate (**59**) was therefore investigated and a mixture of methyl acrylate (2 moles) and *cis*-stilbene (2 moles) stirred over the Grubbs II catalyst (1 mole) for 2 hours at 40 °C. The ^{31}P NMR spectrum (Figure 4.37) of the reaction mixture, however, displayed only the Grubbs II

(**125**) (δ 28.9 ppm) and phosphine oxide (δ 50.8 ppm) resonances. On addition of cresol (4 moles) to the mixture, oligomers derived from the expected zwitterionic phosphonium compound (**291**) and its protonated form (**295**) with resonances at δ 31.5 and 32.5 as well as a peak at 34.2 ppm, most probably an oligomer of (**291**), were observed in the ^{31}P NMR spectrum (Figure 4.27). Since no indication of the cross-metathesis product (**195**) was found during this reaction, it could be concluded that the cinnamate (**195**) formed during the reaction of β-methylstyrene with acrylate in the presence of cresol was not the result of a secondary metathesis process involving the primary stilbene product and the acrylate. A computational study by Paredes-Gil *et al*.,[27] supports this hypothesis as their results showed that the postulated metallacyclobutane intermediate formed during the reaction of stilbene with acrylate, would be very unstable.

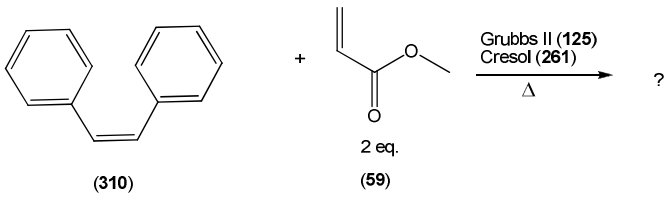

Figure 4.36: Metathesis reaction of *cis*-stilbene (**310**) and methyl acrylate (**59**).

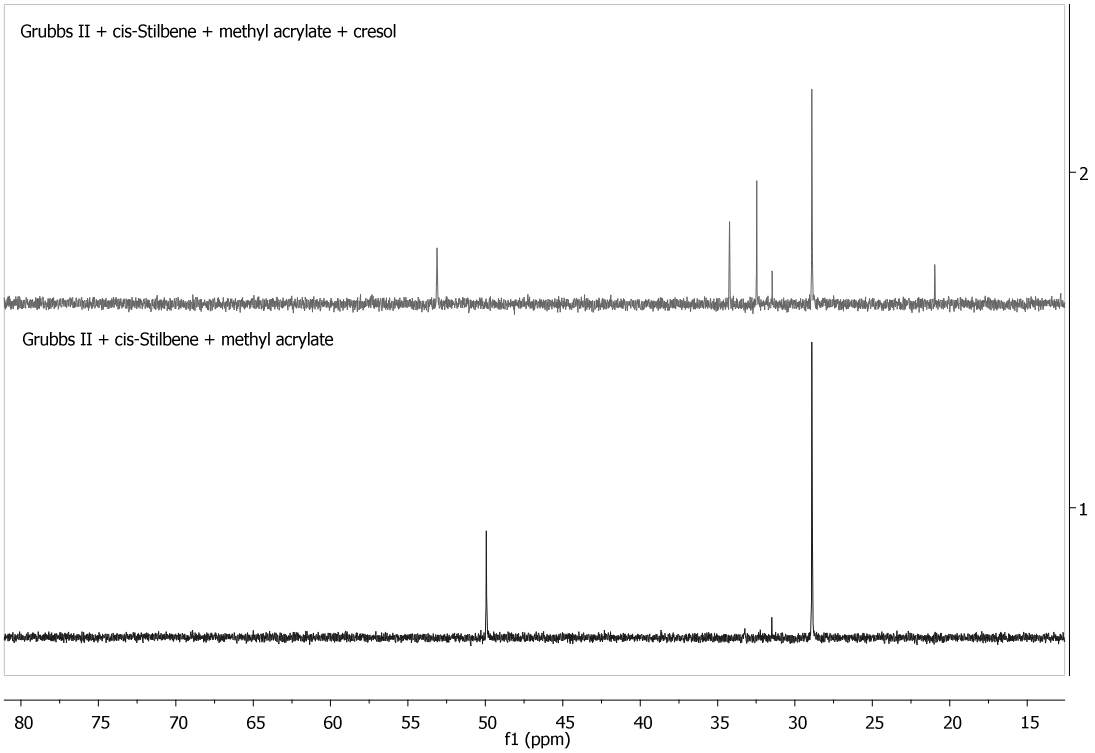

Figure 4.37: ^{31}P spectrums of Grubbs II, *cis*-stilbene (**310**) and methyl acrylate (**59**), with and without cresol (**266**) after 2 hours.

With the possibility of a secondary metathesis reaction being the cause of the enhanced formation of the cross-metathesis product excluded, and the fact that the relative reactivity of the two reactants in the presence of cresol could also not encounter for this phenomenon, attention was again turned towards the interaction of cresol with the Grubbs catalyst. Although Forman *et al*.[11] ascribed the enhanced cross-metathesis when cresol was added to the reaction between alkenes and acrylate to improved stability of the catalyst and a more available co-ordination site due to enhanced dissociation of the tricyclohexylphosphine from the metal centre (vide supra), this postulate falls short of explaining the observed reaction outcome as it does not take into account that the β-methylstyrene is the more reactive of the two reactants.

These authors, however, also postulated the formation of complex (**288**) during the addition of phenol to the Grubbs II catalyst (Figure 4.5). If it is assumed that (**288**) actually is the active form of the catalyst for the cross-metathesis reaction, the reaction with the reactants should change to an associative mechanism (rather than a dissociative process) where the co-ordination number of the ruthenium increases from 5 to 6 to allow for the additional extra ligand to attach itself to the metal centre. In this instance the catalyst complex would become sterically more crowded and the steric size of the incoming ligand (reactant) would play a decisive role in its ability to react with the metal centre in the first step of the reaction. Since acrylate would be sterically less demanding when compared to *trans*-β-methylstyrene, this aspect of the reaction could explain the enhanced formation of the cross-metathesis product when cresol is added to the reaction mixture. In order to probe the possibility of steric size playing a role during the metathesis reaction with the Grubbs catalyst (**125**), methyl acrylate (**59**) was substituted with methyl crotonate (**311**) in a metathesis reaction under the same reaction conditions as before (*cf*. 4.3.1) and it was found that the cinnamate (**195**) only formed in 31% yield. The possibility of an associative mechanism being the cause of the enhanced cross-metathesis process during metathesis reactions with acrylate in the presence of cresol was corroborated by Fogg and co-workers[28,29] who found the cross-metathesis reaction to be the main

reaction when acrylates were reacted with β-methylstyrenes over the Hoveyda-Grubbs catalyst (**128**), which resembles complex (**288**) in structure.

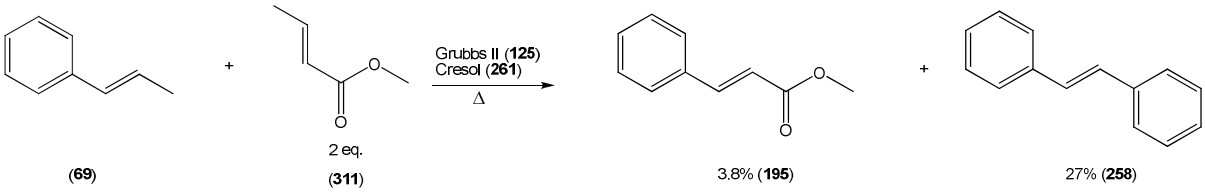

Figure 4.38: Metathesis reaction of methyl crotonate (**311**) and methyl acrylate (**59**).

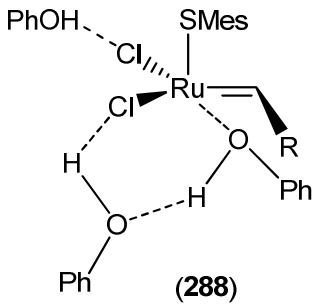

Figure 4.39: Proposed active Grubbs II complex (**288**).

4.7 UV investigation

With the different cinnamates (**7**, **35**, **195**, **278**, **281** and **282**) and unsaturated ketones (**277** and **280**) (Figure 4.40) in hand, it was decided to investigate the UV-B blocking abilities of these compounds by UV spectroscopy (Figure 4.41) to see if OMC (**7**) would really be the best sun blocking compound from a scientific point of view. UV absorption spectra of these compounds over the range 200 - 800 nm were therefore obtained. Since the UV-B blocking ability is associated with the absorption of light in the 290 – 320 nm range, the absorption of the different compounds over this wavelength were compared. From the graph (Figure 4.41) it is clear that OMC (**7**) with a UV absorbency of *ca* 1 is a good UV blocker, however, both of the shorter chained *p*-methoxycinnamate analogues, methyl (E)-*p*-methoxycinnamate (**35**) and butyl (E)-*p*-methoxycinnamate (**278**) exhibit better UV-B absorbency (*ca* 1.5 – 1.8) and thus blocking abilities over this range of wavelengths. (E)-4-(4-methoxyphenyl)but-3-en-2-one (**277**) also displayed higher UV absorbency than the commercially used OMC (**7**), but as its absorption is to the higher end of the UV-B

range (*ca* 320 nm), it might not be the ideal UV blocker as these represent less harmful UV-rays. Although all three unsubstituted cinnamates (**195**), (**278**) and (**282**) display almost the same or slightly lower UV absorbency when compared to OMC (**7**), the absorption of these compounds are towards the higher frequency end (*ca* 275 nm) and thus more harmful part of the spectrum. All of the compounds investigated, i.e. (**7**, **35**, **195**, **278**, **280**, **281** and **282**), except 4-phenyl-3-buten-2-one (**277**), which shows virtually no absorption between 290 - 320 nm, should in principle have better UV-B blocking abilities and therefore be better sunscreens. It must however be kept in mind that the effectiveness as sunscreen is also dependent on the absorption of the sunscreen containing lotion into the skin as well as the decomposition rate of the compound when exposed to the sun and other biological effects, like carcinogenicity etc. From a purely scientific point of view, it, however, looks as if five, i.e. (**35**), (**195**), (**278**), (**281**) and (**282**), of the compounds prepared in this study should be taken further into a biological evaluation program to determine if a better sunscreen lotion might not exist or can be developed based on one or more of these compounds.

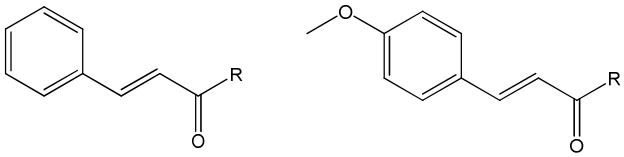

(**195**) R = OMe
(**278**) R = O_nBu
(**282**) R = O-(2-ethylhexyl)
(**277**) R = Me

(**35**) R = OMe
(**281**) R = O_nBu
(**7**) R = O-(2-ethylhexyl)
(**280**) R = Me

Figure 4.40: Structures of cinnamates and unsaturated ketones subjected to UV investigation.

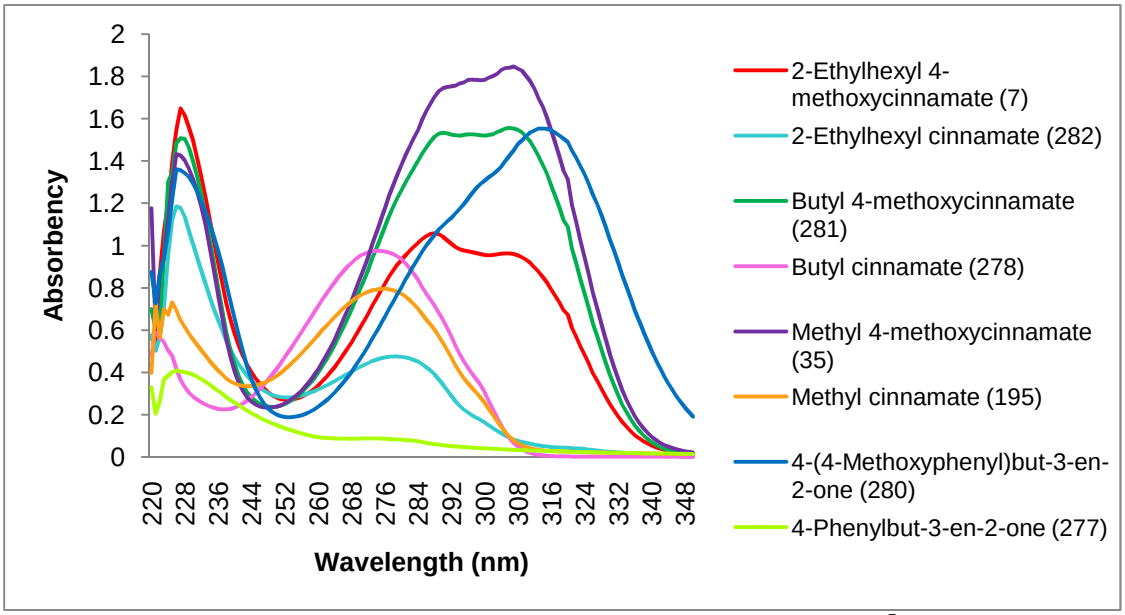

Figure 4.41: Graph of Absorbency *vs* wavelength of OMC analogues ($5x10^{-5}$ M).

4.8 Conclusions and future work

Despite the utilization of a variety of solvents (DCM, THF, and toluene) and reaction conditions (40 - 10 °C), the metathesis reaction between *trans*-β-methylstyrene (**69**) and methyl acrylate (**59**) over the Grubbs II catalyst (**125**) could not be tuned towards the cross-metathesis product and only the stilbene (**258**) was formed in excellent yields (> 99%). When cresol (2eq.) was added to the reaction mixture and the propene side-product stripped away by entrainment with argon, the cross-metathesis product (**195**) could be obtained in moderate yield (38%). By extending the reaction to *trans*–anethole (**11**) and *trans*-4-trifluoromethylsulfonyloxy-β-methylstyrene (**271**), it was determined that with more electron-rich substrates homo-metathesis is enhanced over cross-metathesis (50% vs 36%), while for the electron-poor substrates the a tendency towards the cross-metathesis product (43 vs 4%) was found. Varying the alkyl group of the acrylate from methyl (**59**) to *n*-butyl (**275**) to 2-ethylhexyl (**2**), led to an increase in yield from 38 to 55 to 64%, thus indicating that a sterically more demanding alkyl group attached to the acrylate results in enhanced cross-metathesis to occur. Although MVK (**274**) could also be utilized as substrate in the cross-metathesis reaction, yields were moderate (34%), while with acrolein (**273**) only the homo-metathesis product could be isolated, probably due to polymerization of the acrolein. Finally, it was also shown that the metathesis reaction catalysed by the Grubbs II catalyst (**125**) in the presence of *p*-cresol could be used as a one-step method for the synthesis of OMC (**7**), which was obtained in 47% yield, though not as sole product as stilbene (**259**) concurrently formed in 32% yield.

While it was hoped that an extensive NMR study might shed some light on the mechanism of the reaction and explain how cresol addition influences the reaction to enhance the formation of the cross-metathesis products, ^{1}H,^{13}C and ^{31}P NMR studies were inconclusive as to the mechanism of the metathesis reaction and only indicated that hydrogen bonding between cresol and the catalyst exists, while some dissociation of the tricyclohexylphosphine from the catalyst also occurs. The liberated tricyclohexylphosphine, however, prefers to react with the acrylate rather than form a complex with the cresol as was postulated by Forman *et al*.[10,11]

Although Forman *et al.*[10,11] proposed the addition of phenols to stabilize the Grubbs II catalyst by slowing down the dissociation of the tricyclohexylphosphine from the metal and once dissociated, prevents the phosphine from binding to the metal again, this explanation does not allow for the fact that the more reactive styrene analogue becomes less reactive than the acrylate moiety when cresol is added to the reaction mixture as is evident from the fact that cresol addition enhances cross-metathesis. It was also determined during the current study that the cross-metathesis products are indeed the result of the primary metathesis process and are not formed through secondary metathesis of the stilbene products. In order to explain the formation of the cross-metathesis over homo-metathesis products in the presence of cresol, it is proposed that an associative mechanism rather than a dissociative process is prevailing when cresol is added to the reaction mixture. In this instance the co-ordination number of the ruthenium temporarily increases from 5 to 6 to allow for the additional ligand to be attached to the metal centre. The catalyst complex therefore becomes sterically more crowded and the steric size of the incoming ligand (reactant) would play a decisive role in its ability to react with the metal centre in the first step of the reaction. Since acrylate is a terminal olefin and the O-alkyl group in a remote position with regards to the active centre, it would be sterically less demanding when compared to *trans*-β-methylstyrene, thus presenting a possible explanation for the enhanced formation of the cross-metathesis product. This assumption was proven by substituting methyl acrylate (**195**) with methyl crotonate (**311**) during the reaction and the resulting drop in cross-metathesis product from 38% to 31%. Support for this proposal also comes from results by Fogg and co-workers,[28,29] who reported cross-metathesis to be the dominant if not the only reaction when β-methylstyrenes were reacted with acrylates over the Hoveyda-Grubbs catalyst. It is envisaged that the proposal of an associative rather than a dissociative mechanism for the formation of cross-metathesis products during the reaction in the presence cresol, be evaluated through a molecular modelling study and more experimentation in future.

With the different cinnamates, i.e. OMC (**7**), methyl *p*-methoxycinnamate (**35**), methyl cinnamate (**195**), *n*-butyl cinnamate (**278**), *n*-butyl *p*-methoxycinnamate (**281**), and 2-

ethylhexyl cinnamate (**282**), and unsaturated ketones, 4-phenyl-3-buten-2-one (**277**) and 4-(4-methoxyphenyl)-3-buten-2-one (**280**), in hand, it was decided to investigate the UV-B blocking abilities of these compounds by UV spectroscopy to see if OMC (**7**) would really be the best sun blocking compound of the series form a purely scientific point of view. From the UV absorption spectra (Figure 4.34), four of these compounds, i.e. (**195**), (**278**), (**35**) and (**281**), show better UV-B absorption properties than OMC (**7**) and should be taken further into a biological evaluation program to determine if a better sunscreen lotion might not exist or can be developed based on one or more of these compounds.

References

[1] Stabile, R. G.; Dicks, A. P. *J. Chem. Educ*. **2004**, *81*, 1488 – 1491.

[2] Li. J. J.; Gribble, G. W. *Palladium in Heterocyclic Chemistry: A guide for the Synthetic Chemist*, Gulf Professional Publishing, **2006**, p599.

[3] Lipshutz, B. H.; Taft, B. R. *Org Lett*. **2008**, *10*, 1329 – 1332.

[4] Taylor, H. S.; Vernon, A. A. *J. Am. Chem. Soc*. **1931**, *53*, 2527 – 2536.

[5] Miller, B. J. M.Sc. thesis, University of the Free State, Bloemfontein, SA, 2010.

[6] Senra, J. D.; Malta, L. F. B.; da Costa, M. E. H. M.; Michel, R. C.; Aguiar, L. C. S.; Simas, A. B. C.; Antunes, O. A. C. *Adv. Synth. Catal*. **2009**, *351*, 2411 – 2422.

[7] Kniese, M; Meier, M. A. R. *Green Chem*. **2010**, *12*, 169 – 173.

[8] Lee, K. S.; Choi, T. *Org. Lett.* **2011**, *13*, 2908 – 3911.

[9] Samak, B. A.; Amir-Ebrahimi, V.; Corry, D. G.; Hamilton, J. G.; Rigby, S.; Rooney, J. J.; Thompson, J. M. *J. Mol. Catal. A-Chem.* **2000**, *160*, 13 – 21.

[10] Forman, G. S.; Tooze, R.P. *J. Organomet.Chem*. **2005**, *690*, 5863 – 8566.

[11] Forman, G. S.; McConnell, A. E.; Tooze, R.P.; Janse van Rensburg, W.; Meyer, W. H.; Kirk, K. M.; Dwyer, C. L.; Serfontein, D. W. *Organometallics* **2005**, *24*, 4582 – 4542.

[12] Van Tonder, J. H. Ph.D thesis, University of the Free State, Bloemfontein, SA, 2014.

[13] Tan, E. W.; Chan, B.; Blackman, A. G. *J. Am. Chem. Soc*. **2002**, *124*, 2078 – 2079.

[14] Gardner, E. P.; Sperry, P. D.; Calvert, J. G. *J. Phys. Chem*. **1987**, *91*, 1922 – 1930.

[15] Scholl, M.; Ding, S.; Lee, C.W.; Grubbs, R.H. *Org. Lett*. **1999**, *1*, 953 – 956

[16] Schwab, P.; Grubbs, R. H.; Ziller, J. W. *J. Am. Chem. Soc.* **1996**, *118*, 100 – 110.

[17] Gallagher, M.M.; Rooney, A.D.; Rooney, J.J. *J. Organomet. Chem.* **2008**, *693*, 1252 – 1260.

[18] Kühl, O. *Phosphoros-31 NMR Spectroscopy: A concise introduction for the synthetic organic and organometallic chemist*, Springer-Verlag Berlin Heidelberg, 2008, p22.

[19] Gholivand, K.; Shariatinia, Z.; Pourayoubi, M. *Z. Anorg. Allg. Chem*. **2005**, *631*, 961 – 967.

[20] Gholivand, K.; Hosseini, Z.; Pourayoubi, M.; Shariatinia, Z. *Z. Anorg. Allg. Chem*. **2005**, *631*, 3074 – 3079.

[21] Olah, G. A.; McFarland, C. W. *J. Org. Chem*. **1969**, *34*, 1832 – 1834.

[22] Caraballo, R.; Rahm, M.; Vongvilai, P.; Brinck, T.; Ramström, O. *Chem. Commun.* **2008**, 6603 – 6605.

[23] Hilliard, C. R.; Bhuvanesh, N.; Gladsz, J. A.; Blümel, J. *Dalton Trans*. **2012**, *41*, 1742 – 1754.

[24] Hu, B.; Gay, I. D. *Langmuir* **1995**, *11*, 3845 – 3847.

[25] Lummiss, J.A.M.; Higman, C.S.; Fyson, D.L.; McDonald, R.; Fogg, D.E. *Chem. Sci.* **2015**, *6*, 6739 – 6746.

[26] Bailey, G.A; Fogg, D.E. *J. Am. Chem. Soc*. **2015**, *137*, 7318 – 1321.

[27] Paredes-Gil, K.; Solans-Monfort; X.; Rodriguez-Santiago, L; Sodupe, M.; and Jaqeu, P. *Organometallics*, **2014**, 33, 6065 – 6075.

[28] Lummiss, J. A. M.; Oliveira, K. C.; Pranckevicius, A. M. T.; Santos, A. G.; dos Santos, E. N.; Fogg, D. E. *J. Am. Chem. Soc*. **2012**, *134*, 18889 − 18891.

[29] Bailey, G. A.; Fogg, D. E. *J. Am. Chem. Soc*. **2015**, *137*, 7318 − 7321.

EXPERIMENTAL

Chapter 5: Experimental

5.1: Chromatography

5.1.1: Thin-Layer Chromatography (TLC)

Qualitative TLC was conducted on Merck TLC-aluminium plates: Silica Gel F_{254} (0.2 mm layer) divided into strips (*ca* 2.5 cm x 5 cm). Eluent was prepared v/v. R_f values are those observed in these qualitative TLC assessments. Bands were distinguished by making use of a UV light (254 nm).

5.1.2: Preparative Thin-Layer Chromatography (PLC)

PLC was conducted on glass plates (20 cm x 20 cm) coated with a layer (1 mm) of Merck Kieselgel 60 PF_{254} that had been air-dried overnight at room temperature. Eluent was prepared v/v. Crude mixture (15 – 20 mg per plate) was applied and after development, in the appropriate solvent system, the plates were air-dried. Bands were distinguished by making use of a UV light (254 nm) after which the bands were scraped off and the product removed from the silica with acetone. The solvent was then removed under reduced pressure on a water bath at *ca* 40 °C.

5.1.3: Flash Column Chromatography (FCC)

A glass column was charged with 100 g of silica gel (Machery - Nagel silica gel 60, 0.063 – 0.2mm / 70 – 230 mesh ASTM) for every 1 g of crude product. Air was disposed of by elution with the appropriate solvent under N_2-pressure. The crude product was dissolved in the minimum amount of appropriate solvent and loaded onto the column. The purified products were recovered by elution under N_2-pressure with the appropriate solvent system. Fractions were collected, clean fractions combined (TLC) and the solvent removed under reduced pressure on a water bath at *ca* 40 °C.

5.2 Spectroscopical Methods

5.2.1 Nuclear Magnetic Resonance Spectroscopy (NMR)

NMR-spectroscopy was performed on a Bruker AM 600 FT spectrometer at 20 ºC unless specified differently. $CDCl_3$ (deuterochloroform) was used as solvent. Chemical shifts are reported in parts per million (ppm) with the solvent peak of $CDCl_3$ being observed at δ 7.26 ppm for the proton spectra and at δ 77.16 ppm for the carbon spectra respectively[1] on the δ-scale, whereas coupling constants are given in Hz. A chemical impurity in proton spectra resonating at δ 1.56 ppm is identified as moisture in accordance with Gottlieb *et al.*[1] Trifluoromethane sulphonic acid and phosphoric acid resonances were determined to appear at δ 10.75 and 9.10 ppm respectively. ^{19}F NMR[2]-spectra were calibrated according to added hexafluorobenzene as reference (δ -164.9 ppm) and ^{31}P NMR[3]-spectra according to phosphoric acid (in a glass capillary; δ 0 ppm).

5.2.2 Infrared Spectroscopy (IR)

IR analysis was performed on a Bruker Tensor 27 infrared spectrometer. Acquisition was obtained over 16 scans and manual baseline corrections performed post analysis.

5.2.3 Ultraviolet Visible Spectroscopy (UV)

UV analysis was conducted on a Cary 50 ultraviolet-visible spectrometer with automated baseline correction over a range of 220 – 800 nm.

5.3 Spectrometrical methods

5.3.1 Mass Spectrometry (MS)

Mass spectrometry was performed by means of electron impact (EI) ionization on a Shimadzu GC-MS QP-2010 fitted with a J & W Scientific DB-5ms capillary column (0.25 µm film thickness, 0.32 mm ID, 30 m), helium as carrier gas at a linear velocity of 27.5 cm/s and an injector temperature of 250 °C. Injections were made in the split mode. The initial column temperature of 50 °C was kept

for 3 min, where after it was increased to 250 °C at 10 °C/min and kept at this temperature for the rest of the analysis.

Alternatively, MS was performed by means of a Matrix Assisted Laser Desorption Ionization Time-Of-Flight (MALDI-TOF) Bruker Microflex LRF20 in either positive or negative mode with the minimum laser power (337 nm) required to observe signals. Spectra obtained were compared to simulated spectra generated by Bruker Daltonics Molecular Formula Generator 1.0.

5.3.2 High Resolution Mass Spectrometry (HR-MS)

HR-MS spectra were conducted at the University of KwaZulu-Natal, Pietermaritzburg, South Africa.

5.4 Melting points (mp)

Melting points were determined with a Barloworld Scientific Stuart Melting Point (SMP3) apparatus and are uncorrected.

5.5 Anhydrous solvents

Solvents were dehydrated by filtering through a small column of activated neutral alumina (10% v/v) prior to use.

5.6 Standard Work-up Procedure

Unless specified otherwise, the solvent was first distilled off after which EtOAc (*ca*. 50 mL) was added to the reaction mixture. H_2O was added to this reaction mixture and the aqueous (*aq*.) phase extracted into EtOAc. The organic extract was then dried over either $MgSO_4$ and the solvent removed *in vacuo* at *ca*. 40 °C. Subsequent purification *via* PLC afforded the product.

5.7 Triflate esterification [4]

To a cooled (-20°C) solution of substrate (1 eq.) and DMAP (1.1 eq.) in DCM (50 mL), under Ar, was added dropwise a solution, also at -20°C, of triflic anhydride (1.1 eq.) in dry DCM (25 mL). The reaction mixture was allowed to

warm to rt. and stirred overnight. The reaction mixture was then subjected to FCC (DCM) to yield the purified product.

5.7.1 4-Propionylphenyl trifluoromethanesulfonate (268)

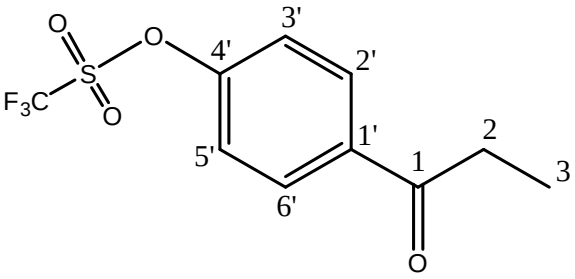

4'-Hydroxypropiophenone (**267**) (2.00 g, 13.3 mmol), DMAP (1.79 g, 14.7 mmol) and triflic anhydride (**269**) (4.13 g, 14.7 mmol) was allowed to react overnight according to the general triflate esterification procedure (5.7). The reaction was worked up (5.6) and separated using PLC (DCM) to give 4-propionylphenyl trifluoromethanesulfonate (**268**) as a *light yellow oil*. (3.4 g, 90%): R_f 0.86 (DCM); ^{1}H NMR [600 MHz, $CDCl_3$, plate 11a]: δ 8.02 (2H, d, *J* = 8.9 Hz, H-3',5'), 7.33 (2H, d, *J* = 8.9 Hz, H-2',6'), 2.97 (2H, q, *J* = 7.2 Hz, H-2), 1.18 (3H, t, *J* = 7.2 Hz, H-3); ^{13}C NMR [151 MHz, $CDCl_3$, plate 11b]: δ 198.9 (C-1), 152.4 (C-1'), 136.8 (C-4'), 130.3 (C-3',5'), 121.6 (C-2',6'), 118.7 (q, *J* = 320.7 Hz, CF_3), 32.0 (C-2), 7.9 (C-3); ^{19}F NMR [565 MHz, $CDCl_3$, plate 11f] δ -75.83 (CF_3); IR (neat, cm^{-1}) 1693 (CO); HR-MS (AP+) (*m/z*) calcd for $C_{10}H_{10}O_4F_3S$ $[M]^+$ 283.0252, found 283.0256.

5.8 $NaBH_4$ reduction[5]

The substrate (1 eq.) was added to a solution of $NaBH_4$ (1.5 eq.) in THF:EtOH (1:1, v/v; 50 mL) and stirred until the reaction was deemed to be complete by TLC. After completion of the reaction (TLC), the reaction mixture was concentrated *in vacuo*, washed with acetone (3 x 20 mL) and concentrated again. The crude product was then obtained by following the standard work-up procedure (5.6) and purified using FCC.

5.8.1 Preparation of 4-(1-hydroxypropyl)phenyl trifluoromethanesulfonate (270)

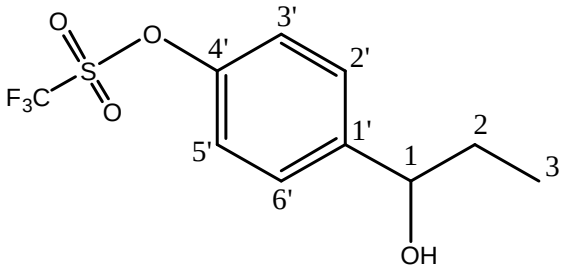

4-Propionylphenyl trifluoromethanesulfonate (**268**) (2.5 g, 8.9 mmol), $NaBH_4$ (0.503 g, 13.3 mmol, 1.5 eq.) was reacted, according to the general $NaBH_4$ reduction procedure (par. 5.8), and monitored using TLC. After completion of the reaction, the mixture was worked up (par. 5.6) and separated using FCC to yield 4-(1-hydroxypropyl)phenyl trifluoromethanesulfonate (**270**) as a *light yellow oil* (1.97 g, 78%): Rf 0.47 (H:A 8:2); ^{1}H NMR [600 MHz, $CDCl_3$, plate 12a]: δ 7.41 (2H, d, *J* = 8.7 Hz, H-2',6'), 7.24 (2H, d, *J* = 8.7 Hz, H-3',5'), 4.63 (1H, t, *J* = 6.5 Hz, H-1), 1.81-1.69 (2H, m, H-2), 1.16 (1H, d, *J* = 6.2 Hz, -OH), 0.91 (3H, t, *J* = 7.4 Hz, H-3); ^{13}C NMR [151 MHz, $CDCl_3$, plate 12b]: δ 148.8(C-4'), 145.3 (C-1'), 127.9 (C-2',6'), 121.3 (C-3',5'), 118.9 (q, J = 320.8Hz, CF_3), 75.0 (C-1), 32.2 (C-2), 10.1 (C-3); ^{19}F NMR [565 MHz, $CDCl_3$, plate 12f] δ -75.95 (CF_3); HR-MS (ES-) (*m/z*) calcd for $C_{10}H_{12}O_4F_3S$ $[M]^+$ 283.0252, found 283.0255.

5.9 Elimination reaction[6]

The substrate (1 eq.) was dissolved in dry hexane (40 mL) and anhydrous $CuSO_4$ (1.5 eq.) added after which the reaction mixture was refluxed overnight or until the reaction was deemed complete by TLC, under Ar atmosphere. The solvent was then removed *in vacuo*, and the solvent distilled off after which hexane (*ca* 50 mL) was added to the reaction mixture. H_2O was added to this reaction mixture and the aqueous (*aq*.) phase extracted into hexane. The organic extract was then dried over $MgSO_4$ and the solvent removed *in vacuo* at *ca*. 40 °C. Subsequent purification *via* PLC afforded the product.

5.9.1 (E)-4-(prop-1-en-1-yl)phenyl trifluoromethanesulfonate (271)

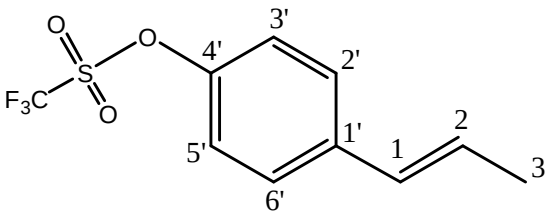

Following the general elimination reaction procedure (par. 5.9) 4-(1-hydroxypropyl)phenyl trifluoromethanesulfonate (**270**) (1.0 g, 3.5 mmol) and anh. $CuSO_4$ (10.84 g, 5.3 mmol) were stirred in dry hexane (40 mL) for 4 days. After which the reaction was worked up (par. 5.6) and separated using FCC to yield (*E*)-4-(prop-1-en-1-yl)phenyl trifluoromethanesulfonate (**271**) as a *light yellow oil* (0.56 g, 60%): R_f 0.76 (H:A 8:2); ^{1}H NMR [600 MHz, $CDCl_3$, plate 13a]: δ 7.37 (2H, d, *J* = 8.6 Hz, H-2',6'), 7.18 (2H, d, *J* = 8.6 Hz, H-3',5'), 6.39 (1H, br d, *J* = 15.8 Hz, H-1), 6.29-6.23 (1H, m, H-2), 1.90 (3H, m, H-3); ^{13}C NMR [151 MHz, $CDCl_3$ plate 13b]: δ 148.3 (C-4'), 138.5 (C-1'), 129.4 (C-1), 128.3 (C-2), 127.5 (C-2',6'), 121.5 (C-3',5'), 118.9 (q, J = 320.8Hz, CF_3), 18.6 (C-3); ^{19}F NMR [565 MHz, $CDCl_3$, plate 13f] δ -75.85 (CF_3); *m/z* (EI)* 266 (M^+, 19).

5.10 Metathesis reactions

5.10.1 Method A[7]

The styrene analogue (1 eq.), acrylate (2 eq.) and Grubbs II catalyst (5 mol%), was stirred in dry solvent (10 mL), under Ar atmosphere, at the specified temperature for *ca*. 2 hours until completion of the reaction (TLC). The reaction mixture was then filtered and washed with cold DCM (3 x 30 mL) to yield the purified product.

*Sample decomposed before HR-MS was obtained.

5.10.1.1 Metathesis of trans-β-methylstyrene (69) and methyl acrylate (59)

5.10.1.1.1 Initial conditions

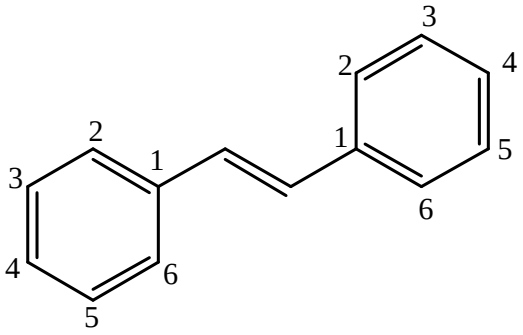

trans-β-Methylstyrene (**69**) (0.20 mL, 1.5 mmol, 1 eq.), methyl acrylate (**59**) (0.28 mL, 3.1 mmol, 2 eq.) and Grubbs II catalyst (**125**) (6.5 mg, 0.0077 mmol, 0.5 mol%) were refluxed in dry DCM (10 mL) for 2 h according to method A to yield *trans-stilbene*[8] (**258**) as colourless platelets (0.27 g, 99%): R_f 0.87 (H:A 8:2); mp 123.6°C; ^{1}H NMR (600 MHz, $CDCl_3$, plate 1a) δ 7.55 (4H, br d, *J* = 8.2 Hz, H-2,6), 7.39 (4H, t, *J* = 7.7 Hz, H-3,5), 7.29 (2H, m, H-4), 7.14 (2H, s, CH=CH); ^{13}C NMR (151 MHz, $CDCl_3$, plate 1b) δ 137.5 (C-1), 128.8 (C-3,5 and CH=CH), 127.8 (C-4), 126.7 (C-2,6); *m/z* (EI) 180 (M^+, 100).

5.10.1.2 Temperature

Repeating the reaction above at 25 and 10 °C, yielded *trans*-stilbene[7] (**258**) as only product (*cf*. 5.8.1) (>99% and 98 %, respectively).

5.10.1.3 Solvent

Replacement of DCM in the reaction above with THF or toluene or performing the reaction under neat conditions yielded stilbene[7] (**258**) (*cf*. 5.8.1) (>99%, 98% and 99%, respectively) as only product at 40 °C.

5.10.1.4 Reagent ratio

The above metathesis reaction, using DCM as solvent, was repeated with different reagent ratios at 40 °C:

trans-β-Methylstyrene (**69**) (0.2 mL, 1.5 mmol, 1 eq.) and methyl acrylate (**59**) (0.69 mL, 7.7 mmol, 5 eq.) yielded *trans*-stilbene[7] (**258**) (97%); *cf*. par. 5.10.1.1.1.

trans-β-Methylstyrene (**69**) (0.2 mL, 1.5 mmol, 1 eq.) and methyl acrylate (**59**) (0.13 mL, 1.5 mmol, 1 eq.) yielded *trans*-stilbene[7] (**258**) (>99%); *cf*. par. 5.10.1.1.1.

trans-β-Methylstyrene (**69**) (1.0 mL, 7.5 mmol, 5 eq.) and methyl acrylate (**59**) (0.13 mL, 1.5 mmol, 1 eq.) yielded *trans*-stilbene[7] (**258**) (>99%); *cf*. par. 5.10.1.1.1.

5.10.1.2 Metathesis of anethole (11) and methyl acrylate (59)

Anethole (**11**) (0.20 mL, 1.3 mmol, 1 eq.), methyl acrylate (**59**) (0.24 mL, 2.7 mmol, 2 eq.) and Grubbs II (**125**) (5.7 mg, 0.0067 mmol, 0.5 mol%) were reacted for 2 h according to method A to yield *trans-4,4'-dimethoxystilbene*[7] (**259**) as colourless platelets (0.28 g, 98%): R_f : 0.54 (H:A 8:2); mp 214.2°C; ^{1}H NMR (600 MHz, $CDCl_3$, plate 2a) δ 7.43 (4H, d, *J* = 8.8 Hz, H-2,6), 6.93 (2H, s, C<u>H</u>=C<u>H</u>), 6.89 (4H, d, *J* = 8.8 Hz, H-3,5), 3.83 (6H, s, -OC<u>H</u>$_3$); ^{13}C NMR (151 MHz, $CDCl_3$, plate 2b) δ 159.2 (C-4), 130.6 (C-1), 127.6 (C-2,6), 126.3 (<u>C</u>H=<u>C</u>H), 114.2 (C-3,5), 55.5 (O<u>C</u>H$_3$); *m/z* (EI) 240 (M^+, 100).

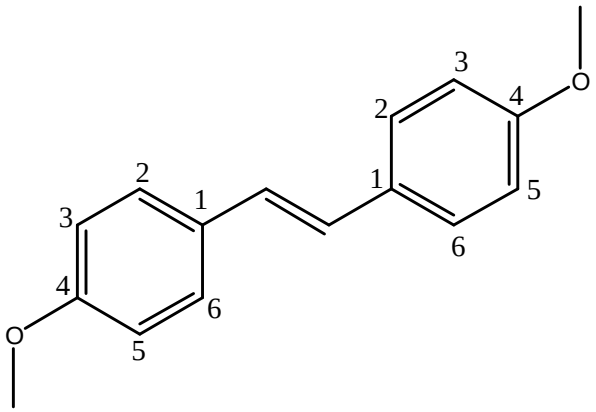

5.10.2 Method B[9]

Grubbs II catalyst (0.5 mol%), *p*-cresol (0.25 eq.) and dry DCM (10 mL) were heated to reflux, stirring, with a steady stream of argon bubbling through the mixture, whilst employing a -20°C condenser. The styrene (1 eq.) and acrylate (2 eq.) were then added to the mixture which was allowed to react for a further *ca*. 2 hours until completion (TLC). The standard work-up procedure (par. 5.6),

followed by PLC of the liquid mixture and washing of the formed precipitate with cold acetone, gave the purified products.

5.10.2.1 Metathesis of trans-β-methylstyrene (69) and methyl acrylate (59)

trans-β-Methylstyrene (**69**) (0.20 mL, 1.5 mmol, 1 eq.), methyl acrylate (**59**) (0.28 mL, 3.1 mmol, 2 eq.), Grubbs II (**125**) (6.5 mg, 0.0077 mmol, 0.5 mol%) and *p*-cresol (**266**) (0.083 g, 0.77 mmol, 0.25 eq.) were subjected to metathesis procedure B for 2 hours. Work-up according to the general work-up procedure (par. 5.6) followed by PLC and purification of the precipitate yielded two products:

trans-Stilbene[7] (**258**) as colourless platelets (49.7 mg, 18%.): R_f 0.87 (H:A 8:2); *cf*. par. 5.8.1.

Methyl cinnamate[10] (**195**) as colourless platelets (94.7 mg, 38%): R_f 0.67 (H:A 8:2); mp 34.6°C; ^{1}H NMR (600 MHz, $CDCl_3$, plate 3a) δ 7.70 (1H, d, *J* = 16.0 Hz, H-3), 7.52 – 7.50 (2H, m, H-2',6'), 7.37 – 7.36 (3H, m, H-3',4',5'), 6.44 (1H, d, *J* = 16.0 Hz, H-2), 3.79 (3H, s, H-1''); ^{13}C NMR (151 MHz, $CDCl_3$, plate 3b) δ 167.4 (C-1), 144.9 (C-3), 134.4 (C-1'), 130.3 (C-4'), 128.9 (C-3',5'), 128.1 (C-2',6'), 117.8 (C-3), 51.7 (C-1''); IR (neat, cm^{-1}) 1712 (CO); *m/z* (EI) 162 (M^+, 53); UV ($CHCl_3$) λ_{max}, nm (ε): 225 (14614), 276 (15916).

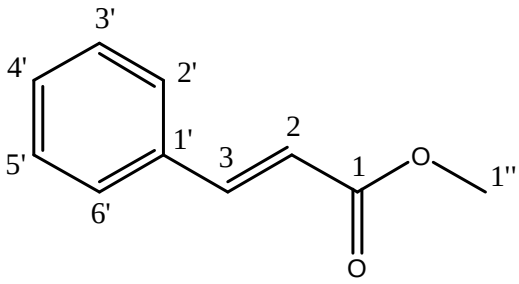

5.10.2.2 Metathesis of trans-β-methylstyrene (69) and butyl acrylate (275)

trans-β-Methylstyrene (**69**) (0.20 mL, 1.5 mmol, 1 eq.), butyl acrylate (**275**) (0.44 mL, 3.1 mmol, 2 eq.), Grubbs II (**125**) (6.5 mg, 0.0077 mmol, 0.5 mol%) and *p*-cresol (**266**) (0.083 g, 0.77 mmol, 0.25 eq.) yielded two products when subjected to method B:

trans-Stilbene[7] (**258**) as colourless platelets (25.6 mg, 9%): R_f 0.87 (H:A 8:2); *cf*. par. 5.8.1.

Butyl cinnamate[9] (**278**) as a light yellow oil (173 mg, 55%): R_f 0.79 (H:A 8:2); ^{1}H NMR (600 MHz, $CDCl_3$, plate 4a) δ 7.57 (1H, d, *J* = 16.0 Hz, H-3), 7.42-7.36 (2H, m, H-2',6'), 7.25-7.21 (3H, m, H-3',4',5'), 6.33 (1H,d, *J* = 16.0 Hz, H-2), 4.09 (2H, t, *J* = 6.7 Hz, H-1''), 1.59-1.55 (2H, m, H-2''), 1.35-1.29 (2H, m, H-3''), 0.85 (3H, t, *J* = 7.4 Hz, H-4''); ^{13}C NMR (151 MHz, $CDCl_3$, plate 4b) δ 167.0 (C-1), 144.5 (C-3), 134.4 (C-1'), 130.2 (C-4'), 128.8 (C-2',6'), 128.0 (C-3',5'), 118.2 (C-2), 64.3 (C-1''), 30.8 (C-2''), 19.2 (C-3''), 13.7 (C-4''); IR (neat, cm^{-1}) 1709 (CO); *m/z* (EI) 204 (M^+, 13); UV ($CHCl_3$) λ_{max}, nm (ε): 218 (16258), 274 (19492).

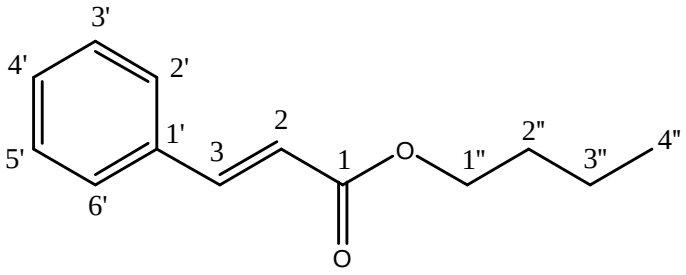

5.10.2.3 Metathesis of trans-β-methylstyrene (69) and 2-ethylhexyl acrylate (2)

trans-β-Methylstyrene (**69**) (0.20 mL, 1.5 mmol, 1 eq.), 2-ethylhexyl acrylate (**2**) (0.64 mL, 3.1 mmol, 2 eq.), Grubbs II (**125**) (6.5 mg, 0.0077 mmol, 0.5 mol%) and *p*-cresol (**266**) (0.083 g, 0.77 mmol, 0.25 eq.) were reacted according to method B to produce two products:

trans-Stilbene[7] (**258**) as colourless platelets (16.8 mg, 6%): R_f 0.87 (H:A 8:2); *cf*. par. 5.8.1.

2-Ethylhexyl cinnamate (**282**) as a *light yellow oil*. (255 mg, 64%): R_f 0.84 (H:A 8:2); ^{1}H NMR (600 MHz, $CDCl_3$, plate 5a) δ 7.68 (1H, d, *J* = 16.0 Hz, H-3), 7.55-7.51 (2H, m, H-2',6'), 7.40-7.35 (3H, m, H-3',4',5'), 6.45 (1H, d, *J* = 16.0 Hz, H-2), 4.17-4.09 (2H, m, H-1''), 1.69-1.61 (1H, m, H-2''), 1.47-1.29 (8H, m, H-3'',4'',5'',1'''), 0.94-.089 (6H, m, H-6'',2'''); ^{13}C NMR (151 MHz, $CDCl_3$, plate 5b) δ 167.3 (C-1), 144.6 (C-3), 134.6 (C-1'), 130.3 (C-4'), 128.9 (C-3',5'),

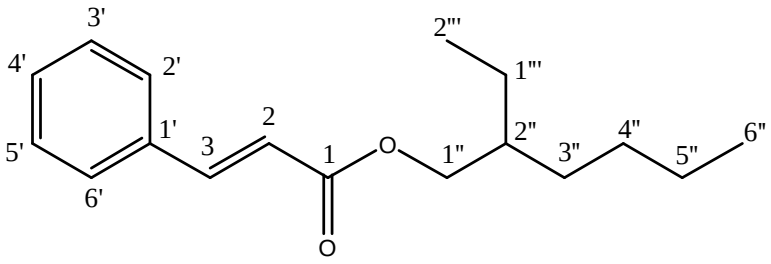

128.1 (C-2',6'), 118.4 (C-2), 67.1 (C-1''), 38.9 (C-2''), 30.6, 29.1, 23.9, 23.1 (C-3'',4'',5'',1'''), 14.2, 11.1 (C-6'',2'''); IR (neat, cm^{-1}) 1712 (CO); HR-MS (AP+) (*m/z*) calcd for $C_{17}H_{24}O_2$ $[M]^+$ 260.1776, found 260.1779 ;UV ($CHCl_3$) λ_{max}, nm (ε): 226 (23694), 278 (9518).

5.10.2.4 Metathesis of trans-β-methylstyrene (69) and 3-buten-2-one (274)

trans-β-Methylstyrene (**69**) (0.20 mL, 1.5 mmol, 1 eq.), 3-buten-2-one (**274**) (0.25 mL, 3.1 mmol, 2 eq.), Grubbs II (**125**) (6.5 mg, 0.0077 mmol, 0.5 mol%) and *p*-cresol (**266**) (0.083 g, 0.77 mmol, 0.25 eq.) were reacted according to the method B to yield two products:

trans-Stilbene[7] (**258**) as colourless platelets (104 mg, 38%): R_f 0.87 (H:A 8:2); *cf*. par. 5.8.1.

(E)-4-Phenylbut-3-en-2-one (**277**) as a *light yellow oil* (77 mg, 34%): R_f 0.49 (H:A 8:2); ^{1}H NMR (600 MHz, $CDCl_3$, plate 6a) δ 7.51 (3H, m, H-4,2',6'), 7.39 (3H, m, H-3',4',5'), 6.71 (1H, d, *J* = 16.3 Hz, H-3), 2.37 (3H, s, H-1); ^{13}C NMR (151 MHz, $CDCl_3$, plate 6b) δ 198.55 (C-2), 143.56 (C-4), 134.45 (C-1'), 130.60 (C-4'), 129.04 (C-3',5'), 128.33 (C-2',6'), 127.18 (C-3), 27.56(C-1); IR (neat, cm^{-1}) 1667 (CO); HR-MS (AP+) (*m/z*) calcd for $C_{10}H_{10}O$ $[M]^+$ 146.0732, found 146.0731 ;UV ($CHCl_3$) λ_{max}, nm (ε): 227 (8104).

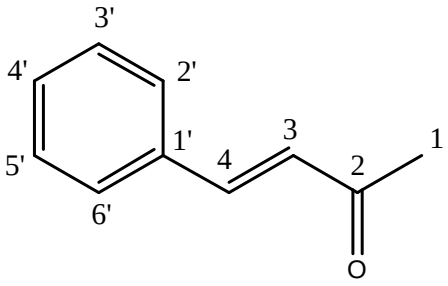

5.10.2.5 Metathesis of trans-β-methylstyrene (69) and acrolein (273)

Following method B, *trans*-β-methylstyrene (**69**) (0.20 mL, 1.5 mmol, 1 eq.), acrolein (**273**) (0.21 mL, 3.1 mmol, 2 eq.), Grubbs II (**125**) (6.5 mg, 0.0077 mmol, 0.5 mol%) and *p*-cresol (**266**) (0.083 g, 0.77 mmol, 0.25 eq.) were reacted for 2 hours to give *trans*-stilbene[7] (**258**) as colourless platelets (161 mg, 58%): R_f 0.87 (H:A 8:2); *cf*. 5.8.1.

GC-MS (EI) did show the presence of cinnamaldehyde[11] (**276**), *m/z* 132 (M^+, 10), in low yield (<5% according to GC). As attempts to retrieve the pure product by PLC failed, no further characterization was possible.

5.10.2.6 Metathesis of t-anethole (11) and methyl acrylate (59)

t-Anethole (**11**) (0.20 mL, 1.3 mmol, 1 eq.), methyl acrylate (**59**) (0.24 mL, 2.7 mmol, 2 eq.), Grubbs II (**125**) (5.7 mg, 0.0067 mmol, 0.5 mol%) and *p*-cresol (**266**) (0.072 g, 0.67 mmol, 0.25 eq.) were reacted according to method B to form two products:

trans-4,4'-Dimethoxystilbene[7] (**259**) as colourless platelets (140 mg, 49%): R_f 0.54 (H:A 8:2); *cf*. par. 5.10.1.2.

Methyl (E)-3-(4-methoxyphenyl)acrylate[12] (**35**)

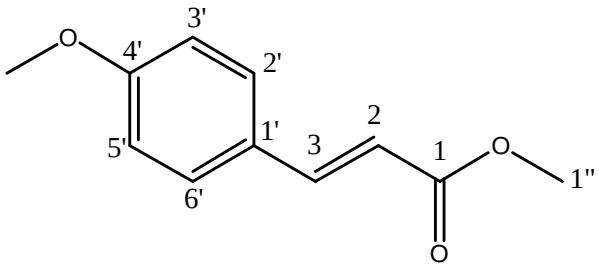

as colourless platelets (85.7 mg, 36%): R_f 0.46 (H:A 8:2); mp 88.3°C; ^{1}H NMR [600 MHz, $CDCl_3$,plate 7a]: δ 7.63 (1H, d, *J* = 16.0 Hz, H-3), 7.45 (2H, d, *J* = 8.8 Hz, H-2',6'), 6.88 (2H, d, *J* = 8.8 Hz, H-3',5'), 6.29 (1H, d, *J* = 16.0 Hz, H-2), 3.80 (3H, s, Ar-O<u>Me</u>), 3.77 (3H, s, H-1"); ^{13}C NMR [151 MHz, $CDCl_3$, plate 7b]: δ 167.8 (C-1), 161.4 (C-4'), 144.6 (C-3), 129.8 (C-2',6'), 127.1 (C-1'), 115.3 (C-2), 114.4 (C-3',5'), 55.4 (-O<u>Me</u>), 51.6 (C-1"); IR (neat, cm^{-1}) 1712 (CO); *m/z* (EI) 192 (M^+, 61); UV ($CHCl_3$) λ_{max}, nm (ε): 226 (28628), 297 (sh,35706), 307 (36928).

5.10.2.7 Metathesis of t-anethole (11) and butyl acrylate (275)

Following method B, *t*-anethole (**11**) (0.20 mL, 1.3 mmol, 1 eq.), butyl acrylate (**275**) (0.38 mL, 2.7 mmol, 2 eq.), Grubbs II (125) (5.7 mg, 0.0067 mmol, 0.5 mol%) and *p*-cresol (**266**) (0.072 g, 0.67 mmol, 0.25 eq.) gave two products:

Butyl (E)-3-(4-methoxyphenyl)acrylate[13] (**281**)

as a light yellow oil (126.4 mg, 41%): R_f 0.62 (H:A 8:2); ^{1}H NMR [600 MHz, $CDCl_3$, plate 8a]: δ 7.62 (1H, d, *J* = 16.0 Hz, H-3), 7.45 (2H, d, *J* = 8.7 Hz, H-3',5'), 6.87 (2H, d, *J* = 8.7 Hz, H-2',6'), 6.29 (1H, d, *J* = 16.0 Hz, H-2), 4.18 (2H, t, *J* = 6.7 Hz, H-1"), 3.80 (3H, s, - OMe), 1.71 – 1.61 (2H, m, H-2"), 1.46 – 1.36 (2H, m, H-3"), 0.95 (3H, t, *J* = 7.4 Hz, H-4"); ^{13}C NMR [151 MHz, $CDCl_3$, plate 8b]: δ 167.4(C-1), 161.4 (C-4'), 144.2 (C-3), 129.7 (C-2',6'), 127.2 (C-1'), 115.8 (C-2), 114.3 (C-3',5'), 64.3 (C-1"), 55.3 (-OMe), 30.9 (C-2"), 19.3 (C-3"), 13.8 (C-4"). IR (neat, cm^{-1}) 1707 (CO); *m/z* (EI) 234 (M^+, 28); UV ($CHCl_3$) λ_{max}, nm (ε): 227 (30150), 290(sh, 30672), 306 (31108).

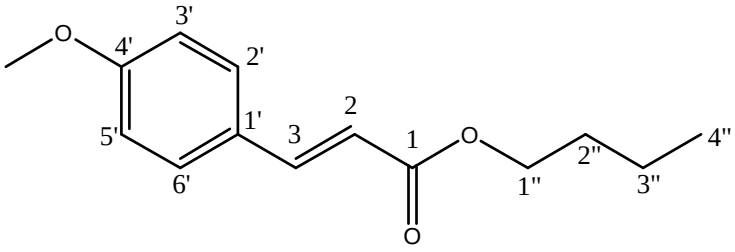

trans-4,4'-Dimethoxystilbene[7] (**259**) as colourless platelets (102 mg, 36%); *cf*. par. 5.10.1.2.

5.10.2.8 Metathesis of t-anethole (11) and 2-ethylhexyl acrylate (2)

Method B with *t*-anethole (**11**) (0.20 mL, 1.3 mmol, 1 eq.), 2-ethylhexyl acrylate (**2**) (0.56 mL, 2.7 mmol, 2 eq.), Grubbs II (**125**) (5.7 mg, 0.0067 mmol, 0.5 mol%) and *p*-cresol (**266**) (0.072 g, 0.67 mmol, 0.25 eq.) yielded two products:

2-Ethylhexyl (E)-3-(4-methoxyphenyl)acrylate[14] (**7**)

as a light yellow oil (181 mg, 47%): R_f 0.69 (H:A 8:2); ^{1}H NMR [600 MHz, $CDCl_3$, plate 9a]: δ 7.62 (1H, d, *J* = 16.0 Hz, H-3), 7.45 (2H, d, *J* = 8.7 Hz, H-2',6'), 6.87 (2H, d, *J* = 8.7 Hz, H3',5'), 6.30 (1H, d, *J* = 16.0 Hz, H-2), 4.09 (1H, m, H-1''), 3.79 (3H, s, -OCH_3), 1.67 – 1.58 (1H, m, H-2''), 1.47 – 1.24 (8H, m, H-3'',4'',5'',1'''), 0.94 – 0.86 (6H, m, H-6'',2'''); ^{13}C NMR [151 MHz, $CDCl_3$, plate 9b]: δ 167.5 (C-1), 161.3 (C-4'), 144.2 (C-3), 129.7 (C-2',6'), 127.2 (C-1'), 115.8 (C-2), 114.3 (C-

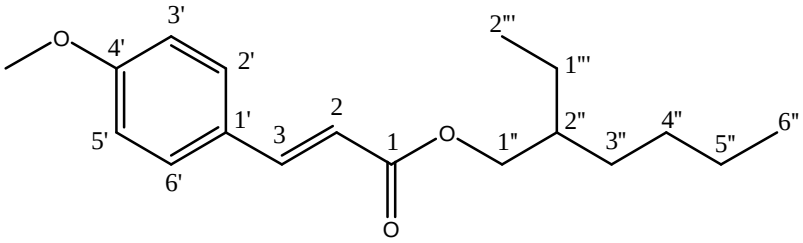

3',5'), 66.8 (C-1''), 55.3 (-OMe), 38.9 (C-2''), 30.5, 29.0, 23.9, 23.0 (C-3'',4'',5'',1'''), 14.1, 11.0 (C-6'',2'''); IR (neat, cm^{-1}) 1706 (CO); *m/z* (EI) 290 (M^+, 8); UV ($CHCl_3$) λ_{max}, nm (ε): 227 (32954), 288(21178), 305(sh, 19272).

trans-4,4'-Dimethoxystilbene[7] (**259**) as colourless platelets (90.7 mg, 32%): R_f 0.54 (H:A 8:2); *cf*. par. 5.10.1.2.

5.10.2.9 Metathesis of t-anethole (11) and 3-buten-2-one (274)

t-Anethole (**11**) (0.20 mL, 1.3 mmol, 1 eq.), 3-buten-2-one (**274**) (0.22 mL, 2.7 mmol, 2 eq.), Grubbs II (**125**) (5.7 mg, 0.0067 mmol, 0.5 mol%) and *p*-cresol (**266**) (0.072 g, 0.67 mmol, 0.25 eq.) were reacted according to method B to form two products:

trans-4,4'-Dimethoxystilbene[7] (**266**) as colourless platelets (77 mg, 27%), *cf*. par. 5.10.1.2.

(E)-4-(4-methoxyphenyl)but-3-en-2-one (**280**)

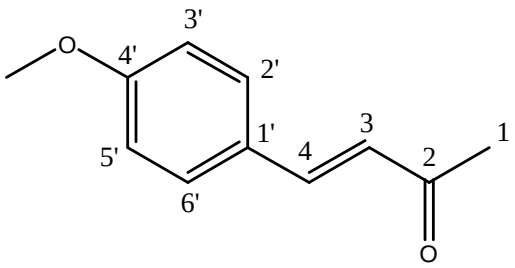

as *colourless platelets* (75.7 mg, 32%): R_f 0.32 (H:A 8:2); mp 71.9°C; ^{1}H NMR [600 MHz, $CDCl_3$, plate 10a]: δ 7.37 (3H, m, H-4,2',6'), 6.89 (2H, d, *J* = 8.7 Hz, H-3',5'), 6.58 (1H, d, *J* = 16.2 Hz, H-3), 3.81 (3H, s, -OC$\underline{H_3}$), 2.33 (3H, s, H-1); ^{13}C NMR [151 MHz, $CDCl_3$, plate 10b]: δ 198.4 (C-2), 161.6 (C-4'), 143.3 (C-4), 130.0 (C-2',6'), 127.1 (C-1'), 125.0 (C-3), 114.5 (C-3',5'), 55.4 (-OMe), 27.4 (C-1). IR (neat, cm^{-1}) 1660 (CO); HR-MS (EI) (*m/z*) calc for $C_{11}H_{12}O_2$ $[M]^+$ 176.0837, found 176.0840; UV ($CHCl_3$) λ_{max}, nm (ε): 226 (27216), 313 (31060).

5.10.2.10 Metathesis of t-anethole (11) and acrolein (273)

t-Anethole (**11**) (0.20 mL, 1.3 mmol, 1 eq.), acrolein (**273**) (0.18 mL, 2.7 mmol, 2 eq.), Grubbs II (**125**) (5.7 mg, 0.0067 mmol, 0.5 mol%) and *p*-cresol (**266**) (0.072 g, 0.67 mmol, 0.25 eq.) were reacted for 2 hours following the method B to yield *trans*-4,4'-dimethoxystilbene[7] (**259**) as colourless platelets (147 mg, 52%); *cf*. par. 5.10.1.2.

GC-MS did indicate the presence of small amounts of (*E*)-3-(4-methoxyphenyl)acrylaldehyde[15] (**279**), *m/z* 162 (M^+, 99), but this product could not be isolated.

5.10.2.11 Metathesis of (E)-4-(prop-1-enyl) phenyltrifluoromethanesulfonate (271) and methyl acrylate (59)

trans-4-(Prop-1-en-1-yl) phenyltrifluoromethanesulfonate (**271**) (0.15 g, 0.60 mmol, 1 eq.), methyl acrylate (**59**) (0.10 mL, 1.1 mmol, 2 eq.), Grubbs II (**125**) (2.4 mg, 0.0030 mmol, 0.5 mol%) and *p*-cresol (**261**) (0.031 g, 0.30 mmol, 0.25 eq.) were subjected to metathesis procedure B for 2 hours. Work-up according to the general work-up procedure (par. 5.6) followed by PLC yielded two products:

(*E*)-4,4'-bis(trifluoromethanesulfonyloxy)stilbene (**272**) as light yellow oil 9.4 mg, 4%.): R_f 0.58 (H:A 8:2); ^{1}H NMR [600 MHz, $CDCl_3$, plate 14a]: δ 7.58 (4H, d, *J* = 8.8 Hz, H-2,6), 7.29 (4H, d, *J* = 8.8 Hz, H-3,5), 7.09 (2H, s, C<u>H</u>=C<u>H</u>); ^{13}C NMR [151 MHz, $CDCl_3$, plate 14b]: δ 149.1 (C-4), 137.2 (C-1), 128.8 (<u>C</u>H=<u>C</u>H), 128.1 (C-2,6), 121.9 (C-3,5), 118.9 (q, J = 320.8Hz, CF_3); ^{19}F NMR [565 MHz, $CDCl_3$, plate 14f] δ -75.91 (CF_3); *m/z* (EI)* 477 (M^+, 6).

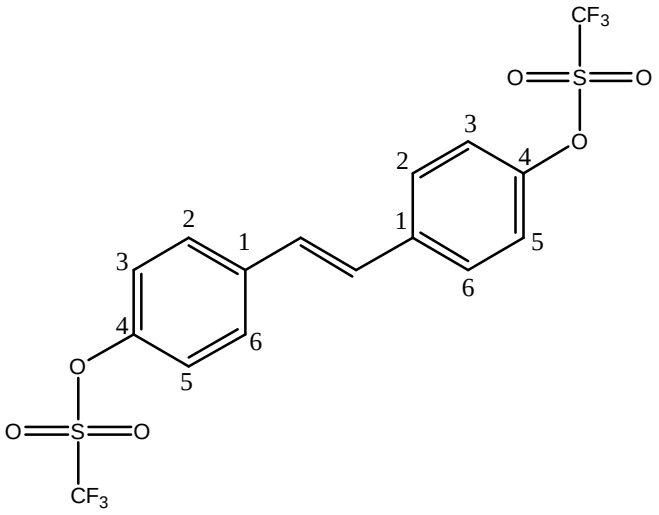

Methyl (E)-3-(4-(trifluoromethylsulfonyloxy)phenyl)acrylate (**273**) as a *light yellow oil* (74.5 mg, 43%): R_f 0.49 (H:A 8:2); ^{1}H NMR (600 MHz, $CDCl_3$, plate 15a) δ 7.66 (1H, d, *J* = 16.0

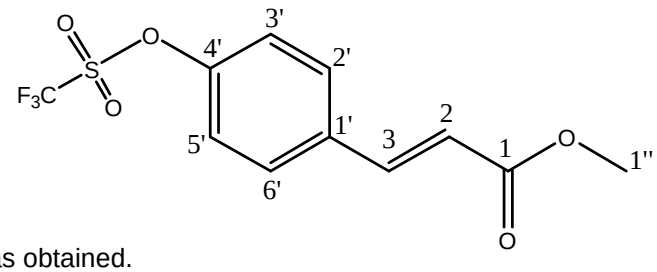

* Sample decomposed before HR-MS was obtained.

Hz, H-3), 7.59 (2H, d, *J* = 8.7 Hz, H-2',6'), 7.29 (2H, d, *J* = 8.7 Hz, H-3',5'), 6.44 (1H, d, *J* = 16.0 Hz, H-2), 3.81 (3H, s, H-1''); ^{13}C NMR (151 MHz, $CDCl_3$, plate 15b) δ 166.9 (C-1), 150.5(C-4'), 142.5 (C-3), 134.9 (C-1'), 129.9 (C-2',6'), 122.1(C-3',5'), 120.0 (C-2), 118.8 (q, J = 320.9Hz, $\underline{C}F_3$), 52.0(C-1''); ^{19}F NMR [565 MHz, $CDCl_3$, plate 11f] δ -75.87 (CF_3); IR (neat, cm^{-1}) 1718 (CO); *m/z* (EI)* 310 (M^+, 43).

5.11 NMR investigation

5.11.1 Grubbs 2nd generation catalyst (125) + p-cresol (266)

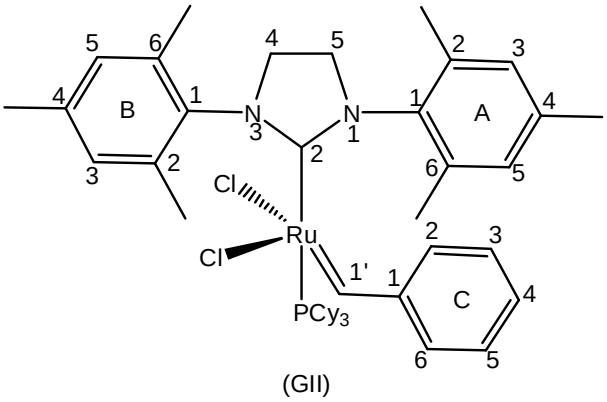

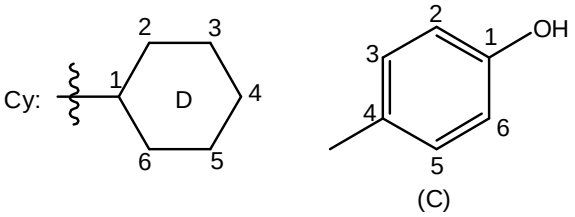

Grubbs II (**125**) (20 mg, 0.024 mmol) and *p*-cresol (**266**) (10.2 mg, 0.094 mmol, 4 eq.) were dissolved in $CDCl_3$ (0.6mL) and stirred at 40°C for 1 hour. NMR was then obtained of the reaction mixture.

^{1}H NMR [600 MHz, $CDCl_3$, plate 17a]: δ 19.12 (s, GII:H-1'), 17.84 (s), 10.00 (s), 9.01 (s, GII:H-2(C)), 7.42 – 7.39 (m, GII:H-4(C)), 7.18 – 7.10 (m), 7.06 (d, *J* = 8.3 Hz, C: H-3,5), 6.86 (d, *J* = 8.3 Hz, C:H2,6), 6.79 – 6.72 (m), 6.43 (s, C:-OH), 5.85 (s, GII:H-3(A)), 4.12 – 3.76 (m, GII:H-4,5), 2.81 (s, GII:H-2-Me(B)), 2.67 (s), 2.62 (s, GII:H-6-Me(B)), 2.54 (s, GII:H-6-Me(A)), 2.48 – 2.41 (m), 2.37 (s, GII:H-4-Me(B)), 2.31 (s, GII:H-4-Me(B)), 2.30(s, C:Me), 2.29 – 2.19 (m), 2.09 (s, GII: H-2-Me(A)), 1.95 (s, GII:H-4-Me(A)), 1.87 – 1.65 (m), 1.62 – 1.30 (m, GII:H-2-6(D)), 1.28 – 1.21 (m), 1.17 – 0.79 (m, GII:H-2-6(D)); ^{13}C NMR [151 MHz, $CDCl_3$, plate 17b]: δ 294.3(GII:C-1'), 219.9(d, J = 76.9Hz, GII:C-2), 155.7, 153.4(C:C-1), 153.2, 151.0(GII:C-

* Sample decomposed before HR-MS was obtained.

1(C)), 139.6, 139.0 and 138.6(GII:C-2,6(A or B)), 138.4(GII:C-4(B)), 137.6(GII:C-4(A)), 137.3, 137.0, 136.6(GII:C-2,6(B or A)), 135.0(GII:C-1(B or A)), 134.8, 131.9, 130.2, 130.1, 129.9(C:C-3,5), 129.8, 129.7, 129.6, 129.5, 129.3, 129.2 128.8, 128.7, 128.6, 128.2, 127.6, 127.1, 126.5, 121.2, 116.3, 115.6, 115.4, 115.2, 112.6, 52.2(d, J = 3.2 Hz, GII:C-4), 51.3(d, J = 1.1 Hz, GII:C-5), 35.1, 34.7, 31.5(d, J = 16.6 Hz, GII:C-2,6(D)), 29.0(d, J = 54.6 Hz, GII:C-1(D)), 27.6(d, J = 9.9 Hz, GII:C-3,5(D)), 26.7, 26.6, 26.1, 25.9, 21.3, 21.1(GII:C-4-Me(B)), 21.0, 20.8(GII:C-4-Me(B)), 20.4(C:Me), 20.3, 19.9(GII:C-2-Me(B),6-Me(B)), 18.5; ^{31}P NMR [243 MHz, $CDCl_3$, plate 17g]: δ 94.6, 55.6, 40.7, 28.9(GII), 20.9.

5.11.2 Tricyclohexylphosphine (289) + 1 eq. p-cresol (266)

Tricyclohexylphosphine (**289**) (20 mg, 0.071 mmol) and *p*-cresol (**266**) (8 mg, 0.071 mmol, 1 eq.) were dissolved in $CDCl_3$ (0.6mL) and stirred at 40°C for 1 hour. NMR was then obtained of the reaction mixture. ^{1}H NMR [600 MHz, $CDCl_3$, plate 20a]: δ 7.60 (s, C: OH), 6.95 (d, *J* = 8.3 Hz, C:H-3,5), 6.81 (d, *J* = 8.3 Hz, C:H-2,6), 2.35 – 2.27 (m, 1H), 2.23 (s, C:Me), 2.02 – 1.62 and 1.52 – 1.11 (m, PCy3:H-1-6); ^{31}P NMR [243 MHz, $CDCl_3$, plate 20g]: δ 59.1, 58.8, 52.9, 50.7, 40.1, 33.3, 12.1.

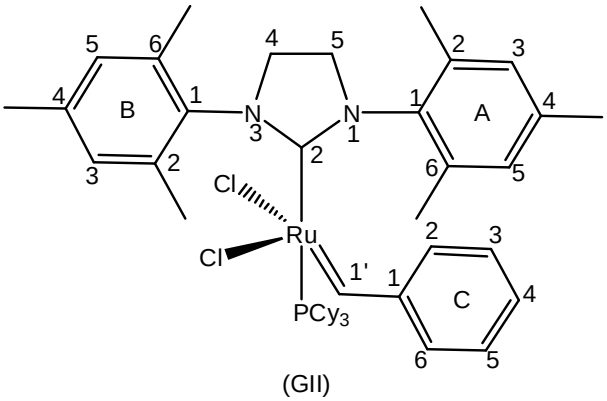

(GII)

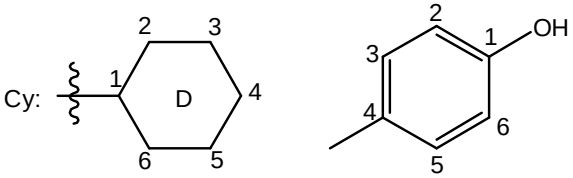

(C)

5.11.3 Tricyclohexylphosphine (289) + 2 eq. p-cresol (266)

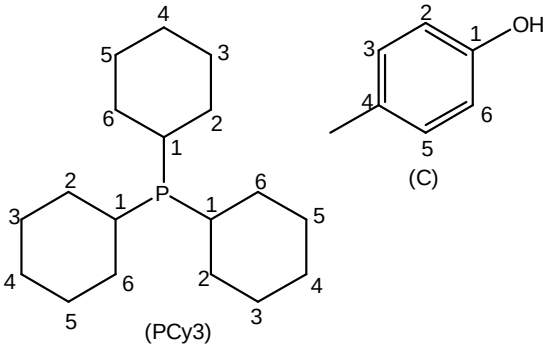

Tricyclohexylphosphine (**289**) (20 mg, 0.071 mmol) and *p*-cresol (**266**) (15 mg, 0.143 mmol, 2 eq.) were dissolved in $CDCl_3$ (0.6mL) and stirred at 40°C for 1 hour. NMR was then obtained of the reaction mixture.^{1}H NMR [600 MHz, $CDCl_3$, plate 21a]: δ 7.27 (s, C: OH), 7.01 (d, *J* = 8.3 Hz, C:H-3,5), 6.85 (d, *J* = 8.3 Hz, C:H-2,6), 2.28 (s, C: Me), 2.05 – 1.68 and 1.54 – 1.17 (m, PCy_3:H-1-6); ^{31}P NMR [243 MHz, $CDCl_3$, plate 21g]: δ 59.9, 59.8, 54.5, 52.0, 33.4, 12.4.

5.11.4 Tricyclohexylphosphine (289) + trifluoromethanesulfonic acid (312)

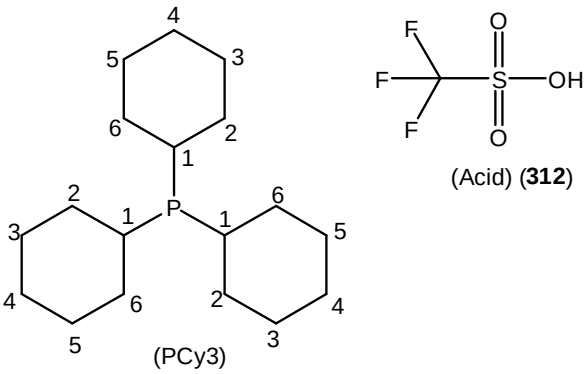

Tricyclohexylphosphine (**289**) (30 mg, 0.11 mmol) and trifluoromethanesulfonic acid (**312**) (0.02 mL, 0.21 mmol, 2 eq.) were dissolved in $CDCl_3$ (0.6mL) and stirred at 40°C for 1 hour. NMR was then obtained of the reaction mixture. ^{1}H NMR [600 MHz, $CDCl_3$, plate 22a]: δ 11.53 – 11.04 (m), 2.69 – 0.71 (m, $POCy_3$:H-1-6); ^{31}P NMR [243 MHz, $CDCl_3$, plate 22g]: δ 86.4, 83.5, 33.4.

5.11.5 Tricyclohexylphosphine oxide (313)

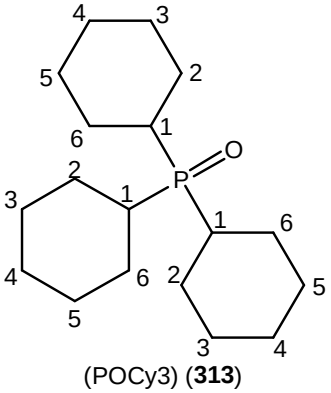

Tricyclohexylphosphine oxide (**313**) was prepared by bubbling medical air through a solution of tricyclohexylphosphine (0.5 g, 1.78 mmol) in DCM (10 mL). The mixture was then concentrated and dried, *in vacuo*, and NMR of the mixture obtained. The ^{1}H NMR [600 MHz, $CDCl_3$, plate 23a]: δ 4.46 – 4.30 (s), 2.01 – 1.15 (m, $POCy_3$:H1-6); ^{31}P NMR [243 MHz, $CDCl_3$,

plate 23g]: δ 57.8, 51.1($POCy_3$), 49.7, 39.9, 31.0, 4.5, -3.1.

5.11.6 Tricyclohexylphosphine oxide (313) + 1 eq. p-cresol (266)

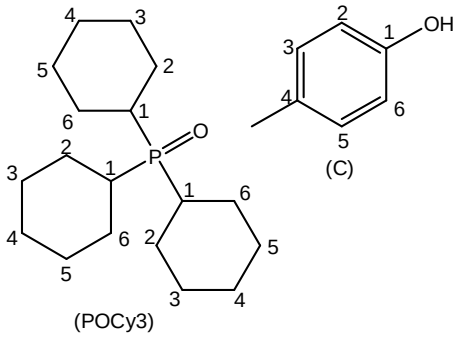

Tricyclohexylphosphine oxide (**313**) (20 mg, 0.068 mmol) and *p*-cresol (**266**) (7 mg, 0.068 mmol, 1 eq.) were dissolved in $CDCl_3$ (0.6mL) and stirred at 40°C for 1 hour. NMR was then obtained of the reaction mixture. ^{1}H NMR [600 MHz, $CDCl_3$, plate 24a]: δ 7.45 (s, C: OH), 7.00 (d, *J* = 8.3 Hz, C:H-3,5), 6.83 (d, *J* = 8.3 Hz, C:H-2,6), 2.27 (s, C:Me), 2.09 – 1.15 (m, POCy3:H-1-6); ^{31}P NMR [243 MHz, $CDCl_3$, plate 24g]: δ 59.1, 53.5, 51.0, 40.4, 31.1, 4.4, -3.4.

5.11.7 Tricyclohexylphosphine oxide (313) + 2 eq. p-cresol (266)

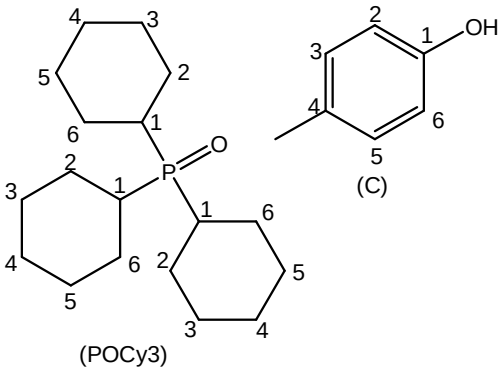

Tricyclohexylphosphine oxide (**313**) (20 mg, 0.068 mmol) and *p*-cresol (**266**) (15 mg, 0.135 mmol, 2 eq.) were dissolved in $CDCl_3$ (0.6mL) and stirred at 40°C for 1 hour. NMR was then obtained of the reaction mixture. ^{1}H NMR [600 MHz, $CDCl_3$, plate 25a]: δ 7.00 (d, *J* = 8.3 Hz, C:H-3,5), 6.78 (d, *J* = 8.3 Hz, C:H-2,6), 5.63 (s), 2.26 (s, C:Me), 2.01 – 1.17 (m, $POCy_3$:H-1-6); ^{31}P NMR [243 MHz, $CDCl_3$, plate 25g]: δ 59.5, 54.1, 51.6, 40.6, 31.2, 4.4, -3.5.

5.11.8 Tricyclohexylphosphine oxide (313) + trifluoromethanesulfonic acid (312)

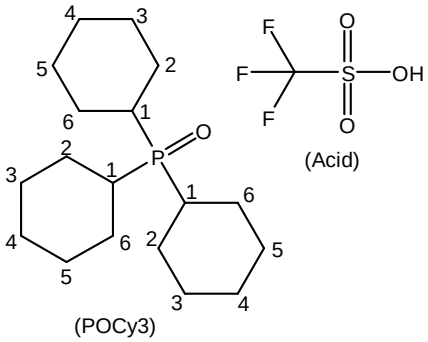

Tricyclohexylphosphine oxide (**313**) (20 mg, 0.07 mmol) and trifluoromethanesulfonic acid (**312**) (0.01 mL, 0.14 mmol, 2 eq.) were dissolved in $CDCl_3$ (0.6mL) and stirred at 40°C

for 1 hour. NMR was then obtained of the reaction mixture. ^{1}H NMR [600 MHz, $CDCl_3$, plate 26a]: δ 11.69 (s), 2.49 – 0.77 (m, $POCy_3$:H-1-6); ^{31}P NMR [243 MHz, $CDCl_3$, plate 26g]: δ 86.0, 85.9, 83.1.

5.11.9 Grubbs 2nd generation catalyst (125) + methyl acrylate (59)

A solution of Grubbs II (**125**) (20 mg, 0.024 mmol) and methyl acrylate (**59**) (0.004 mL, 0.047 mmol, 2 eq.) in dry DCM (5 mL) was refluxed for 1 hour. Concentration of the solution, *in vacuo*, until dry was followed by the addition of $CDCl_3$ (0.6 mL) after which NMR was obtained of the crude reaction mixture. ^{1}H NMR [600 MHz, $CDCl_3$, plate 28a]: δ 19.13 (s, GII: H-1'), 12.04 – 12.01 (m, 1H), 10.03 (s, 1H), 8.24 – 7.98 (m, 1H), 7.89 (d, *J* = 6.3 Hz, 1H), 7.73 – 7.67 (m, *J* = 16.1 Hz, 1H), 7.67 – 7.61 (m, *J* = 7.2 Hz, 1H), 7.54 (dd, *J* = 16.8, 7.9 Hz, 1H), 7.42 – 7.32 (m, 1H), 7.27 (d, *J* = 8.2 Hz, 1H), 7.18 (d, *J* = 7.5 Hz, 1H), 7.11 (s, 1H), 7.09 – 6.79 (m, 1H), 6.45 (d, *J* = 16.0 Hz, 1H), 6.27 (d, *J* = 14.1, MA: H-3a), 5.93 – 5.78 (m, *J* = 7.6 Hz, 1H), 4.57 (s, 1H), 3.99 (dd, *J* = 19.3, 7.1 Hz, 1H), 3.92 – 3.72 (m, GII: H-4,5), 2.99 (d, *J* = 53.3 Hz, 1H), 2.76 (s, GII: H-2-Me(B)), 2.63 (s, 1H), 2.56 (s, GII: H-6-Me(B)), 2.50 (s, GII: H-6-Me(A)), 2.41 – 2.01 (m, 1H), 1.97 – 1.34 and 1.32 – 0.82 (m, GII: H-2-6(D)); ^{13}C NMR [151 MHz, $CDCl_3$, plate 28b]: δ 137.2, 130.0(GII: C-3(B),5(C)), 129.9(GII: C-6(C)), 129.1(GII: C-3(A)), 128.8(GII: C-5(A)), 128.0, 127.7, 126.6, 52.0, 35.6, 35.2, 31.5, 31.4, 29.1, 27.8, 27.1, 27.0, 26.5, 26.4, 26.2, 21.3(GII: C-4-Me(B)), 21.0(GII: C-4-Me(A)), 20.1(GII: C-2-Me(B),6-Me(B)); ^{31}P NMR [243 MHz, $CDCl_3$, plate 28g]: δ 78.0, 50.0, 35.5, 31.5, 28.9(GII).

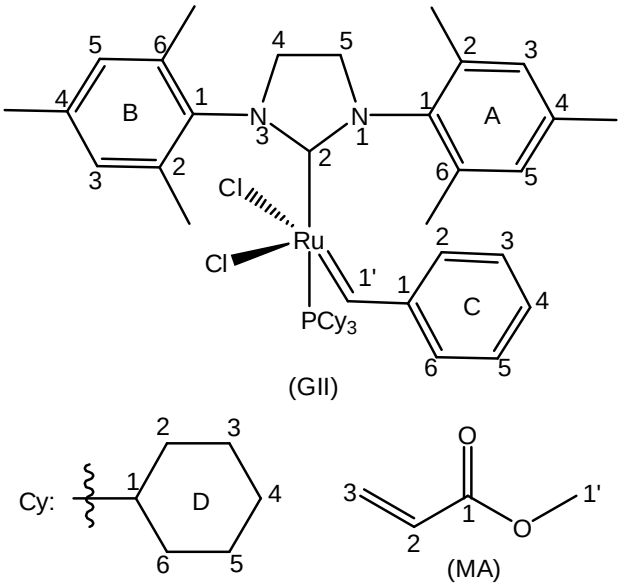

5.11.10 Grubbs 2nd generation catalyst (125) + methyl acrylate (59) + p-cresol (266)

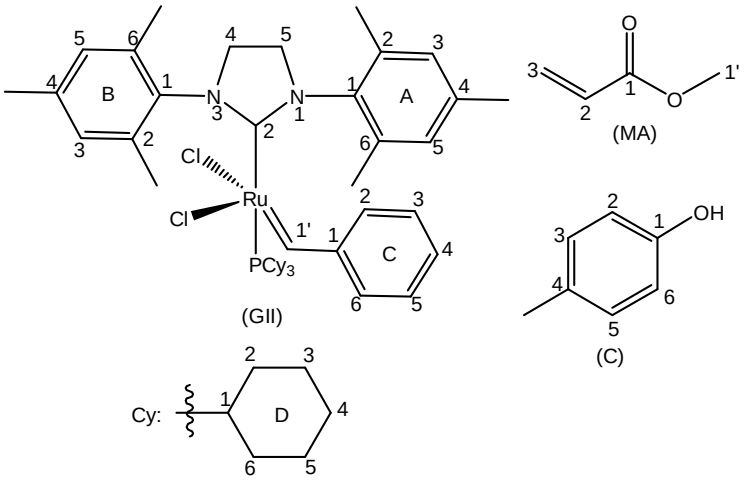

Grubbs II (**125**) (20 mg, 0.024 mmol), methyl acrylate (**59**) (0.004 mL, 0.047 mmol, 2 eq) and *p*-cresol (**266**) (10.2 mg, 0.094 mmol, 4 eq.) were refluxed in dry DCM (5 mL) for 1 hour. The mixture was then concentrated, *in vacuo*, until dry and followed by the addition of $CDCl_3$ (0.6 mL) to the dry mixture. NMR was then obtained of the crude reaction mixture. ^{1}H NMR [600 MHz, $CDCl_3$, plate 29a]: δ 19.07 (s, GII: H-1'), 17.73 (s), 17.52 (s), 8.93 (s), 7.98 (s), 7.62 (d, *J* = 16.0 Hz), 7.48 – 7.38 (m), 7.35 – 7.26 (m), 7.25 – 7.12 (m), 7.25 – 7.12 (m), 7.08 – 6.91 (m, 6H), 6.90 – 6.85 (m), 6.84 – 6.75 (m), 6.75 – 6.43 (m), 6.42 – 6.25 (m), 6.13 – 5.97 (m), 5.97 – 5.83 (m), 5.85 – 5.68 (m), 5.69 – 5.55 (m), 5.31 (s), 4.79 – 4.20 (m), 3.97 – 3.78 (m), 3.76 – 3.71 (m), 3.70 – 3.65 (m), 3.65 – 3.62 (m), 3.61 – 3.58 (m), 3.57 – 3.43 (m), 3.41 – 3.23 (m), 3.23 – 2.92 (m), 2.82 – 2.48 (m), 2.47 – 2.37 (m), 2.36 – 2.32 (m), 2.31 – 2.26 (m), 2.27 – 2.20 (m), 2.18 – 2.11 (m), 2.09 – 0.67 (m); Int. ^{13}C NMR [151 MHz, $CDCl_3$, plate 29b]: δ 294.1, 219.9(d, J = 77.2 Hz), 213.7, 174.8, 171.2 (d, J = 12.5 Hz), 167.3, 166.9, 166.5, 165.1, 154.5, 154.42, 154.36, 154.1, 151.0, 144.8, 138.6 (d, J = 63.3 Hz), 138.1, 137.5, 137.3, 136.9, 136.6 (d, J = 49.3 Hz), 136.1, 135.5, 134.9, 134.8, 134.3, 134.0, 133.1, 131.7, 130.7, 130.2, 129.6, 129.4, 129.2, 128.9, 128.7, 128.5, 128.1, 127.84, 127.77, 126.9, 125.9, 122.5 (d, J = 27.2 Hz), 122.1, 121.5, 119.7, 117.4, 115.2, 69.1, 53.0, 52.3, 52.1, 52.0, 51.4, 51.1, 51.0, 50.6, 50.0, 41.2, 31.2(d, J = 16.6 Hz), 29.8(d, J = 40.0 Hz), 28.8 (d, J = 48.0 Hz), 27.5, 27.4, 26.9, 26.7, 26.5, 26.2, 26.0, 25.9, 25.1, 20.9, 20.7, 20.6, 20.2, 19.7, 18.5, 18.4, 18.2, 18.0, 17.7, 17.4, 11.9, 11.0, 10.6; ^{31}P NMR [243 MHz, $CDCl_3$, plate 29g]: δ 32.2, 28.9(GII).

5.11.11 Grubbs 2nd generation catalyst (125) + trans-β-methylstyrene (69)

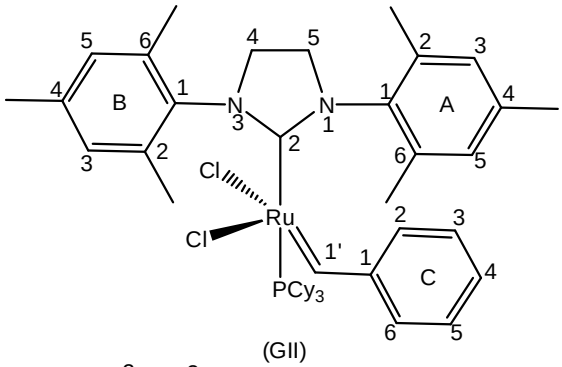

(GII)

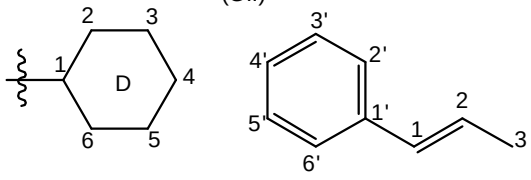

(MS)

Grubbs II (**125**) (20 mg, 0.024 mmol) and *trans*-β-methylstyrene (**69**) (0.005 mL, 0.047 mmol, 2 eq.) were refluxed for 1 hour in dry DCM (5 mL). The mixture was then concentrated, *in vacuo*, until dry and $CDCl_3$ (0.6 mL) added to the crude mixture after which NMR was obtained of the crude reaction mixture. ^{1}H NMR [600 MHz, $CDCl_3$, plate 31a]: δ 19.12 (s, GII:H-1'), 18.52 (q, *J* = 5.5 Hz), 8.98 (s, GII:H-2(C)), 7.54 (d, *J* = 8.1 Hz), 7.41 (d, *J* = 7.4 Hz, MS:H-2',6'), 7.39 – 7.29 (m, MS:H-3',4',5'), 7.28 – 7.22 (m), 7.21 – 7.15 (m), 7.14 – 7.11 (m), 7.11 – 7.07 (m), 7.07 – 7.03 (m), 7.02 (s), 6.95 (s), 6.91 (s), 6.83 (s), 6.78 (s, GII:H-5(A)), 6.71 – 6.59 (m), 6.37 (dd, *J* = 11.5, 6.0 Hz), 6.31 (d, *J* = 15.8 Hz), 6.19 – 6.09 (m, *J* = 15.7, 6.6 Hz), 5.82 – 5.62 (m), 5.48 – 5.33 (m), 3.90 – 3.58 (m, GII:H-4,5), 2.79 – 2.43 (m), 2.38 (s), 2.24 (s), 2.15 (dd, *J* = 19.5, 7.9 Hz), 2.13 – 1.94 (m), 1.84 (s), 1.83 – 1.80 (m), 1.78 (dd, *J* = 6.6, 1.5 Hz), 1.70 – 1.63 (m), 1.70 – 1.14 (m), 1.13 – 0.69 (m); ^{13}C NMR [151 MHz, $CDCl_3$, plate 31b]: δ 315.2, 294.3(GII:C-1'), 220.4 (d, J = 60.2 Hz, GII:C-2), 219.9(d, J = 57.4 Hz), 151.2(GII:C-1(C)), 140.1, 139.0, 138.9, 138.7, 138.4, 138.2, 138.1, 138.0, 137.9, 137.6, 137.53, 137.46, 137.4, 137.3, 137.1, 137.0, 136.9, 135.1, 134.8, 134.6, 133.6, 133.1, 132.4, 131.9, 131.2, 131.0, 129.8, 129.7, 129.4, 128.8, 128.6, 128.4, 128.2, 128.1, 127.8, 127.7, 127.6, 126.7, 126.5, 126.4, 126.3, 125.8, 125.5, 124.5, 51.9(d, J = 38.5 Hz, GII:C-4), 51.1(d, J = 8.2 Hz, GII:C-5), 46.2, 31.6, 31.5, 31.4, 31.3, 29.2, 28.9, 27.8, 27.7, 27.6, 26.3, 26.1, 21.1, 21.0, 20.9, 19.9, 19.7, 18.6, 18.4, 17.9, 14.6, 12.4; ^{31}P NMR [243 MHz, $CDCl_3$, plate 31g]: δ 49.9, 28.9 (GII), 27.4.

5.11.12 Grubbs 2nd generation catalyst (125) + trans-β-methylstyrene (69) + p-cresol (266)

Grubbs II (**125**) (20 mg, 0.024 mmol), *trans*-β-methylstyrene (**69**) (0.005 mL, 0.047 mmol, 2 eq.) and *p*-cresol (**266**) (10.2 mg, 0.094 mmol, 4 eq.) were dissolved in dry DCM (5 mL). The mixture was then refluxed for 1 hour, concentrated, *in vacuo*, until dry and $CDCl_3$ (0.6 mL) added to the crude mixture. NMR was then obtained of the crude reaction mixture. ^{1}H NMR [600 MHz, $CDCl_3$, plate 32a]: δ 19.29 (s, GII: H-1'), 18.76 (q, *J* = 5.5 Hz), 9.18 (s), 7.66 (d, *J* = 7.4 Hz), 7.54 – 7.38 (m), 7.34 (t, *J* = 7.3 Hz, MS: H-4'), 7.32 – 7.24 (m), 7.16 (t, *J* = 7.6 Hz), 7.06 (s), 6.96 (d, *J* = 8.4 Hz), 6.91 – 6.59 (m), 6.55 (m, MS: H-1), 6.39 (dq, *J* = 15.7, 6.6 Hz, MS: H-2), 6.21 (s), 6.04 – 5.88 (m), 5.70 – 5.56 (m), 5.56 – 5.02 (m), 4.84 (dd, *J* = 10.9, 6.0 Hz), 4.17 – 3.78 (m, GII: H-4,5), 2.95 (s), 2.92 – 2.86 (m), 2.79 (s), 2.75 (s), 2.68 (s), 2.60 (s), 2.55 – 2.33 (m), 2.33 – 2.16 (m), 2.11 – 1.98 (m), 1.86 – 1.46 (m), 1.38 – 0.92 (m); ^{13}C NMR [151 MHz, $CDCl_3$, plate 32b]: δ 315.4, 294.4 (GII: C-1'), 220.0(d, *J* = 77.1 Hz, GII; C-2), 219.3(d, J = 74.1 *Hz*), 153.6, 151.1(GII: C-1(C)), 139.0 (d, *J* = 66.9 Hz), 138.6, 138.5, 138.4, 138.1, 138.0, 137.9, 137.6, 137.31, 137.28, 137.1, 136.6, 135.0, 134.8, 134.4, 133.7, 133.5, 133.2, 132.5, 131.8, 131.0, 129.91, 129.85, 129.50, 129.4, 129.2, 128.9, 128.8, 128.7, 128.6, 128.5, 128.4, 128.3, 128.1, 127.8, 127.7, 127.59, 127.55, 127.1, 126.7, 126.5, 126.4, 126.3, 126.2, 126.0, 125.9, 125.84, 125.80, 125.76, 125.6, 124.6, 123.6, 115.3, 65.1, 63.6, 61.4, 52.2, 51.9, 51.3, 51.2, 50.7, 46.3, 31.7, 31.6, 31.5, 31.4, 29.3, 28.9, 27.7, 27.64, 27.56, 26.6, 26.1, 25.6, 21.1, 21.0, 20.9, 20.5(C: Me), 19.9, 19.7, 18.54(MS: C-3), 18.46, 17.9, 14.6, 13.9, 13.6, 12.4, 11.2; ^{31}P NMR [243 MHz, $CDCl_3$, plate 32g]: δ 28.9(GII), 27.3.

5.11.13 Grubbs 2nd generation catalyst (125) + methyl acrylate (59) + trans-β-methylstyrene (69)

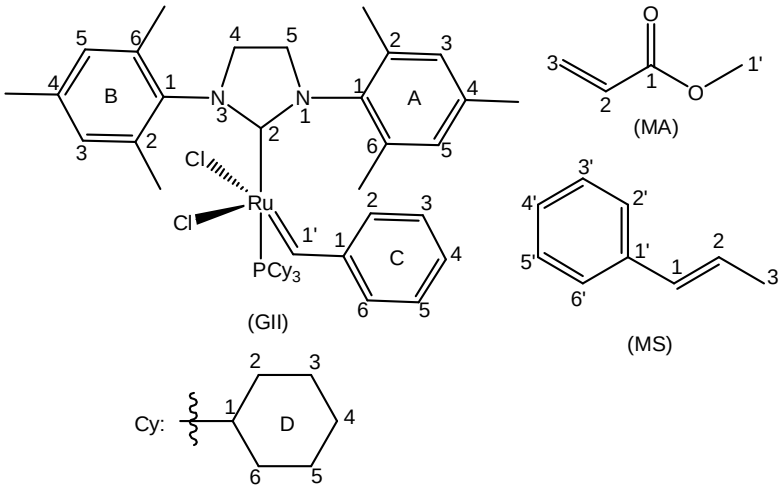

Grubbs II (**125**) (20 mg, 0.024 mmol), methyl acrylate (**59**)(0.004 mL, 0.047 mmol, 2 eq.) and *trans*-β-methylstyrene (**69**) (0.005 mL, 0.047 mmol, 2 eq.) were refluxed for 1 hour in dry DCM (5 mL). The mixture was then concentrated, *in vacuo*, until dry and $CDCl_3$ (0.6 mL) added to the crude mixture after which NMR was obtained of the crude reaction mixture.^{1}H NMR [600 MHz, $CDCl_3$, plate 33a]: δ 19.12 (s, GII:H-1'), 18.52 (q, *J* = 5.3 Hz), 17.77 (s), 8.91 (s), 7.88 – 7.77 (m), 7.68 (s), 7.66 (s), 7.61 (d, *J* = 6.8 Hz), 7.49 (s), 7.48 (s), 7.34 (s), 7.32 (s), 7.31 (s), 7.29 (s), 7.24 (s), 7.23 (s), 7.21 (s), 7.17 – 7.13 (m), 7.08 (s), 7.00 – 6.91 (m), 6.89 (d, *J* = 11.3 Hz), 6.84 (s), 6.74 – 6.51 (m), 6.43 (s), 6.40 (s), 6.36 (s), 6.35 (s), 6.34 – 6.16 (m), 6.15 – 6.06 (m), 5.83 (s), 5.81 (s), 5.75 – 5.65 (m), 5.39 (s), 5.24 (s), 5.20 (s), 5.09 (s), 4.12 – 3.82 (m), 3.77 (s, 2148H), 3.72 (s), 3.68 (s), 3.64 – 3.50 (m), 2.81 – 2.36 (m), 2.33 – 1.87 (m), 1.83 (d, *J* = 6.9 Hz), 1.74 – 0.66 (m); ^{13}C NMR [151 MHz, $CDCl_3$, plate 33b]: δ 167.3, 166.9, 166.6, 165.3, 145.2, 144.8, 144.7, 137.2, 134.3, 133.3, 131.0, 130.7, 130.3, 130.1, 129.8, 128.8, 128.62, 128.59, 128.5, 128.4, 128.1, 128.0, 127.8, 127.7, 127.6, 126.7, 126.5, 126.1, 125.7, 125.6, 122.3, 120.2, 117.7, 113.7, 53.5, 52.3, 51.62, 51.56, 51.3, 50.9, 35.5, 35.1, 31.4, 31.3, 28.8, 27.72, 27.66, 26.9, 26.8, 26.3, 26.1, 25.5, 21.1, 20.9, 19.9, 19.7, 18.6, 18.4, 17.9, 15.3; ^{31}P NMR [243 MHz, $CDCl_3$, plate 33g]: δ 50.04, 32.54, 31.48, 28.90(GII), 27.38.

5.11.14 Tricyclohexylphosphine (289) + methyl acrylate (59) + lithium chloride

Tricyclohexylphosphine (**289**) (0.2 g, 0.7 mmol), methyl acrylate (**59**) (0.06 mL, 0.7 mmol) and lithium chloride (0.03 g, 0.7mmol) was stirred in DCM (5 mL) for 4 hours. The reaction mixture was then concentrated, *in vacuo*, until dry and $CDCl_3$ (0.6 mL) added to the crude mixture. NMR was then obtained of the crude reaction mixture. ^{1}H NMR [600 MHz, $CDCl_3$, plate 34a]: δ 6.00 (s), 5.42 (s), 5.16 (s), 4.30 (s), 3.57 (s), 3.48 (s), 2.39 (dd, *J* = 58.4, 6.9 Hz), 2.19 – 0.96 (m); ^{31}P NMR [243 MHz, $CDCl_3$, plate 34g]: δ 57.8, 51.2, 33.4, 32.6, 32.5, 32.3, 31.9, 31.3.

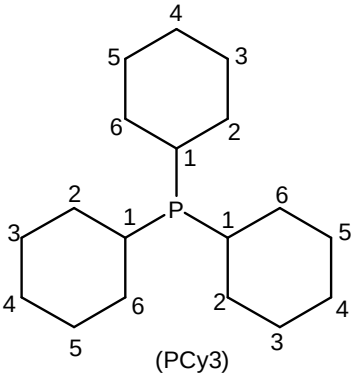

(PCy3)

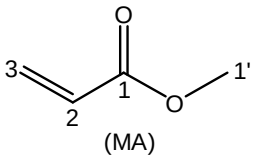

(MA)

5.11.15 Tricyclohexylphosphine (289) + methyl acrylate (59) + lithium chloride + p-cresol (266)

Tricyclohexylphosphine (**289**) (0.2 g, 0.7 mmol), methyl acrylate (**59**) (0.06 mL, 0.7 mmol), lithium chloride (0.03 g, 0.7mmol) and *p*-cresol (**266**) (0.077 g, 0.7 mmol) was stirred in DCM (5 mL) for 4 hours. The reaction mixture was then concentrated, *in vacuo*, until dry and $CDCl_3$ (0.6 mL) added to the crude mixture. NMR was then obtained of the crude reaction mixture. ^{1}H NMR [600 MHz, $CDCl_3$, plate 35a]: δ 8.03(s), 7.11 – 7.01 (m), 6.93 and 6.87 (d, *J* = 8.5 Hz, C: H-Ar), 6.84 – 6.78 (m), 6.43 (dt, *J* = 18.2, 9.1 Hz), 6.20 – 6.09 (m), 5.86 (dd, *J* = 10.5, 1.3 Hz), 5.63 (d, *J* = 1.2 Hz), 5.27 (s), 4.23 (t, *J* = 6.4 Hz), 3.77 (t, *J* = 2.7 Hz), 3.74 (s), 3.71 – 3.68 (m), 3.67

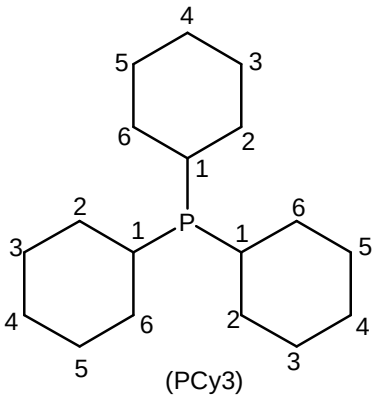

(PCy3)

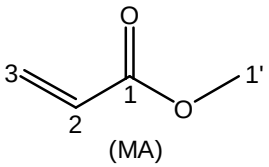

(MA)

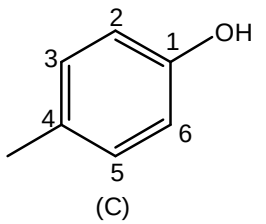

(C)

– 3.62 (m), 3.42 (s), 2.83 – 2.63 (m), 2.59 – 2.28 (m), 2.23 (s, C:H-Me), 2.04 – 1.88 (m), 1.86 – 1.77 (m), 1.73 – 1.42 (m), 1.40 – 0.97 (m); ^{31}P NMR [243 MHz, $CDCl_3$, plate 35g]: δ 60.3, 55.6, 32.3, 32.2, 31.7.

5.11.16 Grubbs 2nd generation catalyst (125) + methyl acrylate (59) + trans-β-methylstyrene (69) + p-cresol (266)

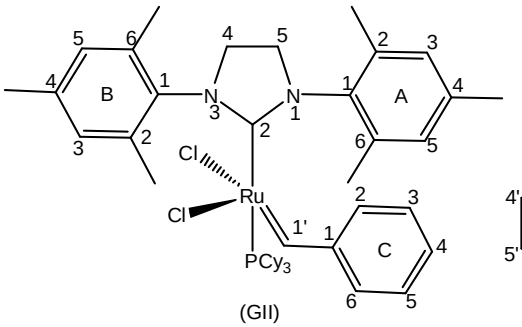

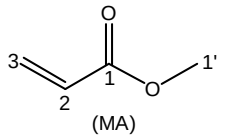

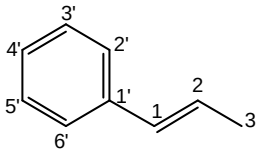

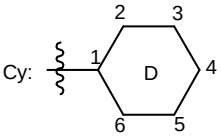

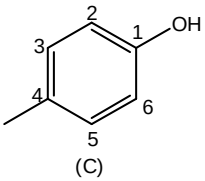

Grubbs II (**125**) (20 mg, 0.024 mmol), methyl acrylate (**59**) (0.004 mL, 0.047 mmol, 2 eq.), *trans*-β-methylstyrene (**69**) (0.005 mL, 0.047 mmol, 2 eq.) and *p*-cresol (**266**) (10.2 mg, 0.094 mmol, 4 eq.) were dissolved in dry DCM (5 mL) and refluxed for 1 hour. The reaction mixture was then concentrated, *in vacuo*, until dry and $CDCl_3$ (0.6 mL) added to the crude mixture. NMR was then obtained of the crude reaction mixture. ^{1}H NMR [600 MHz, $CDCl_3$, plate 36a]: δ 19.12 (s, GII:H-1'), 18.53 (q, *J* = 5.6 Hz), 17.78 (s), 7.94 – 7.77 (m), 7.67 (d, *J* = 16.0 Hz), 7.63 – 7.52 (m), 7.50 – 7.44 (m), 7.38 – 7.30 (m), 7.27 (dd, *J* = 15.7, 8.7 Hz), 7.22 (dd, *J* = 13.5, 6.2 Hz), 7.16 – 7.11 (m), 7.07 (s), 7.00 – 6.91 (m), 6.87 (d, *J* = 19.1 Hz), 6.83 (s), 6.79 (d, *J* = 8.1 Hz), 6.67 (dt, *J* = 22.1, 10.9 Hz), 6.57 – 6.52 (m), 6.41 (d, *J* = 16.0 Hz), 6.38 – 6.06 (m), 5.82 (dd, *J* = 15.5, 1.5 Hz), 5.78 (d, *J* = 11.4 Hz), 5.23 (s), 3.84 (d, *J* = 52.0 Hz), 3.76 (s), 3.75 (s), 3.72 – 3.66 (m), 3.67 (s), 3.64 (d, *J* = 10.6 Hz), 3.55 (s), 2.75 (s), 2.64 – 2.30 (m), 2.29 – 2.24 (m), 2.22 (s), 2.21 – 2.14 (m), 2.11 (s), 2.10 (d, *J* = 1.6 Hz), 2.00 (s), 1.94 – 1.89 (m), 1.86 (d, *J* = 25.7 Hz), 1.82 (dd, *J* = 6.9, 1.4 Hz), 1.76 – 0.72 (m); ^{13}C NMR [151 MHz, $CDCl_3$, plate 36b]: δ 167.4, 167.0, 165.3, 154.33, 144.8, 144.8, 137.2, 134.2, 133.3, 130.9, 130.7, 130.2, 130.1, 129.8, 128.9, 128.8, 128.7, 128.58, 128.55, 128.41, 128.36, 128.2, 128.12, 128.08, 128.0,

127.8, 127.5, 126.6, 126.4, 126.1, 125.7, 125.5, 122.2, 120.1, 117.6, 117.4, 115.2, 77.4, 77.2, 77.0, 53.5, 52.2, 51.6, 51.5, 51.3, 35.2, 34.8, 31.4, 30.8, 28.8, 27.7, 27.6, 27.13, 26.8, 26.7, 26.4, 26.3, 26.1, 26.04, 25.96, 25.3, 21.0, 20.4, 19.9, 18.4, 17.9; ^{31}P NMR [243 MHz, $CDCl_3$, plate 36g]: δ 52.9, 32.4, 31.5, 28.9(GII), 27.4, 25.6, 16.1.

5.12 Investigation of the mechanism

5.12.1 Metathesis of cis-stilbene (310) and methyl acrylate (59)

5.12.1.1 Reaction without p-cresol (266)

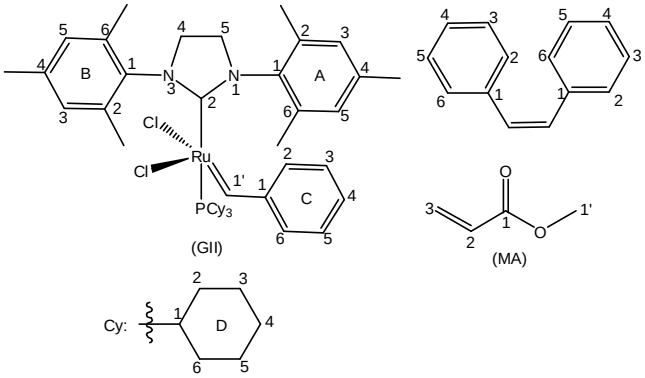

Grubbs 2nd generation catalyst (**125**) (0.02 g, 0.024 mmol), *cis*-stilbene (**310**) (8 mL, 0.047 mmol, 2 eq.) and methyl acrylate (**59**) (0.004 mL, 0.047 mmol, 2 eq.) was dissolved in DCM (5 mL) and refluxed for 2 hours. The reaction mixture was then concentrated, *in vacuo*, until dry and $CDCl_3$ (0.6 mL) added to the crude mixture. NMR was then obtained of the crude reaction mixture. ^{1}H NMR [600 MHz, $CDCl_3$, plate 37a]: δ 19.12 (s, GII: H-1'), 9.04 (s), 7.49 – 7.43 (m), 7.34 – 7.28 (m), 7.23 – 7.19 (m), 7.19 – 7.08 (m), 7.06 (s, GII: H-3(B)), 7.02 – 6.79 (m), 6.55 (s), 6.40 (d, *J* = 16.0 Hz), 5.92 – 5.06 (m), 4.03 – 3.78 (m, GII: H-4,5), 3.74 (s), 3.72 (s), 3.67 – 3.39 (m), 2.75 (s, GII: H-2-Me(B)), 2.63 – 2.42 (m), 2.62 – 2.34 (m), 2.29 (s), 2.19 (s, GII: H-4-Me(B)), 2.20 – 2.12 (m), 2.06 (s, H-2-Me(A)), 2.00 (s, 1.87 (s), 1.93 – 1.63 (m), 1.62 – 0.48 (m, GII: H-2-6(D)); ^{13}C NMR [151 MHz, $CDCl_3$, plate 37b]: δ 220.4 (d, J = 77.4 Hz, GII: C-2), 167.4, 165.4, 151.3(GII: C-1(C)), 144.9, 144.8, 138.3(GII: C-4(B)), 137.6(GII: C-4(A)), 137.4, 137.33, 137.25, 135.2(GII: C-1(B or A)), 134.4, 133.4, 130.29, 130.26, 129.9, 128.9, 128.7, 128.5, 128.2, 128.1, 127.9, 127.8, 127.6, 127.1(GII: C-5(B)), 126.7, 126.5, 126.3, 117.8, 52.2, 51.7, 51.2, 35.5, 35.2, 31.4

(d, J = 16.7 Hz, GII: C-2,6(D)), 30.9, 29.1, 27.8 (d, J = 9.8 Hz, GII: C-3,5(D)), 27.0 (d, J = 11.8 Hz), 26.4 (d, J = 2.7 Hz), 26.2, 21.0 (d, J = 34.8 Hz), 20.0; ^{31}P NMR [243 MHz, $CDCl_3$, plate 37g]: δ 49.9, 31.5, 28.9(GII).

5.12.1.2 Reaction with *p*-cresol (266)

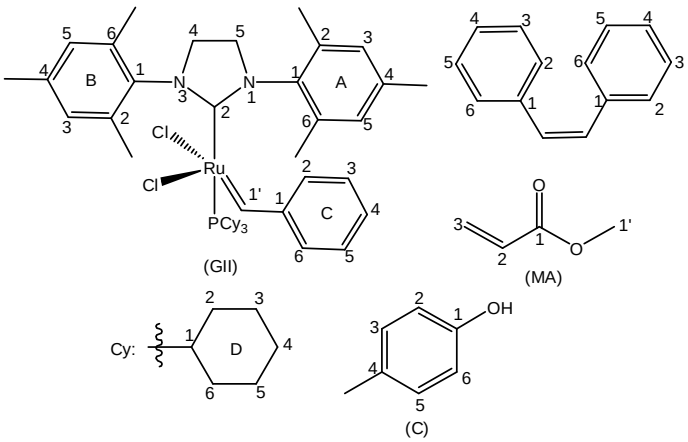

Cis-stilbene (**310**) (8 mL, 0.047 mmol, 2 eq.), methyl acrylate (**59**) (0.004 mL, 0.047 mmol, 2 eq.), Grubbs 2nd generation catalyst (**125**) (0.02 g, 0.024 mmol) and *p*-cresol (**266**) (0.01 g, 0.094 mmol, 4 eq.) was dissolved in DCM (5 mL) and refluxed for 2 hours. The reaction mixture was then concentrated, *in vacuo*, until dry and $CDCl_3$ (0.6 mL) added to the crude mixture. NMR was then obtained of the crude reaction mixture. ^{1}H NMR [600 MHz, $CDCl_3$]: δ 19.12 (s, GII: C-1'), 9.10 (s), 7.89 – 7.79 (m), 7.70 (s), 7.68 (s), 7.63 (d, *J* = 8.2 Hz), 7.52 – 7.47 (m), 7.39 – 7.31 (m), 7.27 – 7.22 (m), 7.20 (s), 7.19 (s), 7.09 (s), 6.99 (d, *J* = 8.1 Hz, C:H-3,5), 6.85 (s), 6.84 (s), 6.78 (d, *J* = 8.1 Hz, C:H-2,6), 6.58 (s), 6.44 (s), 6.42 (s), 6.29 (s), 5.81 (s), 4.02 – 3.82 (m), 3.78 (s), 3.77 (s), 3.70 – 3.63 (m), 2.79 – 2.33 (m), 2.30 (s), 2.24 (s), 2.21 – 1.98 (m), 1.97 – 0.68 (m, GII: C-2-6(D)); Int. ^{13}C NMR [151 MHz, $CDCl_3$]: δ 282.7, 220.2, 167.6, 165.5, 154.1, 145.0, 138.4, 137.64, 137.57, 137.4, 137.3, 137.2, 134.4, 133.5, 130.4, 130.3, 130.0, 129.2, 128.96, 128.94, 128.76, 128.75, 128.6, 128.3, 128.2, 128.0, 127.8, 127.7, 127.2, 126.6, 126.4, 117.8, 115.4, 77.4, 77.2, 77.0, 52.4, 51.8, 31.6, 31.5, 27.9, 27.8, 27.0, 26.9, 26.2, 21.2, 21.0, 20.5, 20.0; ^{31}P NMR [243 MHz, $CDCl_3$]: δ 53.1, 34.2, 32.5, 31.5, 28.9(GII), 21.0.

5.12.2 Metathesis of trans-β-methylstyrene (69) and methyl crotonate (311)

trans-β-Methylstyrene (**69**) (0.20 mL, 1.5 mmol, 1 eq.), methyl crotonate (**311**) (0.33 mL, 3.1 mmol, 2 eq.), Grubbs II (**125**) (6.5 mg, 0.0077 mmol, 0.5 mol%) and *p*-cresol (**266**) (0.083 g, 0.77 mmol, 0.25 eq.) were subjected to metathesis procedure B for 2 hours. Work-up according to the general work-up procedure (par. 5.6) followed by PLC and purification of the precipitate yielded two products:

trans-Stilbene[7] (**258**) as colourless platelets (69 mg, 25%): R_f 0.87 (H:A 8:2); *cf*. par. 5.8.1.

Methyl cinnamate[16] (**195**) as colourless platelets (79 mg, 31%): R_f 0.67 (H:A 8:2); *cf*. par. 5.10.2.1.

References

[1] Gottlieb, H. E.; Kotlyar, V.; Nudelman, A. *J. Org. Chem.* **1997**, *62*, 7512-7515.

[2] ^{19}F NMR reference standards, http://chemnmr.colorado.edu/manuals/19F_NMR_Reference_Standards.pdf (accessed Dec 15, 2015)

[3] Kühl, O., *Phosphoros-31 NMR Spectroscopy: A concise introduction for the synthetic organic and organometallic chemist*, Springer-Verlag Berlin Heidelberg, 2008, p9.

[4] Van Tonder, J. H. Ph.D thesis, University of the Free State, Bloemfontein, SA, 2014.

[5] Van Tonder, B. M.Sc thesis, University of the Free State, Bloemfontein, SA, 2008.

[6] Hoffman, R. V.; Bishop, R. D.; Fitch, P. M.; Hardenstein, R. *J. Org. Chem*. **1980**, *45*, 917-919.

[7] Miller, B. J. M.Sc thesis, University of the Free State, Bloemfontein, SA, 2010.

[8] Senra, J. D.; Malta, L. F. B.; da Costa, M. E. H. M.; Michel, R. C.; Aguiar, L. C. S.; Simas, A. B. C.; Antunes, O. A. C. *Adv. Synth. Catal*. **2009**, *351*, 2411-2422.

[9] Forman, G. S.; McConnell, A. E.; Tooze, R.P.; Janse van Rensburg, W.; Meyer, W. H.; Kirk, K. M.; Dwyer, C. L.; Serfontein, D. W. *Organometallics* **2005**, *24*, 4582-4542.

[10] Sawant, A. D.; Raut, D. G.; Darvatkar, N. B.; Desai, U. V.; Salunkhe, M. M. *Catal. Commun*. **2010**, *12*, 273-276.

[11] Hoover, J. M.; Stahl, S. S. *J. Am. Chem. Soc*. **2011**, *133*, 16901-16910.

[12] Tan, E. W.; Chan, B.; Blackman, A. G. *J. Am. Chem. Soc*. **2002**, *124*, 2078-2079.

[13] Shoa, L.; Qi, C. *Appl. Catal. A Gen*. **2013**, *468,* 26-31.

[14] Aslam, M.; Stansbury, W. F.; Reiter, R. J.; Larkin, D. R. *J. Org. Chem*. **1997**, *62*, 1550-1552.

[15] Wang, T.; Xiang, S.-K.; Qin, C.; Ma, J.-A.; Zhang, L.-H.; Jiao, N. *Tetrahedron Lett*. **2011**, *52*, 3208-3211.

[16] Sawant, A. D.; Raut, D. G.; Darvatkar, N. B.; Desai, U. V.; Salunkhe, M. M. *Catal. Commun*. **2010**, *12*, 273-276.

APPENDIX 1

Plate 1a: *trans*-Stilbene (**258**)

^{1}H NMR [600 MHz, $CDCl_3$]: δ 7.55 (4H, br d, *J* = 8.2 Hz, H-2,6), 7.39 (4H, t, *J* = 7.7 Hz, H-3,5), 7.29 (2H, m, H-4), 7.14 (2H, s, C<u>H</u>=C<u>H</u>).

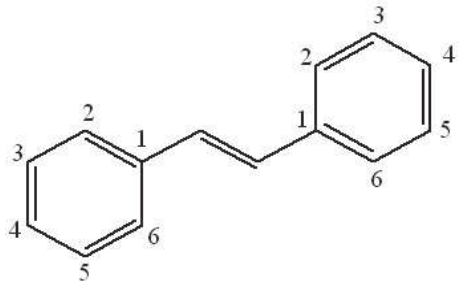

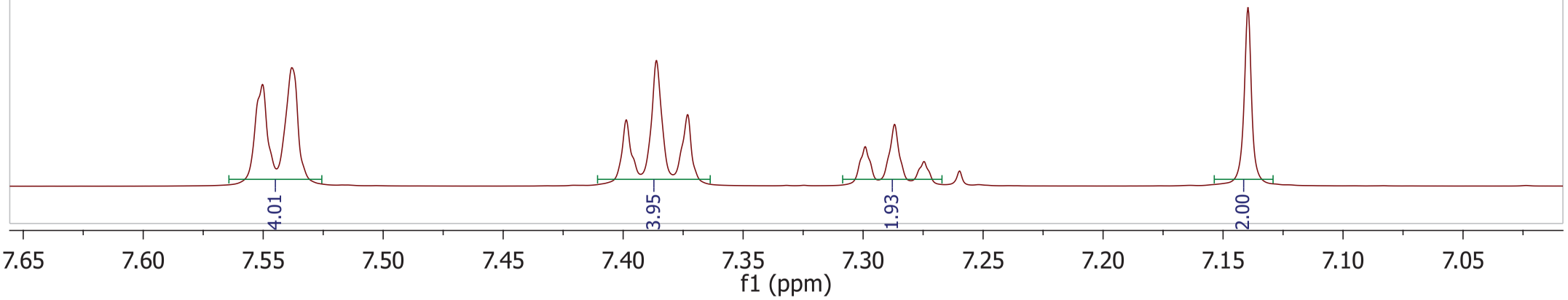

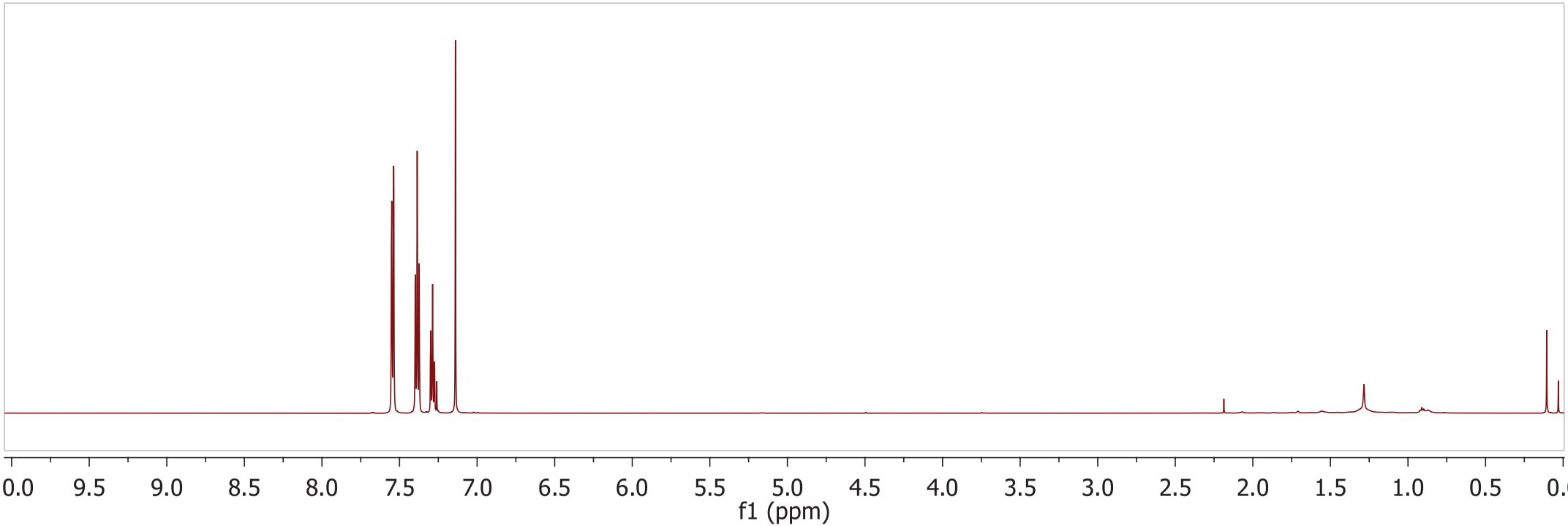

Plate 1b: *trans*-Stilbene (**258**)

^{13}C NMR [151 MHz, $CDCl_3$]: δ 137.5 (C-1), 128.8 (C-3,5 and CH=CH), 127.8 (C-4), 126.7 (C-2,6).

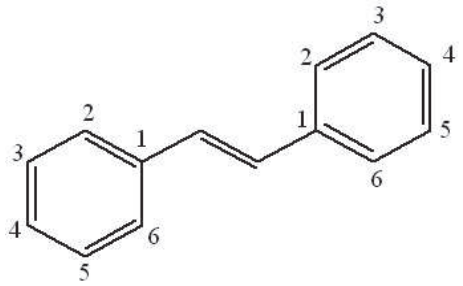

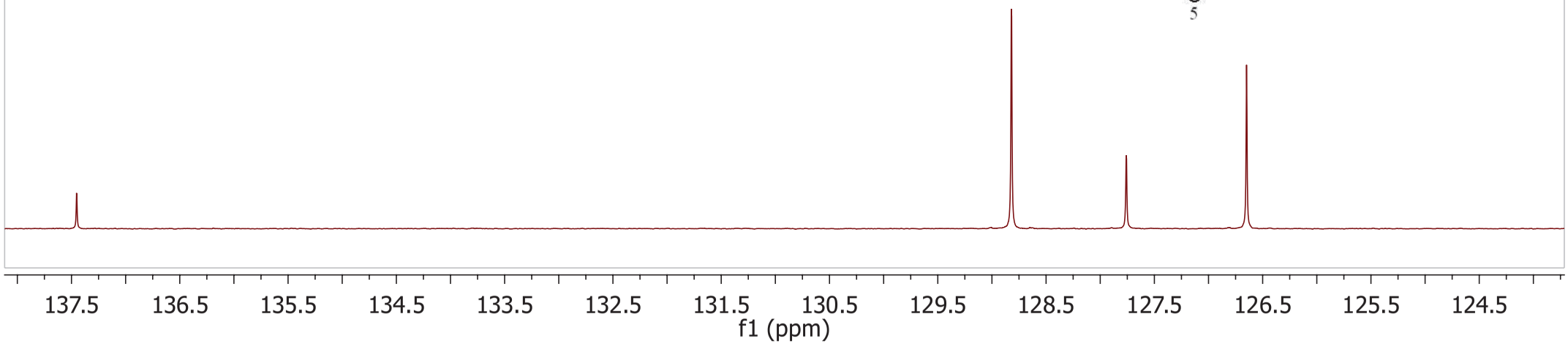

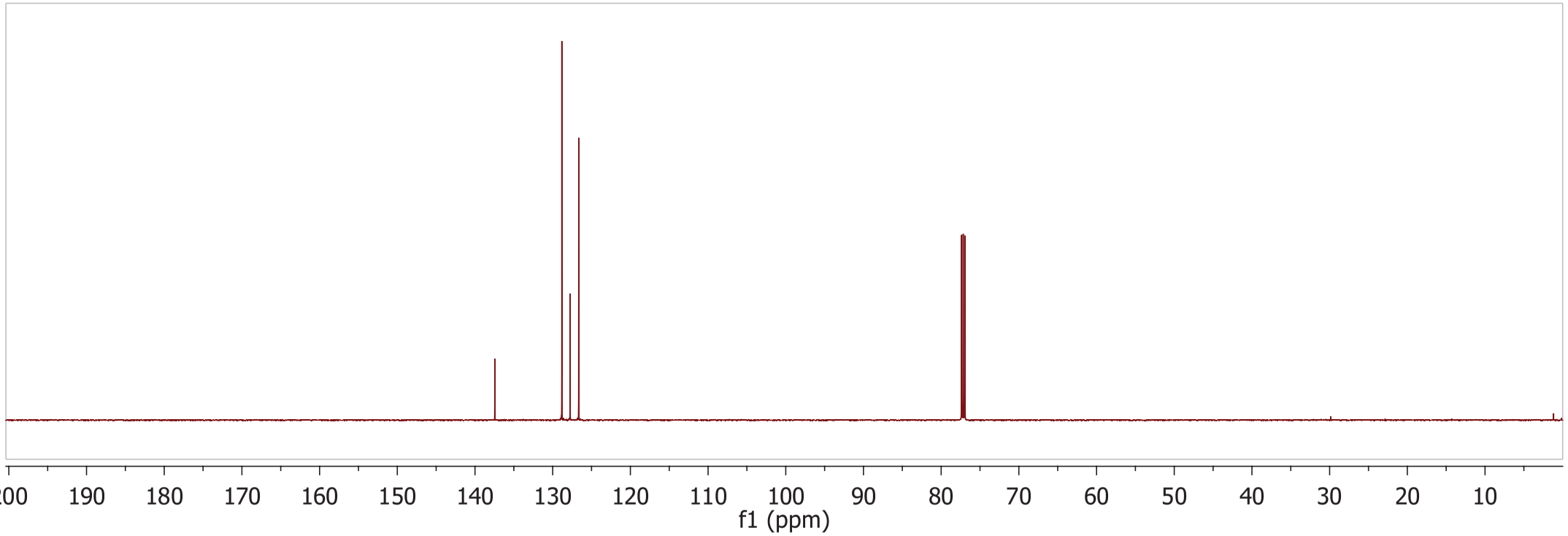

Plate 2a: *trans*-4,4-Dimethoxystilbene (**259**)

^{1}H NMR [600 MHz, $CDCl_3$]: δ 7.43 (4H, d, *J* = 8.8 Hz, H-2,6), 6.93 (2H, s, C<u>H</u>=C<u>H</u>), 6.89 (4H, d, *J* = 8.8 Hz, H-3,5), 3.83 (6H, s, -OC<u>H</u>$_3$).

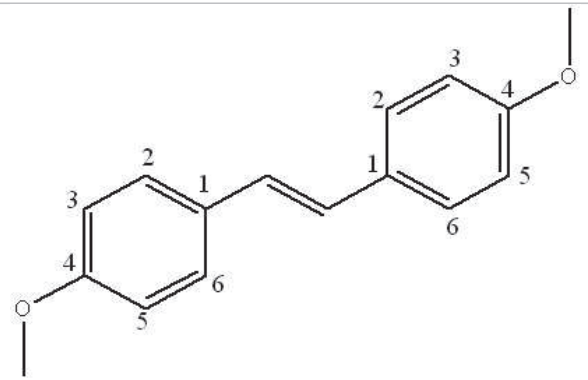

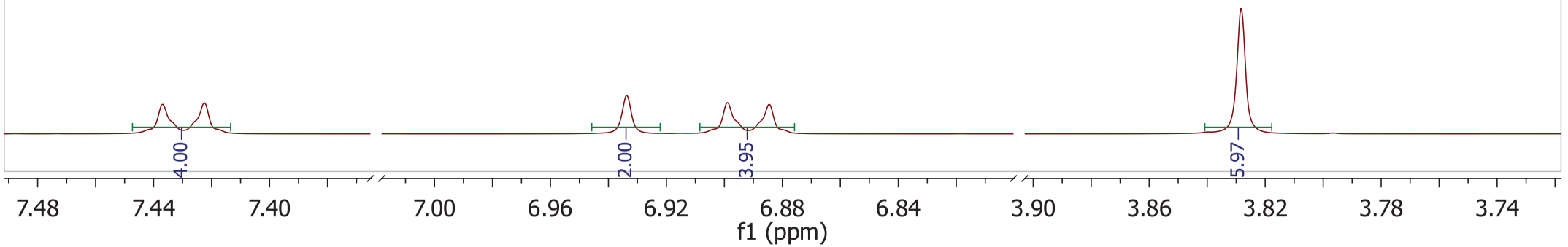

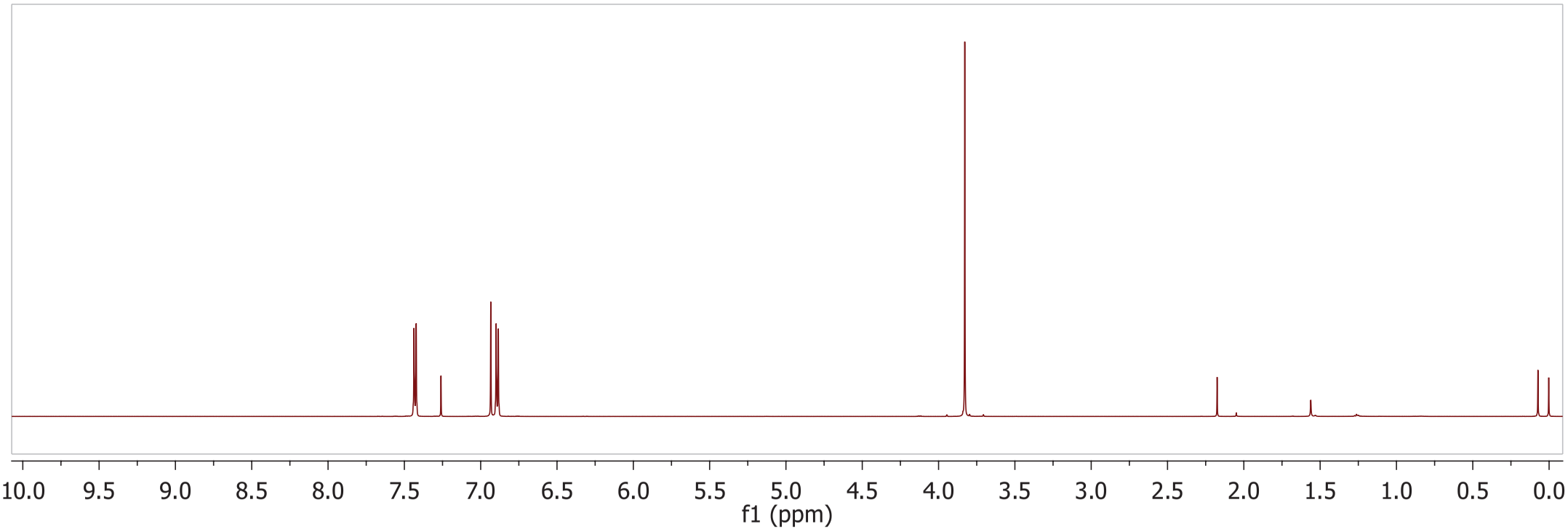

Plate 2b: *trans*-4,4-Dimethoxystilbene (**259**)

^{13}C NMR [151 MHz, $CDCl_3$]: δ 159.2 (C-4), 130.6 (C-1), 127.6 (C-2,6), 126.3 (C=C), 114.2 (C-3,5), 55.5 (OCH_3).

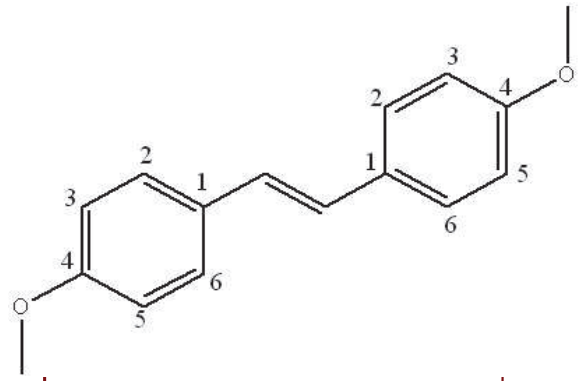

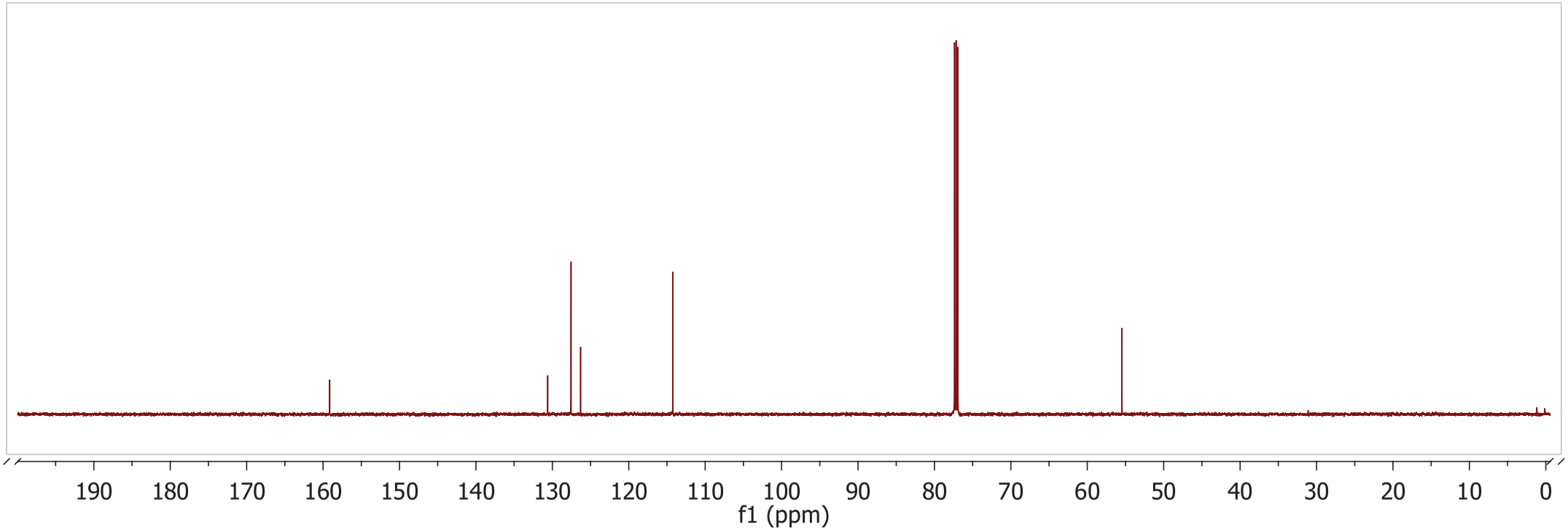

Plate 3a: Methyl cinnamate (**195**)

^{1}H NMR [600 MHz, $CDCl_3$]: δ 7.70 (1H, d, *J* = 16.0 Hz, H-3), 7.52 – 7.50 (2H, m, H-2',6'), 7.37 – 7.36 (3H, m, H-3',4',5'), 6.44 (1H, d, *J* = 16.0 Hz, H-2), 3.79 (3H, s, H-1'').

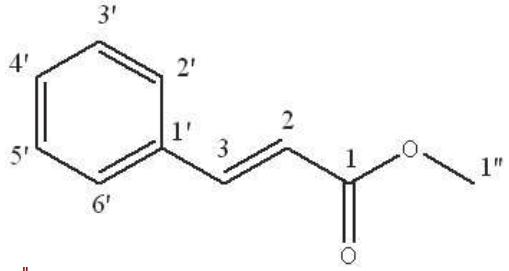

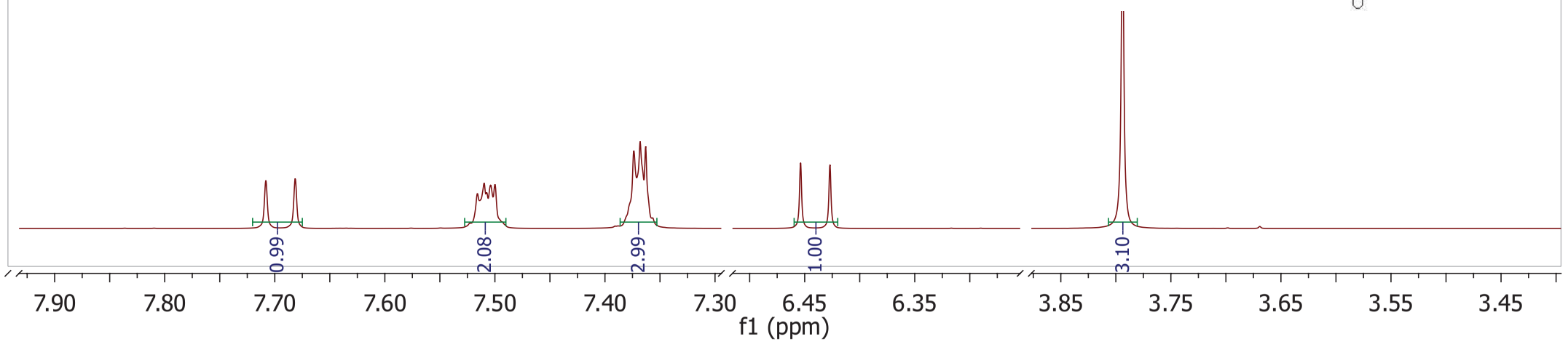

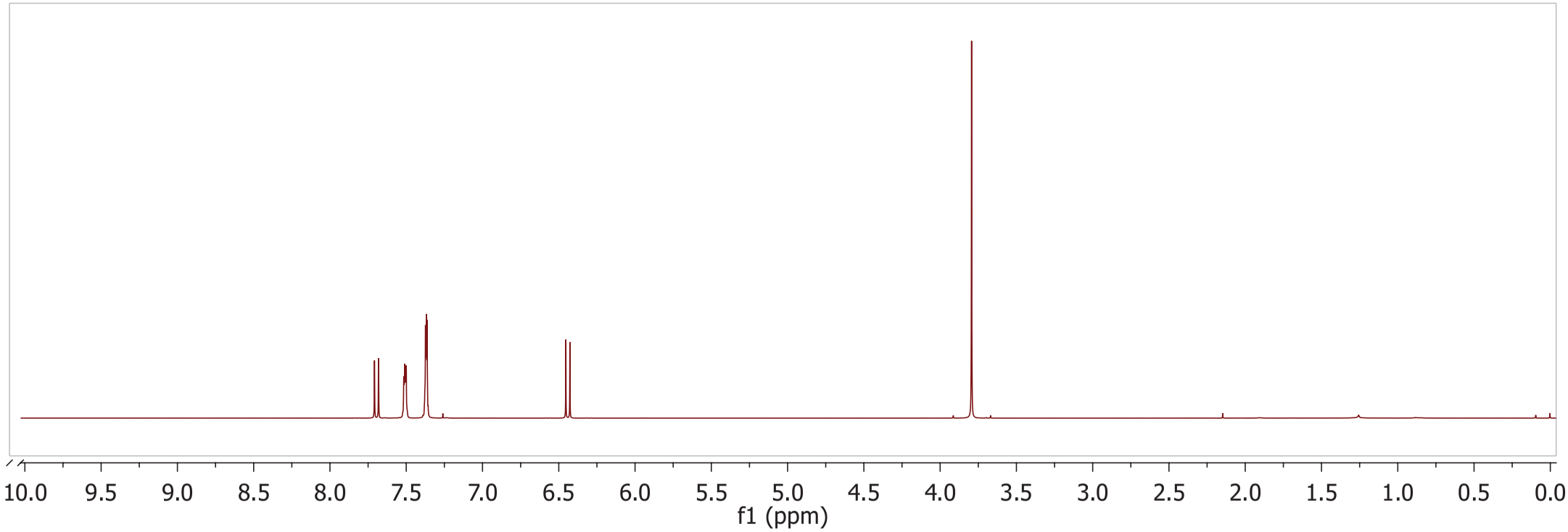

Plate 3b: Methyl cinnamate (**195**)

^{13}C NMR [151 MHz, $CDCl_3$]: δ 167.4 (C-1), 144.9 (C-3), 134.4 (C-1'), 130.3 (C-4'), 128.9 (C-3',5'), 128.1 (C-2',6'), 117.8 (C-3), 51.7 (C-1'').

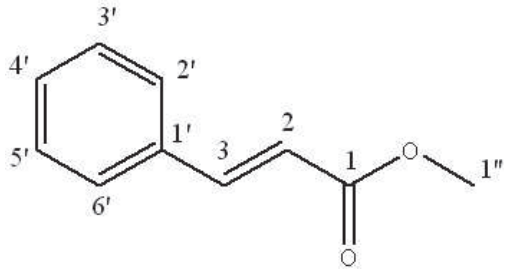

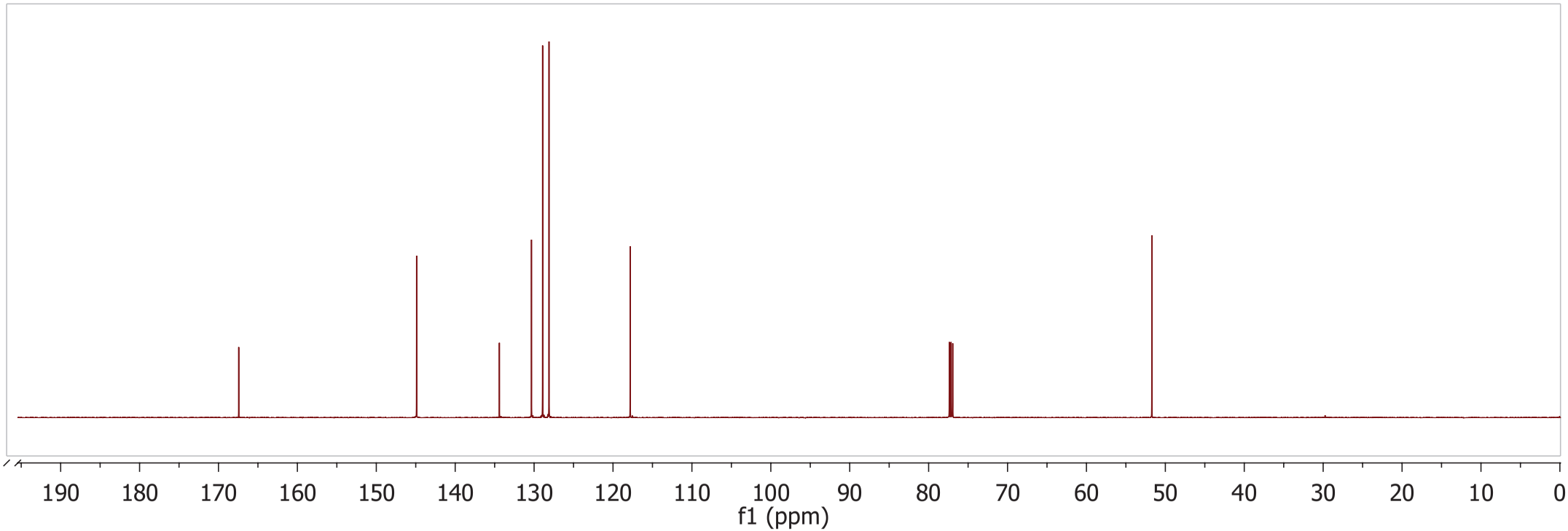

Plate 4a: Butyl cinnamate (**278**)

^{1}H NMR [600 MHz, $CDCl_3$]: δ 7.57 (1H, d, *J* = 16.0 Hz, H-3), 7.42-7.36 (2H, m, H-2',6'), 7.25-7.21 (3H, m, H-3',4',5'), 6.33 (1H,d, *J* = 16.0 Hz, H-2), 4.09 (2H, t, *J* = 6.7 Hz, H-1''), 1.59-1.55 (2H, m, H-2''), 1.35-1.29 (2H, m, H-3''), 0.85 (3H, t, *J* = 7.4 Hz, H-4'').

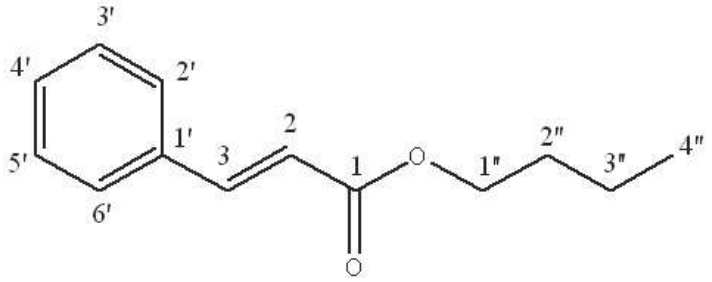

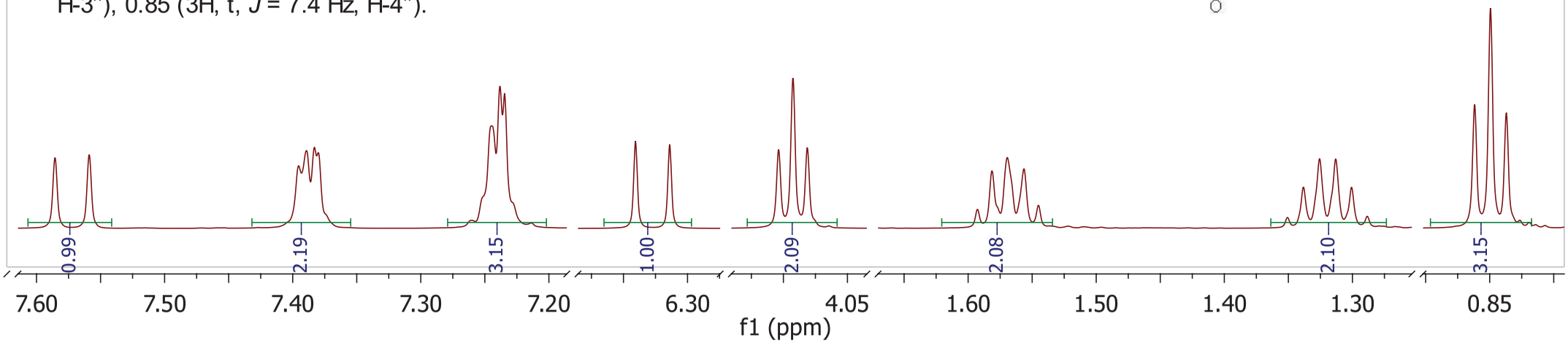

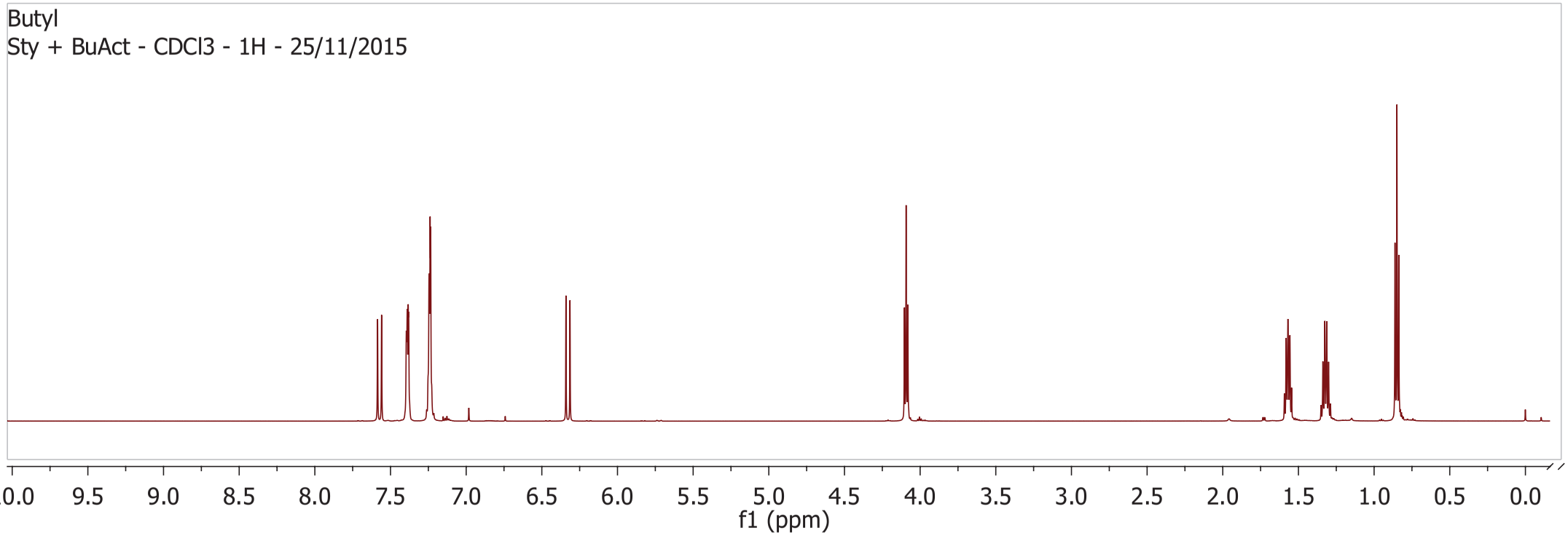

Plate 4b: Butyl cinnamate (**278**)

^{13}C NMR [151 MHz, $CDCl_3$]: δ 167.0 (C-1), 144.5 (C-3), 134.4 (C-1'), 130.2 (C-4'), 128.8 (C-2',6'), 128.0 (C-3',5'), 118.2 (C-2), 64.3 (C-1''), 30.8 (C-2''), 19.2 (C-3''), 13.7 (C-4'').

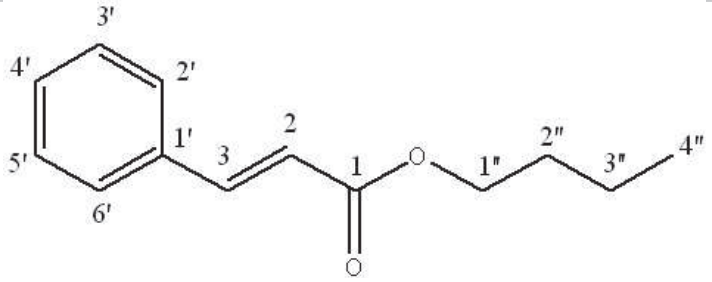

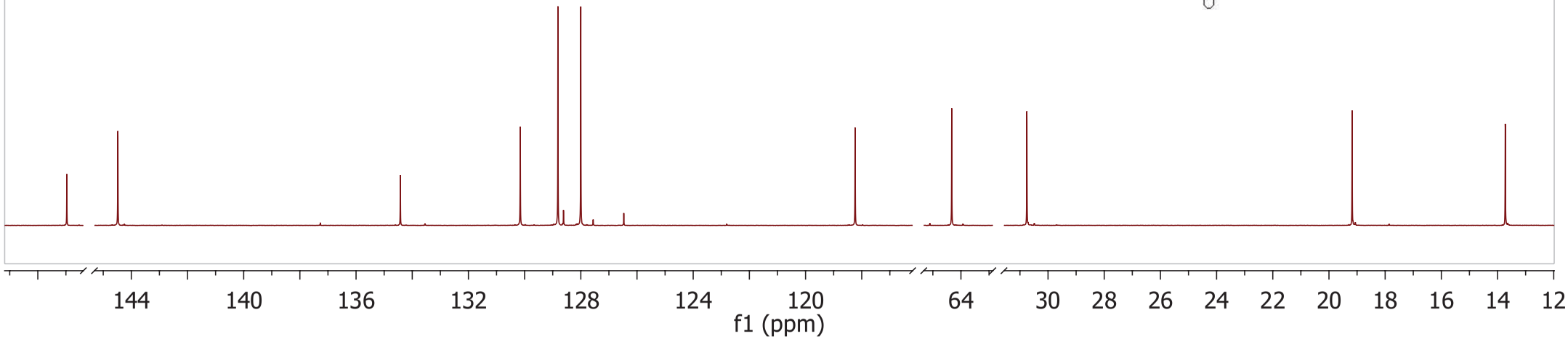

Butyl
Sty + BuAct - CDCl3 - 13C - 25/11/2015

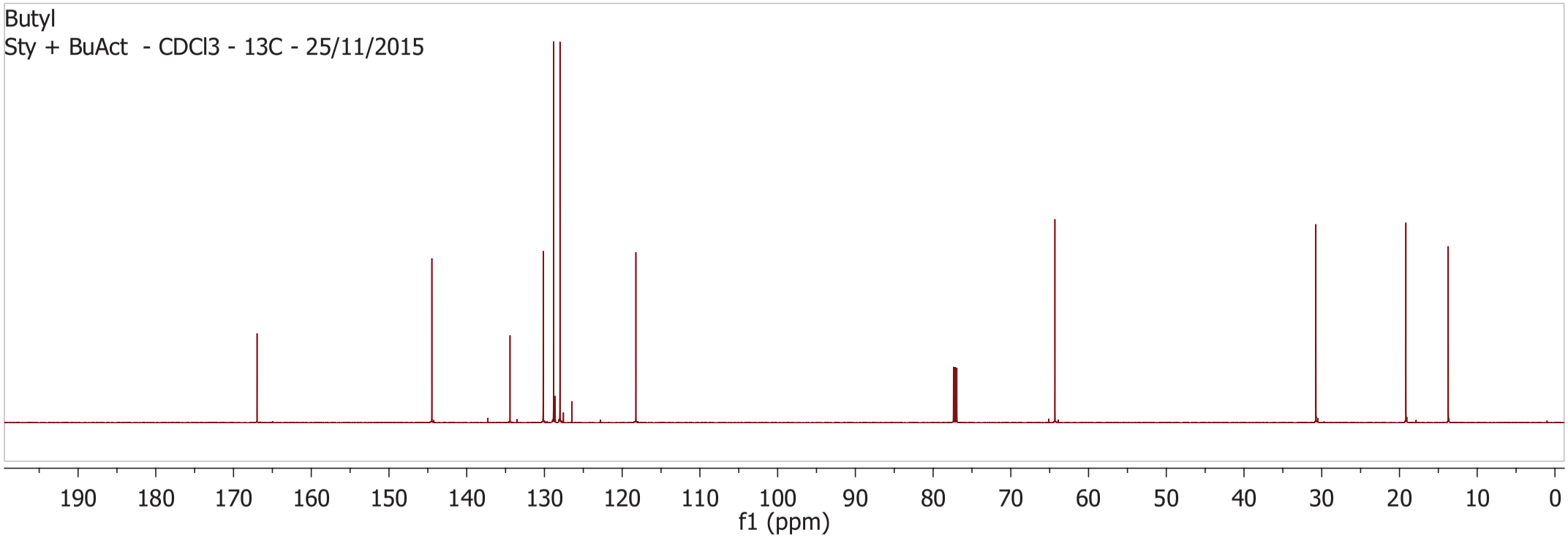

Plate 5a: 2-Ethylhexyl cinnamate (**282**)

^{1}H NMR [600 MHz, $CDCl_3$]: δ 7.68 (1H, d, *J* = 16.0 Hz, H-3), 7.55-7.51 (2H, m, H-2',6'), 7.40-7.35 (3H, m, H-3',4',5'), 6.45 (1H, d, *J* = 16.0 Hz, H-2), 4.17-4.09 (2H, m, H-1''), 1.69-1.61 (1H, m, H-2''), 1.47-1.29 (8H, m, H-3'',4'',5'',1'''), 0.94-.089 (6H, m, H-6'',2''').

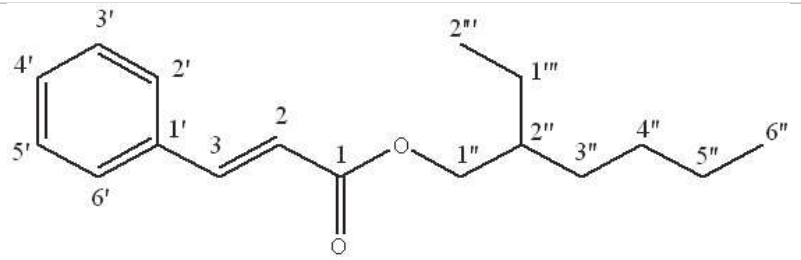

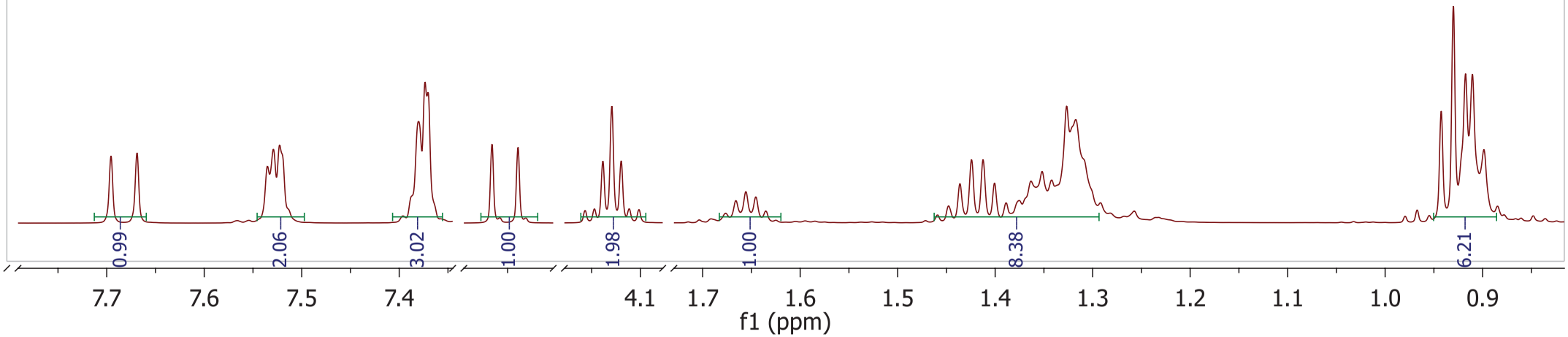

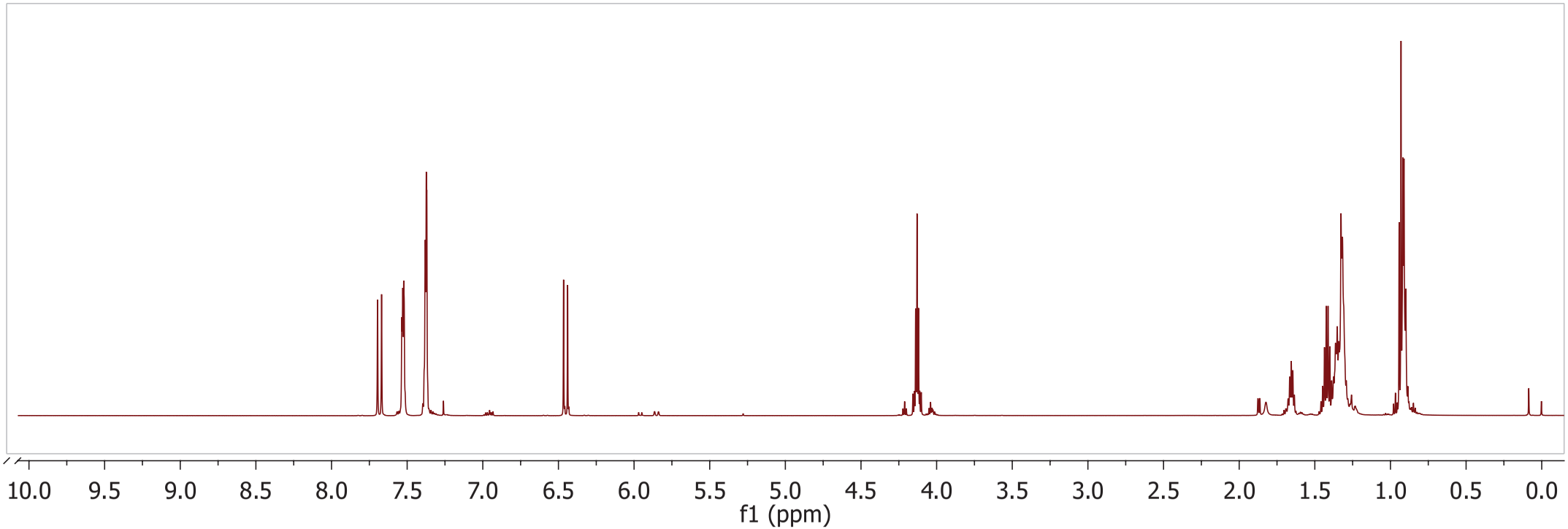

Plate 5b: 2-Ethylhexyl cinnamate (**282**)

^{13}C NMR [151 MHz, $CDCl_3$]: δ 167.3 (C-1), 144.6 (C-3), 134.6 (C-1'), 130.3 (C-4'), 128.9 (C-3',5'), 128.1 (C-2',6'), 118.4 (C-2), 67.1 (C-1''), 38.9 (C-2''), 30.6, 29.1, 23.9, 23.1 (C-3'',4'',5'',1'''), 14.2, 11.1 (C-6'',2''').

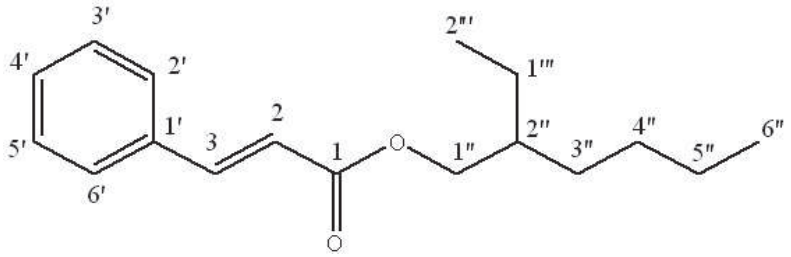

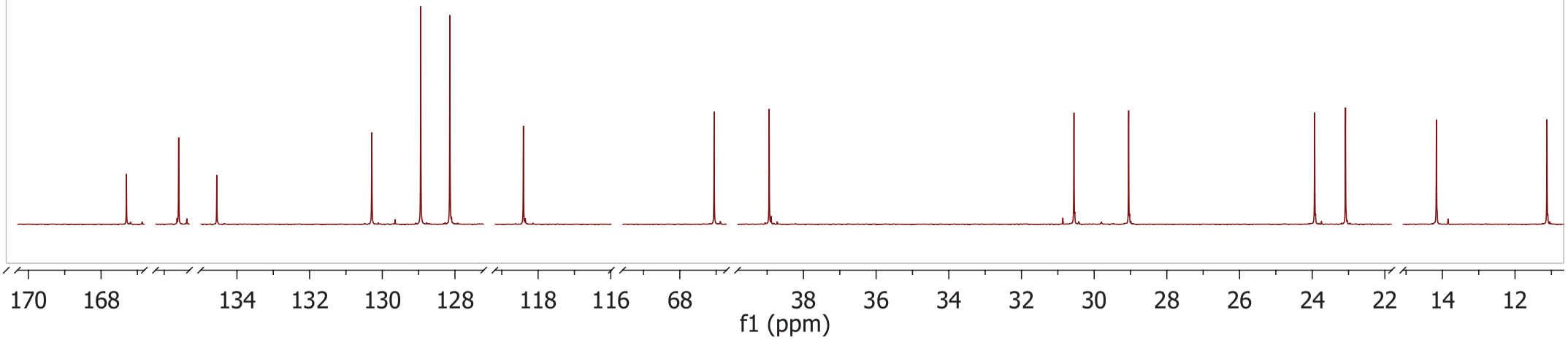

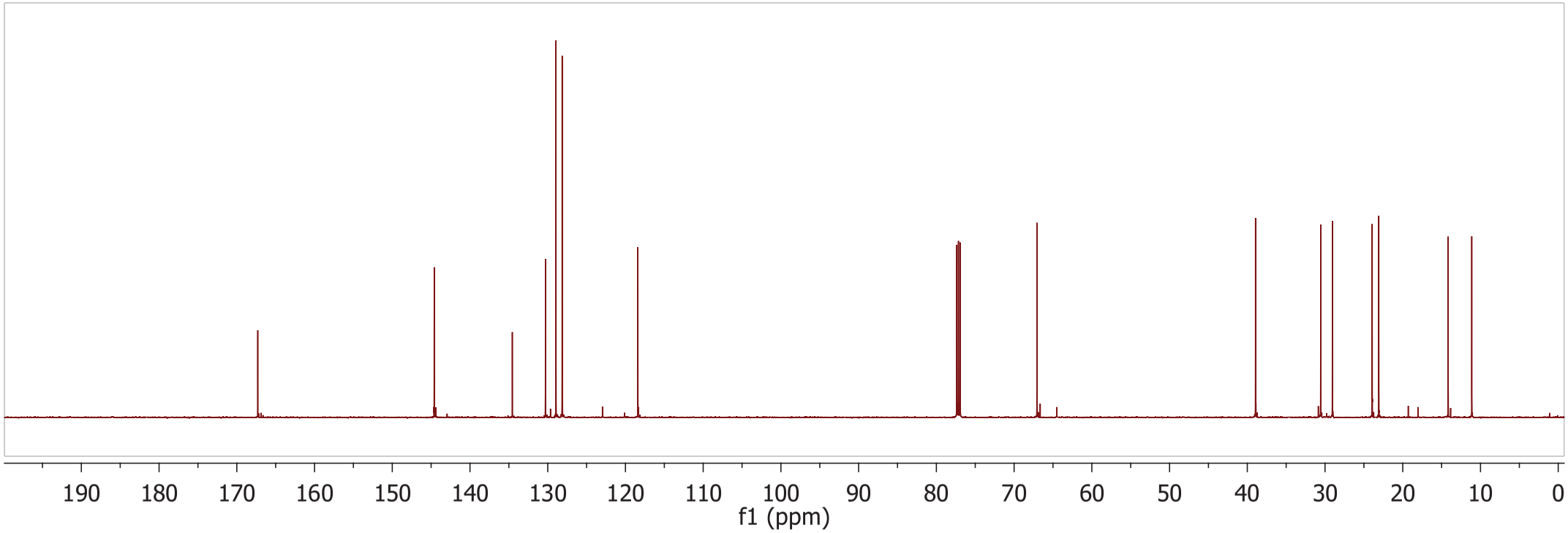

Plate 6a: (E)-4-Phenylbut-3-en-2-one (**277**)

^{1}H NMR [600 MHz, $CDCl_3$]: δ 7.51 (3H, m, H-4,2',6'), 7.39 (3H, m, H-3',4',5'), 6.71 (1H, d, *J* = 16.3 Hz, H-3), 2.37 (3H, s, H-1).

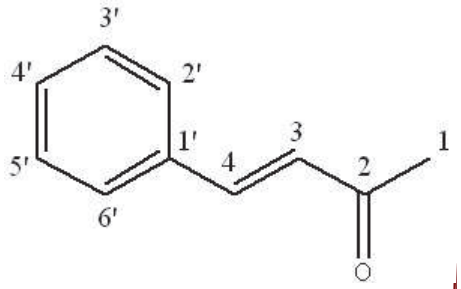

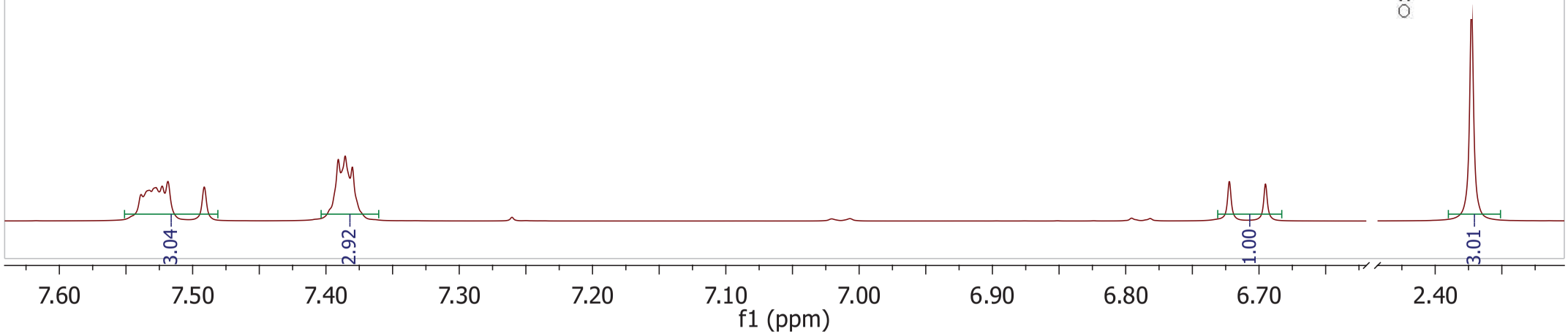

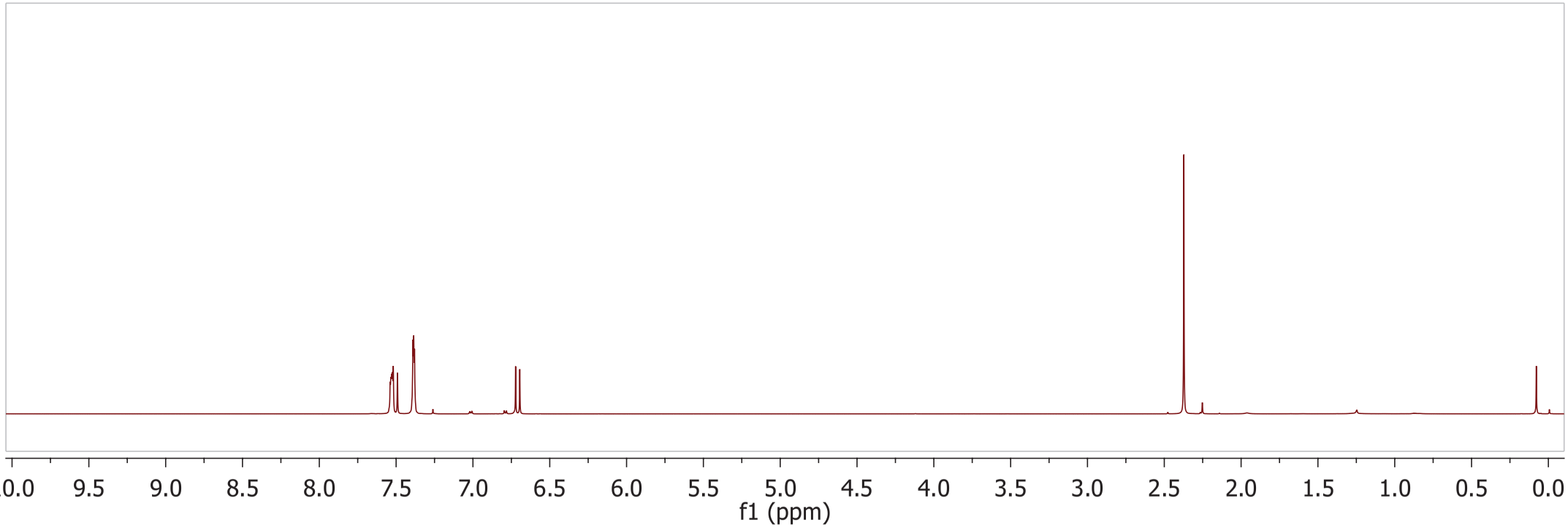

Plate 6b: (E)-4-Phenylbut-3-en-2-one (**277**)

^{13}C NMR [151 MHz, $CDCl_3$]: δ 198.55 (C-2), 143.56 (C-4), 134.45 (C-1'), 130.60 (C-4'), 129.04 (C-3',5'), 128.33 (C-2',6'), 127.18 (C-3), 27.56(C-1).

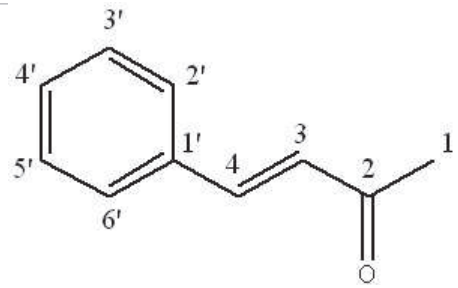

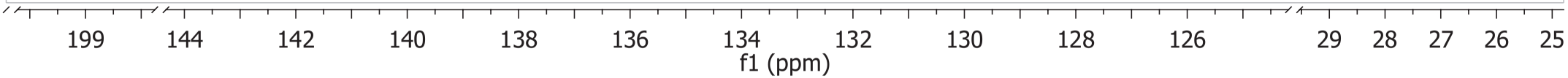

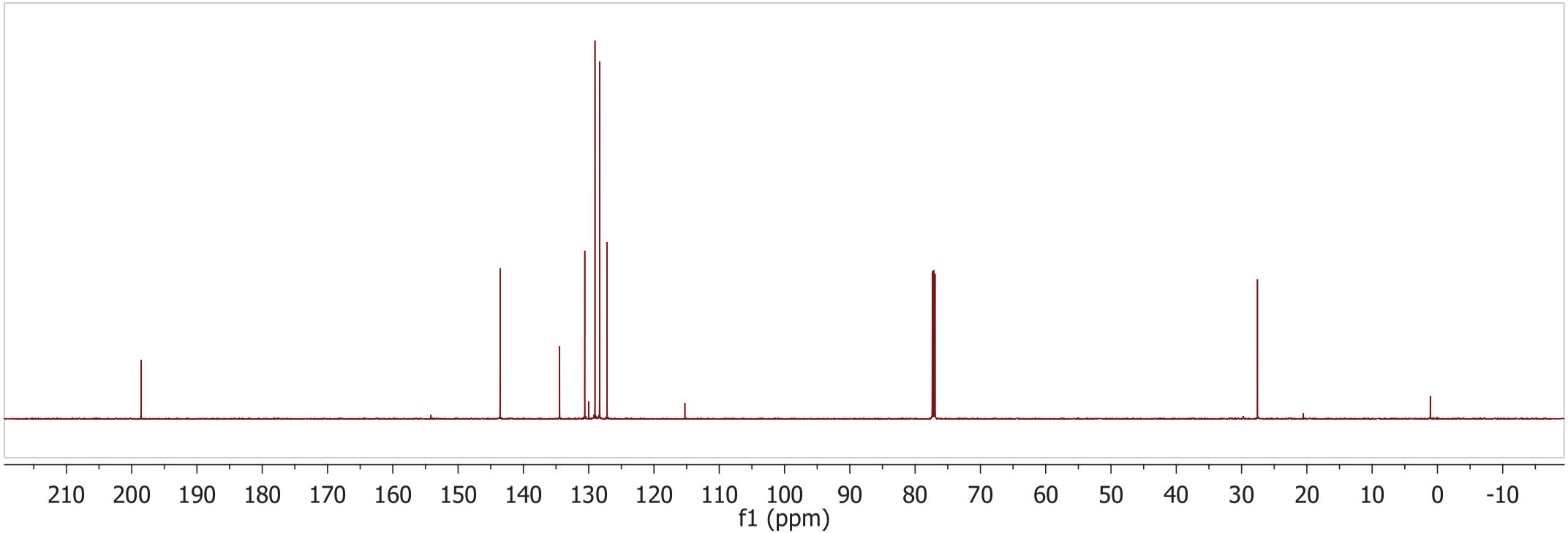

Plate 7a: (E)-methyl 4-methoxycinnamate (**35**)

^{1}H NMR [600 MHz, $CDCl_3$]: δ 7.63 (1H, d, *J* = 16.0 Hz, H-3), 7.45 (2H, d, *J* = 8.8 Hz, H-2',6'), 6.88 (2H, d, *J* = 8.8 Hz, H-3',5'), 6.29 (1H, d, *J* = 16.0 Hz, H-2), 3.80 (3H, s, Ar-O<u>Me</u>), 3.77 (3H, s, H-1").

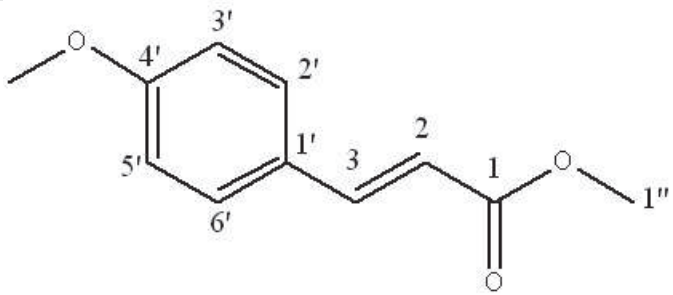

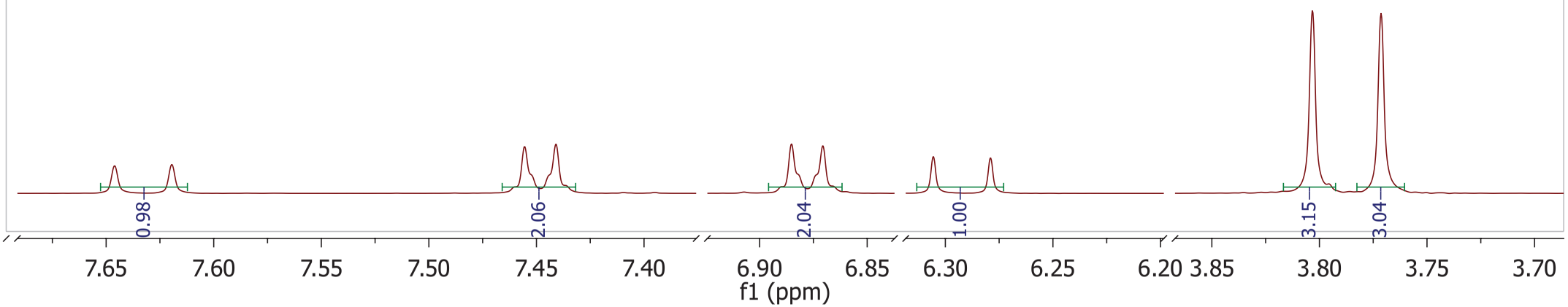

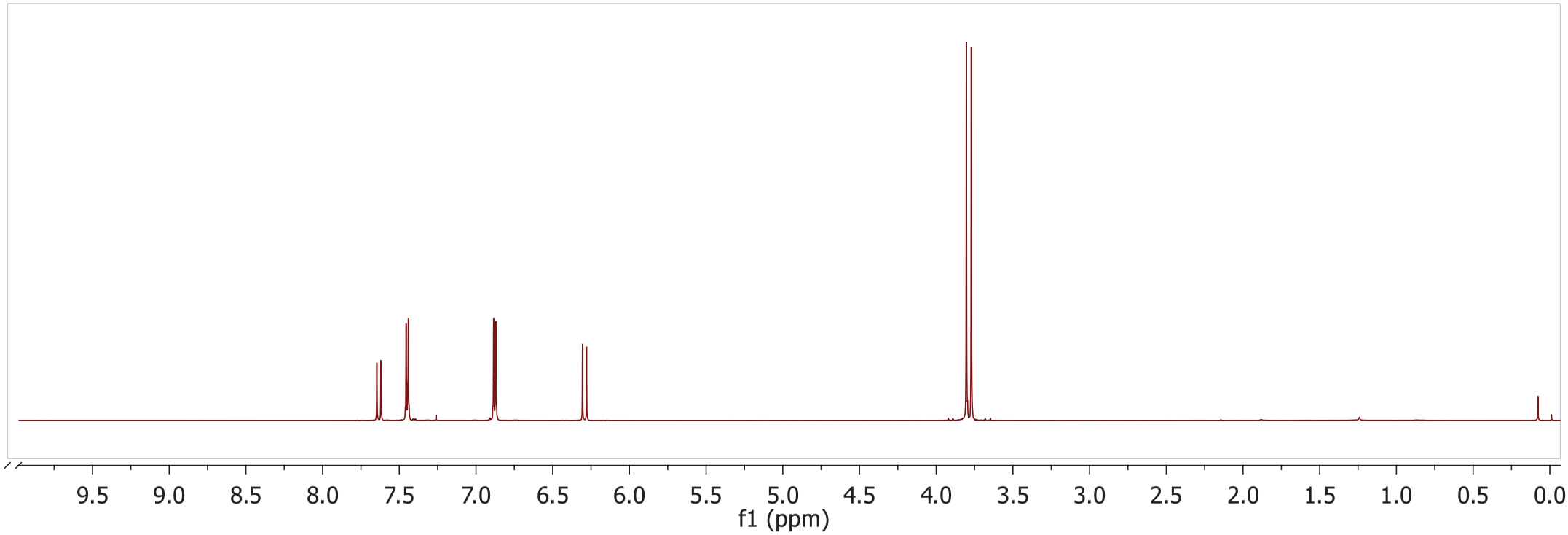

Plate 7b: (E)-methyl 4-methoxycinnamate (**35**)

^{13}C NMR [151 MHz, $CDCl_3$]: δ 167.8 (C-1), 161.4 (C-4'), 144.6 (C-3), 129.8 (C-2',6'), 127.1 (C-1'), 115.3 (C-2), 114.4 (C-3',5'), 55.4 (-OMe), 51.6 (C-1").

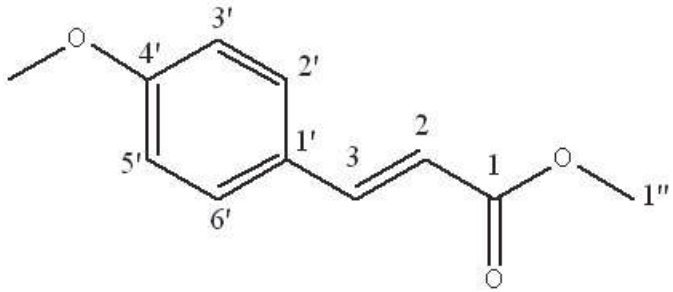

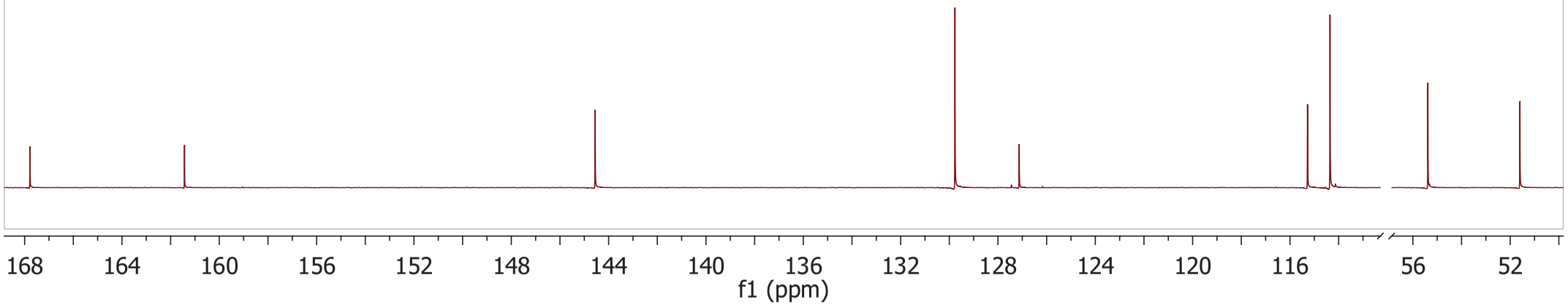

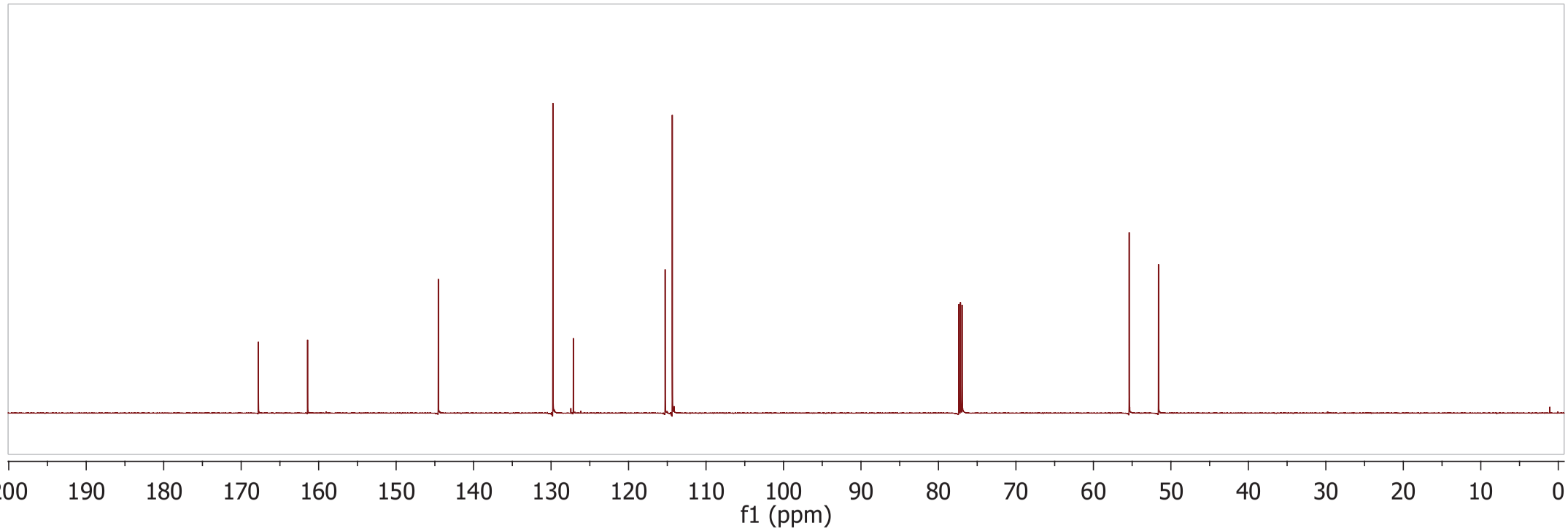

Plate 8a: (E)-butyl 4-methoxycinnamate (**281**)

^{1}H NMR [600 MHz, $CDCl_3$]: δ 7.62 (1H, d, *J* = 16.0 Hz, H-3), 7.45 (2H, d, *J* = 8.7 Hz, H-3',5'), 6.87 (2H, d, *J* = 8.7 Hz, H-2',6'), 6.29 (1H, d, *J* = 16.0 Hz, H-2), 4.18 (2H, t, *J* = 6.7 Hz, H-1"), 3.80 (3H, s, - OMe), 1.71 – 1.61 (2H, m, H-2"), 1.46 – 1.36 (2H, m, H-3"), 0.95 (3H, t, *J* = 7.4 Hz, H-4").

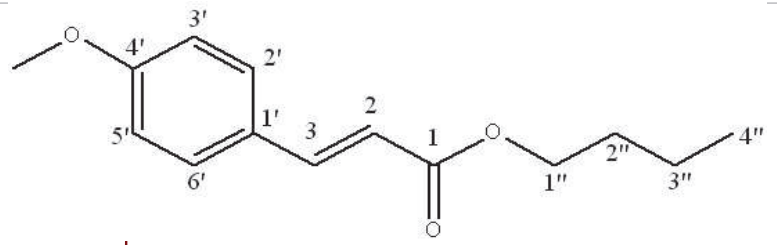

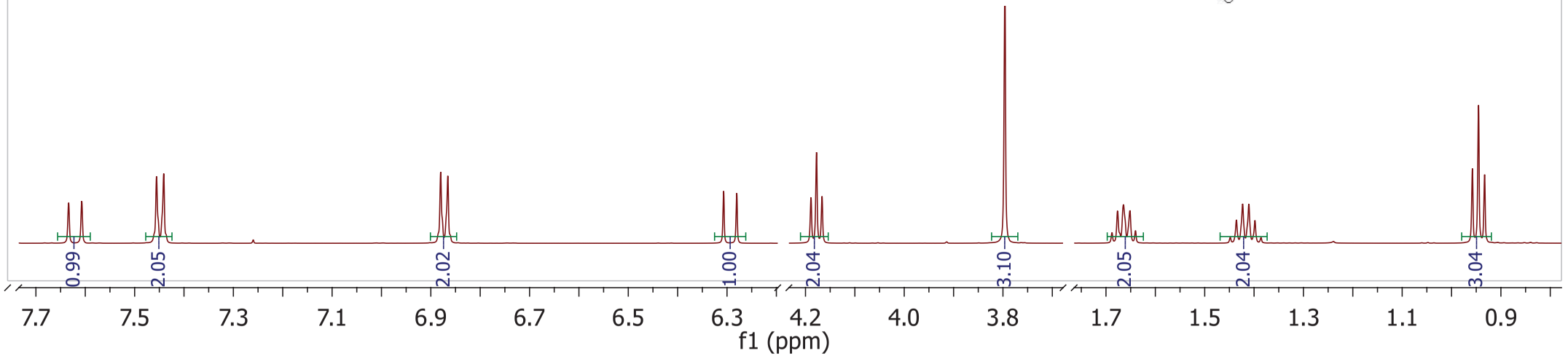

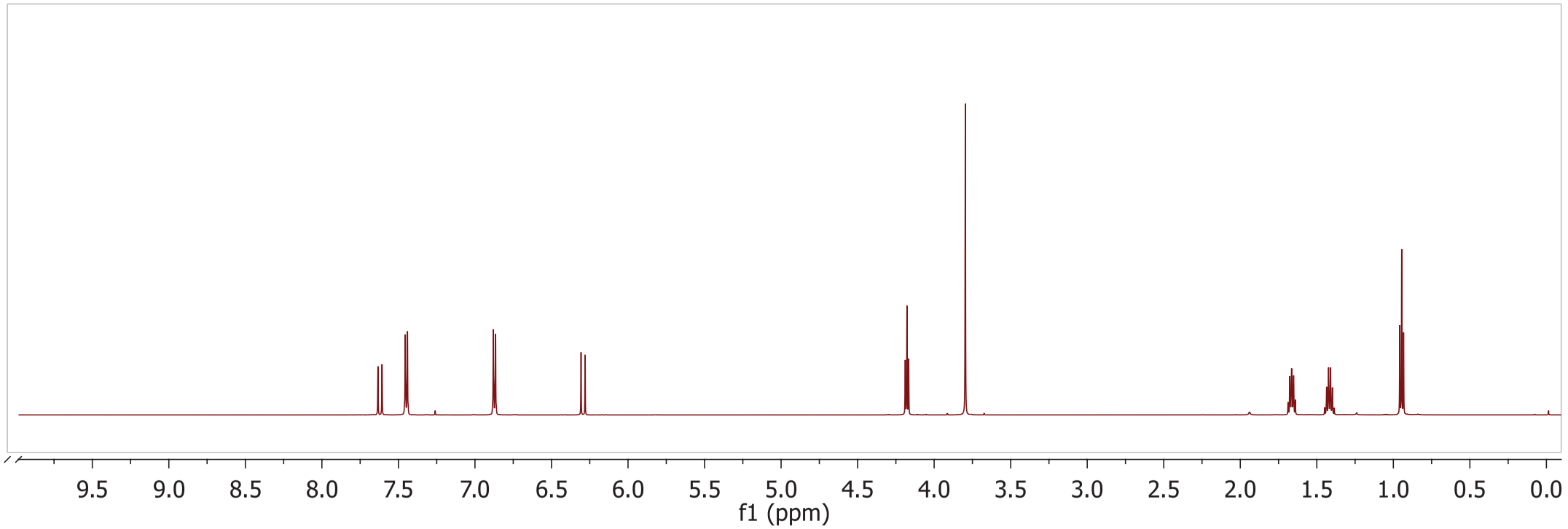

Plate 8b: (E)-butyl 4-methoxycinnamate (**281**)

^{13}C NMR [151 MHz, $CDCl_3$]: δ 167.4(C-1), 161.4 (C-4'), 144.2 (C-3), 129.7 (C-2',6'), 127.2 (C-1'), 115.8 (C-2), 114.3 (C-3',5'), 64.3 (C-1"), 55.3 (-O<u>Me</u>), 30.9 (C-2"), 19.3 (C-3"), 13.8 (C-4").

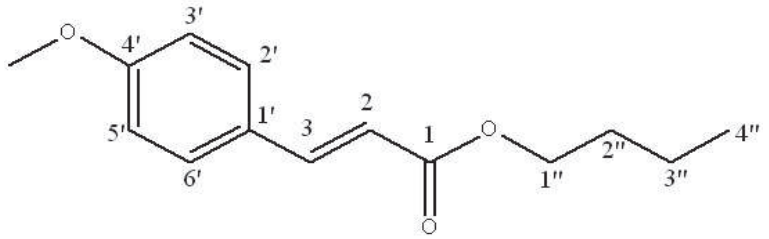

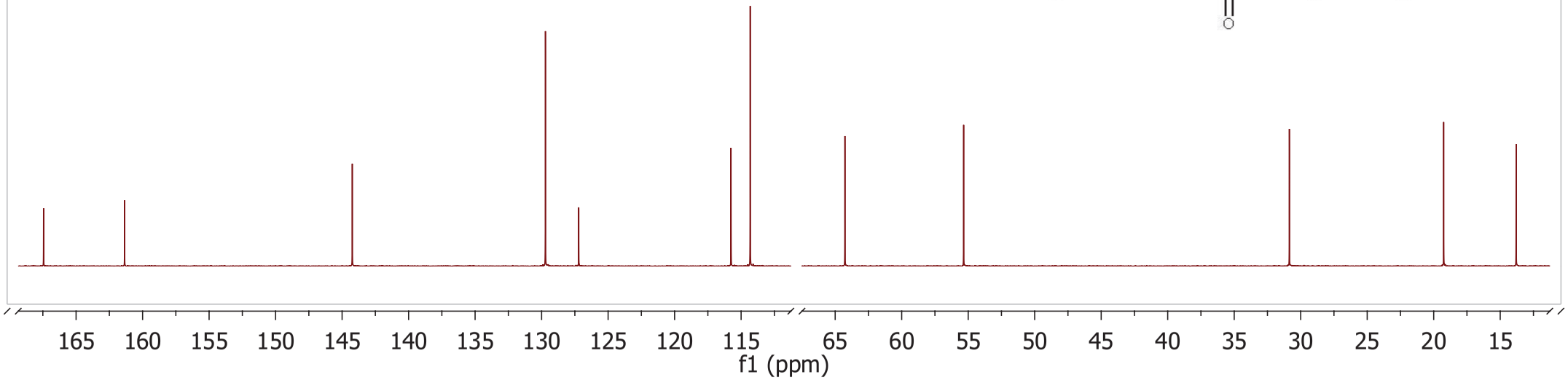

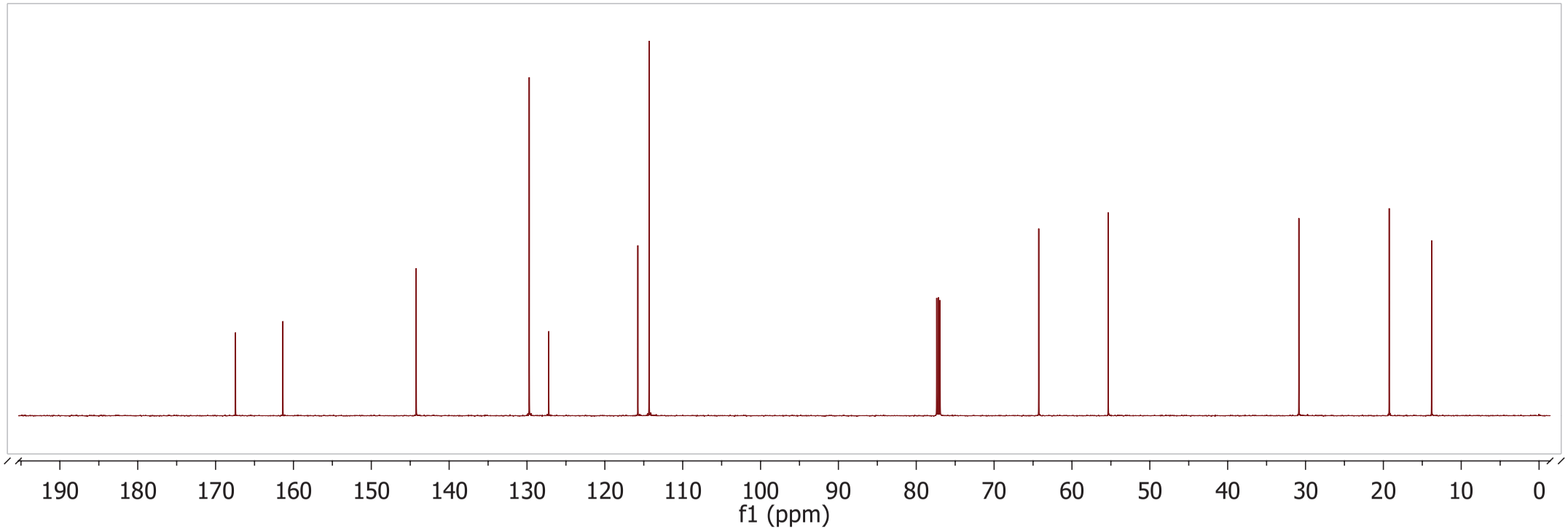

Plate 9a: (E)-2-ethylhexyl 4-methoxycinnamate (**7**)

^{1}H NMR [600 MHz, $CDCl_3$]: δ 7.62 (1H, d, *J* = 16.0 Hz, H-3), 7.45 (2H, d, *J* = 8.7 Hz, H-2',6'), 6.87 (2H, d, *J* = 8.7 Hz, H3',5'), 6.30 (1H, d, *J* = 16.0 Hz, H-2), 4.09 (1H, m, H-1''), 3.79 (3H, s, -OCH_3), 1.67 – 1.58 (1H, m, H-2''), 1.47 – 1.24 (8H, m, H-3'',4'',5'',1'''), 0.94 – 0.86 (6H, m, H-6'',2''').

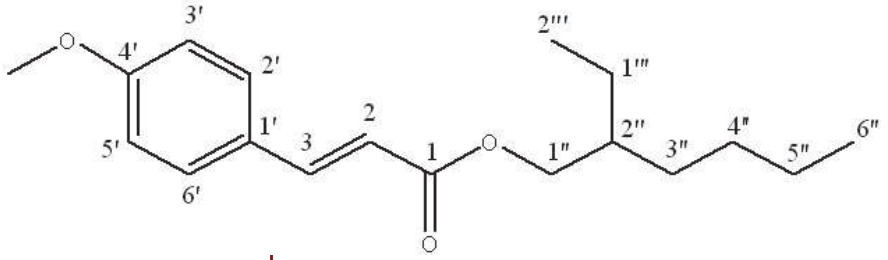

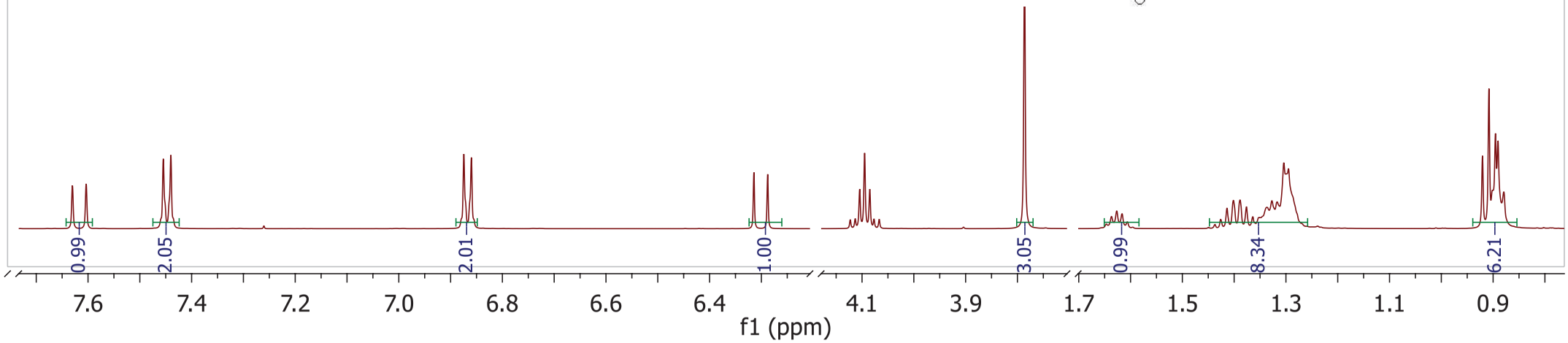

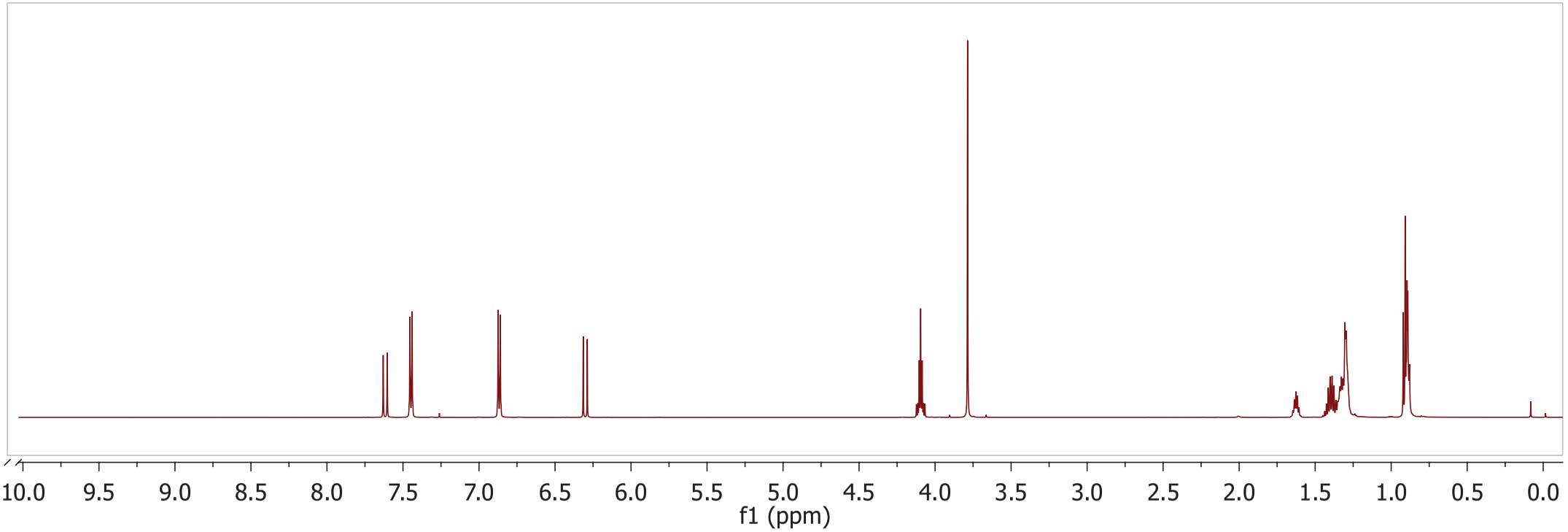

Plate 9b: (E)-2-ethylhexyl 4-methoxycinnamate (**7**)

^{13}C NMR [151 MHz, $CDCl_3$]: δ 167.5 (C-1), 161.3 (C-4'), 144.2 (C-3), 129.7 (C-2',6'), 127.2 (C-1'), 115.8 (C-2), 114.3 (C-3',5'), 66.8 (C-1''), 55.3 (-OMe), 38.9 (C-2''), 30.5, 29.0, 23.9, 23.0 (C-3'',4'',5'',1'''), 14.1, 11.0 (C-6'',2''').

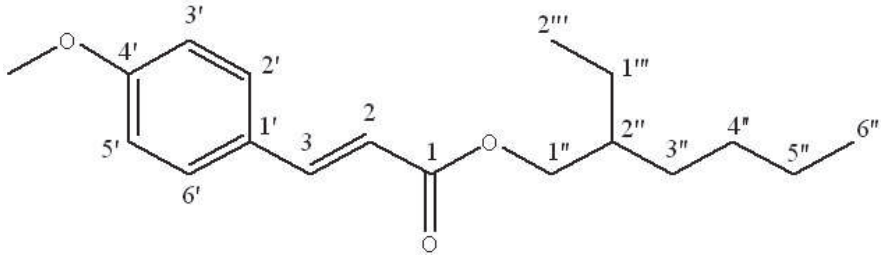

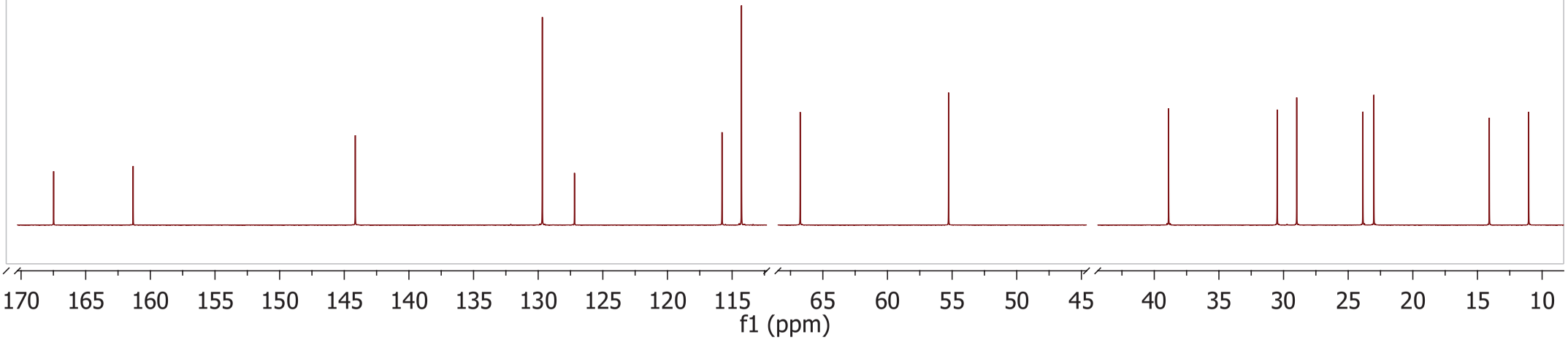

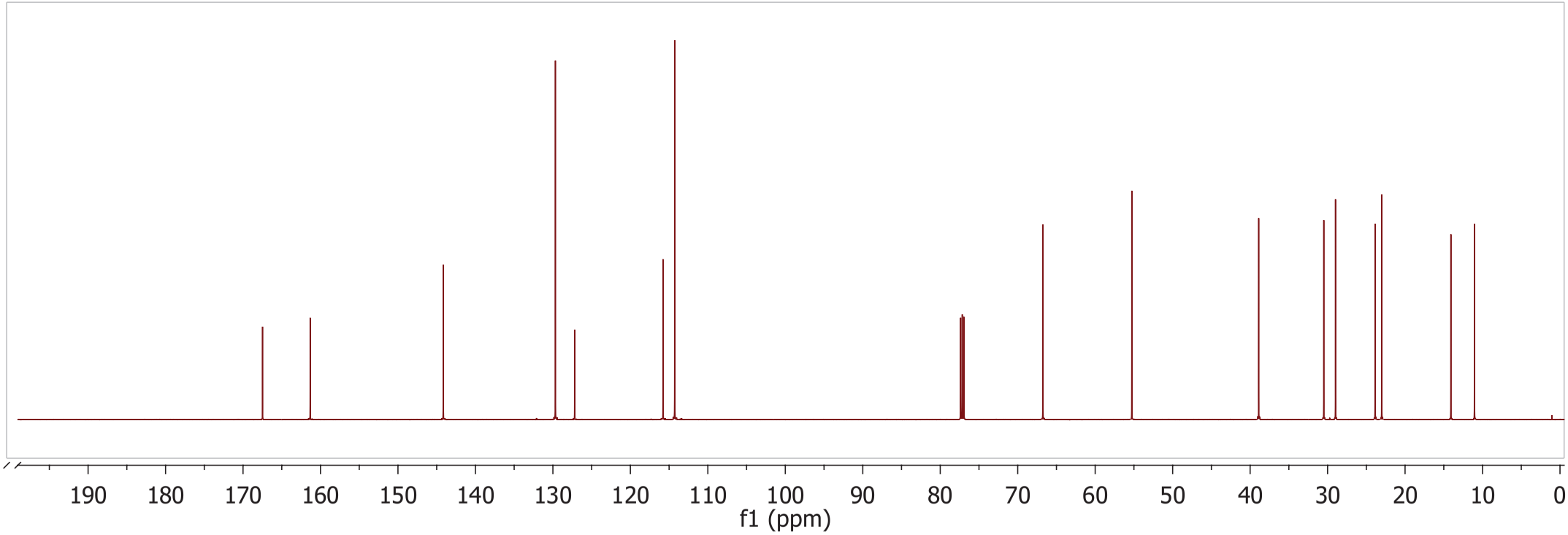

Plate 10a: (E)-4-(4-Methoxyphenyl)but-3-en-2-one (**280**)

^{1}H NMR [600 MHz, $CDCl_3$]: δ 7.37 (3H, m, H-4,2',6'), 6.89 (2H, d, *J* = 8.7 Hz, H-3',5'), 6.58 (1H, d, *J* = 16.2 Hz, H-3), 3.81 (3H, s, -OC<u>H</u>$_3$), 2.33 (3H, s, H-1).

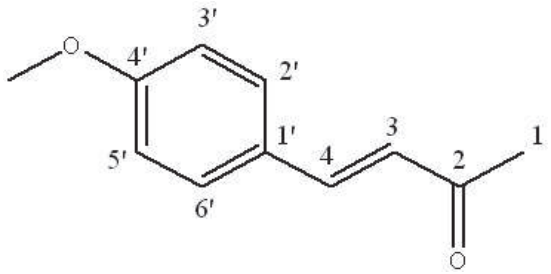

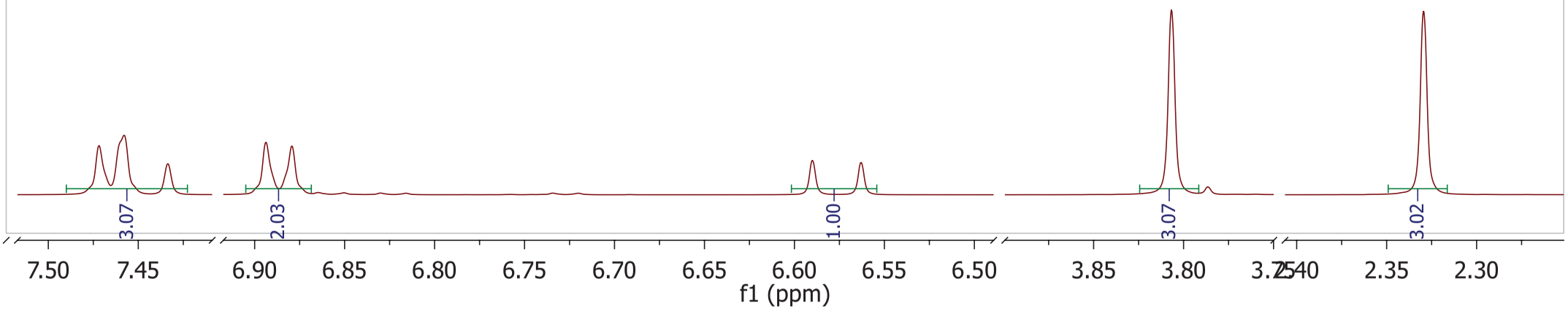

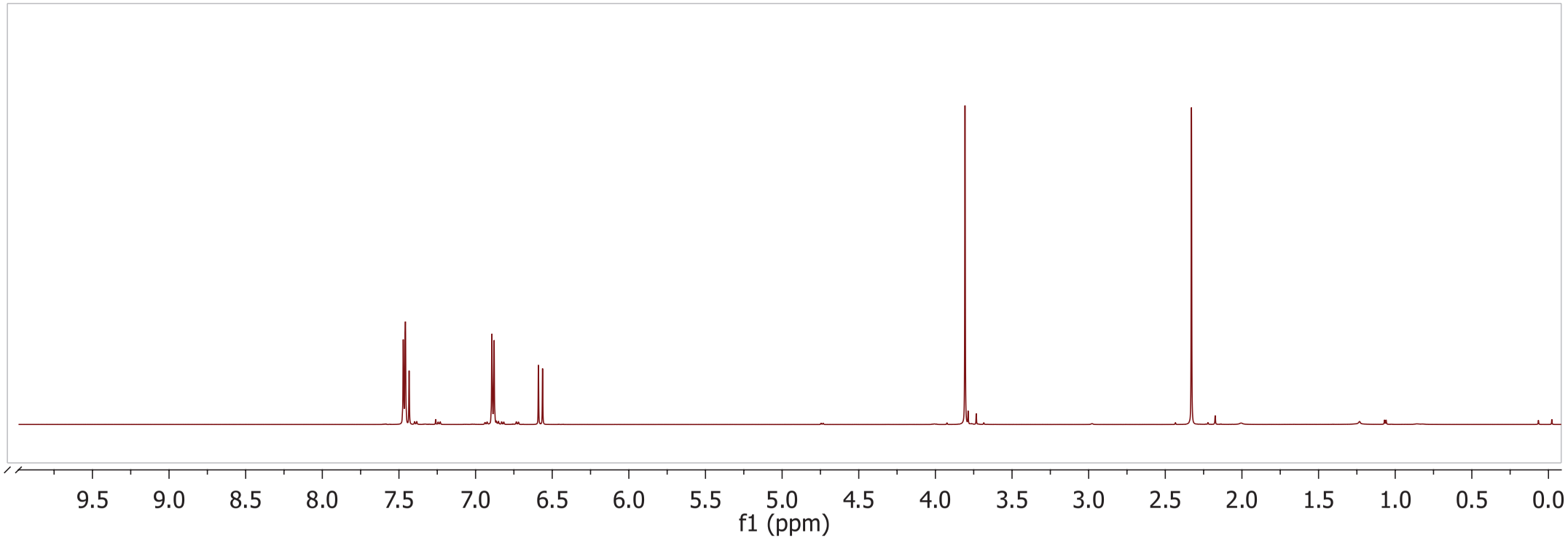

Plate 10b: (E)-4-(4-methoxyphenyl)but-3-en-2-one (**280**)

^{13}C NMR [151 MHz, $CDCl_3$]: δ 198.4 (C-2), 161.6 (C-4'), 143.3 (C-4), 130.0 (C-2',6'), 127.1 (C-1'), 125.0 (C-3), 114.5 (C-3',5'), 55.4 (-OMe), 27.4 (C-1).

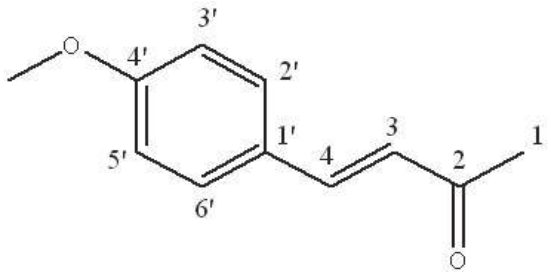

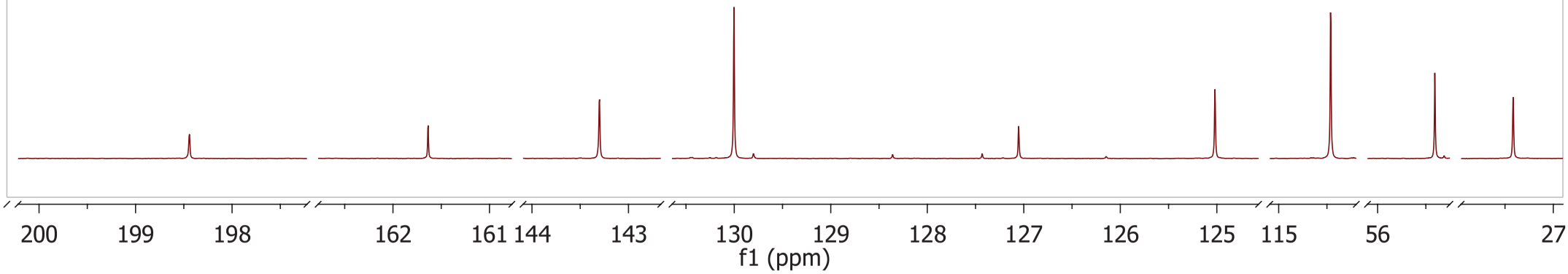

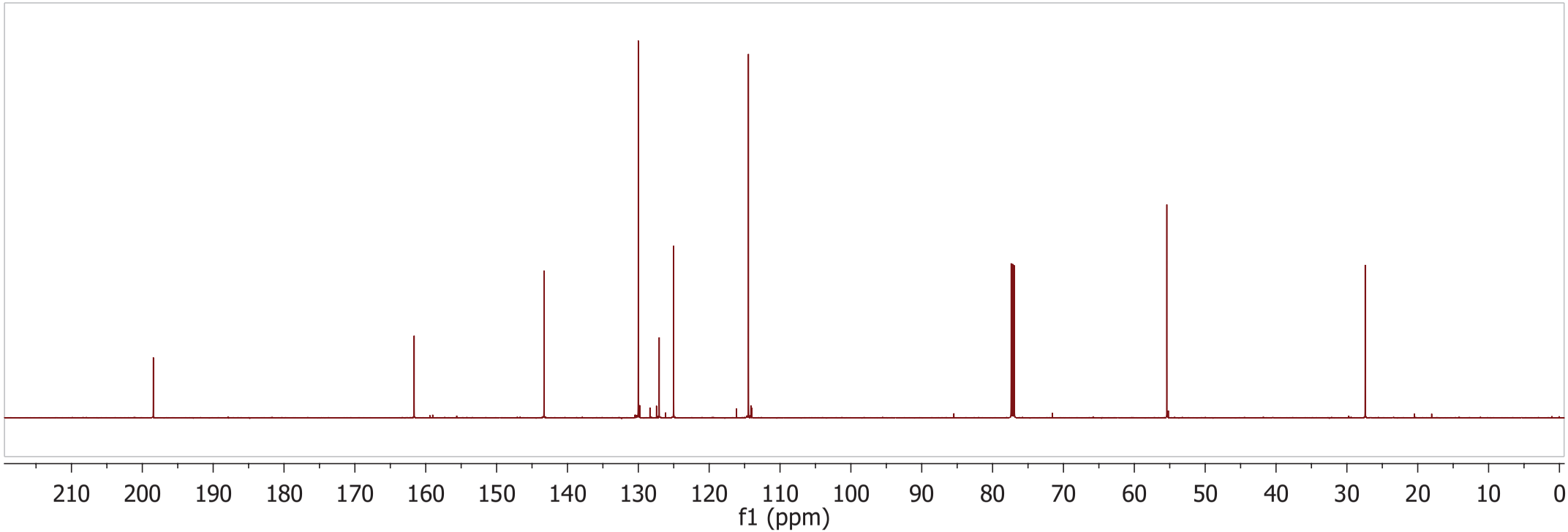

Plate11a: 4-propionylphenyl trifluoromethanesulfonate (**268**)

^{1}H NMR [600 MHz, $CDCl_3$]: δ 8.02 (2H, d, *J* = 8.9 Hz, H-3',5'), 7.33 (2H, d, *J* = 8.9 Hz, H-2',6'), 2.97 (2H, q, *J* = 7.2 Hz, H-2), 1.18 (3H, t, *J* = 7.2 Hz, H-3).

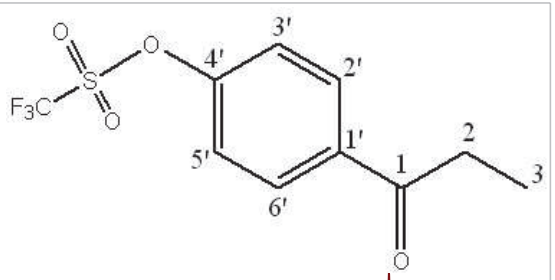

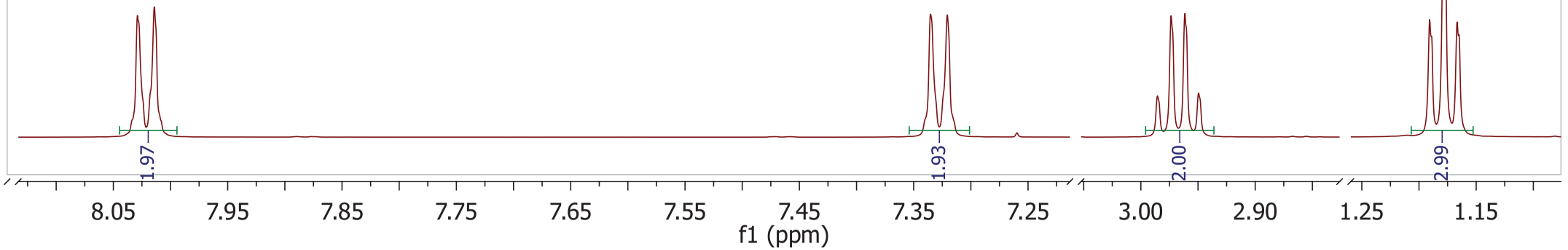

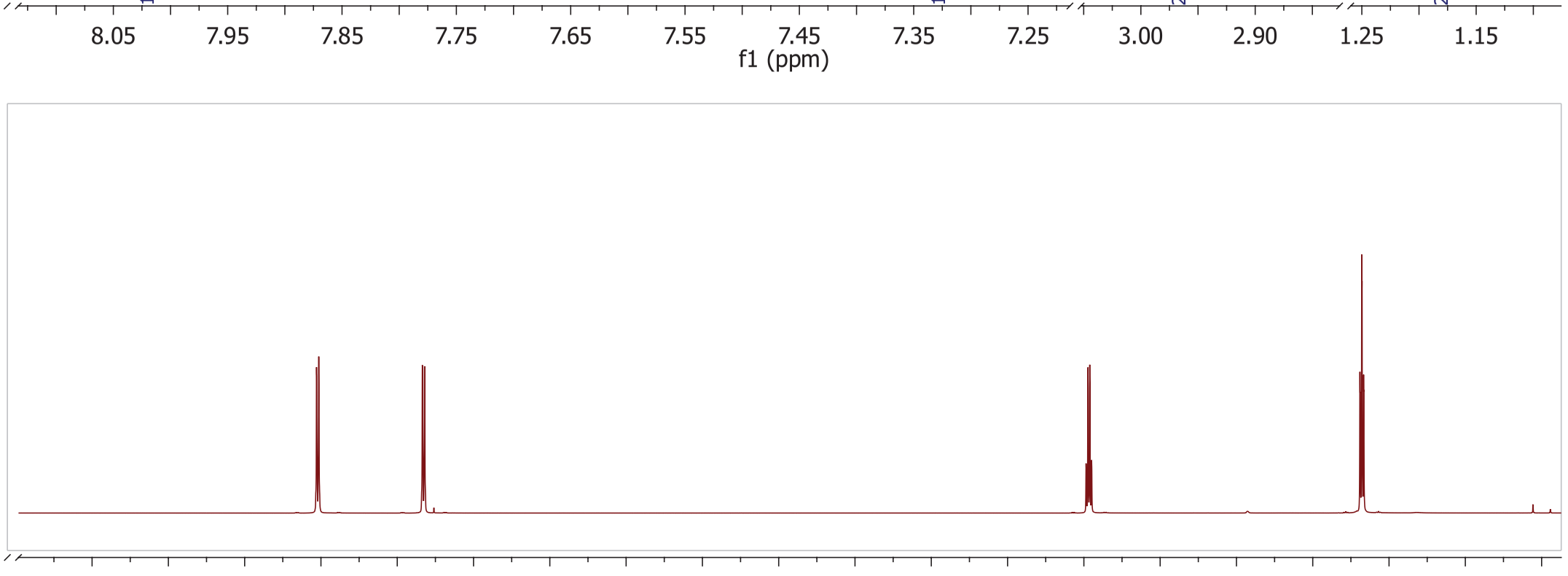

Plate 11b: 4-propionylphenyl trifluoromethanesulfonate (**268**)

^{13}C NMR [151 MHz, $CDCl_3$]: δ 198.9 (C-1), 152.4 (C-1'), 136.8 (C-4'), 130.3 (C-3',5'), 121.6 (C-2',6'), 118.7 (q, J = 320.7 Hz, CF_3), 32.0 (C-2), 7.9 (C-3).

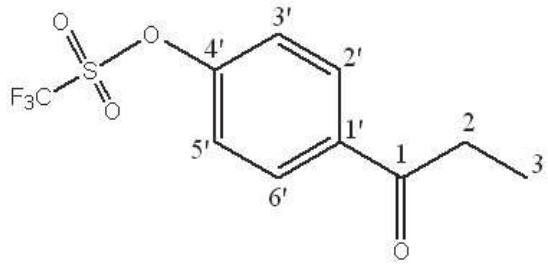

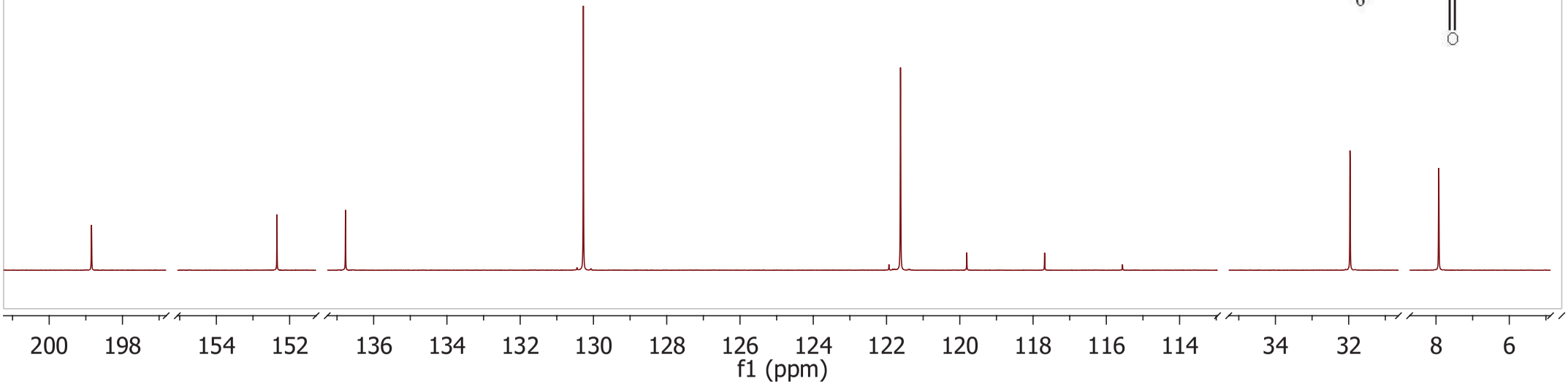

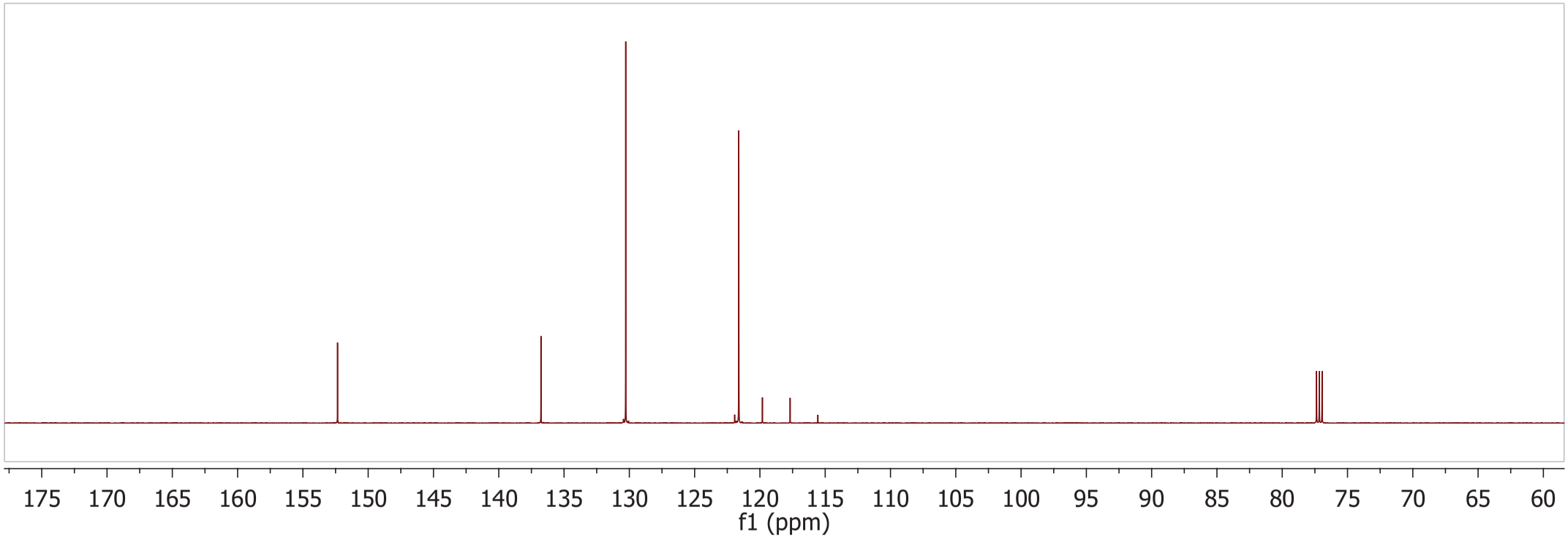

Plate 12a: 4-(1-hydroxypropyl)phenyl trifluoromethanesulfonate (**270**)

^{1}H NMR [600 MHz, $CDCl_3$]: δ 7.41 (2H, d, *J* = 8.7 Hz, H-2',6'), 7.24 (2H, d, *J* = 8.7 Hz, H-3',5'), 4.63 (1H, t, *J* = 6.5 Hz, H-1), 1.81-1.69 (2H, m, H-2), 1.16 (1H, d, *J* = 6.2 Hz, -OH), 0.91 (3H, t, *J* = 7.4 Hz, H-3).

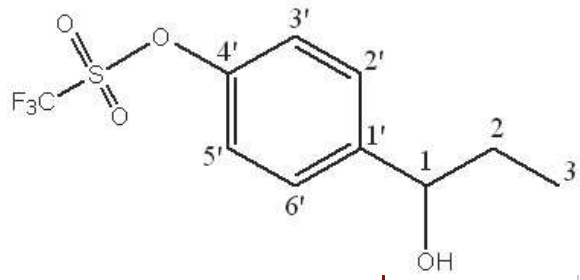

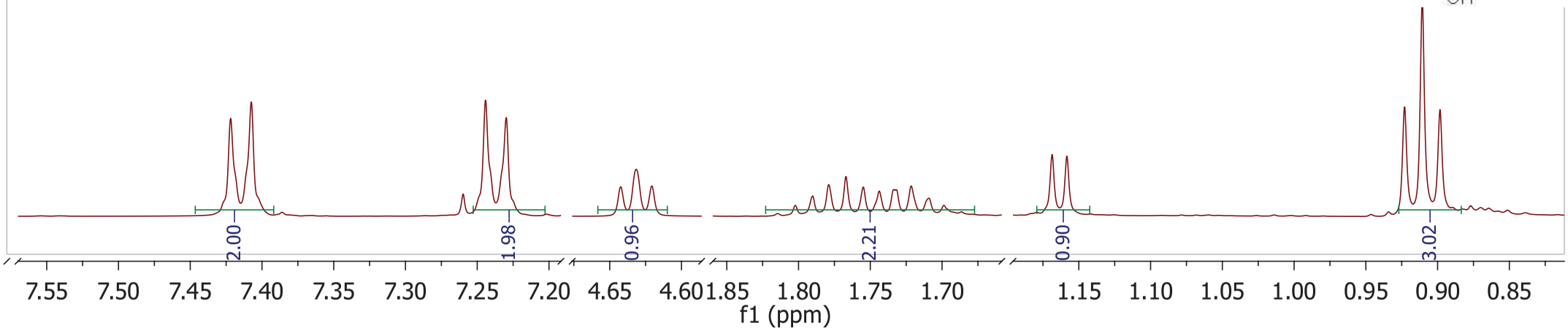

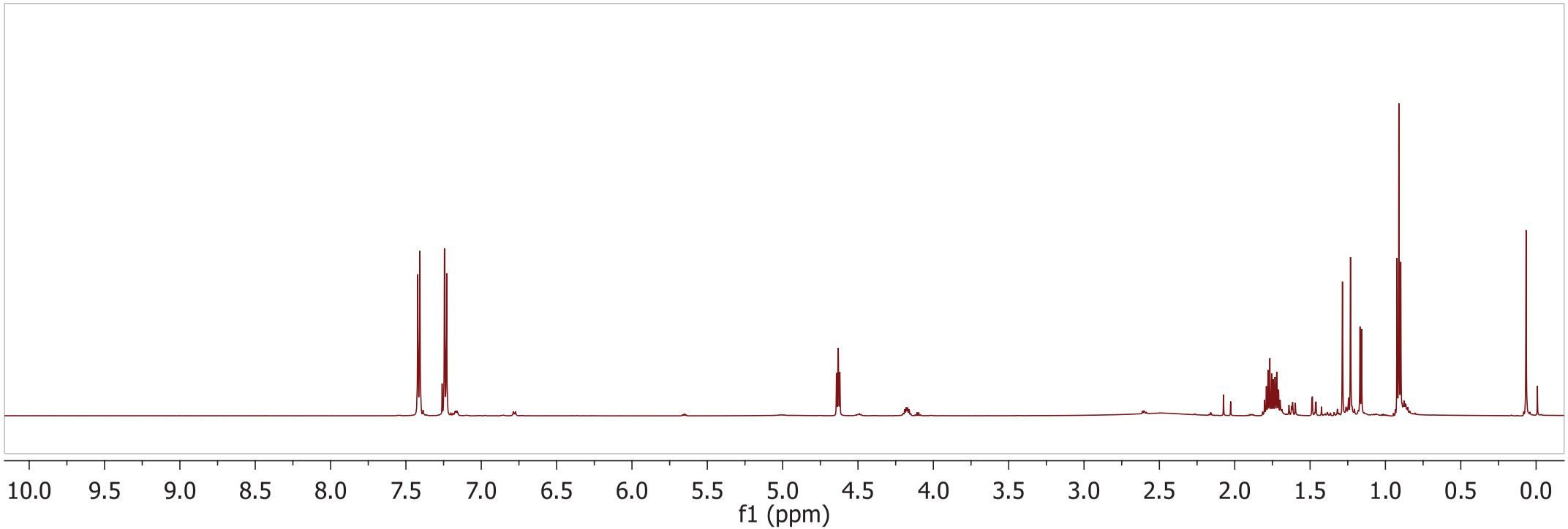

Plate 12b: 4-(1-hydroxypropyl)phenyl trifluoromethanesulfonate (**270**)

^{13}C NMR [151 MHz, $CDCl_3$]: δ 148.8(C-4'), 145.3 (C-1'), 127.9 (C-2',6'), 121.3 (C-3',5'), 118.9 (q, J = 320.8Hz, CF_3), 75.0 (C-1), 32.2 (C-2), 10.1 (C-3).

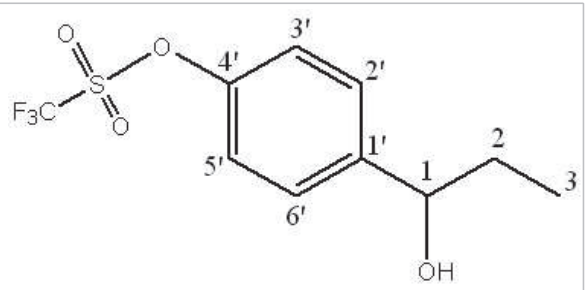

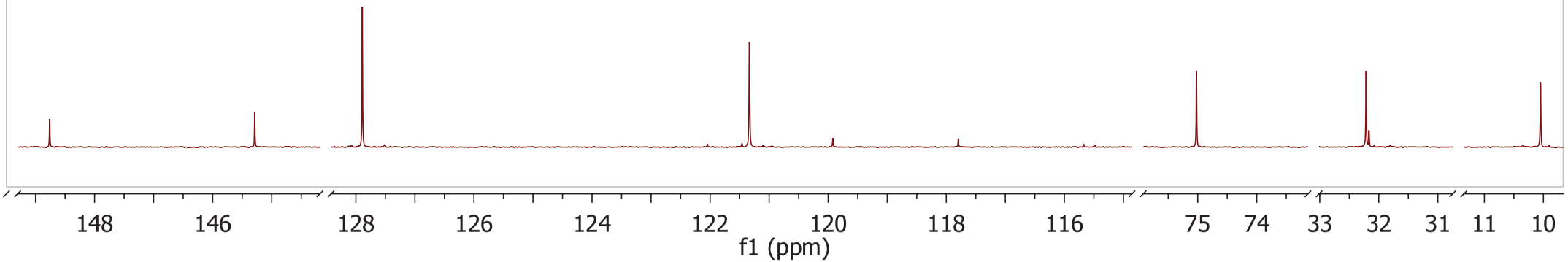

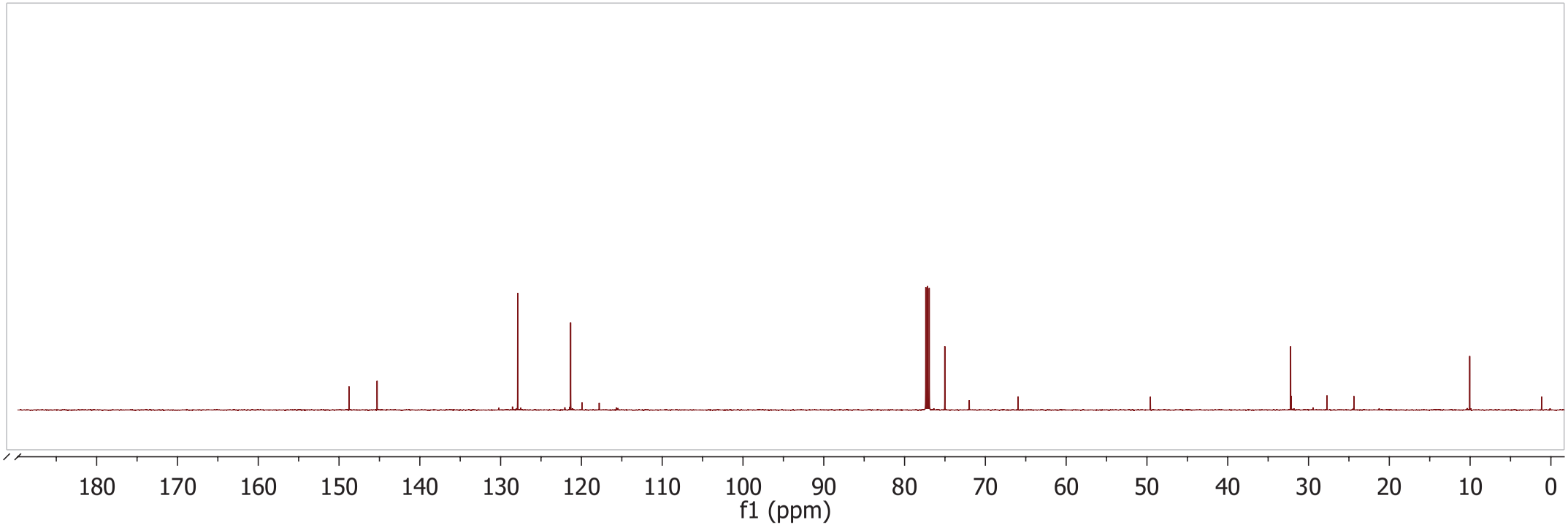

Plate 13a: (E)-4-(prop-1-enyl)phenyl trifluoromethanesulfonate (**271**)

^{1}H NMR [600 MHz, $CDCl_3$]: δ 7.37 (2H, d, *J* = 8.6 Hz, H-2',6'), 7.18 (2H, d, *J* = 8.6 Hz, H-3',5'), 6.39 (1H, br d, *J* = 15.8 Hz, H-1), 6.29-6.23 (1H, m, H-2), 1.90 (3H, m, H-3).

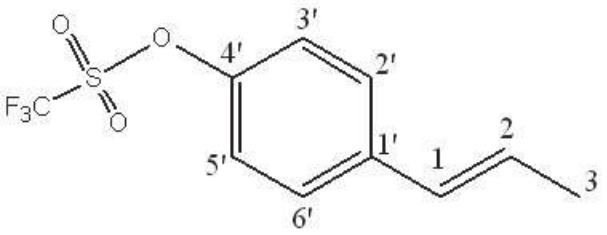

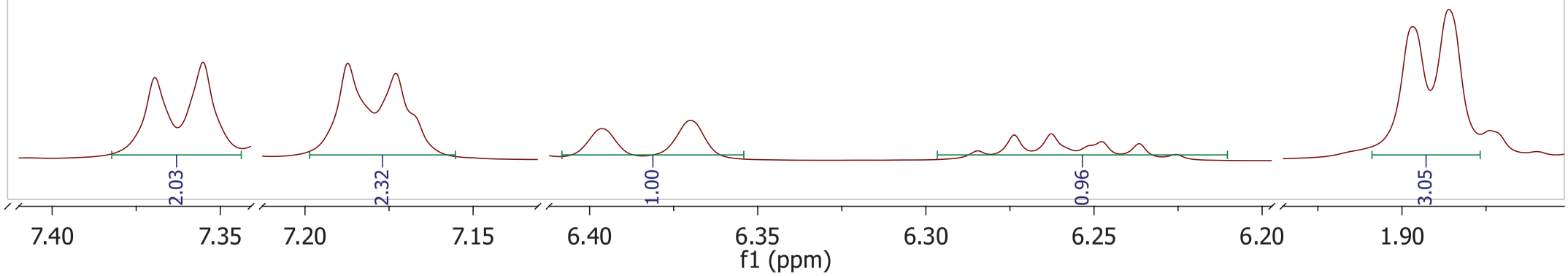

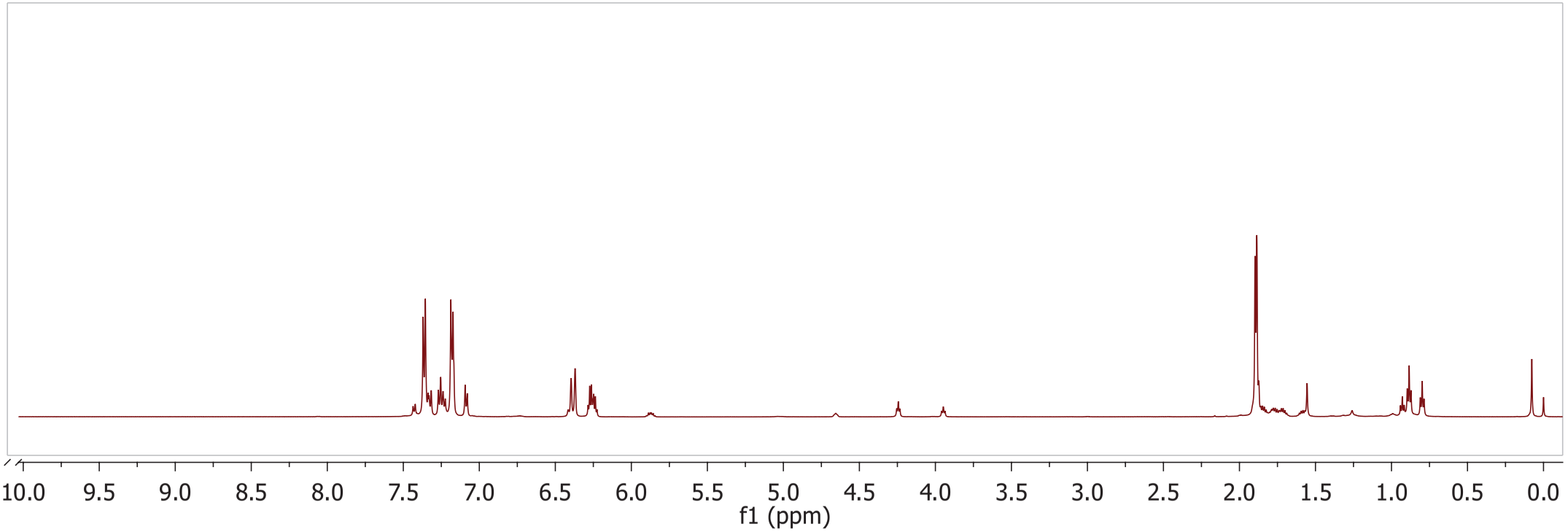

Plate 13b: (E)-4-(prop-1-enyl)phenyl trifluoromethanesulfonate (**271**)

^{13}C NMR [151 MHz, $CDCl_3$]: δ 148.3 (C-4'), 138.5 (C-1'), 129.4 (C-1), 128.3 (C-2), 127.5 (C-2',6'), 121.5 (C-3',5'), 118.9 (q, J = 320.8Hz, CF_3), 18.6 (C-3).

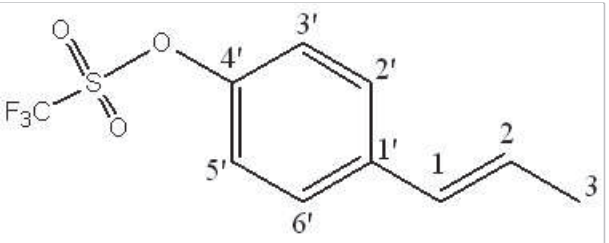

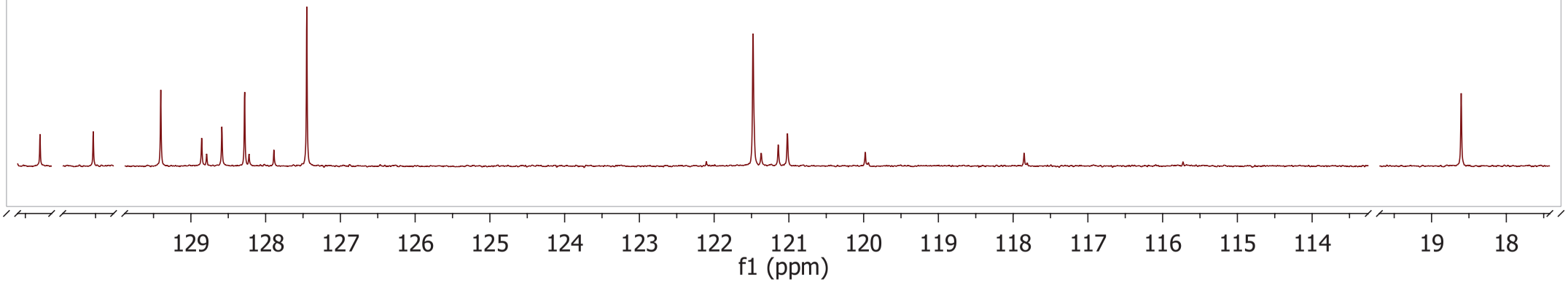

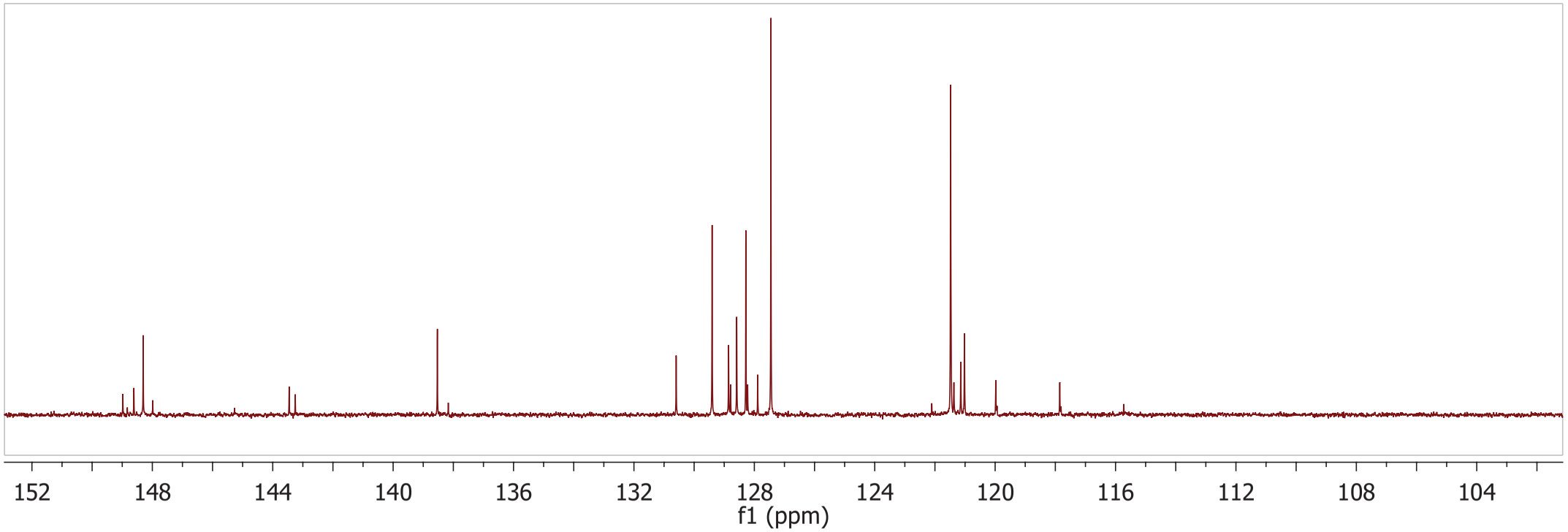

Plate 14a: (E)-4,4'-(ethene-1,2-diyl)bis(4,1-phenylene) bis(trifluoromethanesulfonate) (**272**)

^{1}H NMR [600 MHz, $CDCl_3$]: δ 7.58 (4H, d, *J* = 8.8 Hz, H-2,6), 7.29 (4H, d, *J* = 8.8 Hz, H-3,5), 7.09 (2H, s, CH=CH).

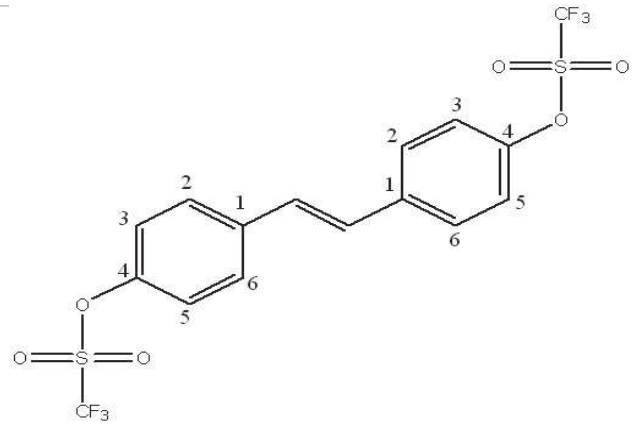

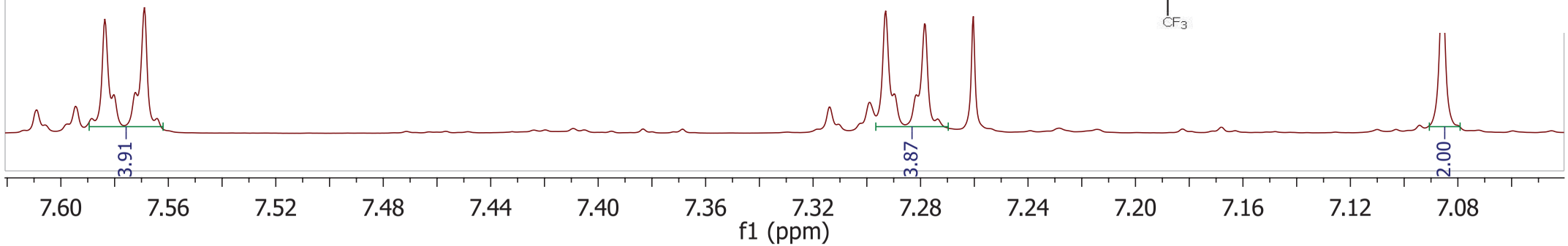

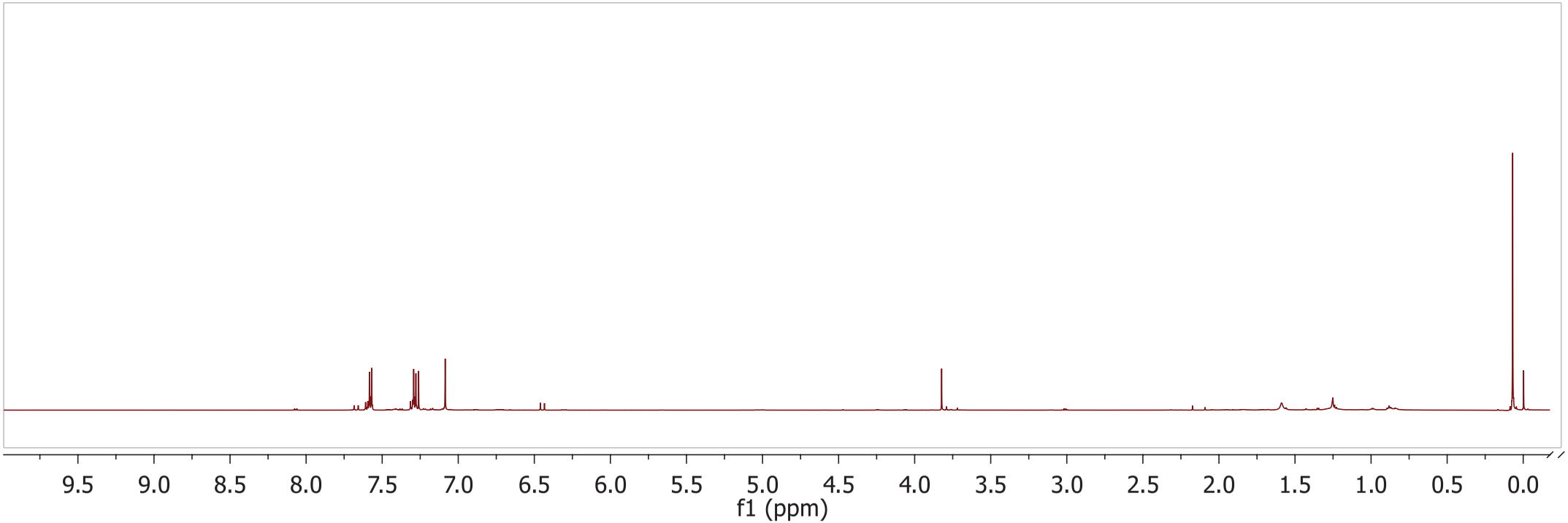

Plate 14b: (E)-4,4'-(ethene-1,2-diyl)bis(4,1-phenylene) bis(trifluoromethanesulfonate) (**272**)

^{13}C NMR [151 MHz, $CDCl_3$]: δ 149.1 (C-4), 137.2 (C-1), 128.8 (CH=CH), 128.1 (C-2,6), 121.9 (C-3,5), 118.9 (q, J = 320.8Hz, CF_3).

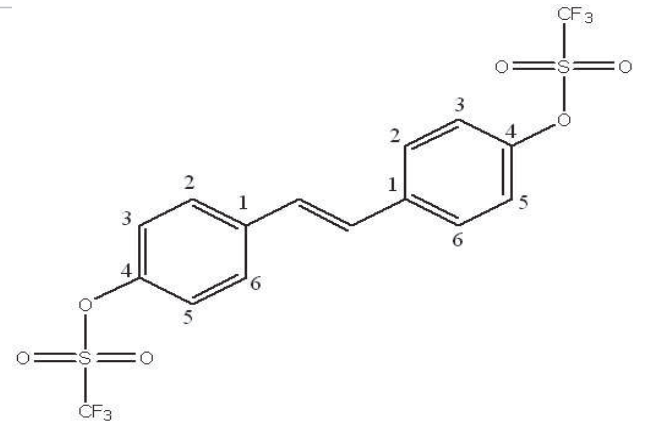

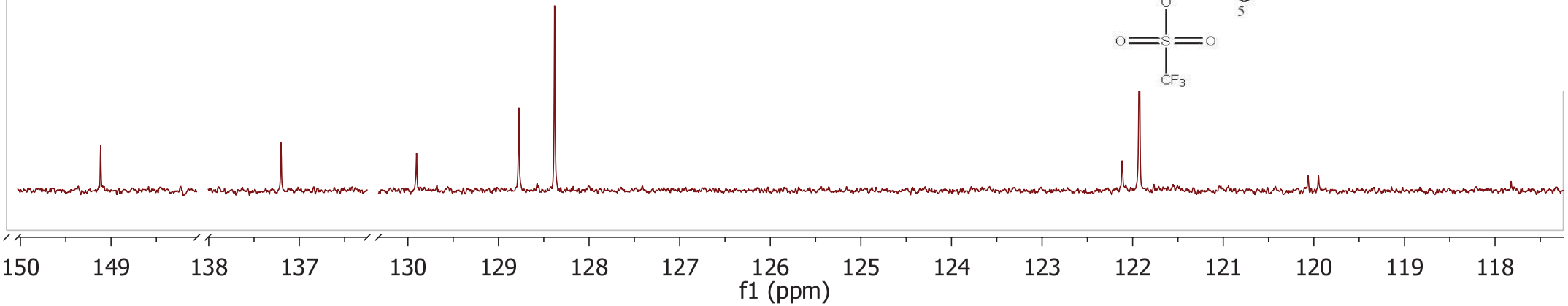

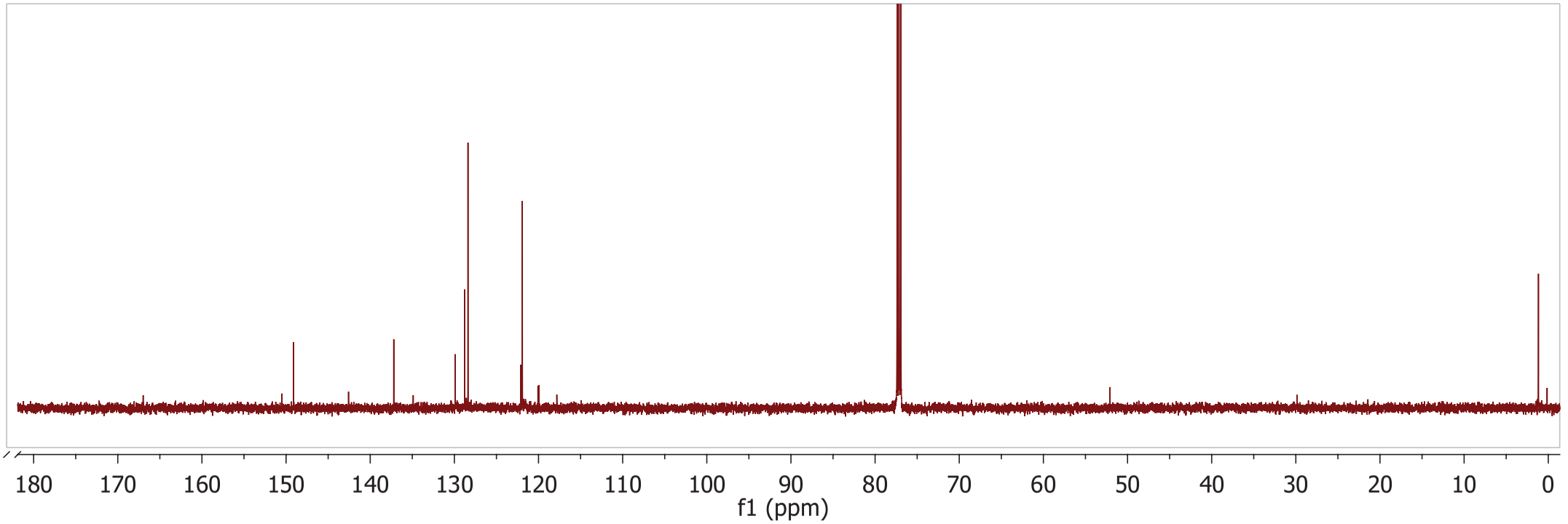

Plate 15a: (E)-methyl 3-(4-(trifluoromethylsulfonyloxy)phenyl)acrylate (**273**)

^{1}H NMR [600 MHz, $CDCl_3$]: δ 7.66 (1H, d, *J* = 16.0 Hz, H-3), 7.59 (2H, d, *J* = 8.7 Hz, H-2',6'), 7.29 (2H, d, *J* = 8.7 Hz, H-3',5'), 6.44 (1H, d, *J* = 16.0 Hz, H-2), 3.81 (3H, s, H-1'').

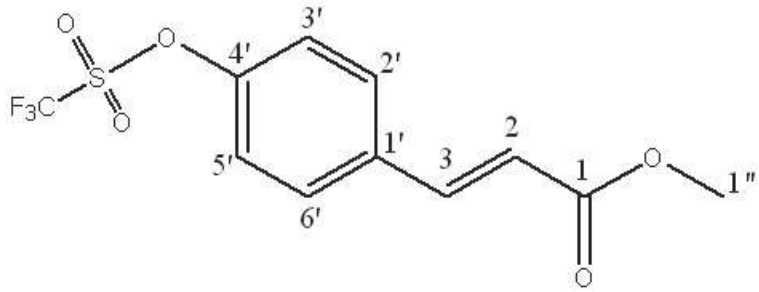

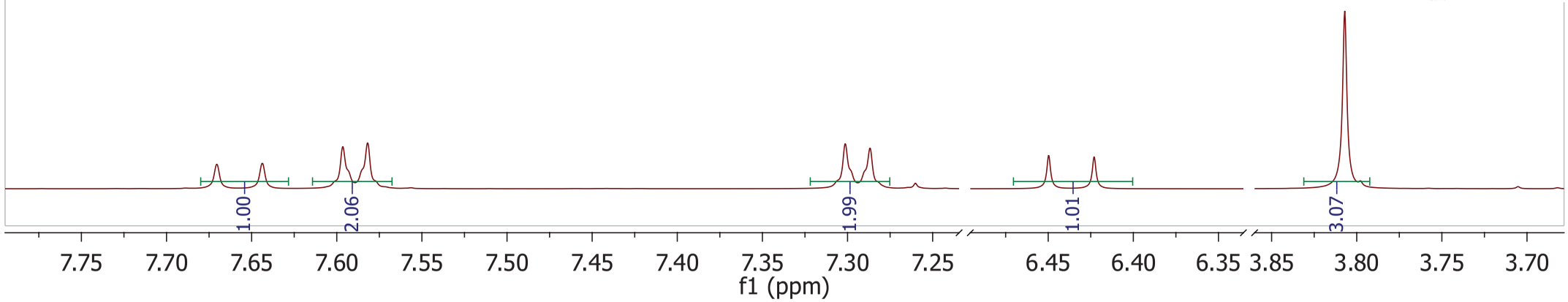

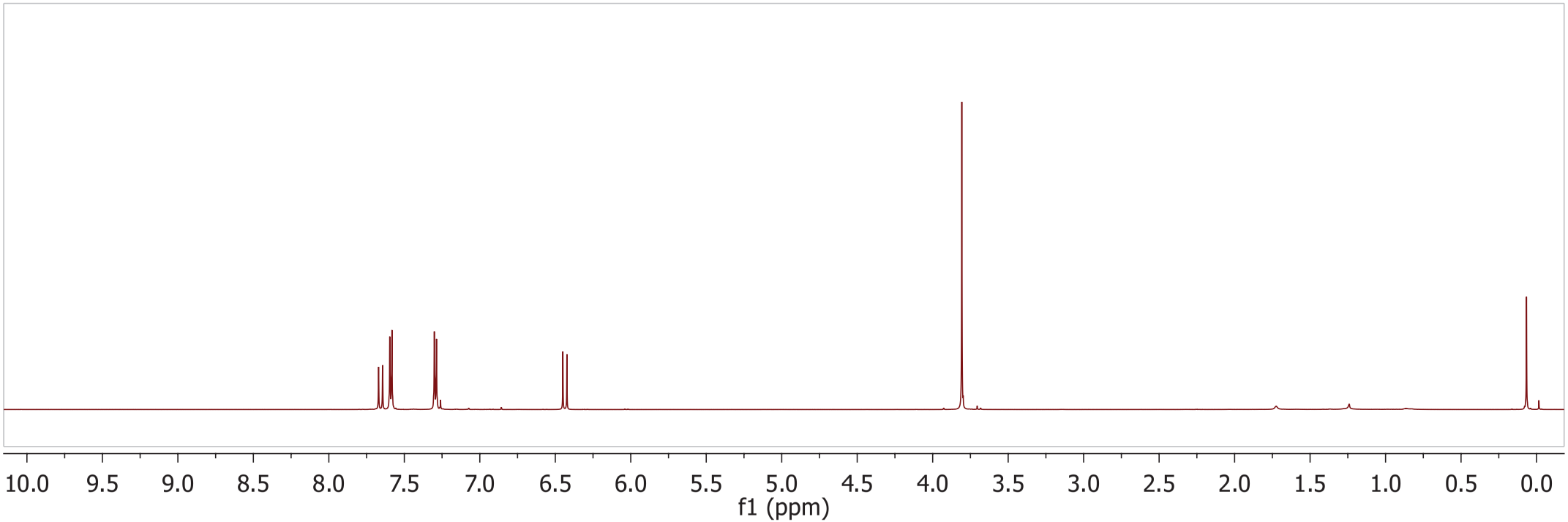

Plate 15b: (E)-methyl 3-(4-(trifluoromethylsulfonyloxy)phenyl)acrylate (**273**)

^{13}C NMR [151 MHz, $CDCl_3$]: δ 166.9 (C-1), 150.5(C-4'), 142.5 (C-3), 134.9 (C-1'), 129.9 (C-2',6'), 122.1(C-3',5'), 120.0 (C-2), 118.8 (q, J = 320.9Hz, $\underline{C}F_3$), 52.0(C-1'').

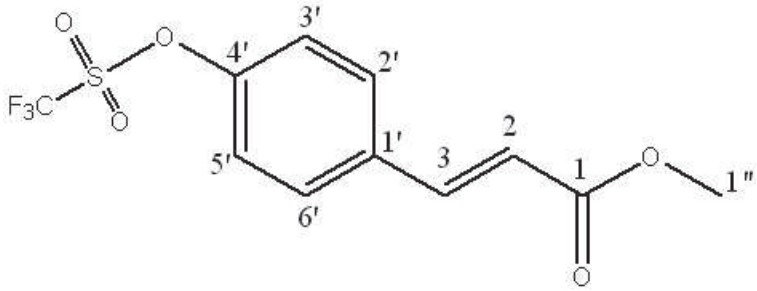

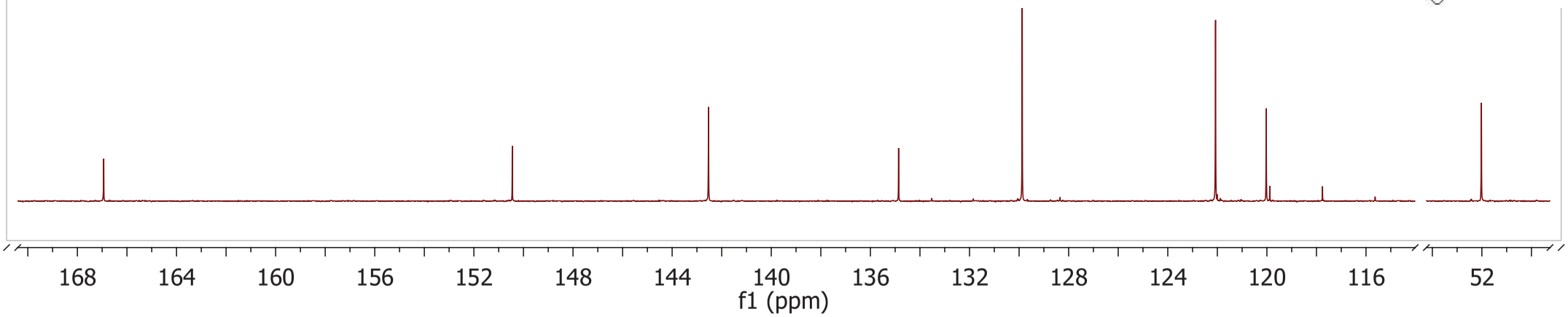

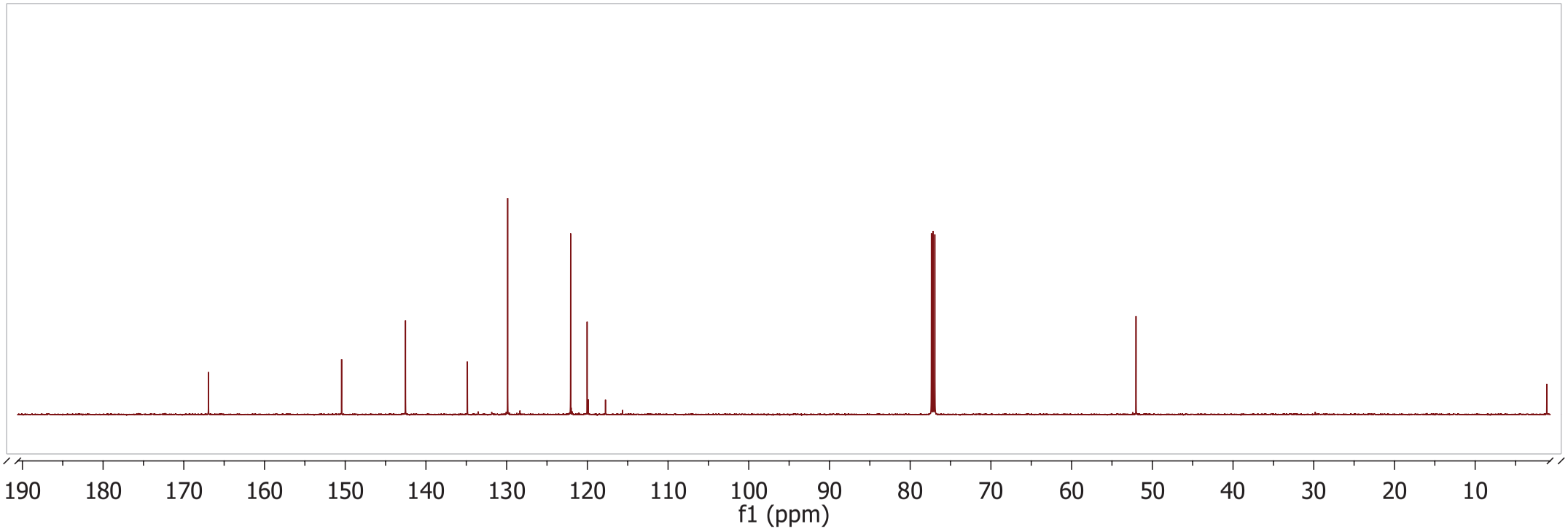

Plate 16a: Grubbs 2nd generation catalyst (**125**)

^{1}H NMR [600 MHz, $CDCl_3$]: δ 19.12 (1H,s, H-1'), 8.97 (1H, s, H-2(C)), 7.37 – 7.34 (1H, m, H-4(C)), 7.16 – 6.91 (3H, m, H-3(C), 5(C), 6(C)), 7.07 (1H, bs, H-3(B)), 7.02 (2H, bs, H-5(B)), 6.74 (1H, s, H-5(A)), 5.81 (1H, s, H-3(A)), 3.97 (3H, bs, H-4,5_b), 3.80 (1H, bs, H-5_a), 2.76 (3H, s, H-2-Me(B)), 2.57 (3H, s, H-6-Me(B)), 2.52 (3H, s, H-6-Me(A)), 2.31 (3H, s, H-4-Me(B)), 2.23 – 2.14 (3H, m, H-1(D)), 2.04 (3H, s, H-2-Me(A)), 1.90 (3H, s, H-4-Me(A)), 1.63 – 1.17 and 1.17 - 0770 (30H, m, H2-6(D)).

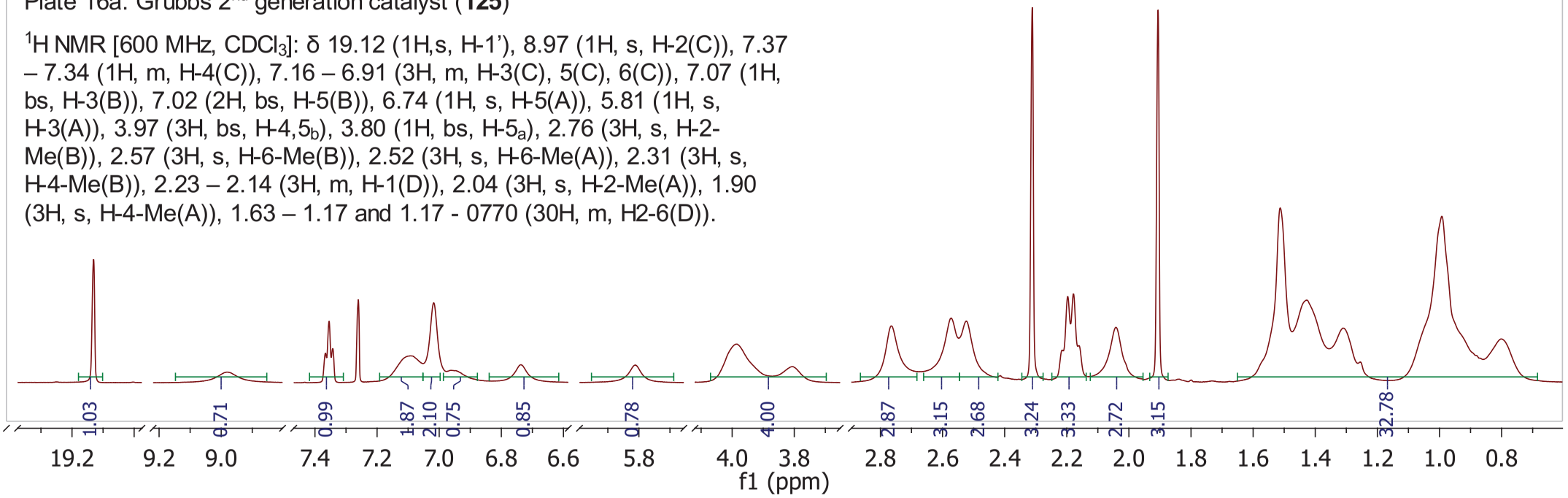

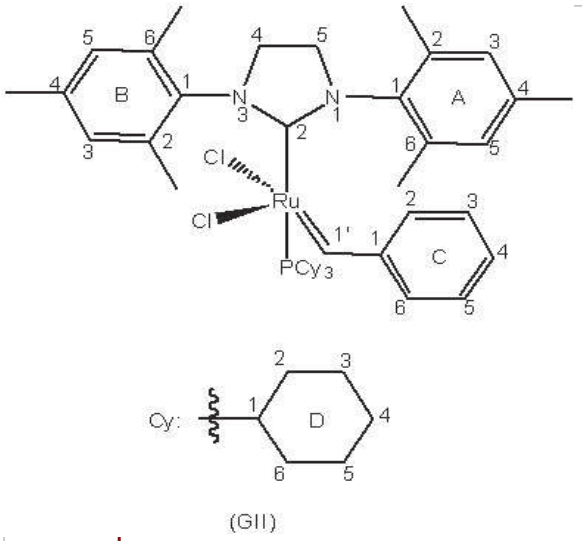

Plate 16b: Grubbs 2nd generation catalyst (**125**)

Int. ^{13}C NMR [151 MHz, $CDCl_3$]: δ 294.4(C-1'), 220.5(d, J = 77.4 Hz, C-2), 151.3(C-1(C)), 139.2 and 139.0(C-2,6(A or B)), 138.4(C-4(B)), 137.7(C-4(A)), 137.3(C-1(A or B)), 137.2 and 136.9(C-2,6(B or A)), 135.3(C-1(B or A)), 132.0(C-2(C)), 130.0(C-3(B),5(C)), 129.8(C-6(C)), 129.3(C-3(A)), 128.9(C-5(A)), 128.2(C-3(C)), 128.0(C-4(C)), 127.2(C-5(B)), 52.3 (d, J = 3.4 Hz, C-4), 51.4 (d, J = 1.7 Hz, C-5), 31.5(d, J = 16.6 Hz, C-2,6(D)), 29.2(d, J = 141.0 Hz, C-1(D)), 27.9(d, J = 9.9 Hz, C-3,5(D)), 26.3(C-4(D)), 21.3(C-4-Me(B)), 21.0(C-4-Me(A)), 20.1(C-2-Me(B),6-Me(B)), 18.9(C-2-Me(A)), 18.6(C-6-Me(A)).

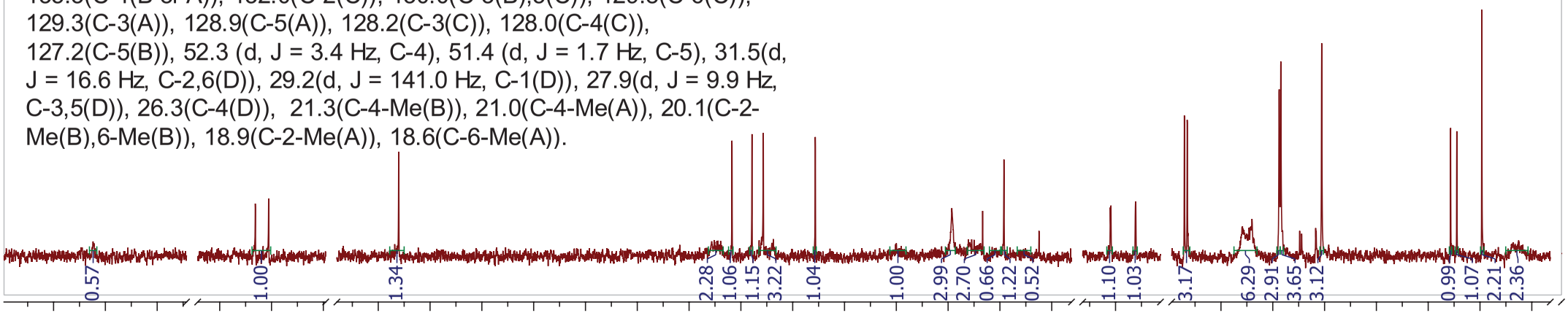

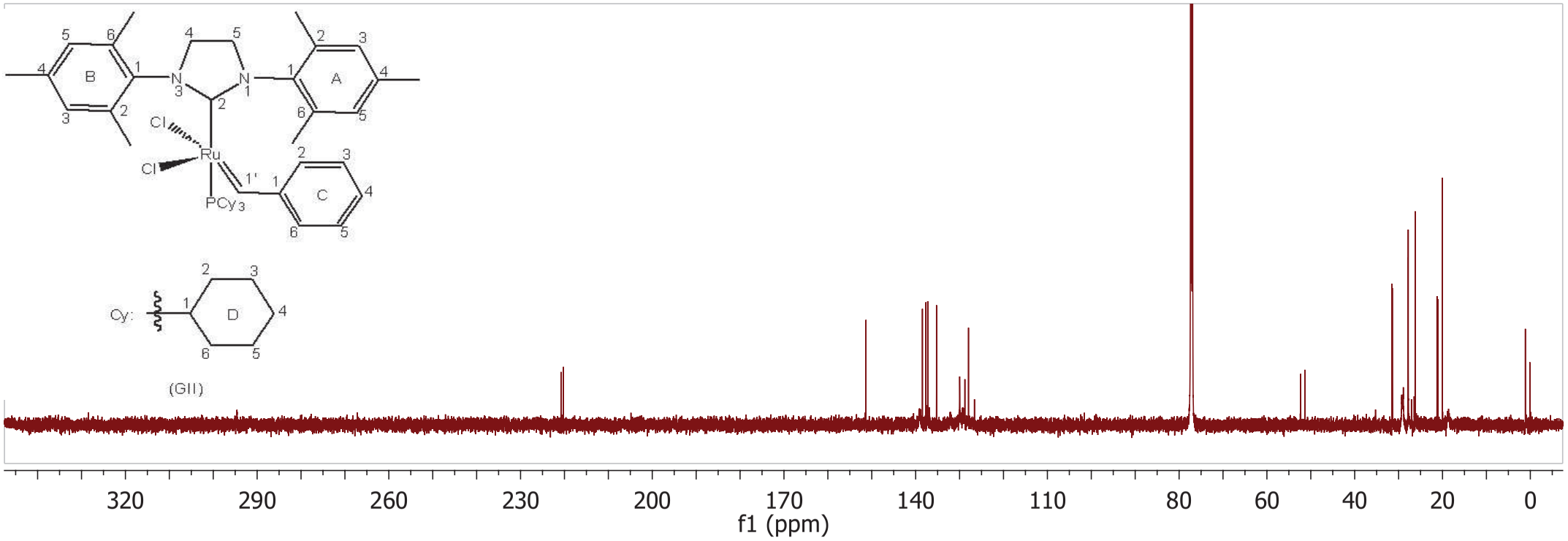

Plate 16a$_2$: Grubbs 2nd generation catalyst (**125**) @ 60°C

^{1}H NMR [600 MHz, $CDCl_3$]: δ 19.25 (1H,s, H-1'), 7.34 (1H, t, *J* = 7.3 Hz), 7.08 (2H, t, *J* = 7.8 Hz), 6.99 (2H, s), 6.28 (2H, s), 4.01 – 3.94 (2H, m, H-4), 3.89 – 3.81 (2H, m, H-5), 2.66 (6H, s), 2.30 (6H, s), 2.17 (4H, q, *J* = 12.0 Hz, C-1(D)), 1.90 (3H,s), 1.55 – 1.32 and 1.08 – 0.84 (30H, m, H-2-6(D)).

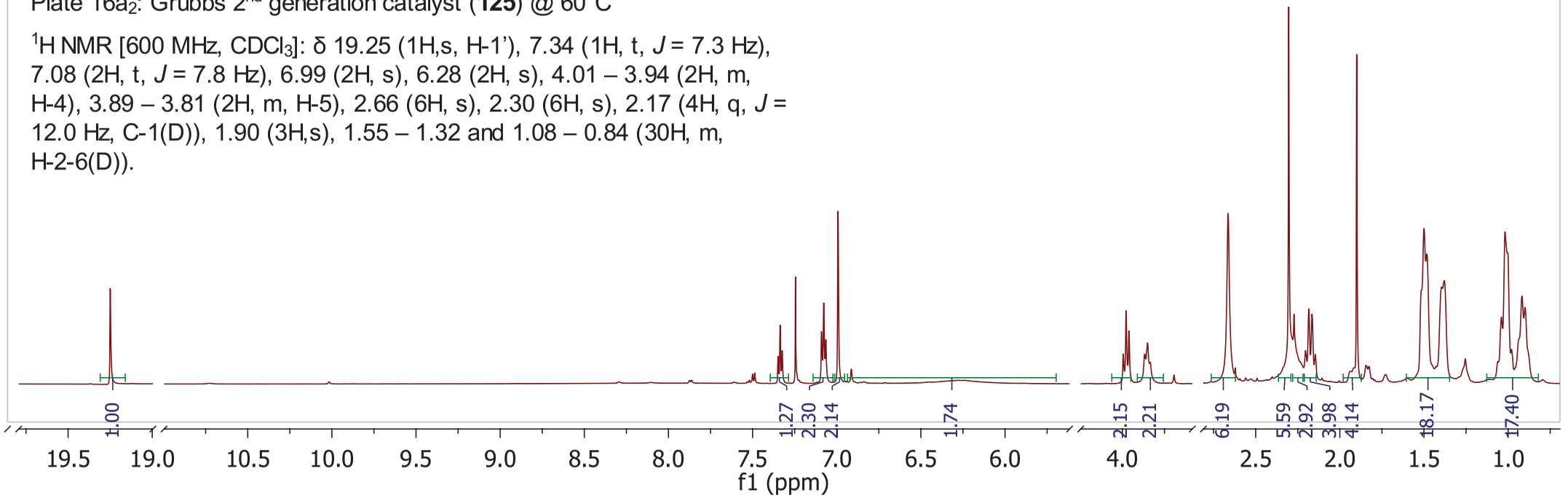

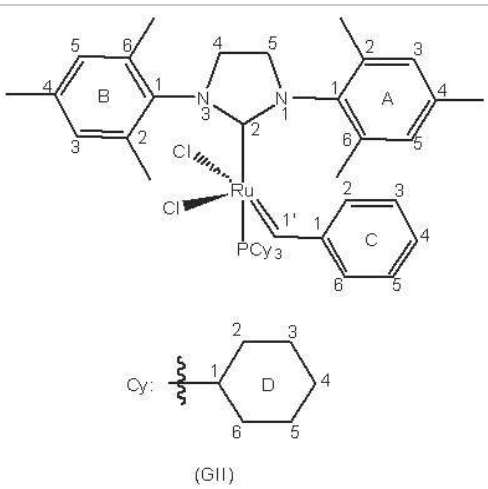

Plate 16b$_2$: Grubbs 2nd generation catalyst (**125**) @ 60°C

^{13}C NMR [151 MHz, $CDCl_3$]: δ 219.8(J = 78.4 Hz), 150.6, 138.1, 137.4, 136.6, 136.4, 136.0, 134.4, 129.0, 128.2, 126.8, 126.6, 125.6, 51.4(d, J = 3.3 Hz, C-4), 50.5(d, J = 1.8 Hz, C-5), 30.9 (d, J = 16.2 Hz), 28.22, 26.8(d, J = 10.1 Hz), 25.28, 20.10, 19.86, 19.03, 17.63.

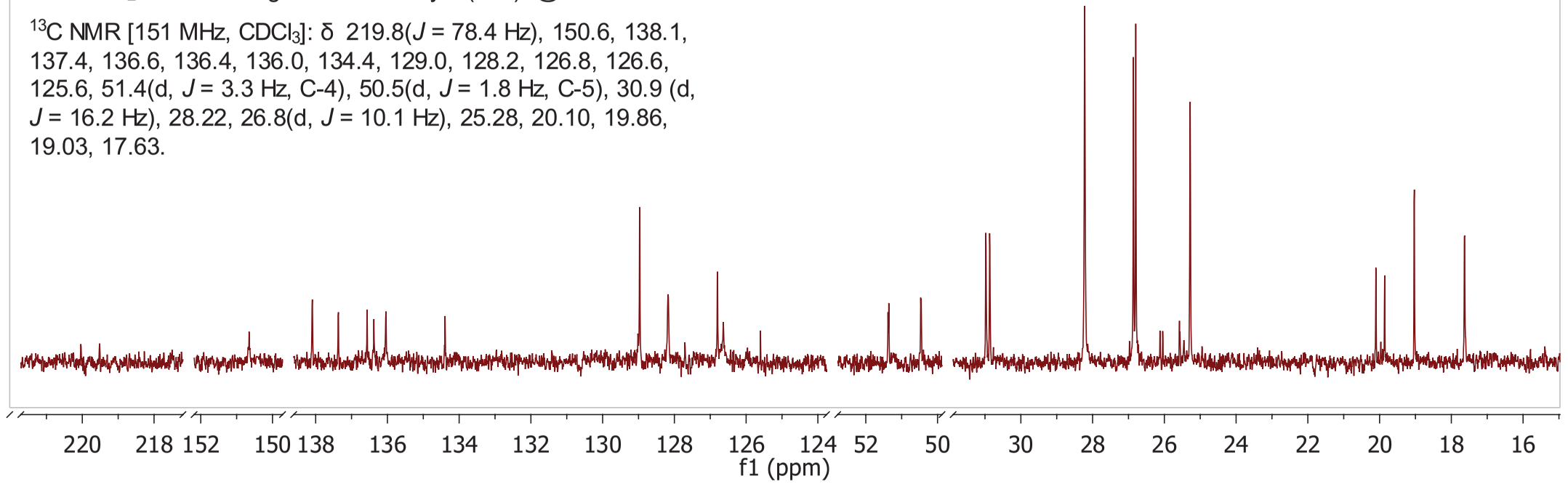

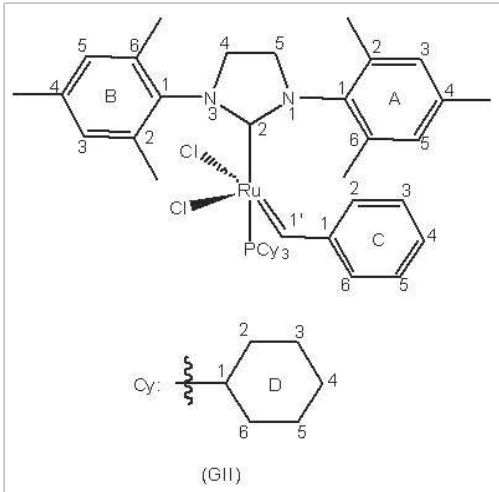

Plate 16a$_3$: Grubbs 2nd generation catalyst (**125**) @ -40°C

^{1}H NMR [600 MHz, $CDCl_3$]: δ 18.94 (1H,s, H-1'), 8.87 (1H, d, *J* = 7.84 Hz, H-2(C)), 7.39 – 3.35 (1H, m, H-4(C)), 7.18 – 7.14 (1H, m, H-3(C)), 7.08 (1H, s, H-3(B)), 7.03 (2H, s, H-5(B)) , 7.09 – 7.04 (1H, m, 5(C)), 6.89 (1H, d, *J* = 7.57 Hz, H-6(C)), 6.75 (1H, s, H-5(A)), 5.77 (1H, s, H-3(A)), 4.08 – 3.91 (3H, bs, H-4,5$_b$), 3.82 (1H, ddd, *J* = 18.27, 17.27, 6.95 Hz, H-5$_a$), 2.77 (3H, s, H-2-Me(B)), 2.57 (3H, s, H-6-Me(B)), 2.52 (3H, s, H-6-Me(A)), 2.31 (3H, s, H-4-Me(B)), 2.25 – 2.07 (3H, m, H-1(D)), 2.03 (3H, s, H-2-Me(A)), 1.90 (3H, s, H-4-Me(A)), 1.67 – 1.11 and 1.11 – 0.51 (30H, m, H2-6(D)).

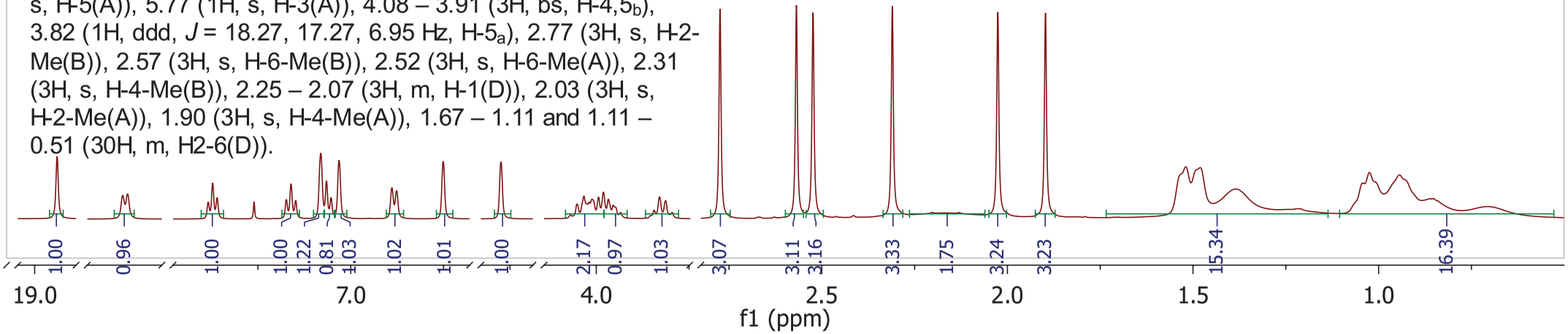

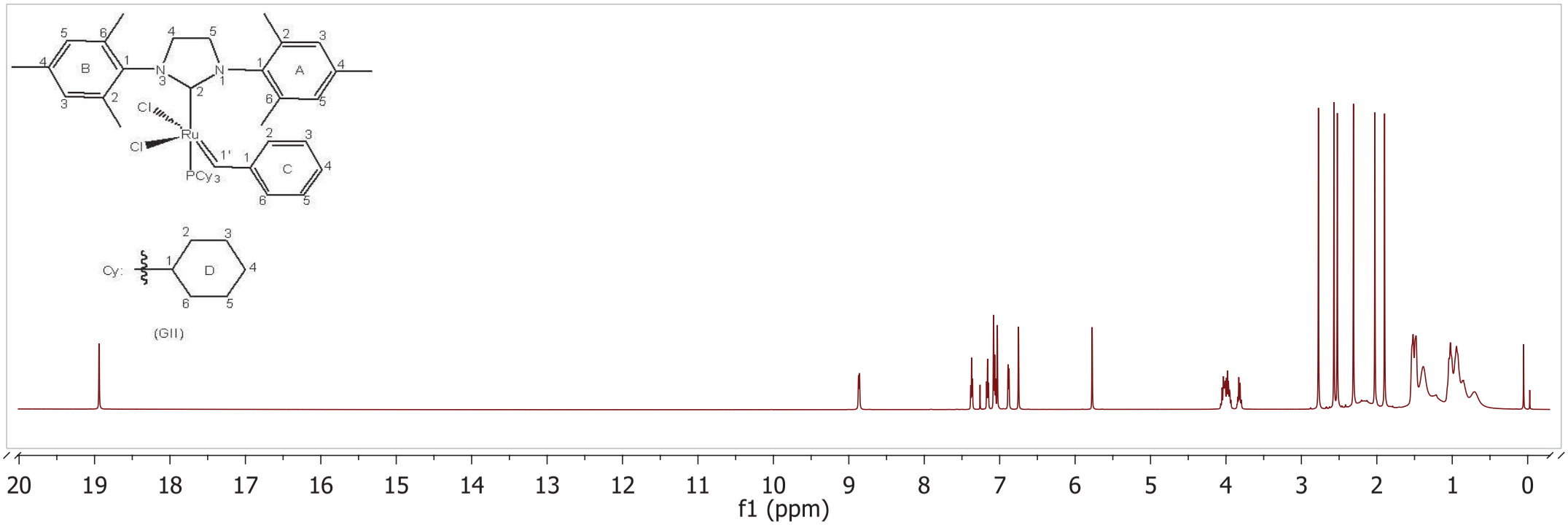

Plate 16b$_3$: Grubbs 2nd generation catalyst (**125**) @ -40°C

^{13}C NMR [151 MHz, $CDCl_3$]: δ 294.4(C-1'), 219.6 (d, *J* = 177.3 Hz, C-2), 150.6(C-1(C)), 138.9 and 138.8 (C-2,6(A or B)), 138.5(C-4(B)), 137.8(C-4(A)), 137.3(C-1(A or B)), 136.9 and 136.7 (C-2,6(B or A)), 134.9(C-1(B or A)), 131.6(C-2(C)), 129.8(C-3(B)), 129.7 (C-5(C)), 129.3(C-6(C)), 128.9(C-3(A)), 128.5(C-5(A)), 128.2(C-3(C)), 128.1(C-4(C)), 127.0(C-5(B)), 52.0 (s, C-4), 50.9 (s, C-5), 30.6(C-1(D)), 28.8(d, *J* = 85.8 Hz, C-2(D),6(D)), 27.6(t, *J* = 9.2 Hz, C-3,5(D)), 25.9(C-4(D)), 21.3(C-4-Me(B)), 21.0(C-4-Me(A)), 19.8(C-2-Me(B),6-Me(B)), 19.0(C-2-Me(A)), 18.4(C-6-Me(A)).

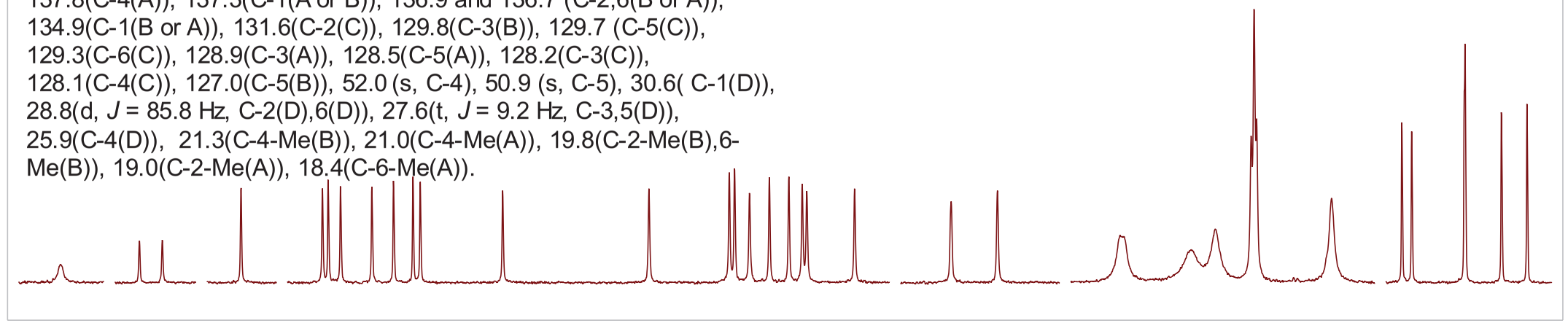

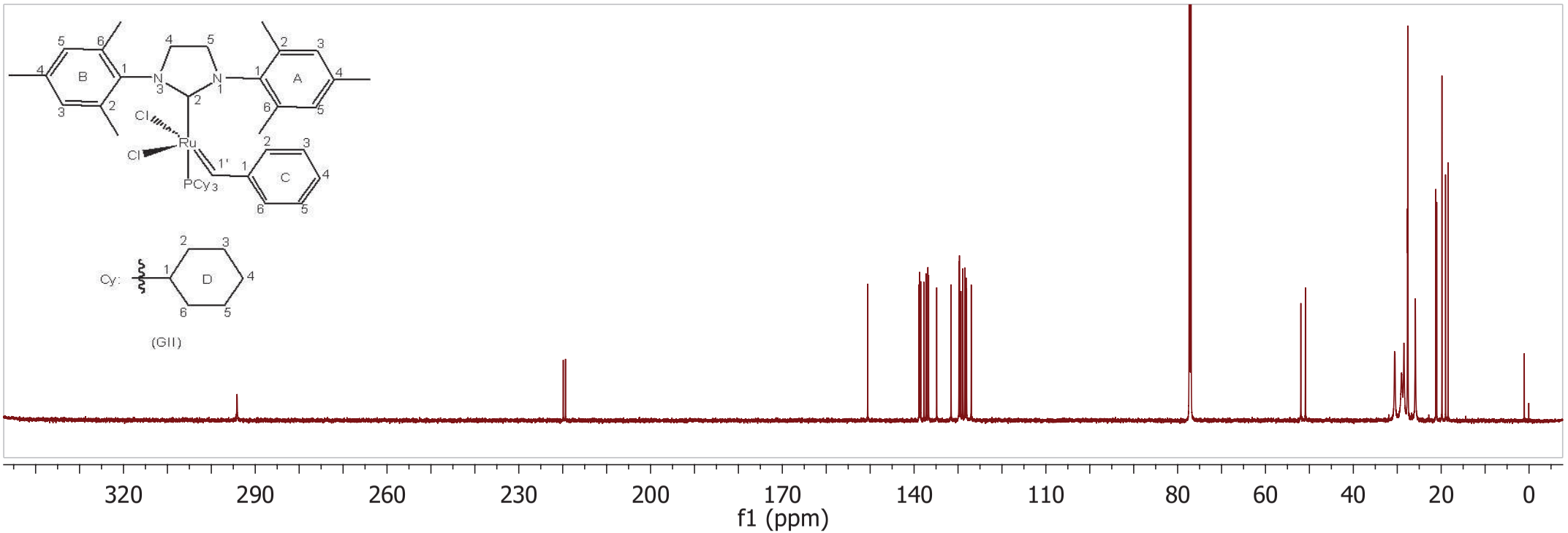

Plate 17a: *p*-Cresol (**266**)

^{1}H NMR [600 MHz, $CDCl_3$]: δ 7.05 (2H, d, *J* = 8.3 Hz, H-3,5), 6.76 (2H, d, *J* = 8.3 Hz, H-2,6), 5.11 (1H, s, -OH), 2.29 (3H, s, H-Me).

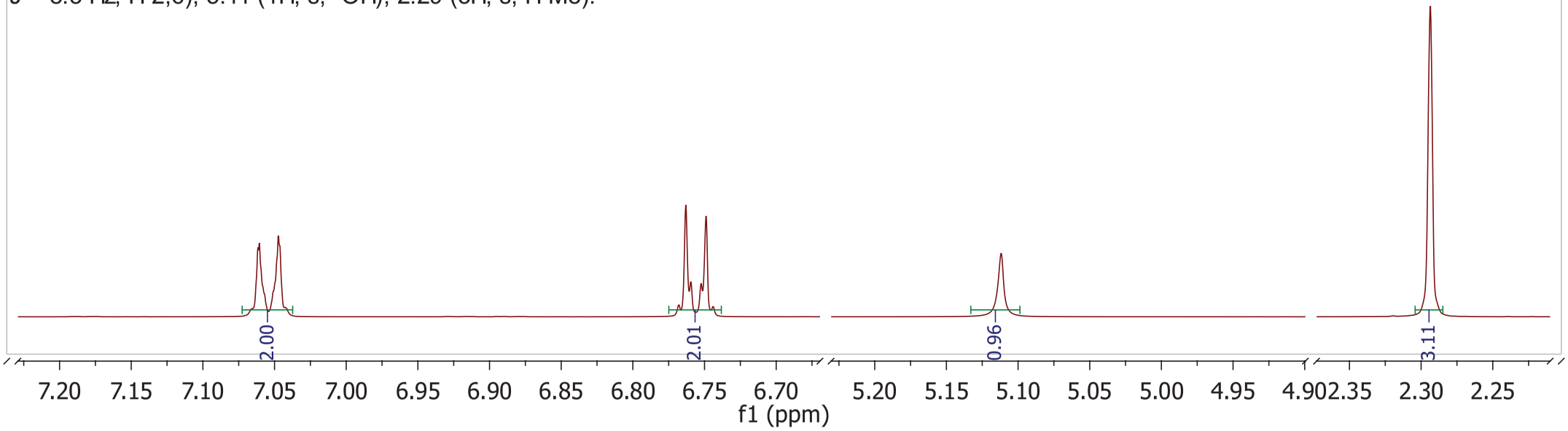

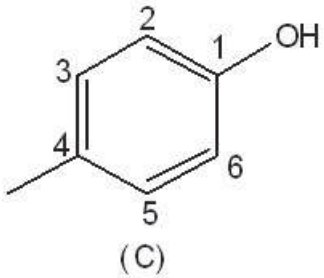

(C)

Plate 17b: *p*-Cresol (**266**)

^{13}C NMR [151 MHz, $CDCl_3$]: δ 153.2(C-1), 130.21(C-3,5), 130.17(C-4), 115.2(C-2,6), 20.6(Me).

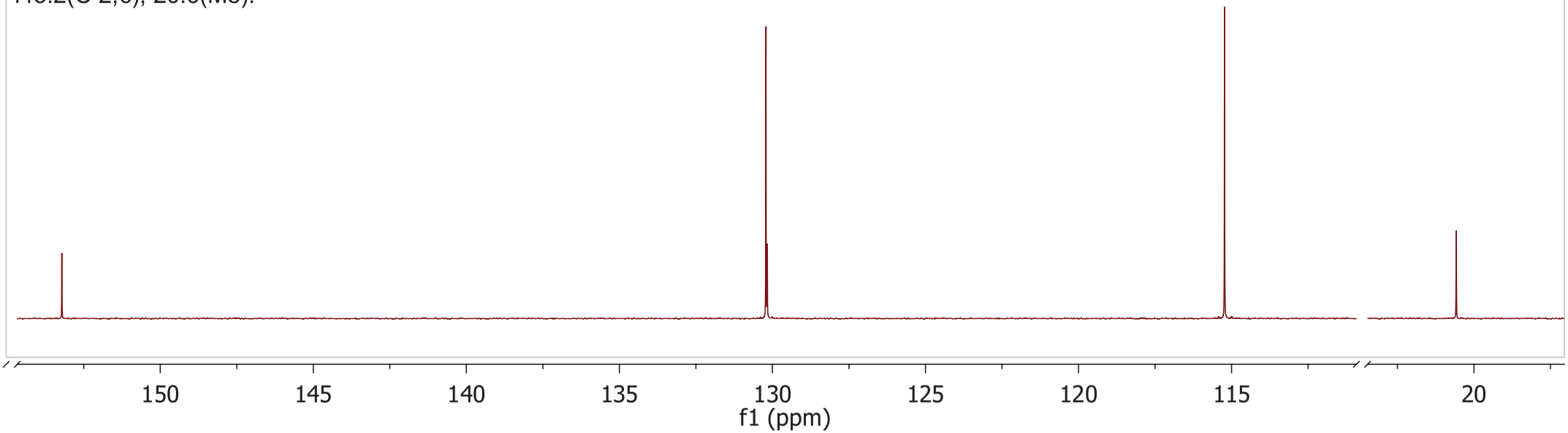

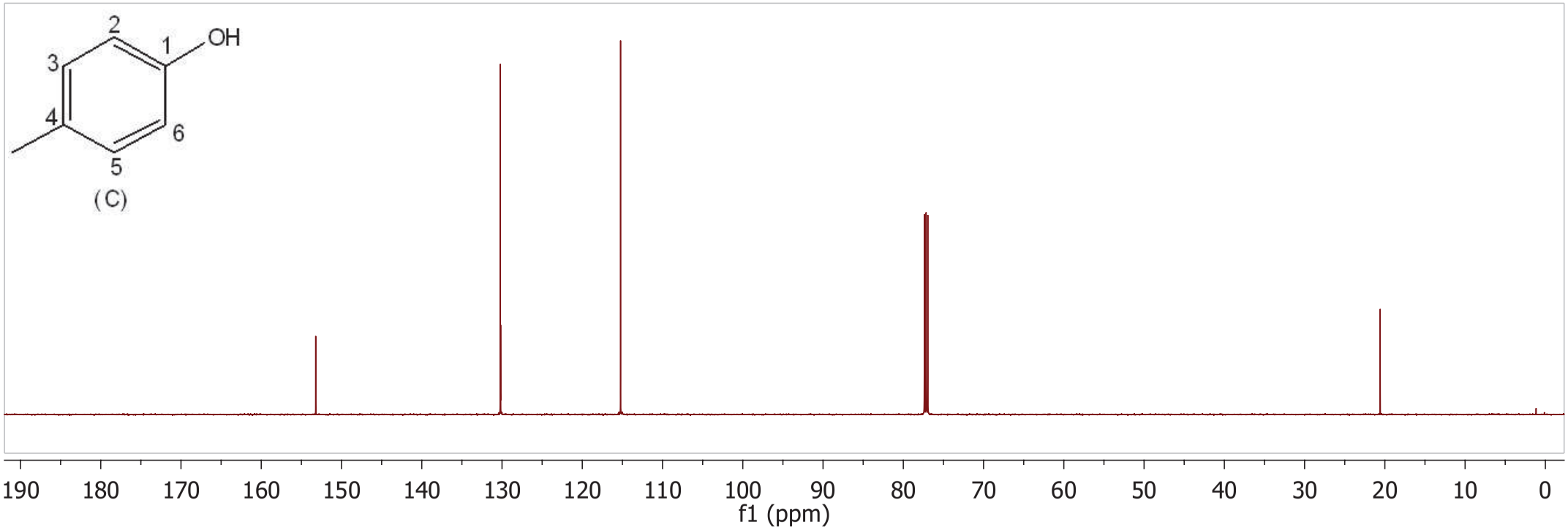

Plate 18a: Grubbs 2nd generation catalyst (**125**) + *p*-cresol (**266**)

^{1}H NMR [600 MHz, $CDCl_3$]: δ 19.12 (s, GII:H-1'), 17.84 (s), 10.00 (s), 9.01 (s, GII:H-2(C)), 7.42 – 7.39(m, GII:H-4(C)), 7.18 – 7.10 (m), 7.06 (d, *J* = 8.3 Hz, C: H-3,5), 6.86 (d, *J* = 8.3 Hz, C:H2,6), 6.79 – 6.72 (m), 6.43 (s, C:-OH), 5.85 (s, GII:H-3(A)), 4.12 – 3.76 (m, GII:H-4,5), 2.81 (s, GII:H-2-Me(B)), 2.67 (s), 2.62 (s, GII:H-6-Me(B)), 2.54 (s, GII:H-6-Me(A)), 2.48 – 2.41 (m), 2.37 (s, GII:H-4-Me(B)), 2.31 (s, GII:H-4-Me(B)), 2.30(s, C:Me), 2.29 – 2.19 (m), 2.09 (s, GII: H-2-Me(A)), 1.95 (s, GII:H-4-Me(A)), 1.87 – 1.65 (m), 1.62 – 1.30 (m, GII:H-2-6(D)), 1.28 – 1.21 (m), 1.17 – 0.79 (m, GII:H-2-6(D)).

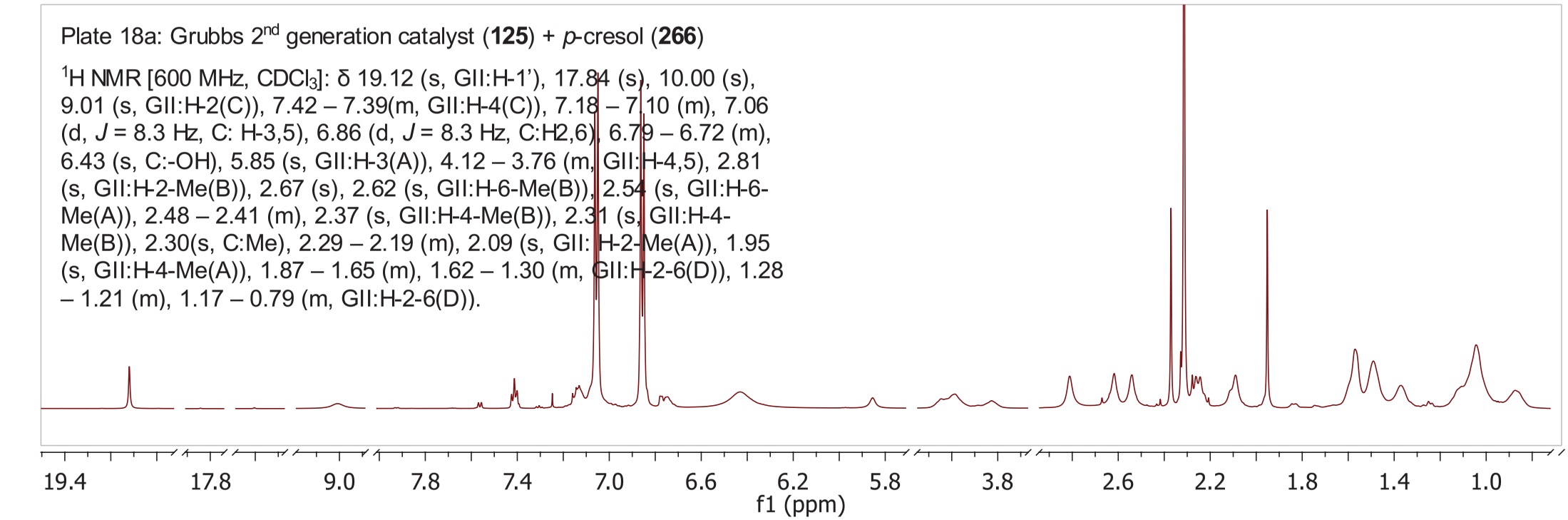

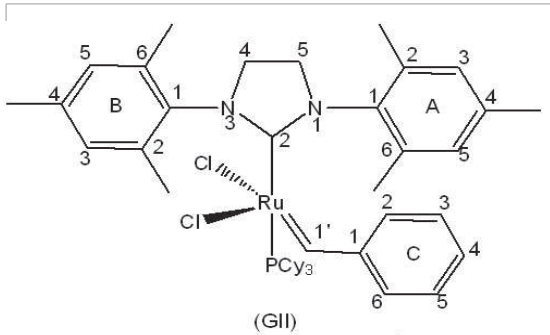

Plate 18b: Grubbs 2nd generation catalyst (**125**) + *p*-cresol (**266**)

^{13}C NMR [151 MHz, $CDCl_3$]: δ 294.3(GII:C-1'), 219.9(d, J = 76.9Hz, GII:C-2), 155.7, 153.4(C:C-1), 153.2, 151.0(GII:C-1(C)), 139.6, 139.0 and 138.6(GII:C-2,6(A or B)), 138.4(GII:C-4(B)), 137.6(GII:C-4(A)), 137.3, 137.0, 136.6(GII:C-2,6(B or A)), 135.0(GII:C-1(B or A)), 134.8, 131.9, 130.2, 130.1, 129.9(C:C-3,5), 129.8, 129.7, 129.6, 129.5, 129.3, 129.2 128.8, 128.7, 128.6, 128.2, 127.6, 127.1, 126.5, 121.2, 116.3, 115.6, 115.4, 115.2, 112.6, 52.2(d, J = 3.2 Hz, GII:C-4), 51.3(d, J = 1.1 Hz, GII:C-5), 35.1, 34.7, 31.5(d, J = 16.6 Hz, GII:C-2,6(D)), 29.0(d, J = 54.6 Hz, GII:C-1(D)), 27.6(d, J = 9.9 Hz, GII:C-3,5(D)), 26.7, 26.6, 26.1, 25.9, 21.3, 21.1(GII:C-4-Me(B)), 21.0, 20.8(GII:C-4-Me(B)), 20.4(C:Me), 20.3, 19.9(GII:C-2-Me(B),6-Me(B)), 18.5.

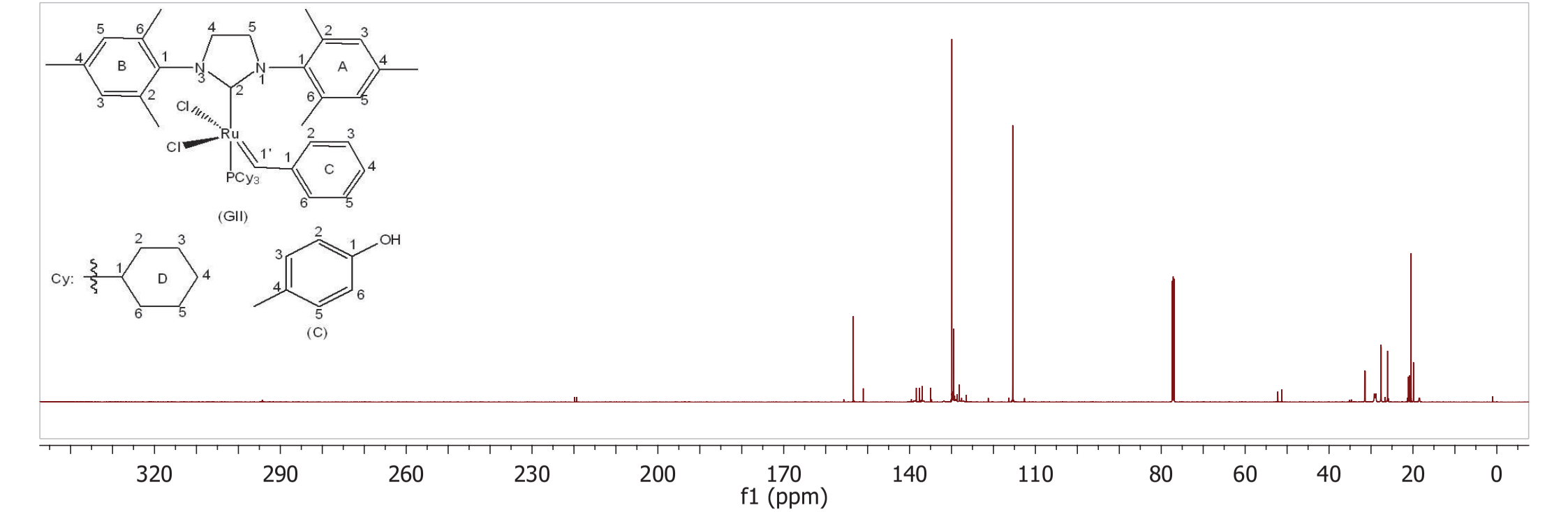

Plate 19a: Tricyclohexylphosphine (**289**)

^{1}H NMR [600 MHz, $CDCl_3$]: δ 1.95 – 1.12 (33H, m, H-1-6).

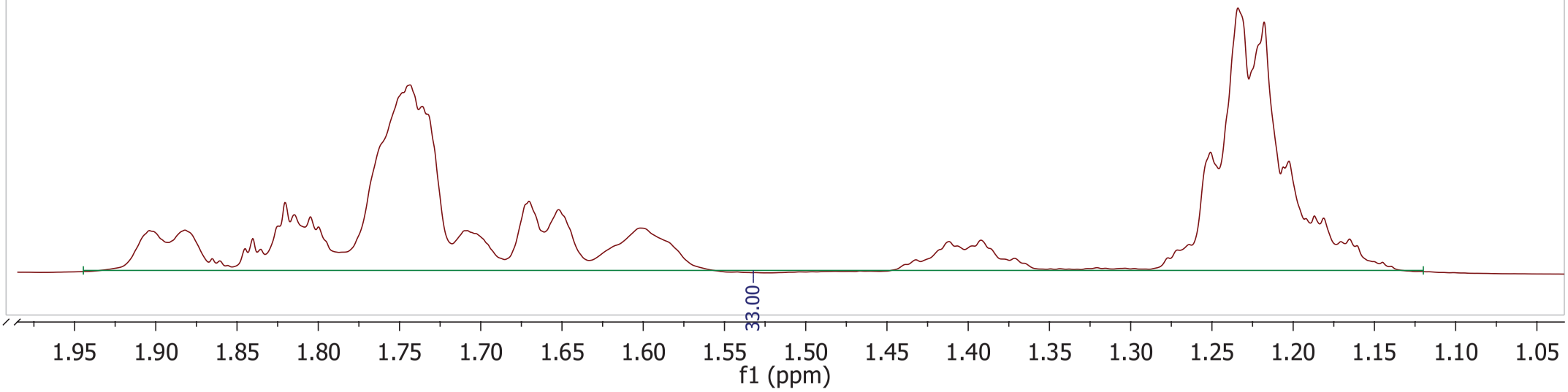

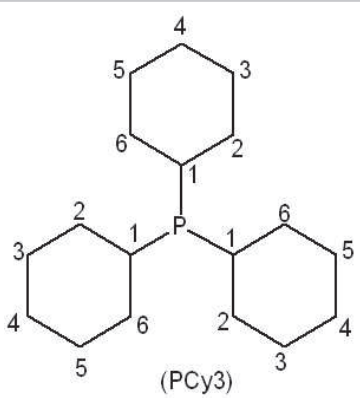

Plate 20a: Tricyclohexylphosphine (**289**) + 1 eq. *p*-cresol (**266**)

^{1}H NMR [600 MHz, $CDCl_3$]: δ 7.60 (s), 6.95 (d, *J* = 8.3 Hz, C:H-3,5), 6.81 (d, *J* = 8.3 Hz, C:H-2,6), 2.35 – 2.27 (m), 2.23 (s, C:Me), 2.02 – 1.62 and 1.52 – 1.11 (m, PCy3:H-1-6).

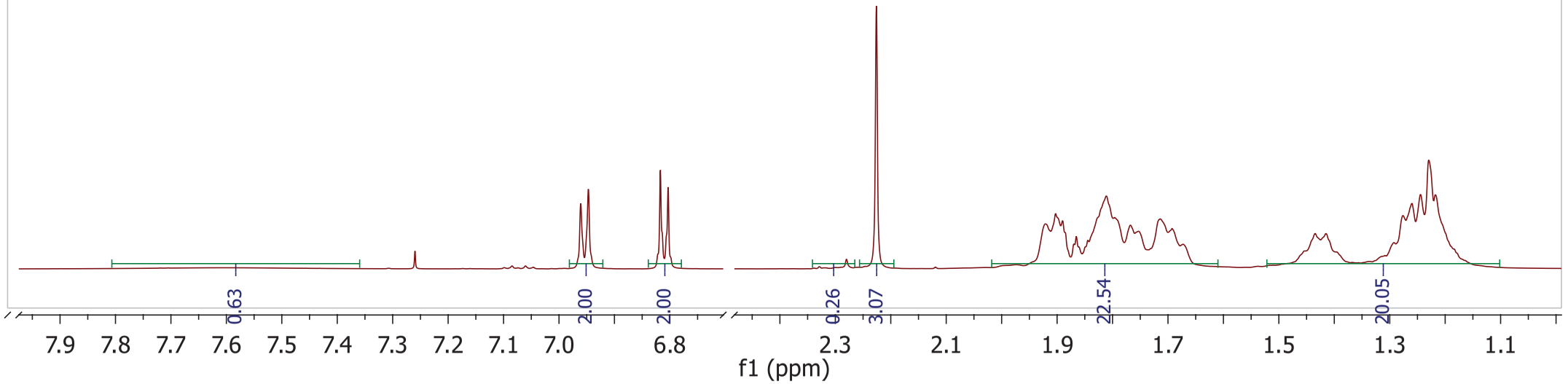

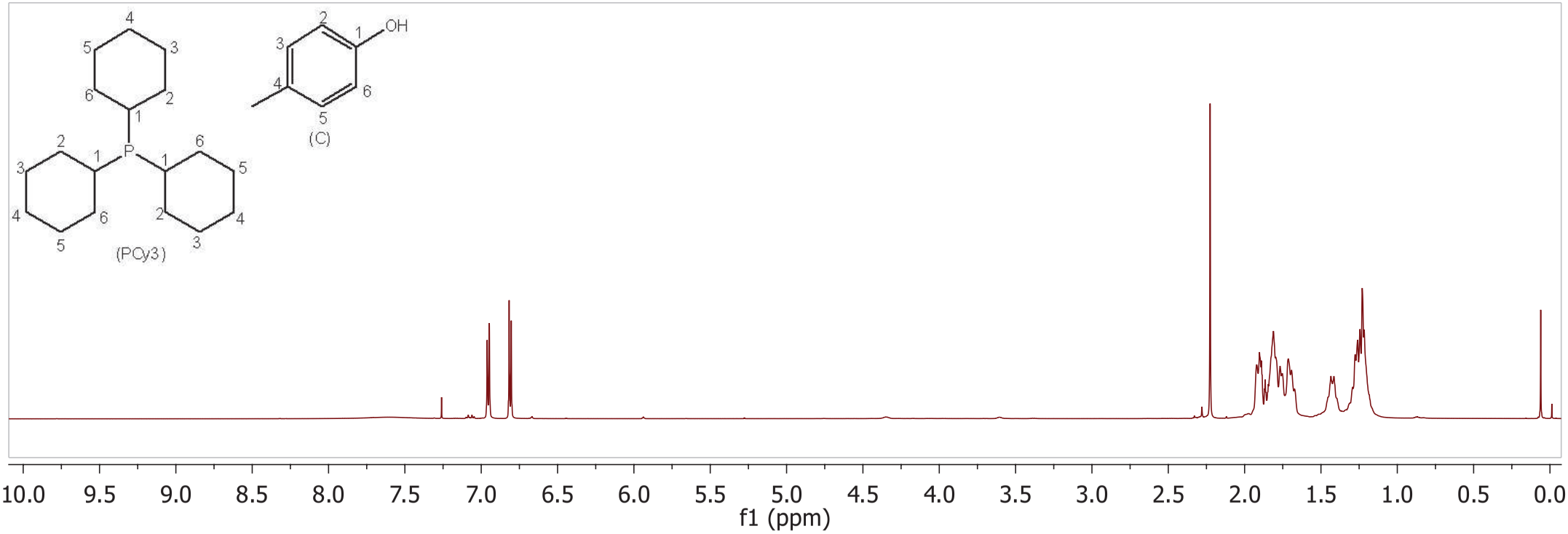

Plate 21a: Tricyclohexylphosphine (**289**) + 2 eq. *p*-cresol (**266**)

^{1}H NMR [600 MHz, $CDCl_3$]: δ 7.27 (s), 7.01 (d, *J* = 8.3 Hz, C:H-3,5), 6.85 (d, *J* = 8.3 Hz, C:H-2,6), 2.28 (s), 2.05 – 1.68 and 1.54 – 1.17 (m, PCy3:H1-6).

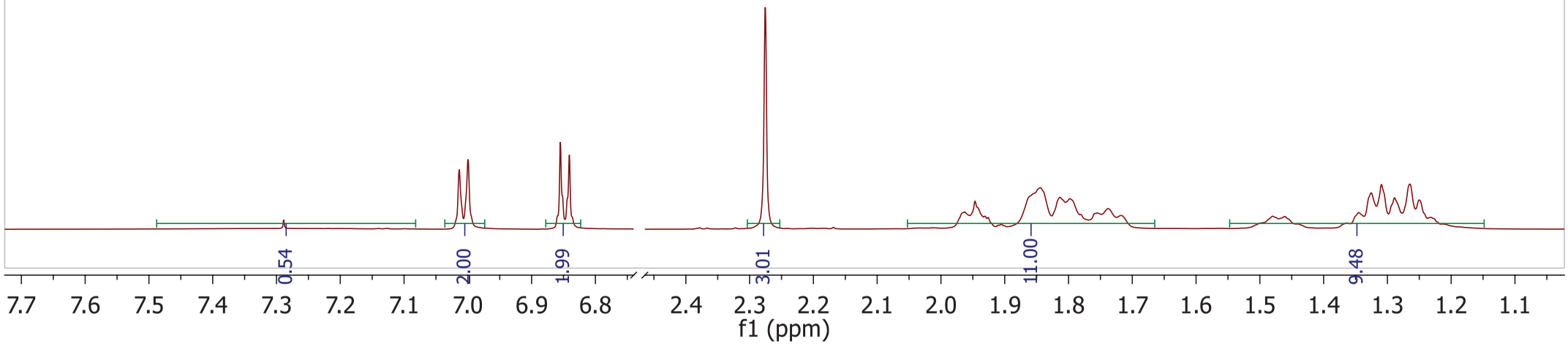

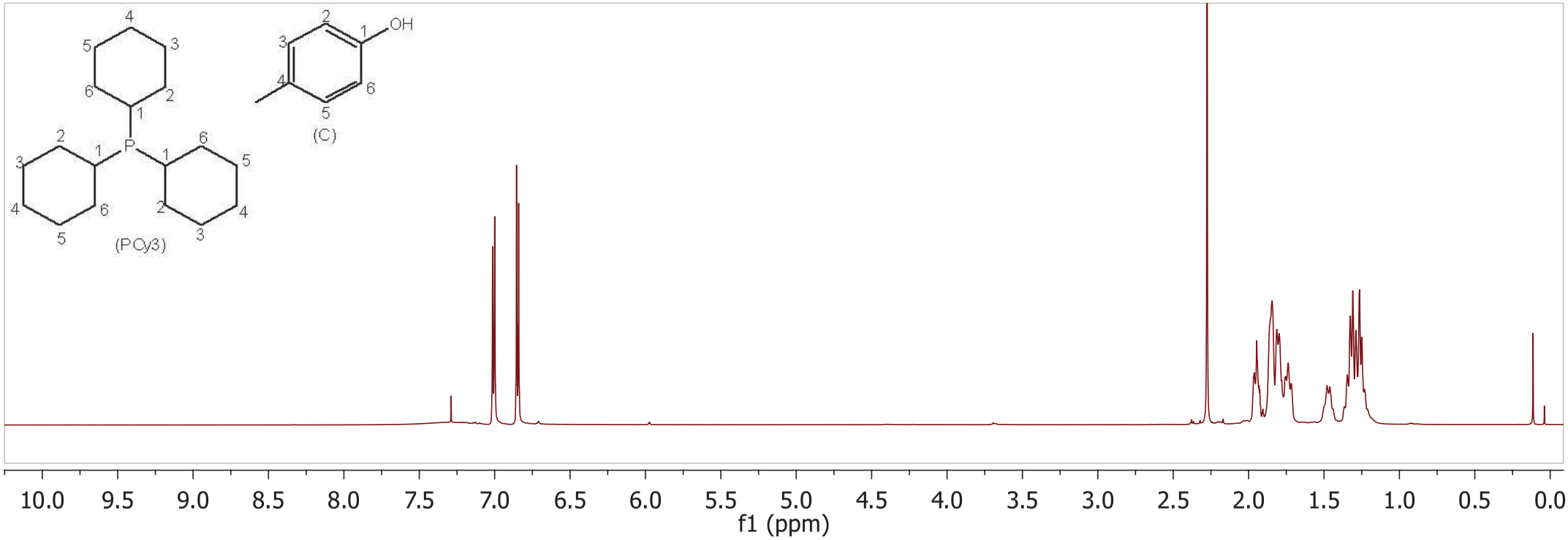

Plate 22a: Tricyclohexylphosphine (**289**) + trifluoromethanesulfonic acid (**312**) ^{1}H NMR [600 MHz, $CDCl_3$]: δ 11.53 – 11.04 (m) , 2.69 – 0.71 (m, POCy3:H-1-6).

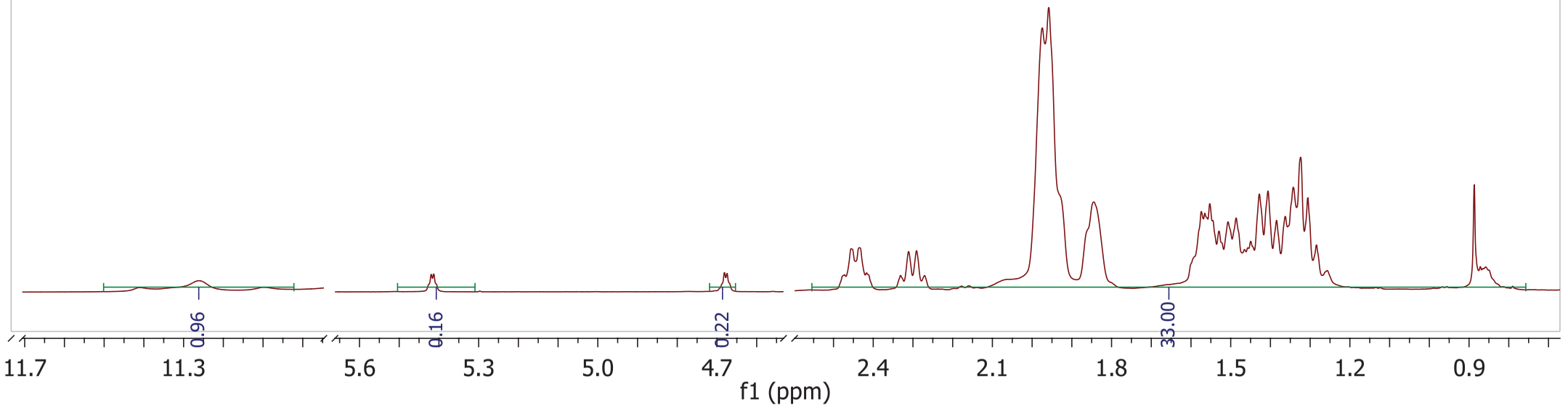

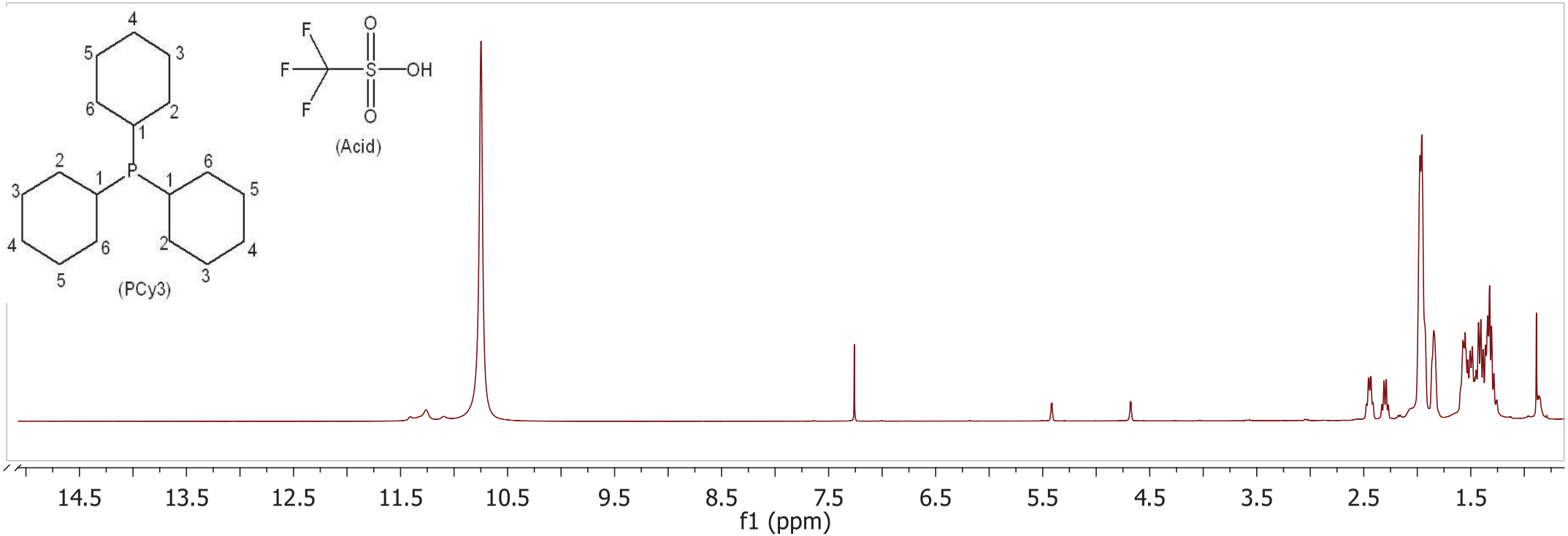

Plate 23a: Tricyclohexylphosphine oxide (**313**)

^{1}H NMR [600 MHz, $CDCl_3$]: δ 4.46 – 4.30 (1H), 2.01 – 1.15 (33H, m, POCy3:H-1-6).

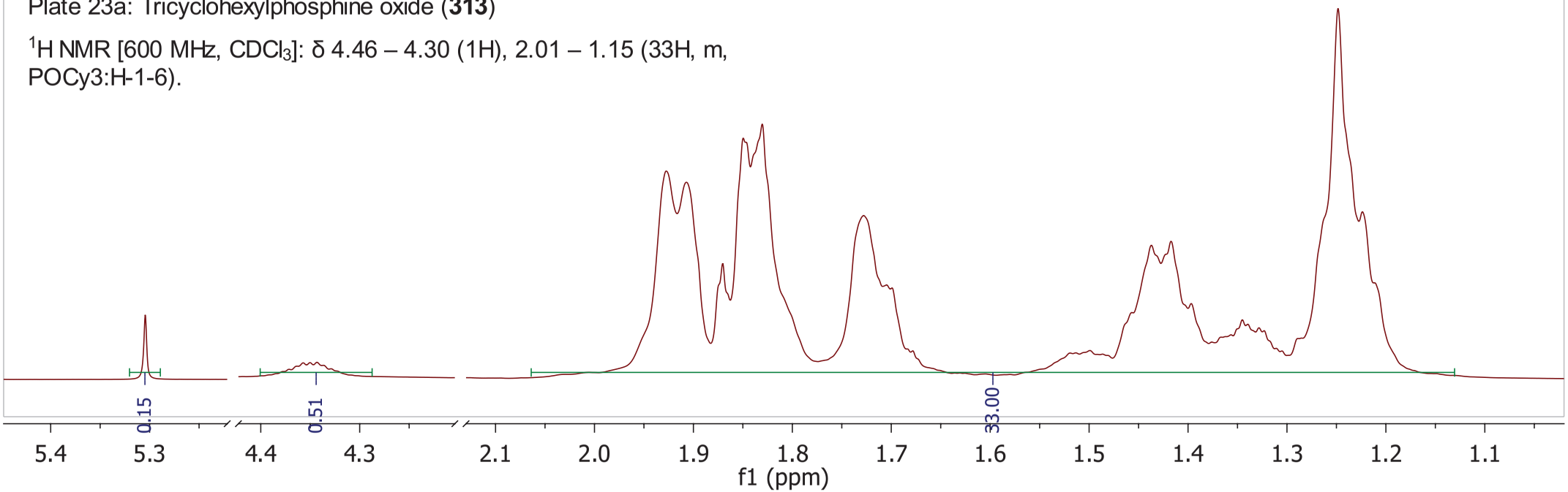

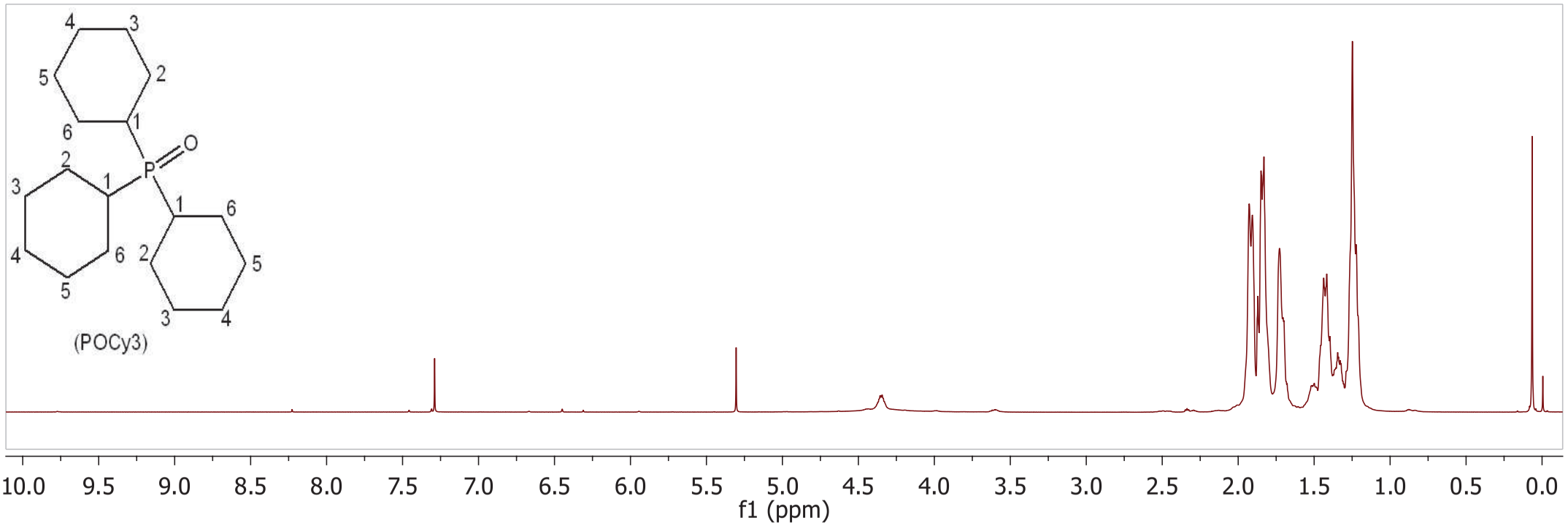

Plate 24a: Tricyclohexylphosphine oxide (**313**) + 1 eq. *p*-cresol (**266**)

^{1}H NMR [600 MHz, $CDCl_3$]: δ 7.45 (s), 7.00 (d, *J* = 8.3 Hz, C:H-3,5), 6.83 (d, *J* = 8.3 Hz, C:H-2,6), 2.27 (s, C:Me), 2.09 – 1.15 (m, POCy3:H-1-6).

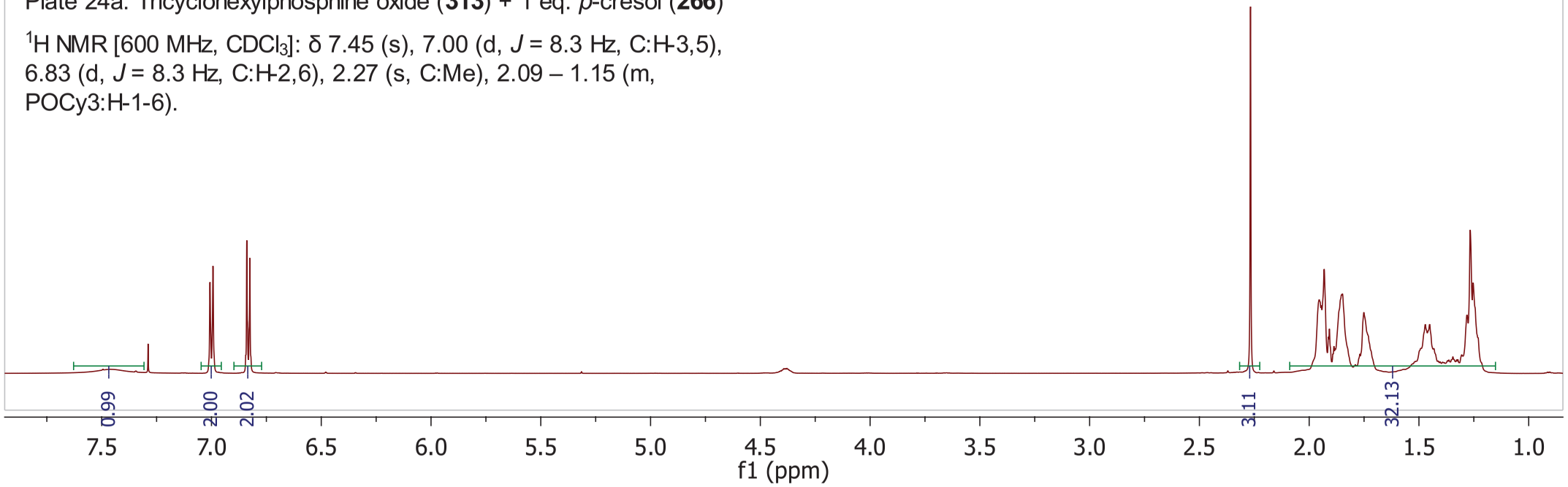

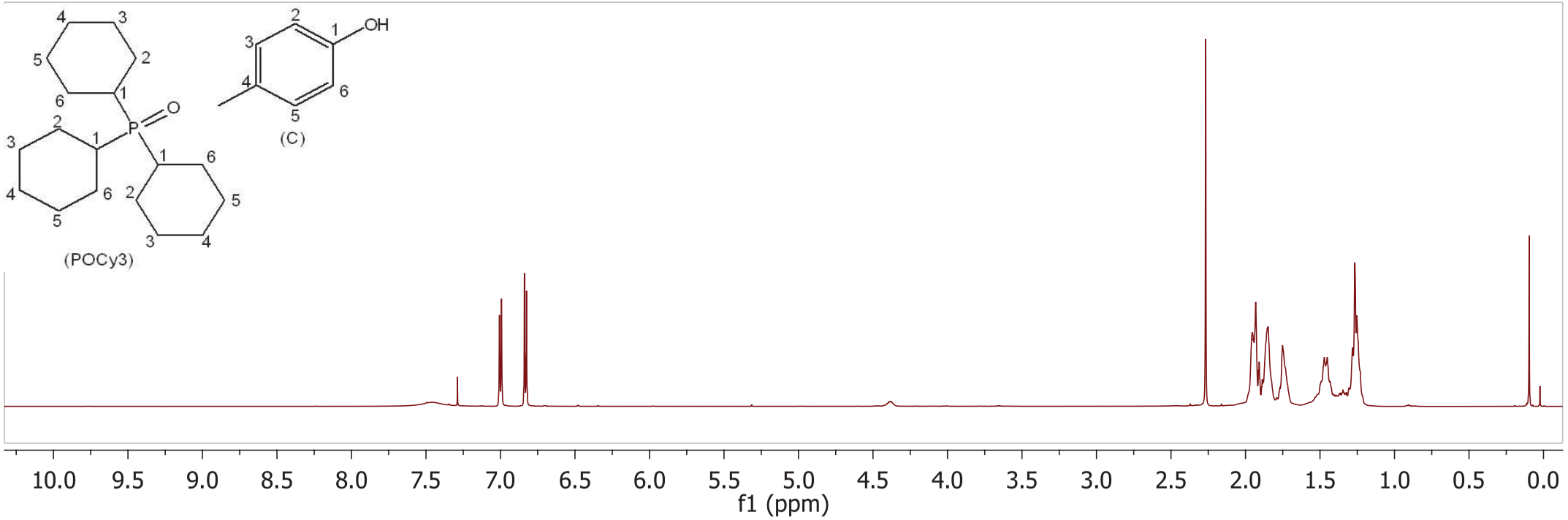

Plate 25a: Tricyclohexylphosphine oxide (**313**) + 2 eq. *p*-cresol (**266**)

^{1}H NMR [600 MHz, $CDCl_3$]: δ 7.00 (d, *J* = 8.3 Hz, C:H-3,5), 6.78 (d, *J* = 8.3 Hz, C:H-2,6), 5.63 (s), 2.26 (s, C:Me), 2.01 – 1.17 (m, POCy3:H-1-6).

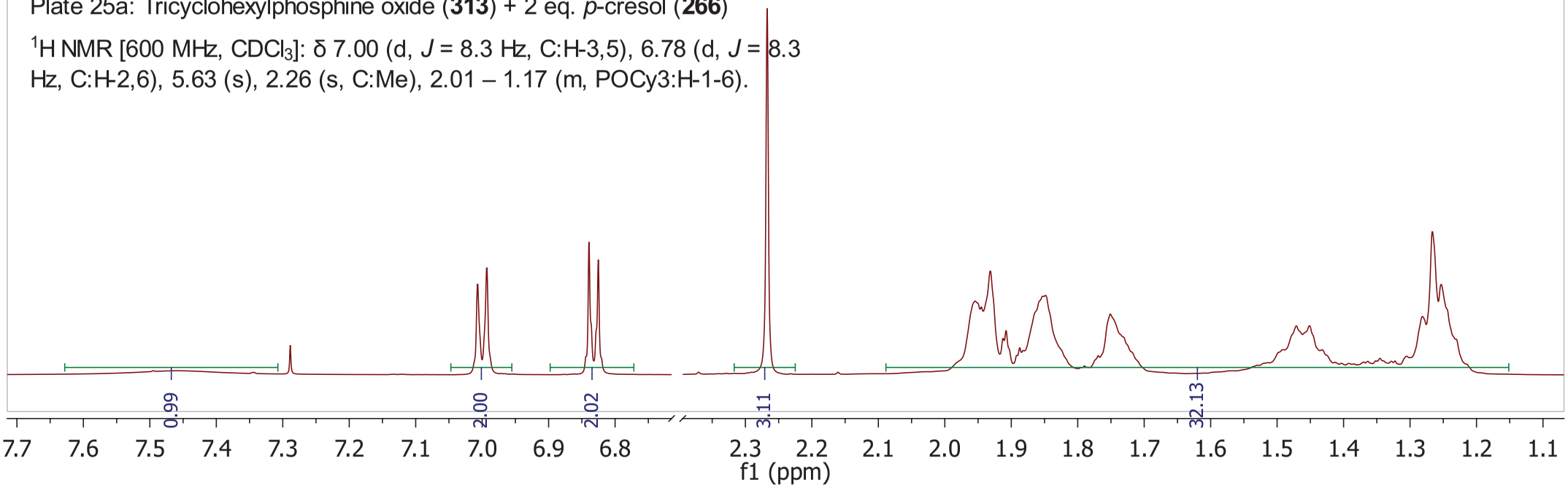

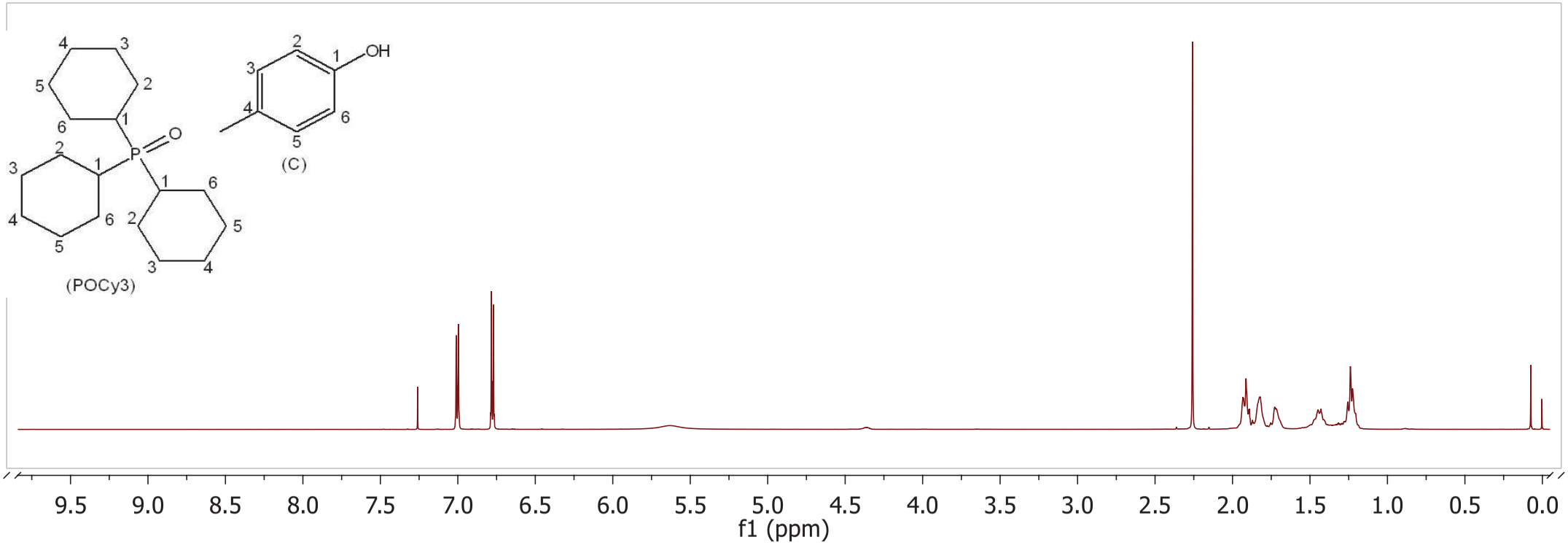

Plate 26a: Tricyclohexylphosphine oxide (**313**) + trifluoromethanesulfonic acid (**312**)

^{1}H NMR [600 MHz, $CDCl_3$]: δ 11.69 (s), 2.49 – 0.77 (m, POCy3:H-1-6).

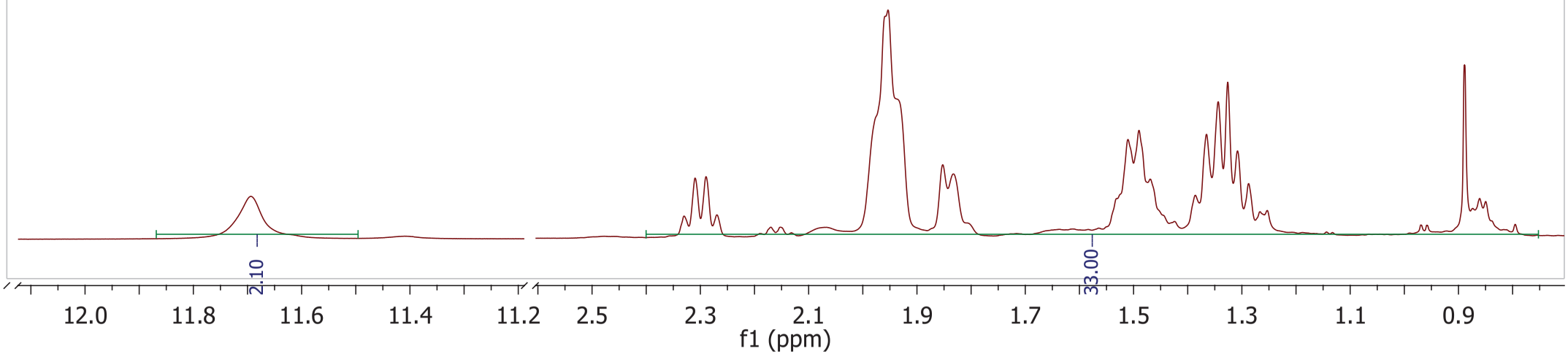

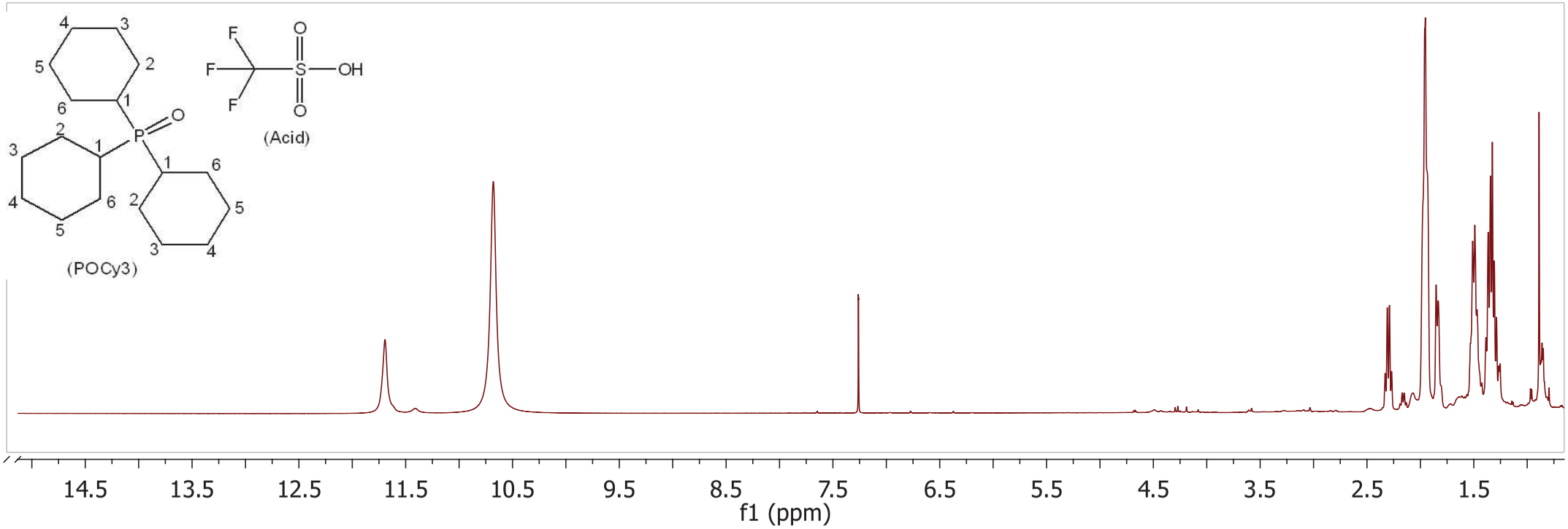

Plate 27a: Methyl acrylate (**59**)

^{1}H NMR [600 MHz, $CDCl_3$]: δ 6.28 (1H, dd, *J* = 17.4, 1.5 Hz, H-3a), 6.01 (1H, dd, *J* = 17.4, 10.5 Hz, H-2), 5.71 (1H, dd, *J* = 10.5, 1.5 Hz, H-3b), 3.64 (3H, s, -OC<u>H</u>$_3$).

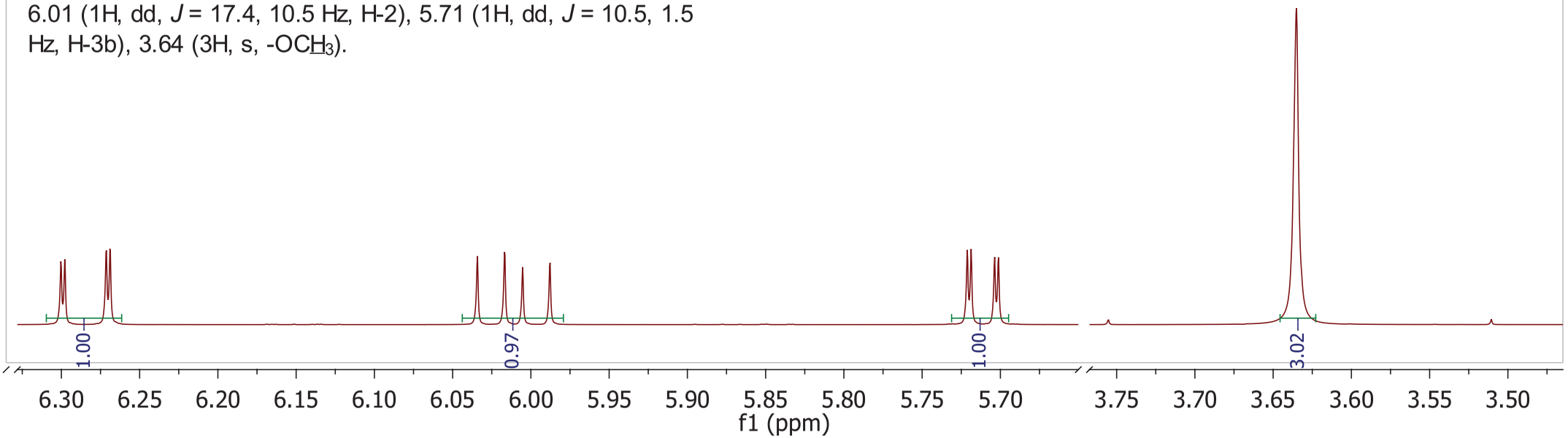

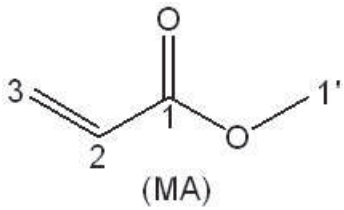

(MA)

Plate 27b: Methyl acrylate (**59**)

^{13}C NMR [151 MHz, $CDCl_3$]: δ 166.5 (C-1), 130.5 (C-3), 128.2 (C-2), 51.4 (C-1').

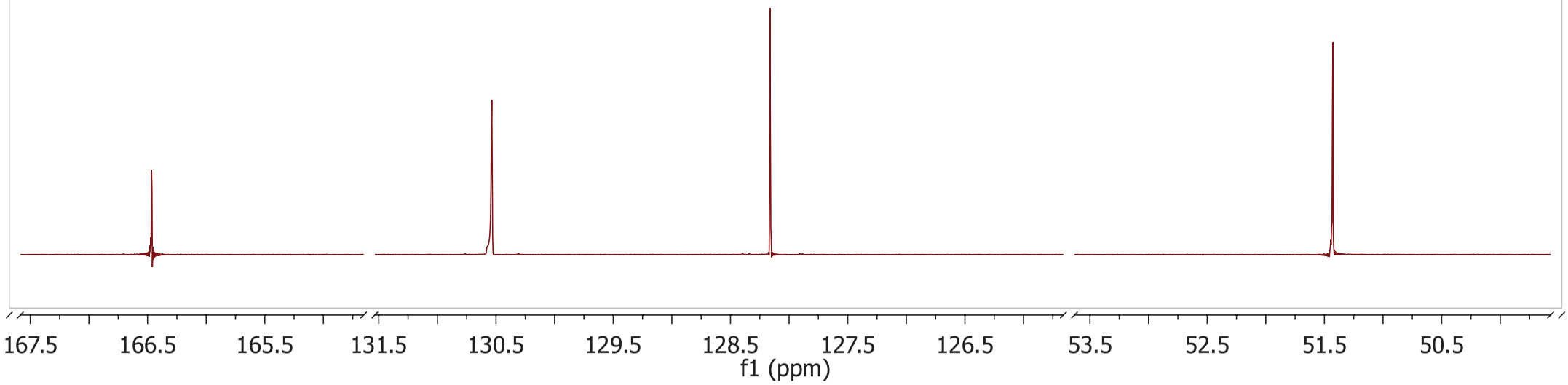

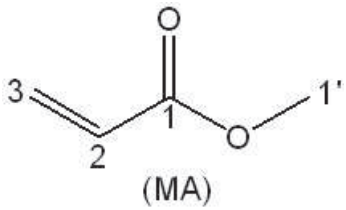

(MA)

Plate 28a: Grubbs 2nd generation catalyst (**125**) + methyl acrylate (**59**)

^{1}H NMR [600 MHz, $CDCl_3$]: δ 19.13 (s, GII: H-1'), 12.04 – 12.01 (m), 10.03 (s), 8.24 – 7.98 (m), 7.89 (d, *J* = 6.3 Hz), 7.73 – 7.67 (m), 7.67 – 7.61 (m), 7.54 (dd, *J* = 16.8, 7.9 Hz), 7.42 – 7.32 (m), 7.27 (d, *J* = 8.2 Hz), 7.18 (d, *J* = 7.5 Hz), 7.11 (s), 7.09 – 6.79 (m), 6.45 (d, *J* = 16.0 Hz), 6.27 (d, *J* = 14.1, MA: H-3a), 5.93 – 5.78 (m), 4.57 (s), 3.99 (dd, *J* = 19.3, 7.1 Hz), 3.92 – 3.72 (m, GII: H-4,5), 2.99 (d, *J* = 53.3 Hz), 2.76 (s, GII: H-2-Me(B)), 2.63 (s), 2.56 (s, GII: H-6-Me(B)), 2.50 (s, GII: H-6-Me(A)), 2.41 – 2.01 (m), 1.97 – 1.34 and 1.32 – 0.82 (m, GII: H-2-6(D)).

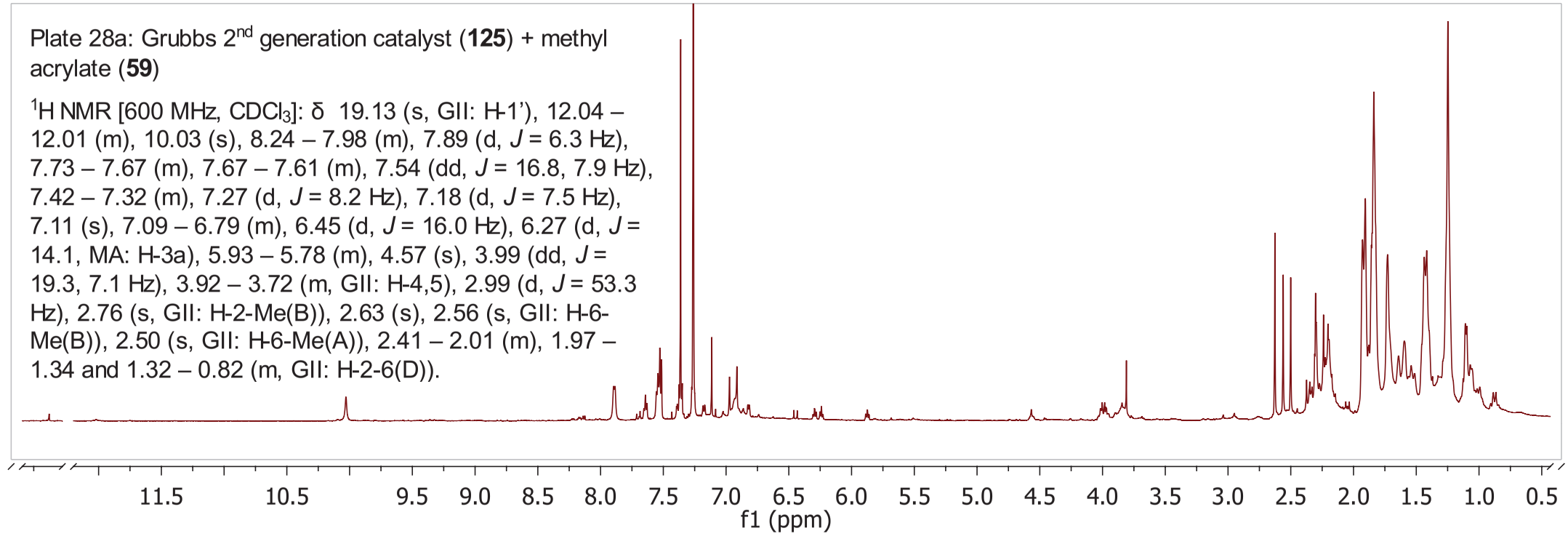

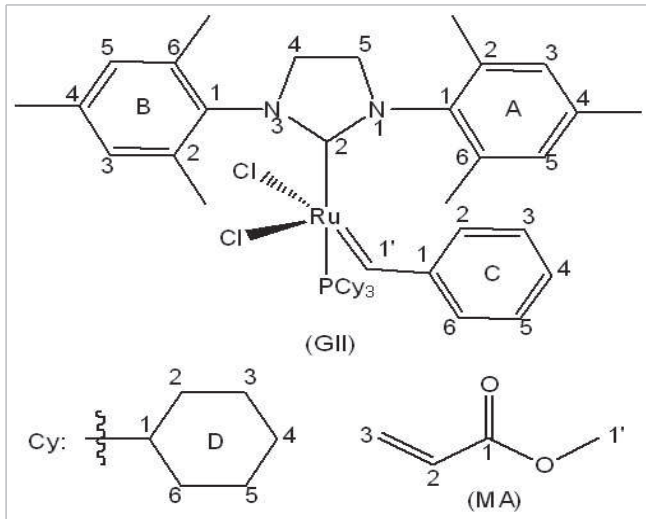

Plate 28b: Grubbs 2nd generation catalyst (**125**) + methyl acrylate (**59**)

^{13}C NMR [151 MHz, $CDCl_3$]: δ 137.2, 130.0(GII: C-3(B),5(C)), 129.9(GII: C-6(C)), 129.1(GII: C-3(A)), 128.8(GII: C-5(A)), 128.0, 127.7, 126.6, 52.0, 35.6, 35.2, 31.5, 31.4, 29.1, 27.8, 27.1, 27.0, 26.5, 26.4, 26.2, 21.3(GII: C-4-Me(B)), 21.0(GII: C-4-Me(A)), 20.1(GII: C-2-Me(B),6-Me(B)).

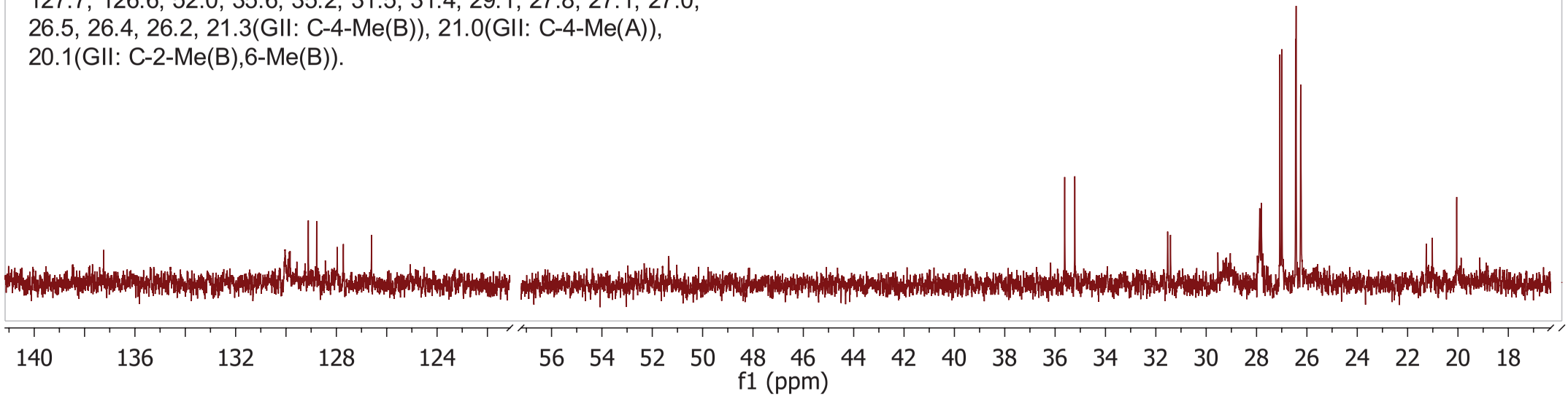

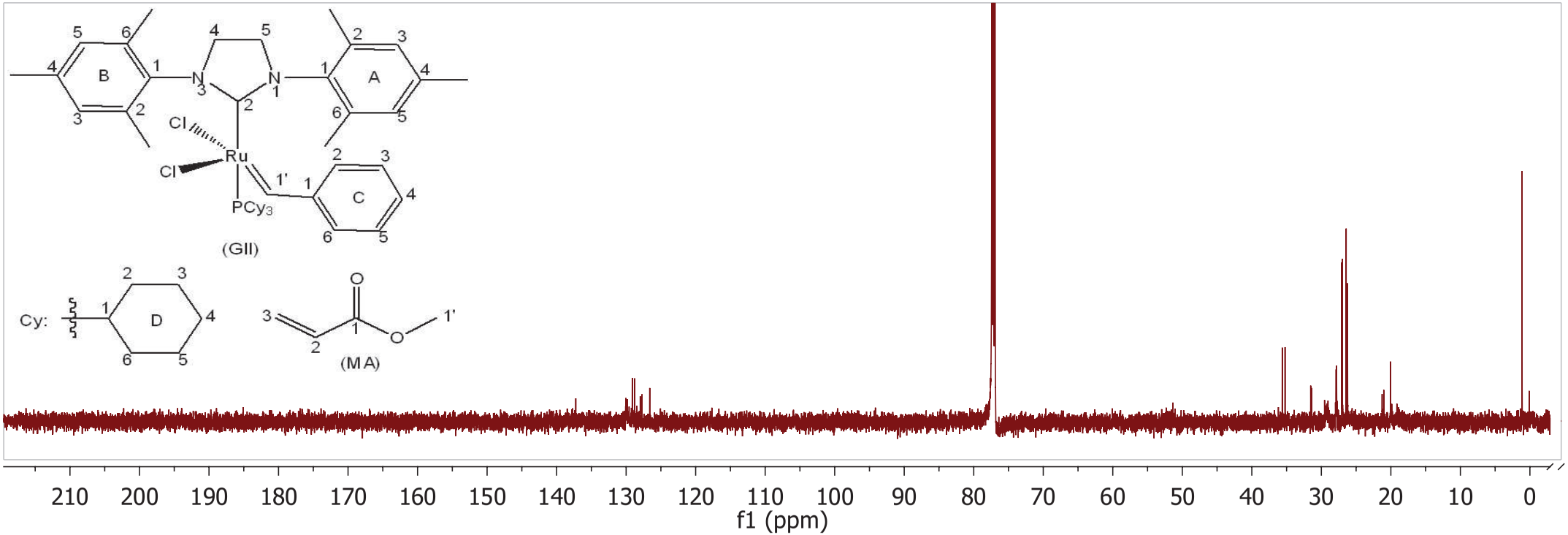

Plate 29a: Grubbs 2nd generation catalyst (**125**) + methyl acrylate (**59**) + *p*-cresol (**266**)

^{1}H NMR [600 MHz, $CDCl_3$]: δ 19.07 (s, GII: H-1'), 17.73 (s), 17.52 (s), 8.93 (s), 7.98 (s), 7.62 (d, *J* = 16.0 Hz), 7.48 – 7.38 (m), 7.35 – 7.26 (m), 7.25 – 7.12 (m), 7.25 – 7.12 (m), 7.08 – 6.91 (m), 6.90 – 6.85 (m), 6.84 – 6.75 (m), 6.75 – 6.43 (m), 6.42 – 6.25 (m), 6.13 – 5.97 (m), 5.97 – 5.83 (m), 5.85 – 5.68 (m), 5.69 – 5.55 (m), 5.31 (s), 4.79 – 4.20 (m), 3.97 – 3.78 (m), 3.76 – 3.71 (m), 3.70 – 3.65 (m), 3.65 – 3.62 (m), 3.61 – 3.58 (m), 3.57 – 3.43 (m), 3.41 – 3.23 (m), 3.23 – 2.92 (m), 2.82 – 2.48 (m), 2.47 – 2.37 (m), 2.36 – 2.32 (m), 2.31 – 2.26 (m), 2.27 – 2.20 (m), 2.18 – 2.11 (m), 2.09 – 0.67 (m).

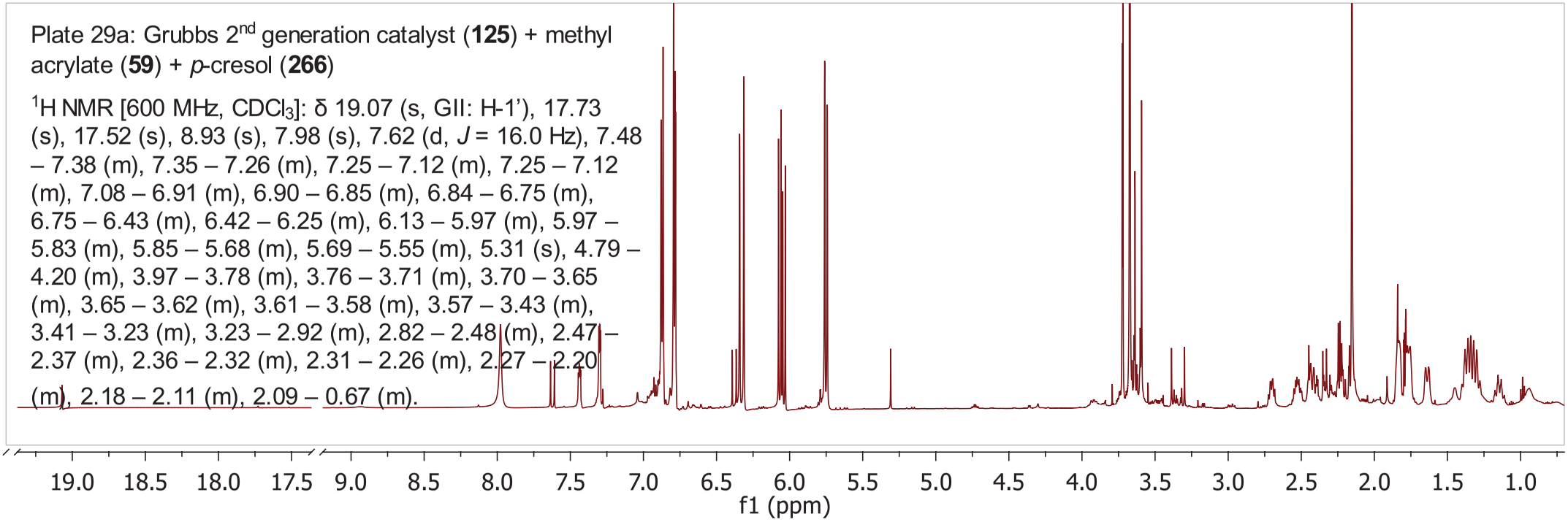

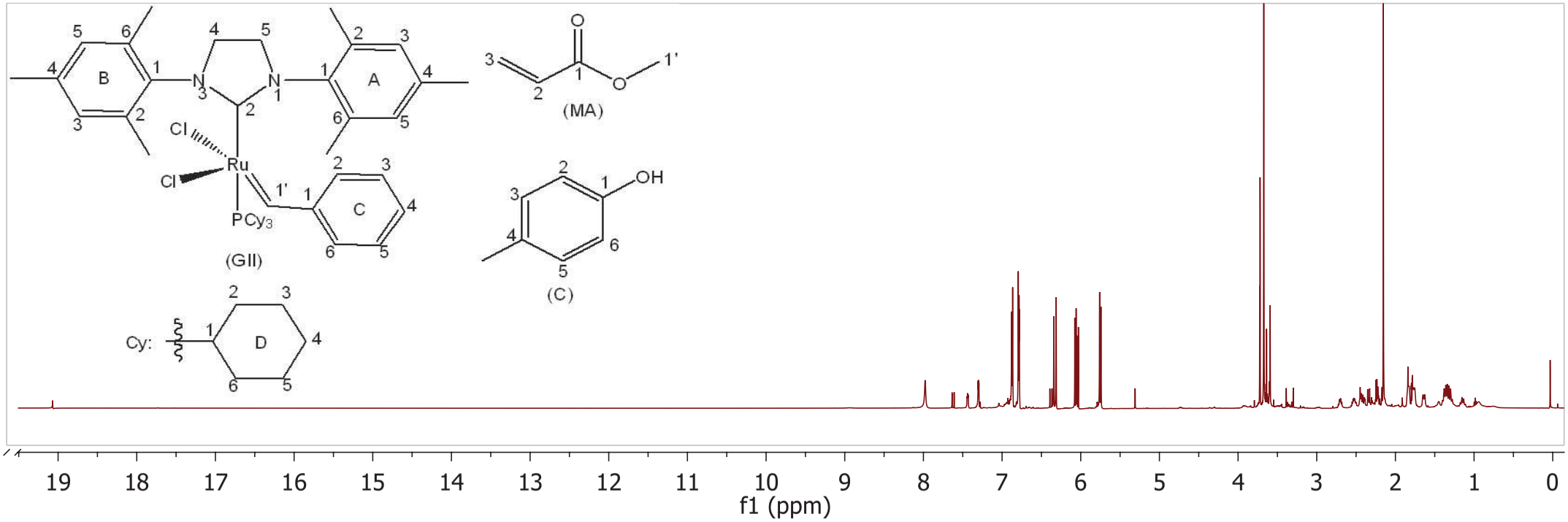

Plate 29b: Grubbs 2nd generation catalyst (**125**) + methyl acrylate (**59**) + *p*-cresol (**266**)

Int. ^{13}C NMR [151 MHz, $CDCl_3$]: δ 294.1, 219.9(d, J = 77.2 Hz), 213.7, 174.8, 171.2 (d, J = 12.5 Hz), 167.3, 166.9, 166.5, 165.1, 154.5, 154.42, 154.36, 154.1, 151.0, 144.8, 138.6 (d, J = 63.3 Hz), 138.1, 137.5, 137.3, 136.9, 136.6 (d, J = 49.3 Hz), 136.1, 135.5, 134.9, 134.8, 134.3, 134.0, 133.1, 131.7, 130.7, 130.2, 129.6, 129.4, 129.2, 128.9, 128.7, 128.5, 128.1, 127.84, 127.77, 126.9, 125.9, 122.5 (d, J = 27.2 Hz), 122.1, 121.5, 119.7, 117.4, 115.2, 69.1, 53.0, 52.3, 52.1, 52.0, 51.4, 51.1, 51.0, 50.6, 50.0, 41.2, 31.2(d, J = 16.6 Hz), 29.8(d, J = 40.0 Hz), 28.8 (d, J = 48.0 Hz), 27.5, 27.4, 26.9, 26.7, 26.5, 26.2, 26.0, 25.9, 25.1, 20.9, 20.7, 20.6, 20.2, 19.7, 18.5, 18.4, 18.2, 18.0, 17.7, 17.4, 11.9, 11.0, 10.6.

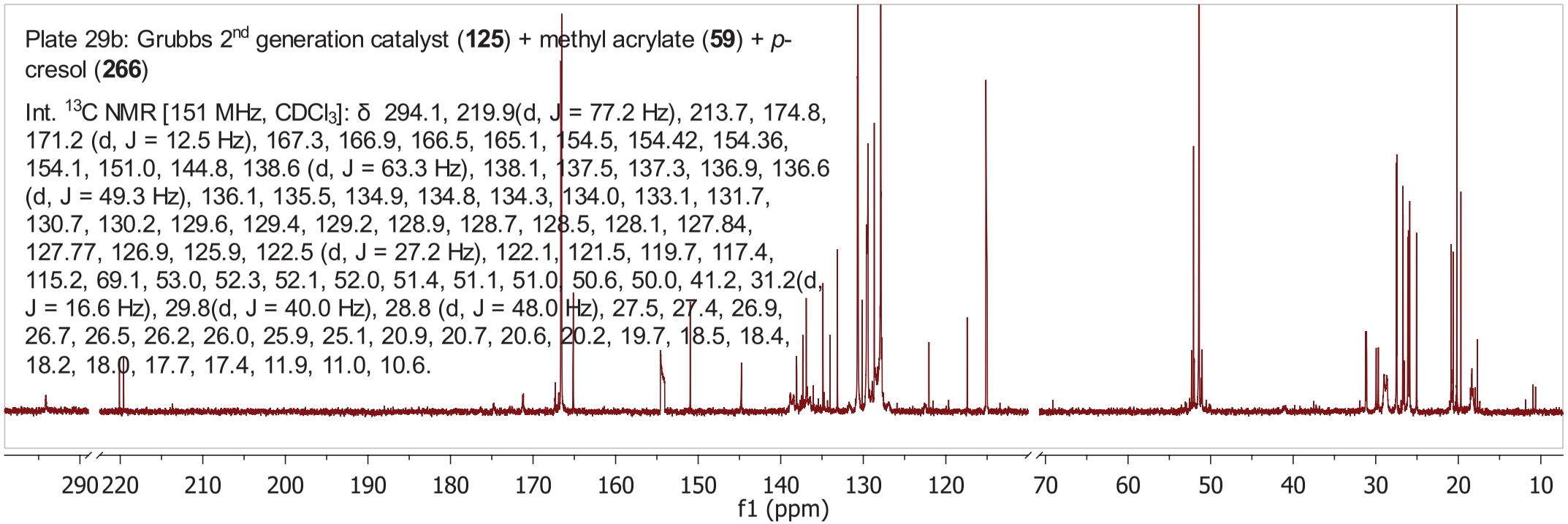

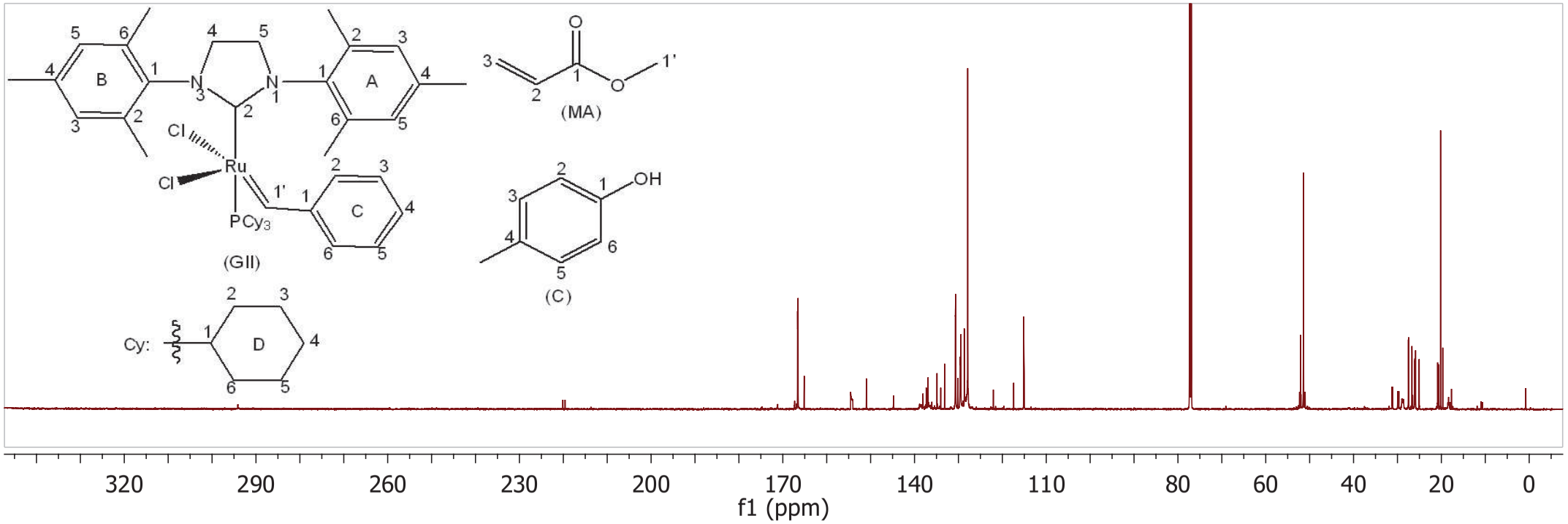

Plate 30a: Methylstyrene (**69**)

^{1}H NMR [600 MHz, $CDCl_3$]: δ 7.49 (2H,dd, *J* = 7.3, 1.0 Hz, H-2',6'), 7.44 (2H, m, H-3',5'), 7.14 (1H,t t, *J* = 6.7, 1.0 Hz, H-4'), 6.56 (1H, qd, *J* = 15.8, 1.7 Hz, H-1), 6.39 (1H, dq, *J* = 15.8, 6.7 Hz, H-2), 2.03 (3H, dd, *J* = 6.7, 1.7 Hz, H-3).

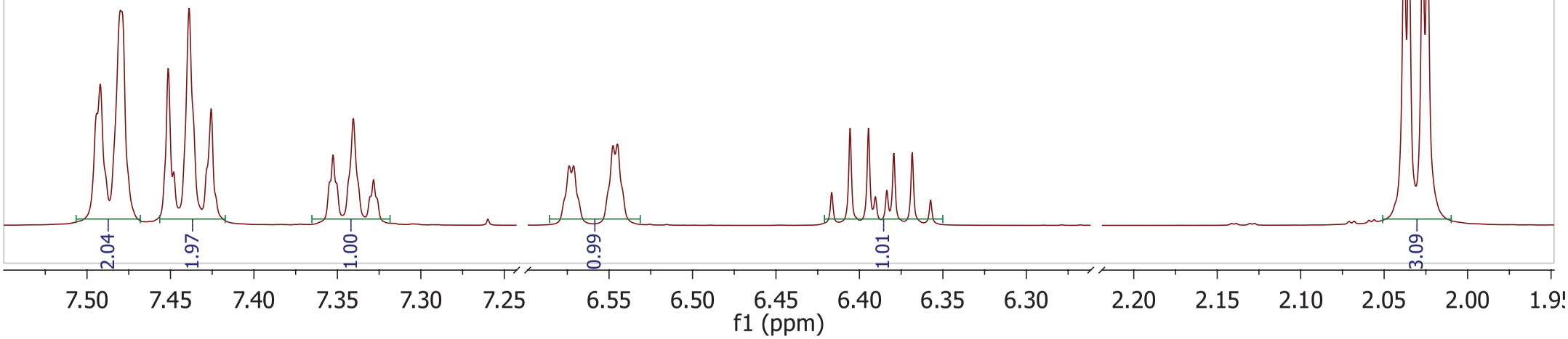

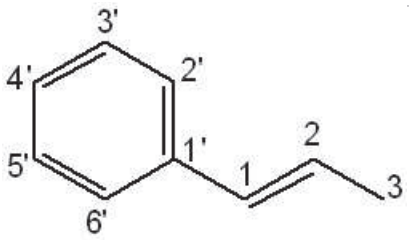

(MS)

Plate 30b: Methylstyrene (**69**)

^{13}C NMR [151 MHz, $CDCl_3$]: δ 138.03 (C-1'), 131.18 (C-1), 128.56 (C-3',5'), 126.83 (C-4'), 125.93 (C-2',6'), 125.68 (C-2), 18.56 (C-3).

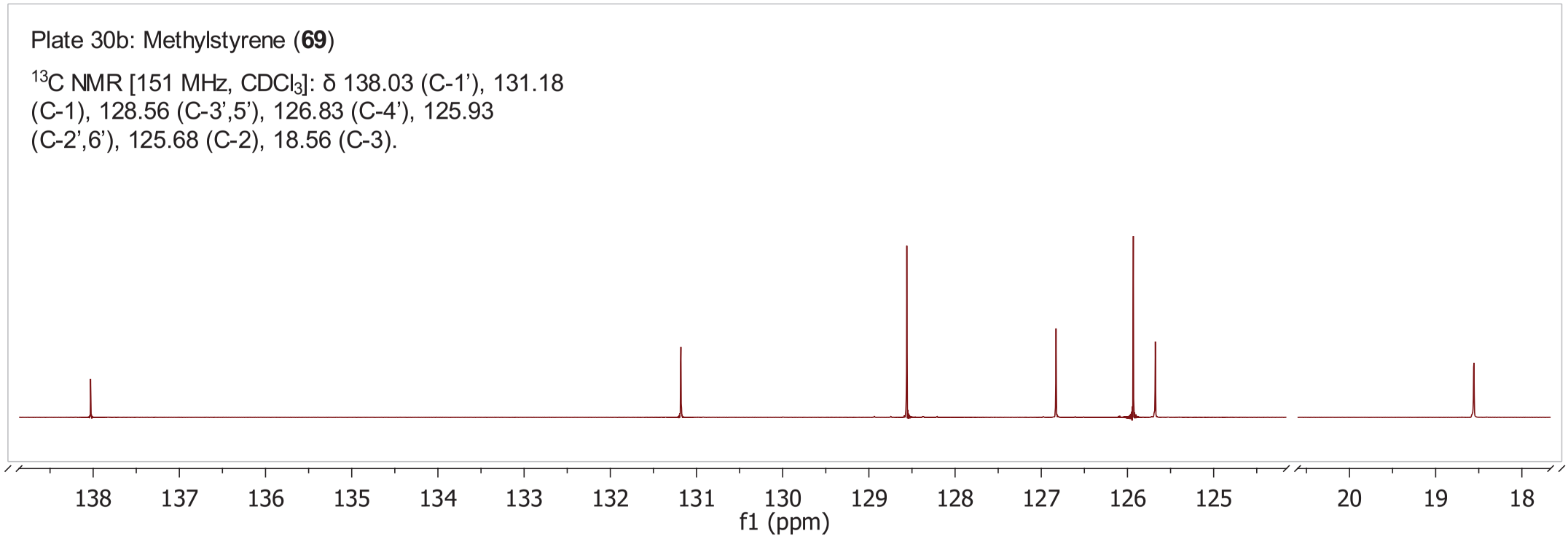

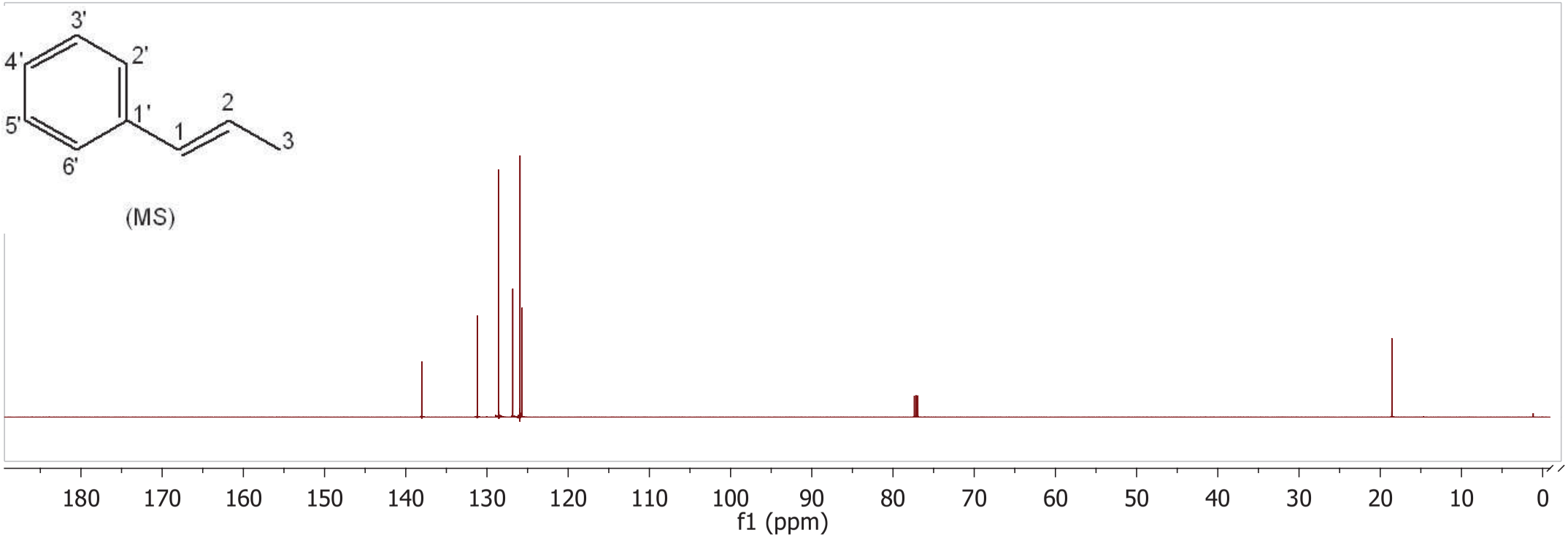

Plate 31a: Grubbs 2nd generation catalyst (**125**) + trans-β-methylstyrene (**69**)

^{1}H NMR [600 MHz, $CDCl_3$]: δ 19.12 (s, GII:H-1'), 18.52 (q, *J* = 5.5 Hz), 8.98 (s, GII:H-2(C)), 7.54 (d, *J* = 8.1 Hz), 7.41 (d, *J* = 7.4 Hz, MS:H-2',6'), 7.39 – 7.29 (m, MS:H-3',4',5'), 7.28 – 7.22 (m), 7.21 – 7.15 (m), 7.14 – 7.11 (m), 7.11 – 7.07 (m), 7.07 – 7.03 (m), 7.02 (s), 6.95 (s), 6.91 (s), 6.83 (s), 6.78 (s, GII:H-5(A)), 6.71 – 6.59 (m), 6.37 (dd, *J* = 11.5, 6.0 Hz), 6.31 (d, *J* = 15.8 Hz), 6.19 – 6.09 (m, *J* = 15.7, 6.6 Hz), 5.82 – 5.62 (m), 5.48 – 5.33 (m), 3.90 – 3.58 (m, GII:H-4,5), 2.79 – 2.43 (m), 2.38 (s), 2.24 (s), 2.15 (dd, *J* = 19.5, 7.9 Hz), 2.13 – 1.94 (m), 1.84 (s), 1.83 – 1.80 (m), 1.78 (dd, *J* = 6.6, 1.5 Hz), 1.70 – 1.63 (m), 1.70 – 1.14 (m), 1.13 – 0.69 (m).

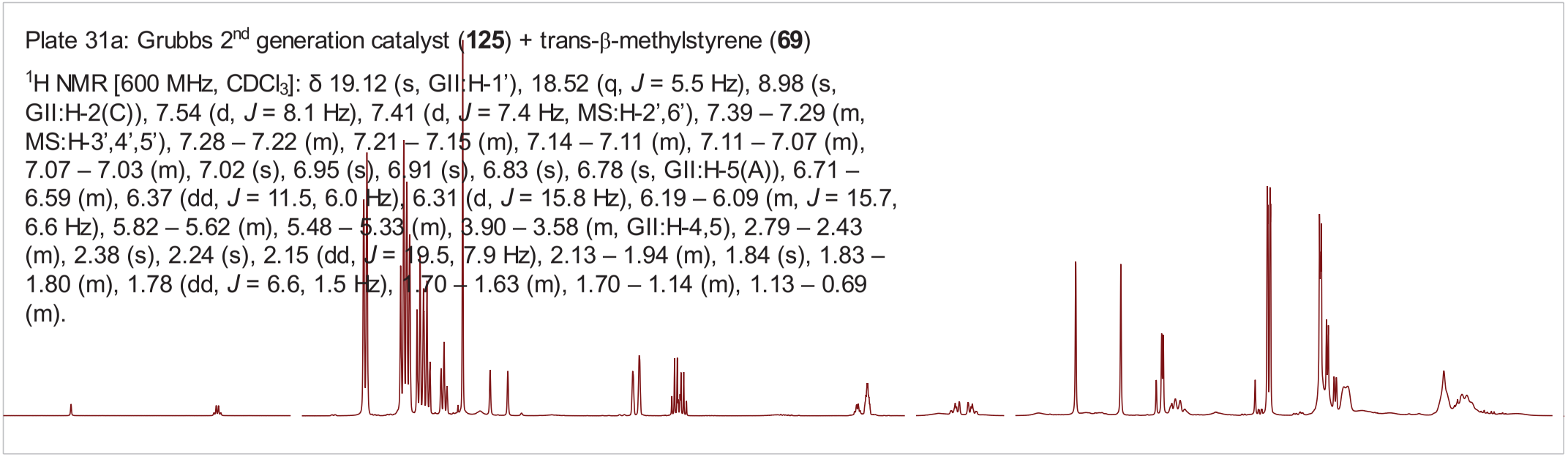

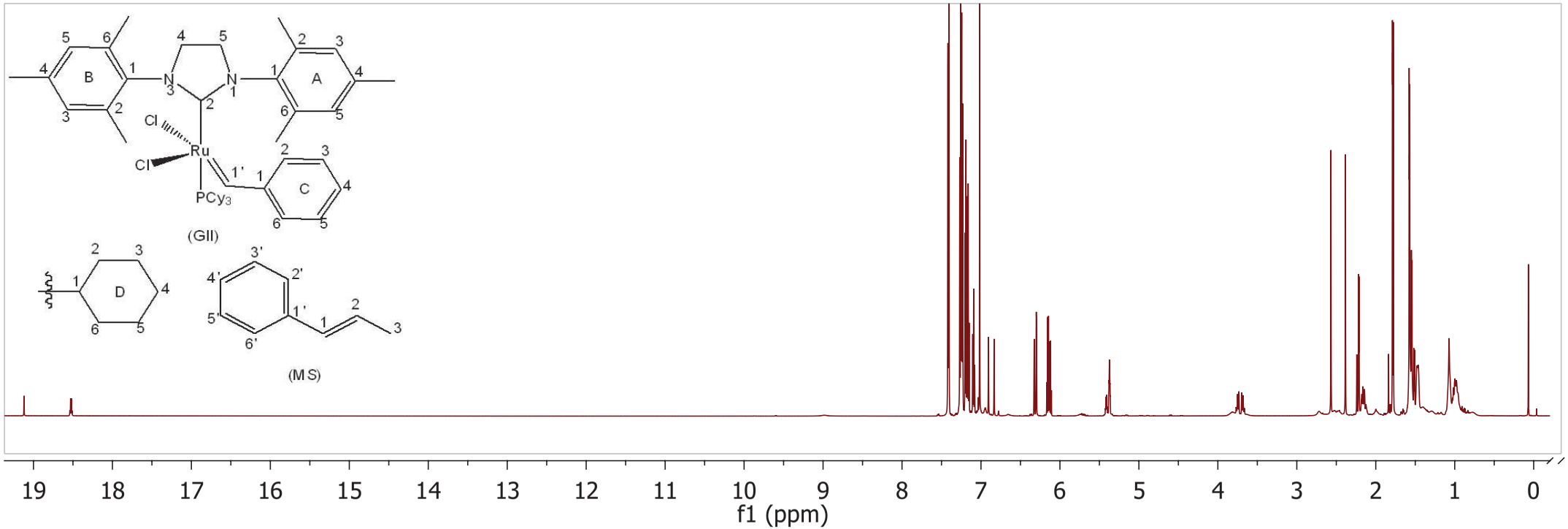

Plate 31b: Grubbs 2nd generation catalyst (**125**) + trans-β-methylstyrene (**69**)

Int. ^{13}C NMR [151 MHz, $CDCl_3$]: δ 315.2, 294.3(GII:C-1'), 220.4 (d, J = 60.2 Hz, GII:C-2), 219.9(d, J = 57.4 Hz), 151.2(GII:C-1(C)), 140.1, 139.0, 138.9, 138.7, 138.4, 138.2, 138.1, 138.0, 137.9, 137.6, 137.53, 137.46, 137.4, 137.3, 137.1, 137.0, 136.9, 135.1, 134.8, 134.6, 133.6, 133.1, 132.4, 131.9, 131.2, 131.0, 129.8, 129.7, 129.4, 128.8, 128.6, 128.4, 128.2, 128.1, 127.8, 127.7, 127.6, 126.7, 126.5, 126.4, 126.3, 125.8, 125.5, 124.5, 51.9(d, J = 38.5 Hz, GII:C-4), 51.1(d, J = 8.2 Hz, GII:C-5), 46.2, 31.6, 31.5, 31.4, 31.3, 29.2, 28.9, 27.8, 27.7, 27.6, 26.3, 26.1, 21.1, 21.0, 20.9, 19.9, 19.7, 18.6, 18.4, 17.9, 14.6, 12.4.

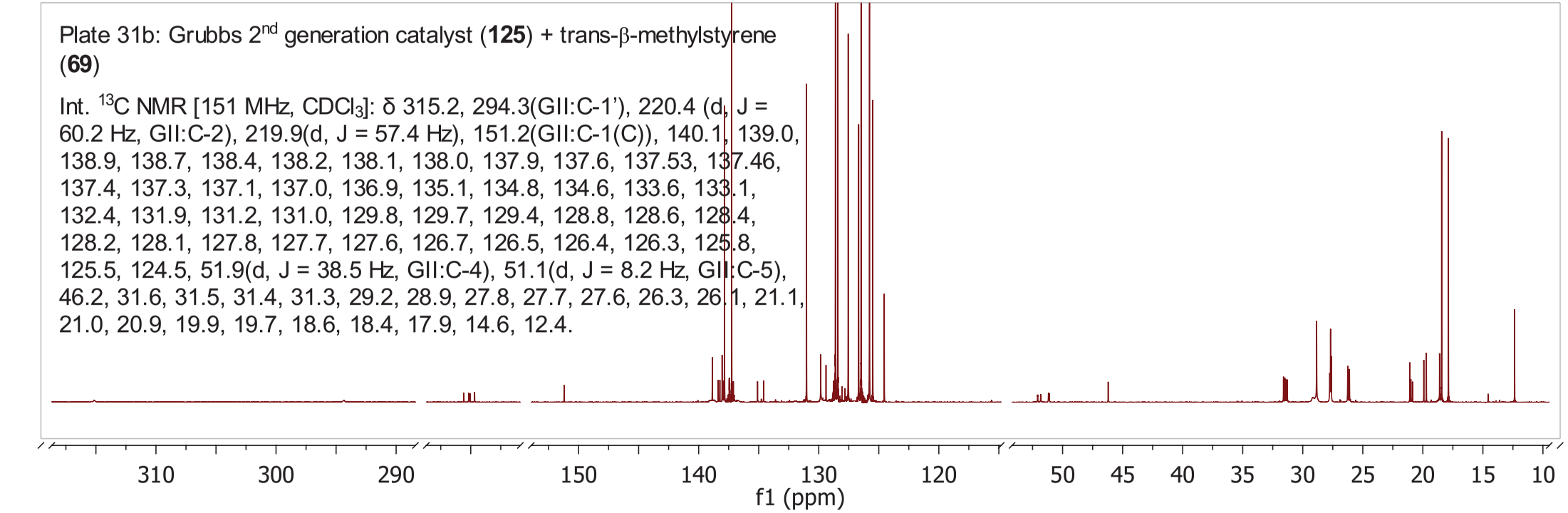

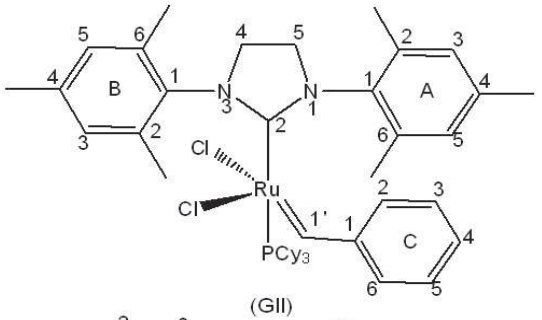

(GII)

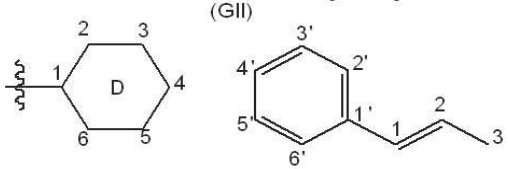

(MS)

Plate 32a: Grubbs 2nd generation catalyst (**125**) + trans-β-methylstyrene (**69**)+ *p*-cresol (**266**)

^{1}H NMR [600 MHz, $CDCl_3$]: δ 19.29 (s, GII: H-1'), 18.76 (q, *J* = 5.5 Hz), 9.18 (s), 7.66 (d, *J* = 7.4 Hz), 7.54 – 7.38 (m), 7.34 (t, *J* = 7.3 Hz, MS: H-4'), 7.32 – 7.24 (m), 7.16 (t, *J* = 7.6 Hz), 7.06 (s), 6.96 (d, *J* = 8.4 Hz), 6.91 – 6.59 (m), 6.55 (m, MS: H-1), 6.39 (dq, *J* = 15.7, 6.6 Hz, MS: H-2), 6.21 (s), 6.04 – 5.88 (m), 5.70 – 5.56 (m), 5.56 – 5.02 (m), 4.84 (dd, *J* = 10.9, 6.0 Hz), 4.17 – 3.78 (m, GII: H-4,5), 2.95 (s), 2.92 – 2.86 (m), 2.79 (s), 2.75 (s), 2.68 (s), 2.60 (s), 2.55 – 2.33 (m), 2.33 – 2.16 (m), 2.11 – 1.98 (m), 1.86 – 1.46 (m), 1.38 – 0.92 (m).

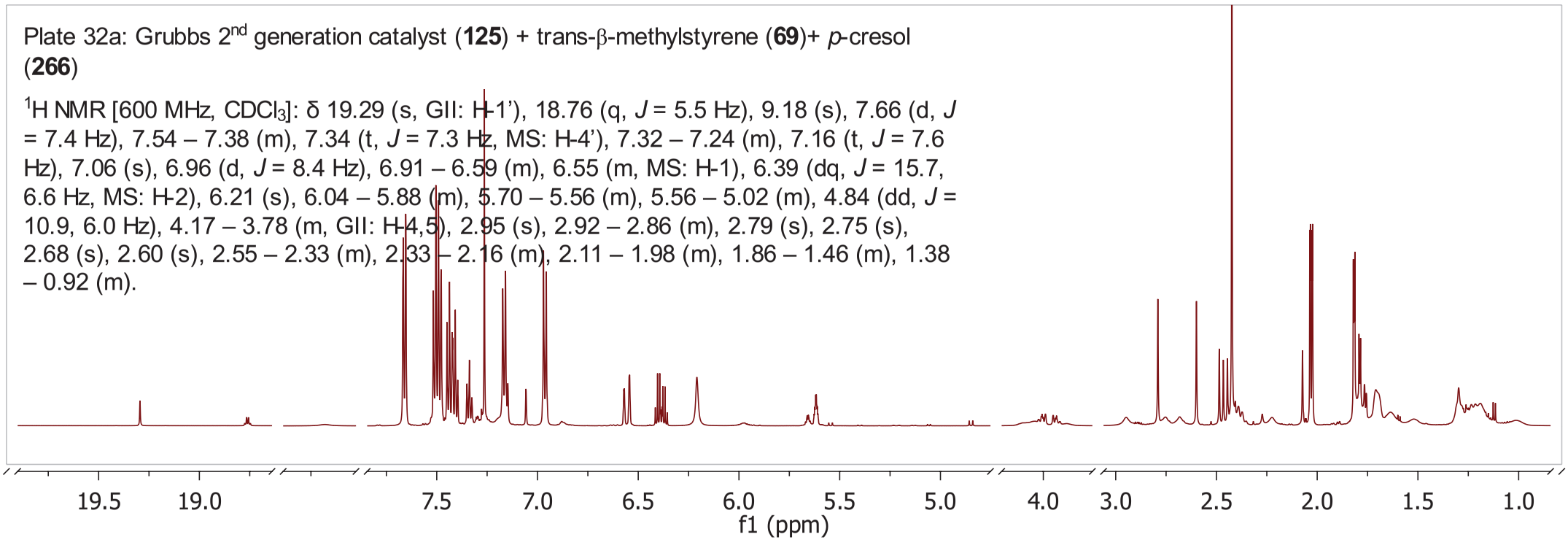

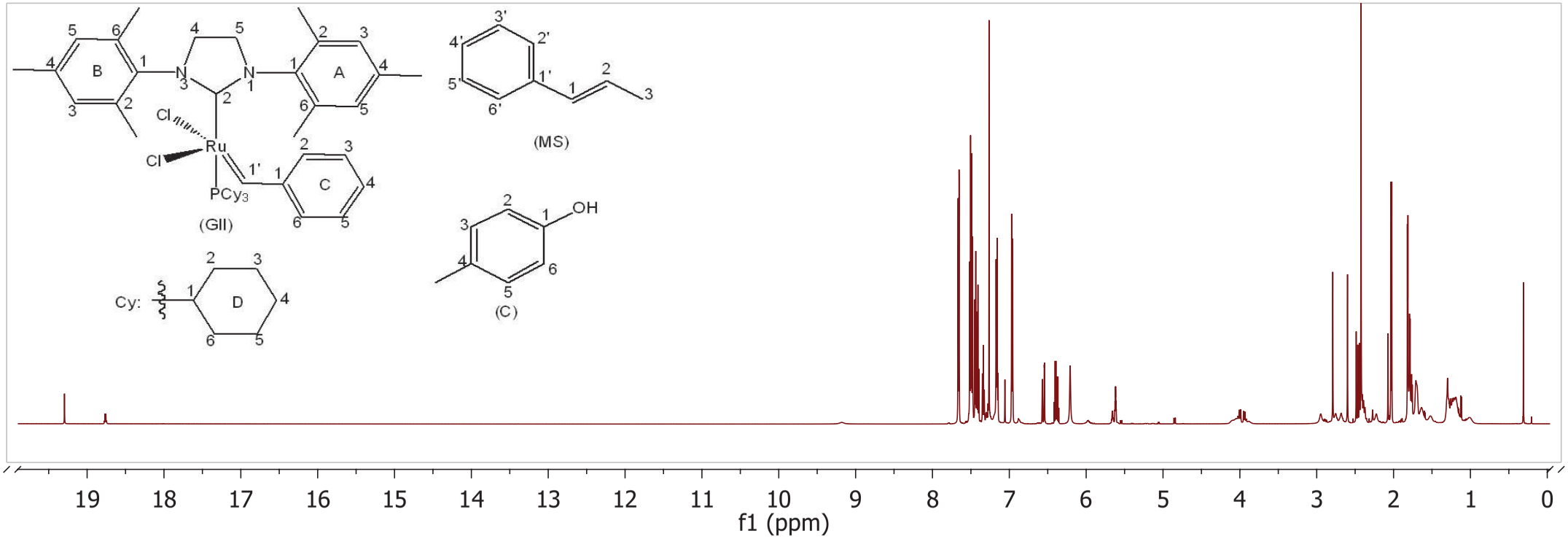

Plate 32b: Grubbs 2nd generation catalyst (**125**) + trans-β-methylstyrene (**69**)+ *p*-cresol (**266**)

^{13}C NMR [151 MHz, $CDCl_3$]: δ 315.4, 294.4 (GII: C-1'), 220.0(d, *J* = 77.1 Hz, GII; C-2), 219.3(d, J = 74.1 *Hz*), 153.6, 151.1(GII: C-1(C)), 139.0 (d, *J* = 66.9 Hz), 138.6, 138.5, 138.4, 138.1, 138.0, 137.9, 137.6, 137.31, 137.28, 137.1, 136.6, 135.0, 134.8, 134.4, 133.7, 133.5, 133.2, 132.5, 131.8, 131.0, 129.91, 129.85, 129.50, 129.4, 129.2, 128.9, 128.8, 128.7, 128.6, 128.5, 128.4, 128.3, 128.1, 127.8, 127.7, 127.59, 127.55, 127.1, 126.7, 126.5, 126.4, 126.3, 126.2, 126.0, 125.9, 125.84, 125.80, 125.76, 125.6, 124.6, 123.6, 115.3, 65.1, 63.6, 61.4, 52.2, 51.9, 51.3, 51.2, 50.7, 46.3, 31.7, 31.6, 31.5, 31.4, 29.3, 28.9, 27.7, 27.64, 27.56, 26.6, 26.1, 25.6, 21.1, 21.0, 20.9, 20.5(C: Me), 19.9, 19.7, 18.54(MS: C-3), 18.46, 17.9, 14.6, 13.9, 13.6, 12.4, 11.2.

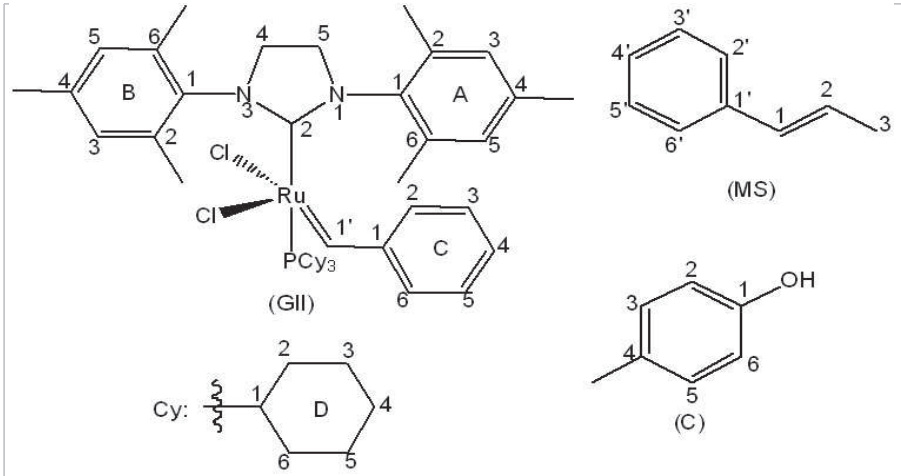

Plate 33a: Grubbs 2nd generation catalyst (**125**) + methyl acrylate (**59**) + trans-β-methylstyrene (**69**)

^{1}H NMR [600 MHz, $CDCl_3$]: δ 19.12 (s, GII:H-1'), 18.52 (q, *J* = 5.3 Hz), 17.77 (s), 8.91 (s), 7.88 – 7.77 (m), 7.68 (s), 7.66 (s), 7.61 (d, *J* = 6.8 Hz), 7.49 (s), 7.48 (s), 7.34 (s), 7.32 (s), 7.31 (s), 7.29 (s), 7.24 (s), 7.23 (s), 7.21 (s), 7.17 – 7.13 (m), 7.08 (s), 7.00 – 6.91 (m), 6.89 (d, *J* = 11.3 Hz), 6.84 (s), 6.74 – 6.51 (m), 6.43 (s), 6.40 (s), 6.36 (s), 6.35 (s), 6.34 – 6.16 (m), 6.15 – 6.06 (m), 5.83 (s), 5.81 (s), 5.75 – 5.65 (m), 5.39 (s), 5.24 (s), 5.20 (s), 5.09 (s), 4.12 – 3.82 (m), 3.77 (s), 3.72 (s), 3.68 (s), 3.64 – 3.50 (m), 2.81 – 2.36 (m), 2.33 – 1.87 (m), 1.83 (d, *J* = 6.9 Hz), 1.74 – 0.66 (m).

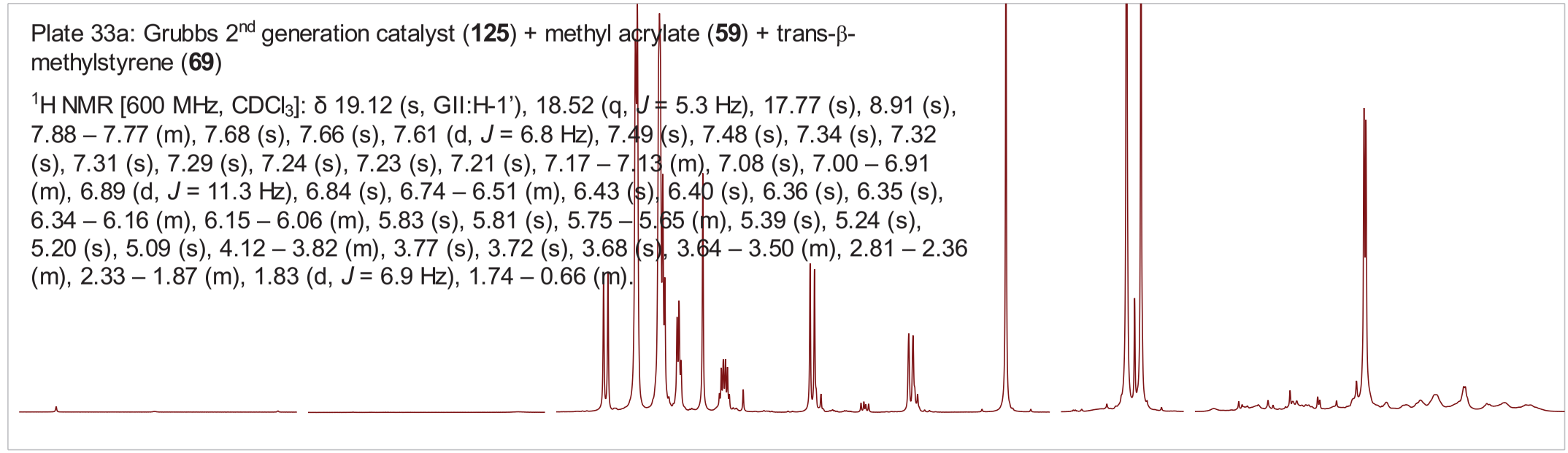

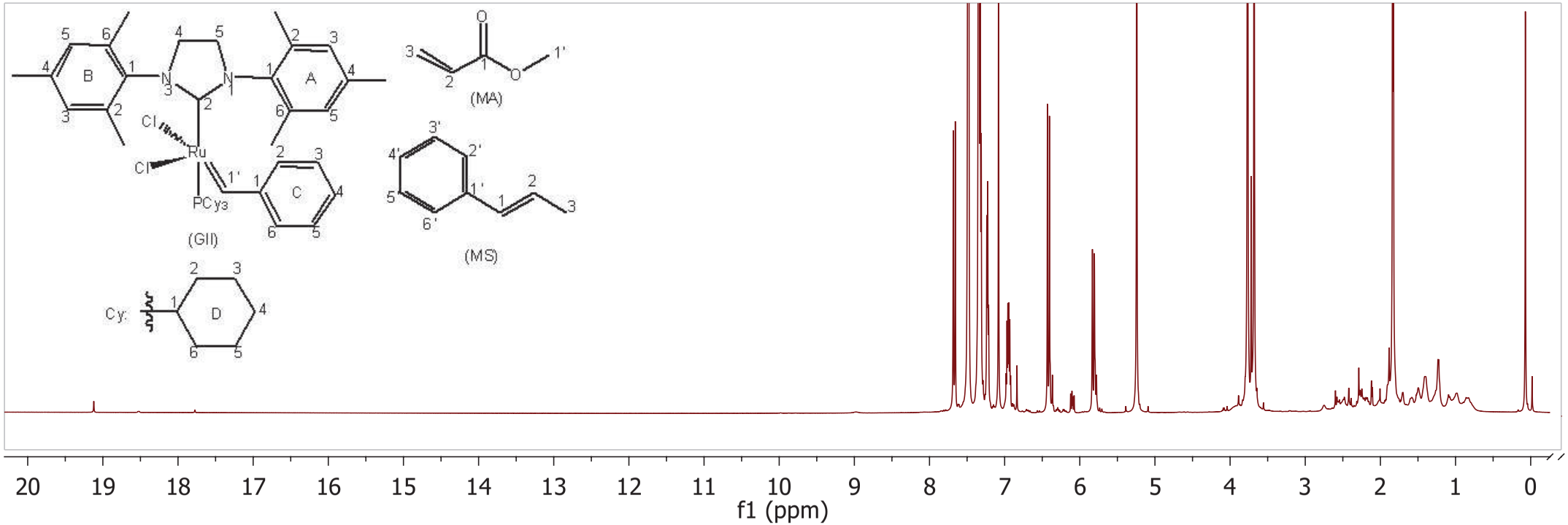

Plate 33b: Grubbs 2nd generation catalyst (**125**) + methyl acrylate (**59**) + trans-β-methylstyrene (**69**)

^{13}C NMR [151 MHz, $CDCl_3$]: δ 167.3, 166.9, 166.6, 165.3, 145.2, 144.8, 144.7, 137.2, 134.3, 133.3, 131.0, 130.7, 130.3, 130.1, 129.8, 128.8, 128.62, 128.59, 128.5, 128.4, 128.1, 128.0, 127.8, 127.7, 127.6, 126.7, 126.5, 126.1, 125.7, 125.6, 122.3, 120.2, 117.7, 113.7, 53.5, 52.3, 51.62, 51.56, 51.3, 50.9, 35.5, 35.1, 31.4, 31.3, 28.8, 27.72, 27.66, 26.9, 26.8, 26.3, 26.1, 25.5, 21.1, 20.9, 19.9, 19.7, 18.6, 18.4, 17.9, 15.3.

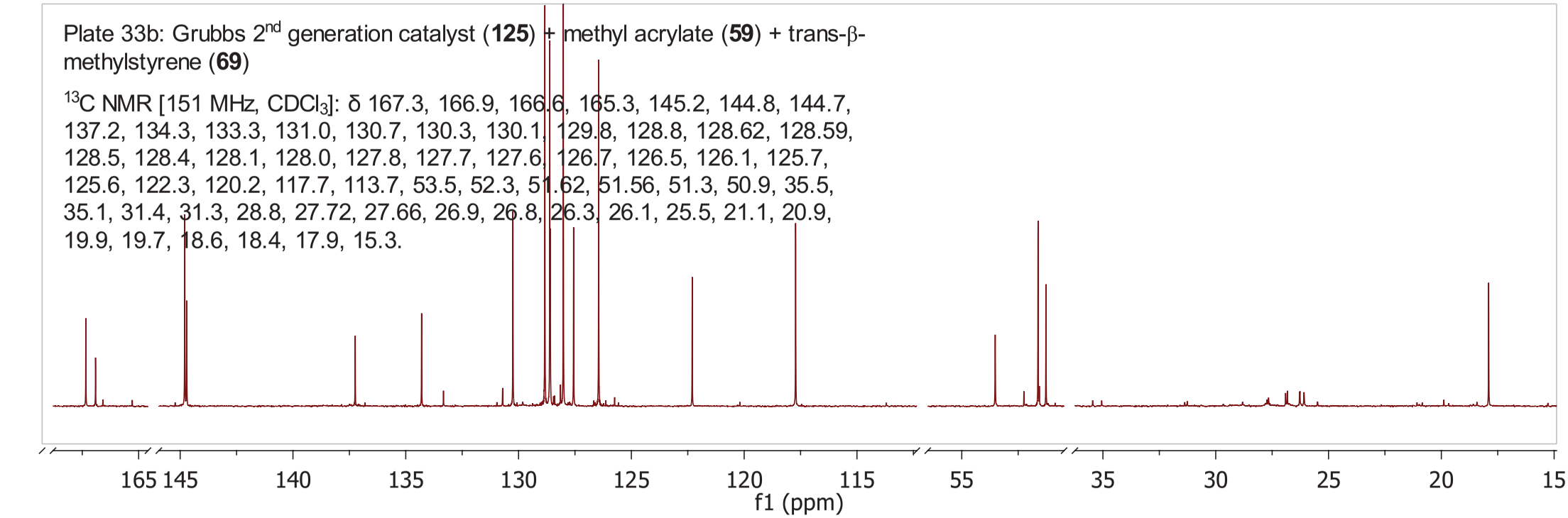

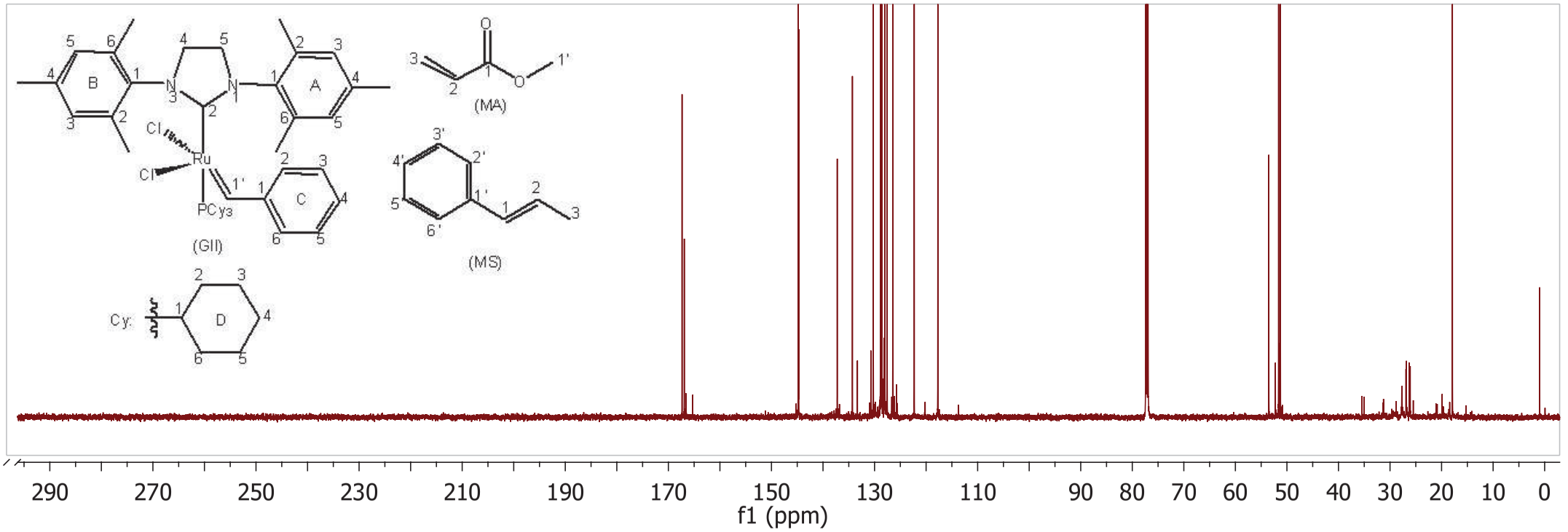

Plate 34a: Tricyclohexylphosphine (**289**) + methyl acrylate (**59**) + LiCl

^{1}H NMR [600 MHz, $CDCl_3$]: δ 6.00 (s), 5.42 (s), 5.16 (s), 4.30 (s), 3.57 (s), 3.48 (s), 2.39 (dd, *J* = 58.4, 6.9 Hz), 2.19 – 0.96 (m).

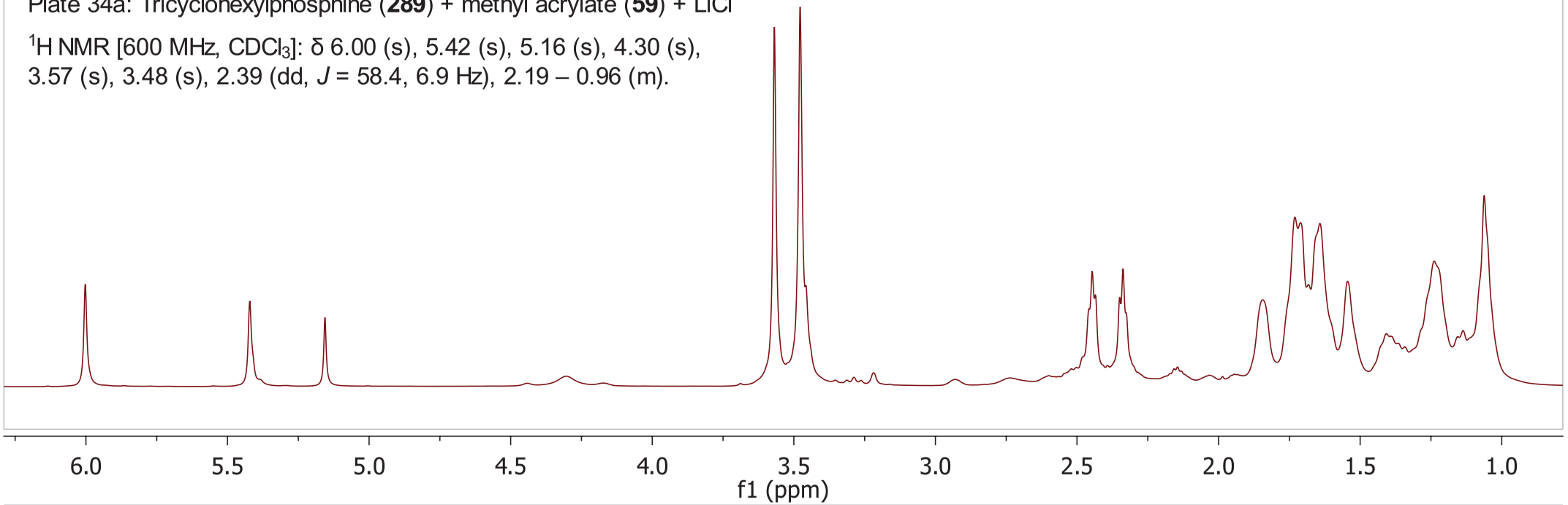

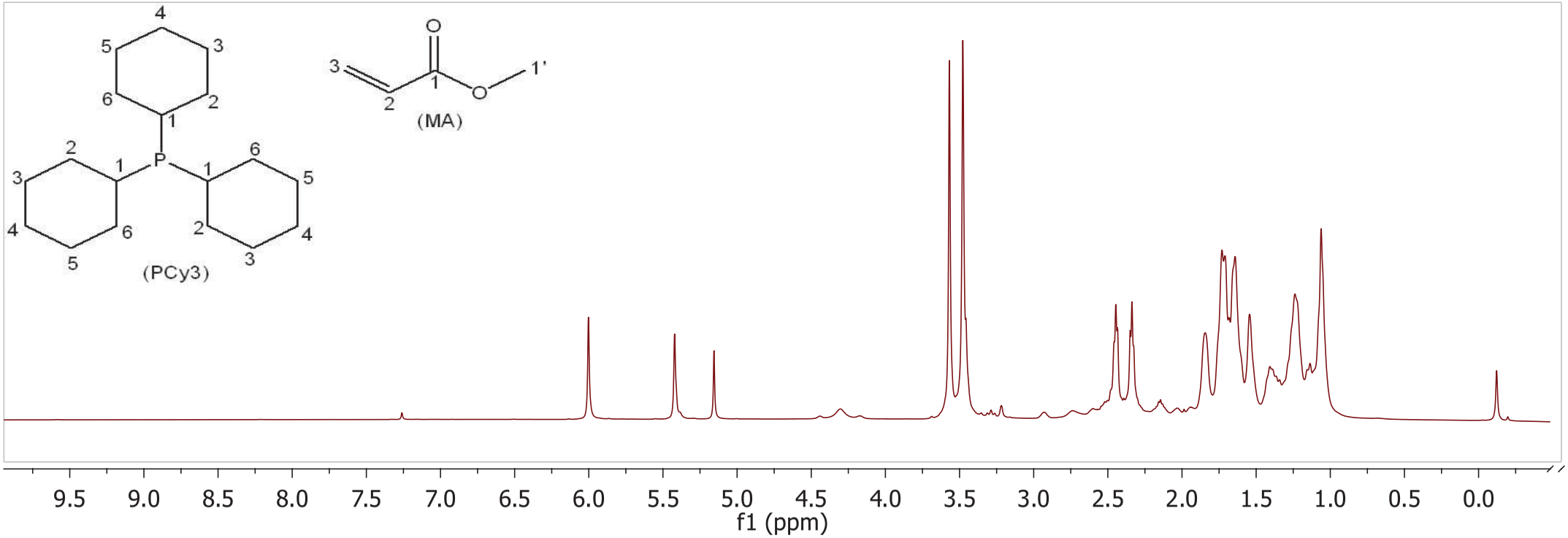

Plate 35a: Tricyclohexylphosphine (**289**) + methyl acrylate (**59**) + LiCl + p-cresol (**266**)

^{1}H NMR [600 MHz, $CDCl_3$]: δ 8.03(s), 7.11 – 7.01 (m), 6.93 and 6.87 (d, *J* = 8.5 Hz, C: H-Ar), 6.84 – 6.78 (m), 6.43 (dt, *J* = 18.2, 9.1 Hz), 6.20 – 6.09 (m), 5.86 (dd, *J* = 10.5, 1.3 Hz), 5.63 (d, *J* = 1.2 Hz), 5.27 (s), 4.23 (t, *J* = 6.4 Hz), 3.77 (t, *J* = 2.7 Hz), 3.74 (s), 3.71 – 3.68 (m), 3.67 – 3.62 (m), 3.42 (s), 2.83 – 2.63 (m), 2.59 – 2.28 (m), 2.23 (s, C:H-Me), 2.04 – 1.88 (m), 1.86 – 1.77 (m), 1.73 – 1.42 (m), 1.40 – 0.97

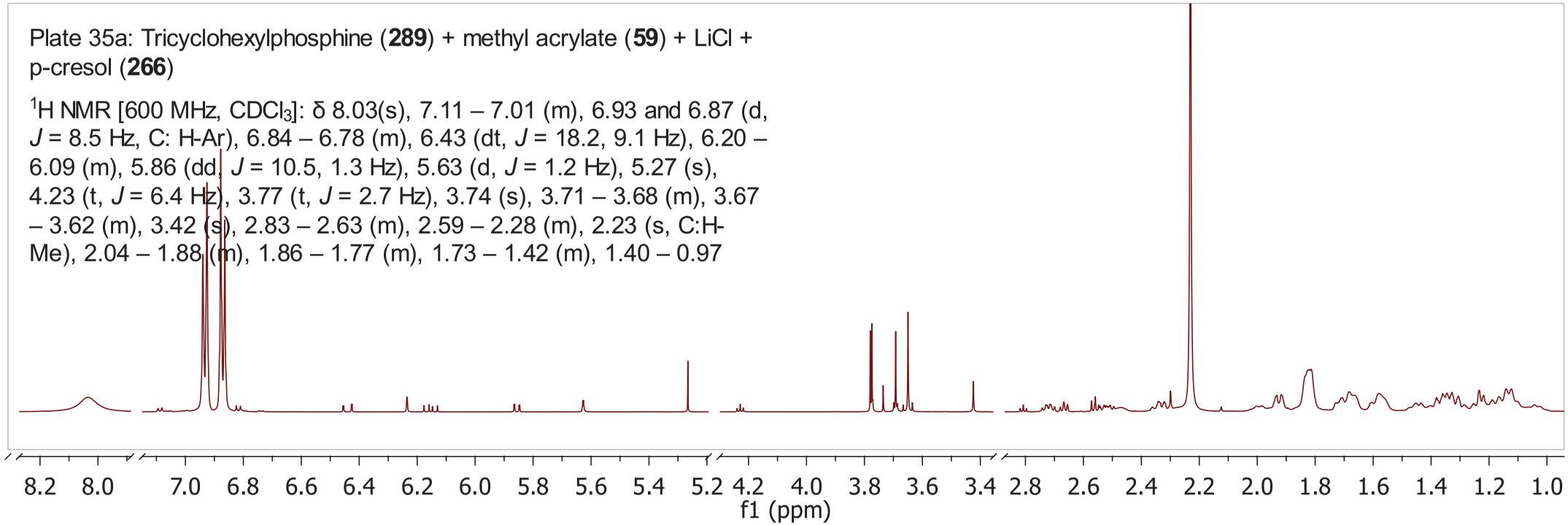

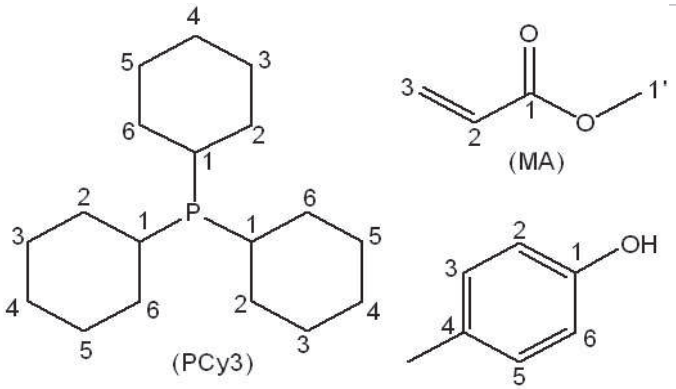

Plate 36a: Grubbs 2nd generation catalyst (**125**) + methyl acrylate (**59**) + trans-β-methylstyrene (**69**) + *p*-cresol (**266**)

^{1}H NMR [600 MHz, $CDCl_3$]: δ 19.12 (s, GII:H-1'), 18.53 (q, *J* = 5.6 Hz), 17.78 (s), 7.94 – 7.77 (m), 7.67 (d, *J* = 16.0 Hz), 7.63 – 7.52 (m), 7.50 – 7.44 (m), 7.38 – 7.30 (m), 7.27 (dd, *J* = 15.7, 8.7 Hz), 7.22 (dd, *J* = 13.5, 6.2 Hz), 7.16 – 7.11 (m), 7.07 (s), 7.00 – 6.91 (m), 6.87 (d, *J* = 19.1 Hz), 6.83 (s), 6.79 (d, *J* = 8.1 Hz), 6.67 (dt, *J* = 22.1, 10.9 Hz), 6.57 – 6.52 (m), 6.41 (d, *J* = 16.0 Hz), 6.38 – 6.06 (m), 5.82 (dd, *J* = 15.5, 1.5 Hz), 5.78 (d, *J* = 11.4 Hz), 5.23 (s), 3.84 (d, *J* = 52.0 Hz), 3.76 (s), 3.75 (s), 3.72 – 3.66 (m), 3.67 (s), 3.64 (d, *J* = 10.6 Hz), 3.55 (s), 2.75 (s), 2.64 – 2.30 (m), 2.29 – 2.24 (m), 2.22 (s), 2.21 – 2.14 (m), 2.11 (s), 2.10 (d, *J* = 1.6 Hz), 2.00 (s), 1.94 – 1.89 (m), 1.86 (d, *J* = 25.7 Hz), 1.82 (dd, *J* = 6.9, 1.4 Hz), 1.76 – 0.72 (m).

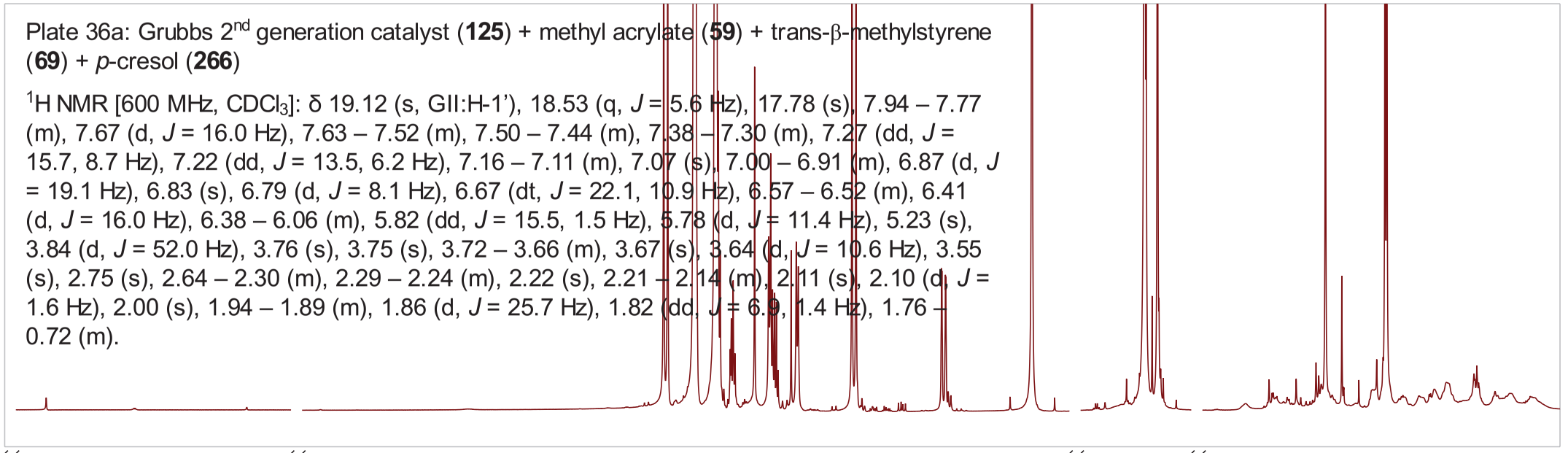

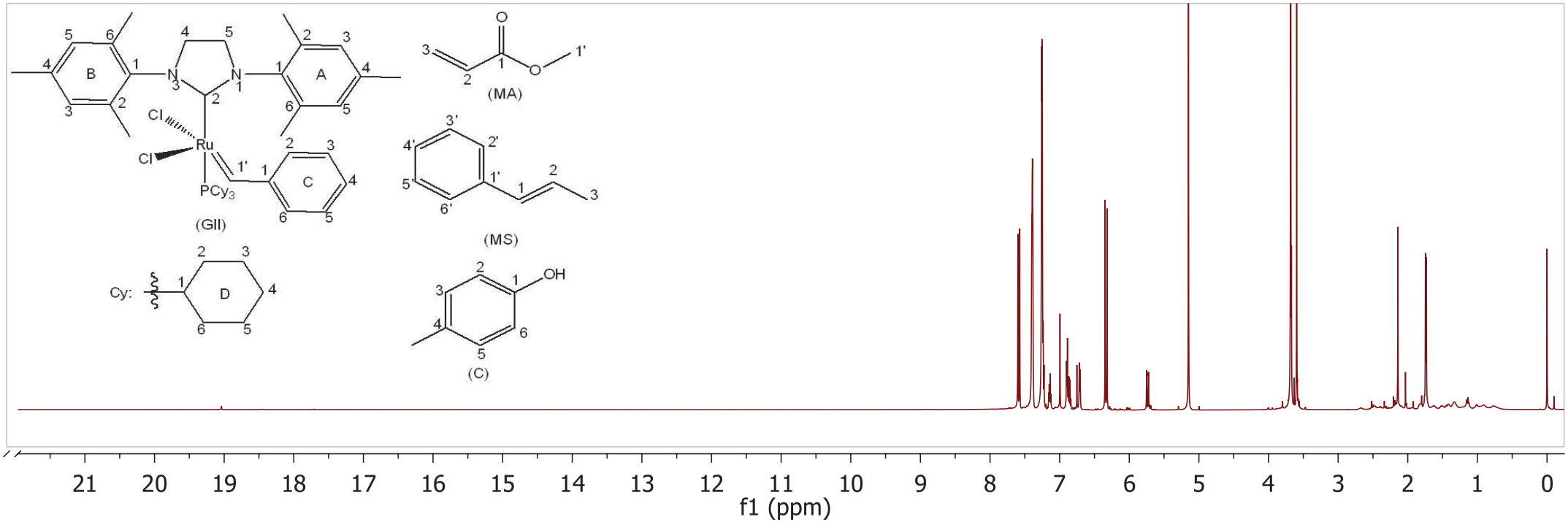

Plate 36b: Grubbs 2nd generation catalyst (**125**) + methyl acrylate (**59**) + trans-β-methylstyrene (**69**) + *p*-cresol (**266**)

^{13}C NMR [151 MHz, $CDCl_3$]: δ 167.4, 167.0, 165.3, 154.33, 144.8, 144.8, 137.2, 134.2, 133.3, 130.9, 130.7, 130.2, 130.1, 129.8, 128.9, 128.8, 128.7, 128.58, 128.55, 128.41, 128.36, 128.2, 128.12, 128.08, 128.0, 127.8, 127.5, 126.6, 126.4, 126.1, 125.7, 125.5, 122.2, 120.1, 117.6, 117.4, 115.2, 77.4, 77.2, 77.0, 53.5, 52.2, 51.6, 51.5, 51.3, 35.2, 34.8, 31.4, 30.8, 28.8, 27.7, 27.6, 27.13, 26.8, 26.7, 26.4, 26.3, 26.1, 26.04, 25.96, 25.3, 21.0, 20.4, 19.9, 18.4, 17.9.

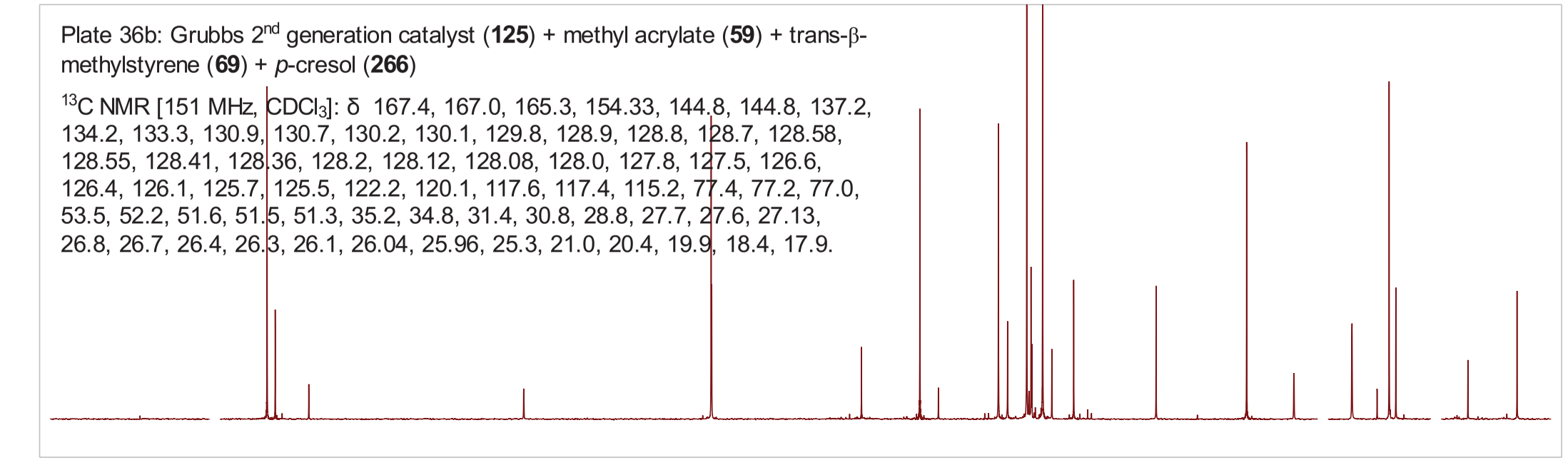

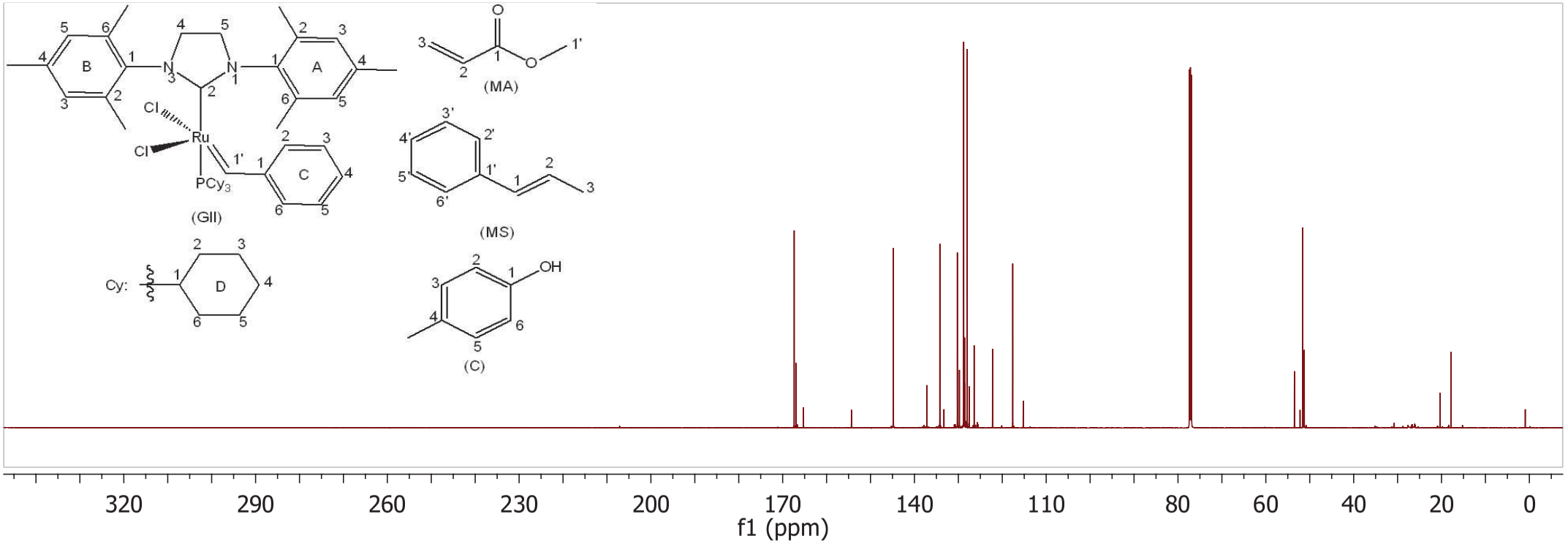

Plate 37a: Grubbs 2nd generation catalyst (**125**) + *cis*-stilbene (**310**) + methyl acrylate (**59**)

^{1}H NMR [600 MHz, $CDCl_3$]: δ 19.12 (s, GII: H-1'), 9.04 (s), 7.49 – 7.43 (m), 7.34 – 7.28 (m), 7.23 – 7.19 (m), 7.19 – 7.08 (m), 7.06 (s, GII: H-3(B)), 7.02 – 6.79 (m), 6.55 (s), 6.40 (d, J = 16.0 Hz), 5.92 – 5.06 (m), 4.03 – 3.78 (m, GII: H-4,5), 3.74 (s), 3.72 (s), 3.67 – 3.39 (m), 2.75 (s, GII: H-2-Me(B)), 2.63 – 2.42 (m), 2.62 – 2.34 (m), 2.29 (s), 2.19 (s, GII: H-4-Me(B)), 2.20 – 2.12 (m), 2.06 (s, H-2-Me(A)), 2.00 (s, 1.87 (s), 1.93 – 1.63 (m), 1.62 – 0.48 (m, GII: H-2-6(D)).

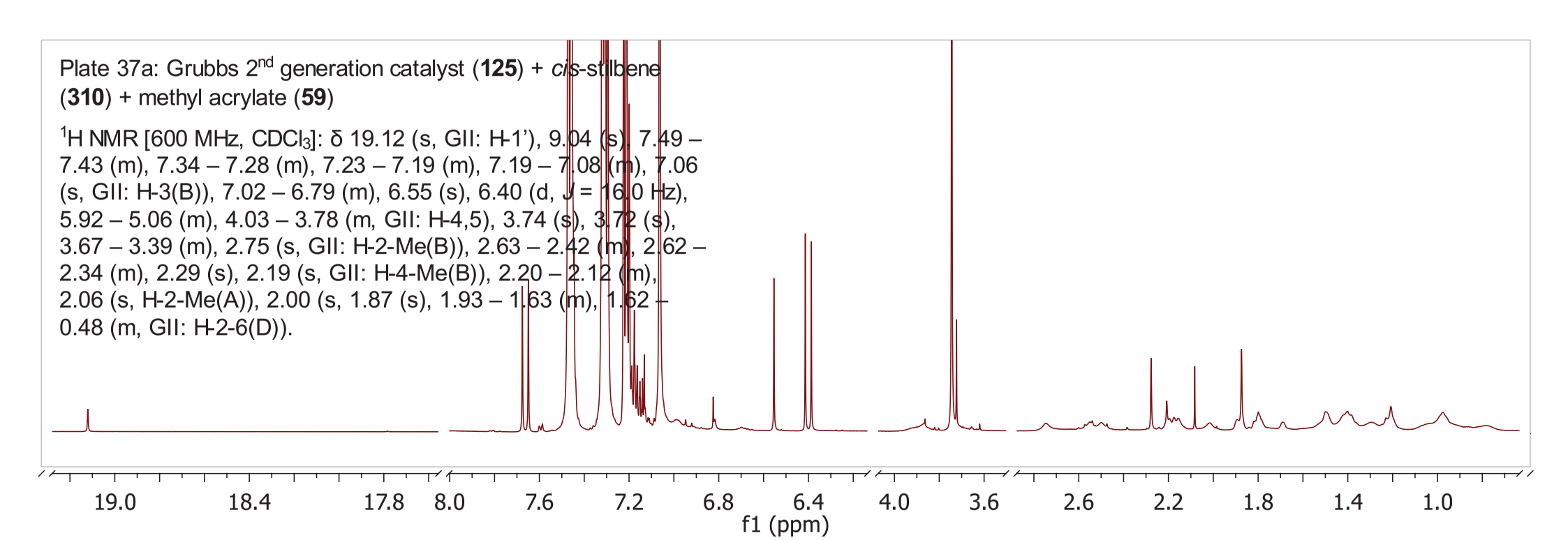

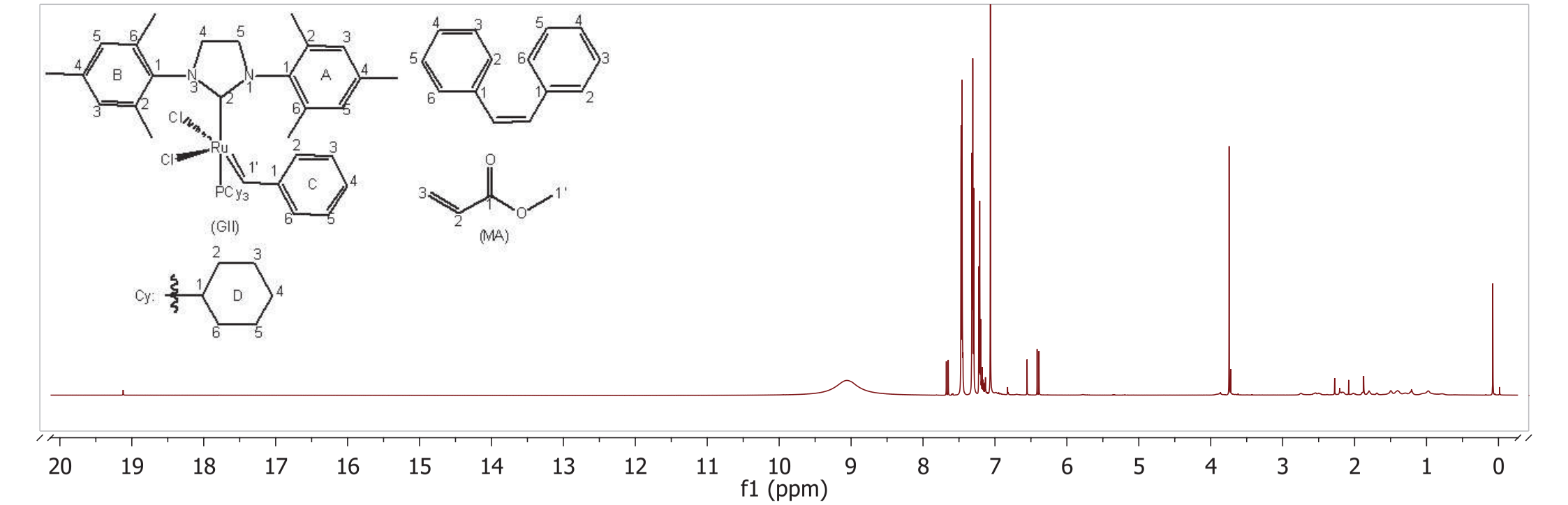

Plate 37b: Grubbs 2nd generation catalyst (**125**) + *cis*-stilbene (**310**) + methyl acrylate (**59**)

^{13}C NMR [151 MHz, $CDCl_3$]: δ 220.4 (d, J = 77.4 Hz, GII: C-2), 167.4, 165.4, 151.3(GII: C-1(C)), 144.9, 144.8, 138.3(GII: C-4(B)), 137.6(GII: C-4(A)), 137.4, 137.33, 137.25, 135.2(GII: C-1(B or A)), 134.4, 133.4, 130.29, 130.26, 129.9, 128.9, 128.7, 128.5, 128.2, 128.1, 127.9, 127.8, 127.6, 127.1(GII: C-5(B)), 126.7, 126.5, 126.3, 117.8, 52.2, 51.7, 51.2, 35.5, 35.2, 31.4 (d, J = 16.7 Hz, GII: C-2,6(D)), 30.9, 29.1, 27.8 (d, J = 9.8 Hz, GII: C-3,5(D)), 27.0 (d, J = 11.8 Hz), 26.4 (d, J = 2.7 Hz), 26.2, 21.0 (d, J = 34.8 Hz), 20.0.

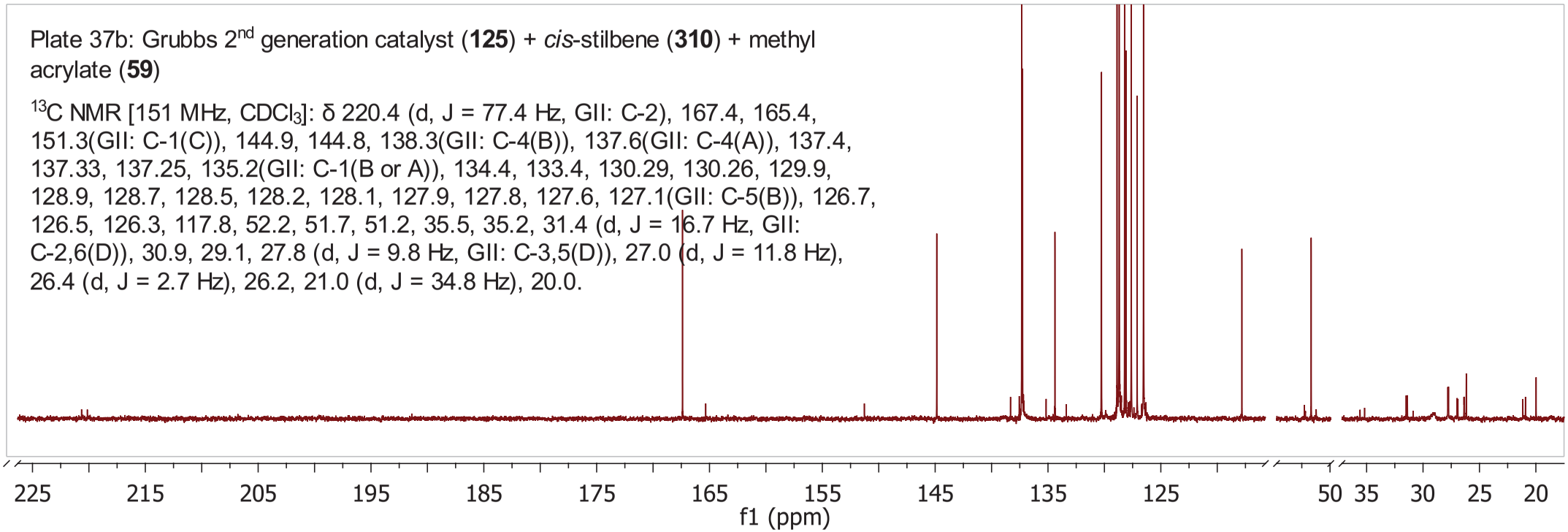

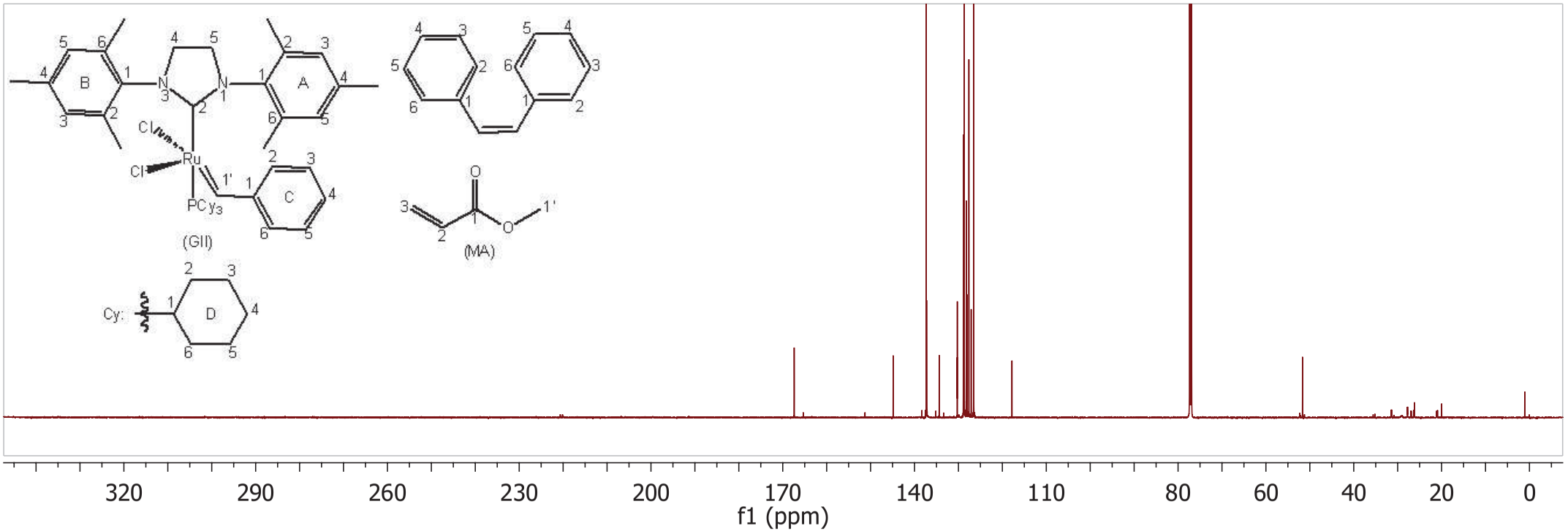

Plate 38a: Grubbs 2nd generation catalyst (**125**) + *cis*-stilbene (**310**) + methyl acrylate (**59**) + *p*-cresol (**266**)

^{1}H NMR [600 MHz, $CDCl_3$]: δ 19.12 (s, GII: C-1'), 9.10 (s), 7.89 – 7.79 (m), 7.70 (s), 7.68 (s), 7.63 (d, *J* = 8.2 Hz), 7.52 – 7.47 (m), 7.39 – 7.31 (m), 7.27 – 7.22 (m), 7.20 (s), 7.19 (s), 7.09 (s), 6.99 (d, *J* = 8.1 Hz, C:H-3,5), 6.85 (s), 6.84 (s), 6.78 (d, *J* = 8.1 Hz, C:H-2,6), 6.58 (s), 6.44 (s), 6.42 (s), 6.29 (s), 5.81 (s), 4.02 – 3.82 (m), 3.78 (s), 3.77 (s), 3.70 – 3.63 (m), 2.79 – 2.33 (m), 2.30 (s), 2.24 (s), 2.21 – 1.98 (m), 1.97 – 0.68 (m, GII: C-2-6(D)).

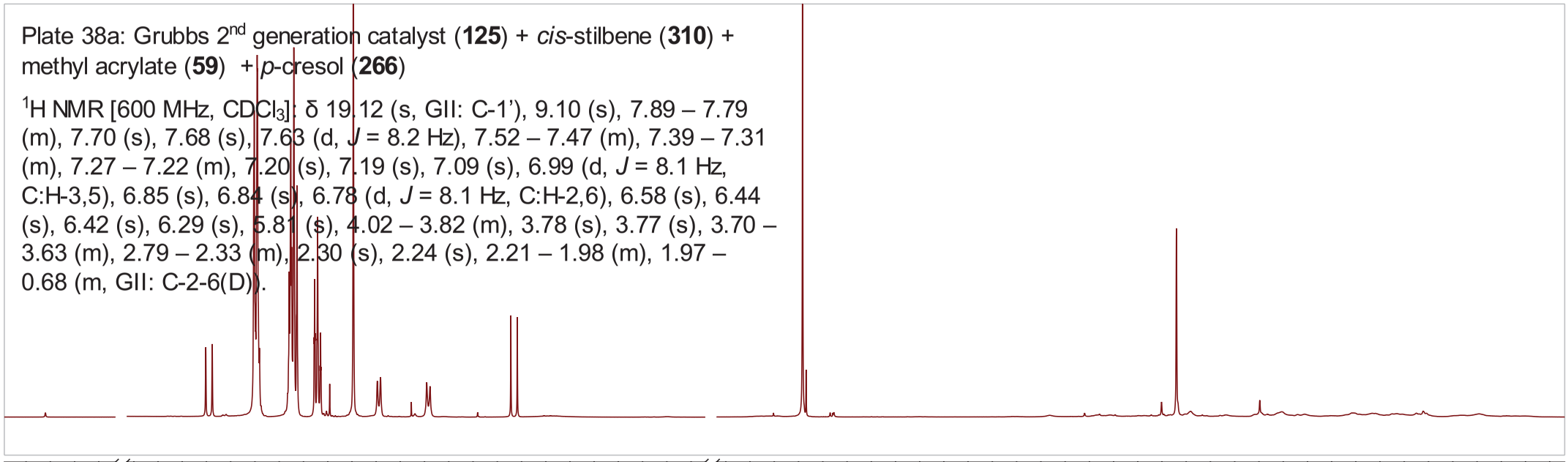

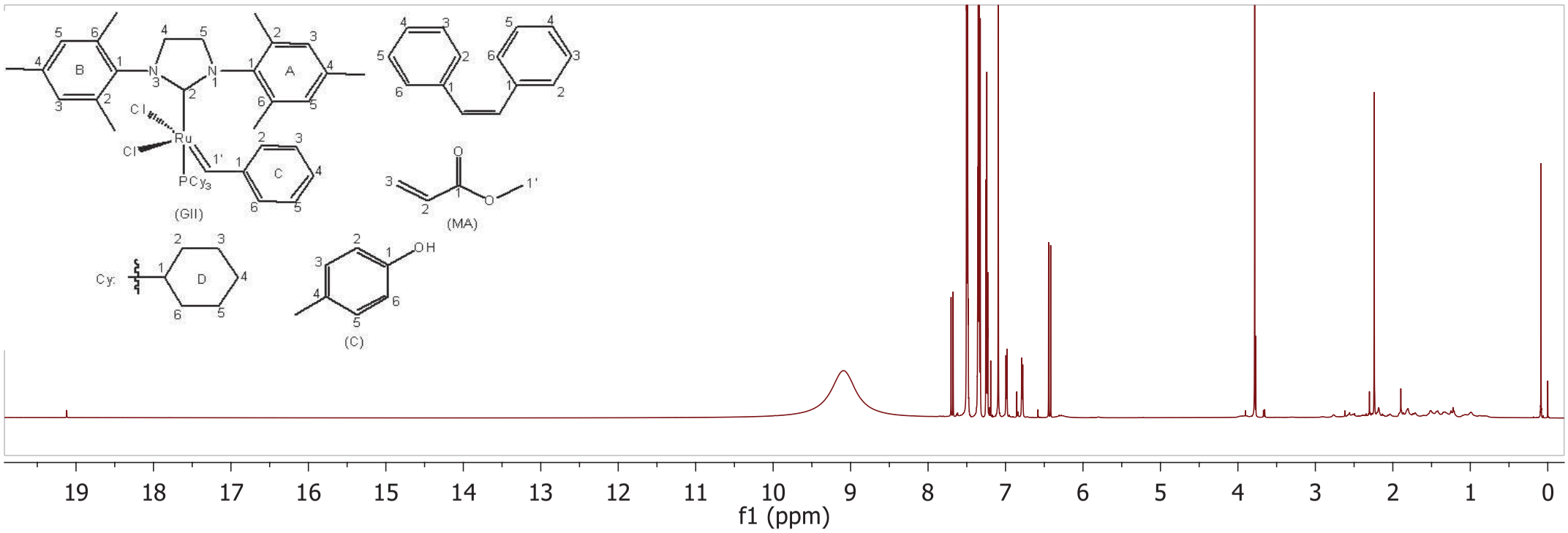

Plate 38b: Grubbs 2nd generation catalyst (**125**) + *cis*-stilbene (**310**) + methyl acrylate (**59**) + *p*-cresol (**266**)

Int. ^{13}C NMR [151 MHz, $CDCl_3$]: δ 282.7, 220.2, 167.6, 165.5, 154.1, 145.0, 138.4, 137.64, 137.57, 137.4, 137.3, 137.2, 134.4, 133.5, 130.4, 130.3, 130.0, 129.2, 128.96, 128.94, 128.76, 128.75, 128.6, 128.3, 128.2, 128.0, 127.8, 127.7, 127.2, 126.6, 126.4, 117.8, 115.4, 77.4, 77.2, 77.0, 52.4, 51.8, 31.6, 31.5, 27.9, 27.8, 27.0, 26.9, 26.2, 21.2, 21.0,

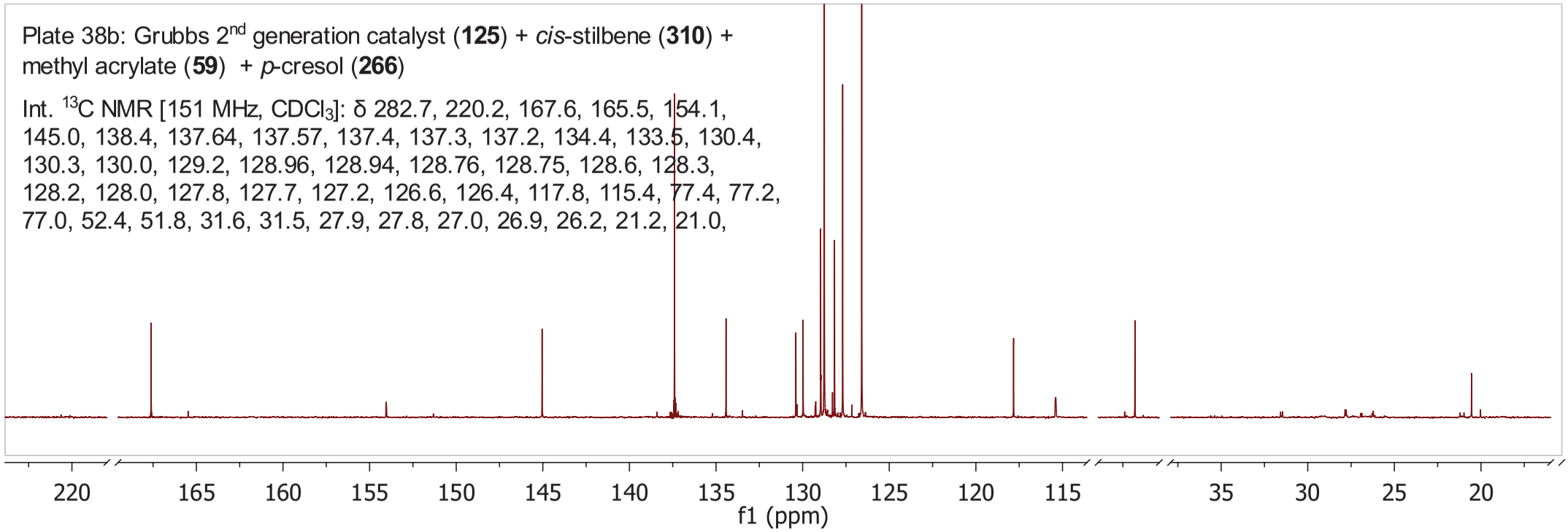

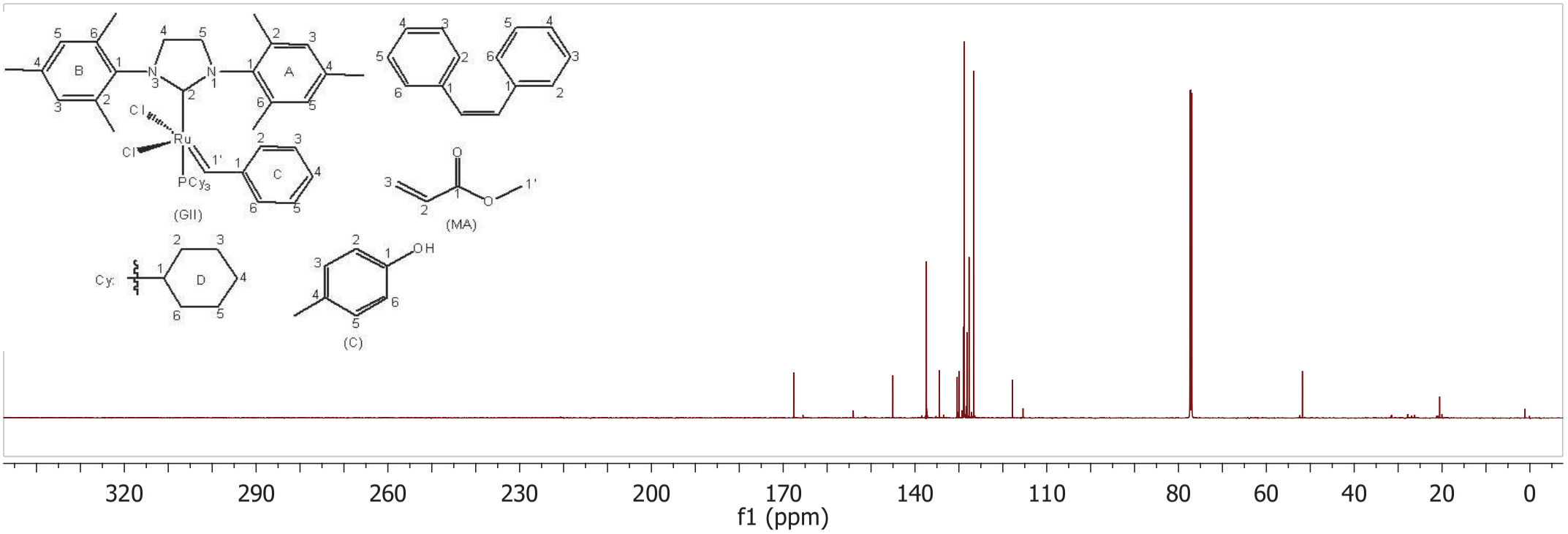

SUMMARY

Summary

2-Ethylhexyl *p*-methoxycinnamate [Octyl methoxycinnamate (OMC)] is an organic compound that is commercially used in the cosmetic industry as a UV blocker in sunscreen creams and lotions. Commercial production of this compound, however, is hampered by multiple synthetic steps, high temperatures, tedious work-up procedures, halogenated by-products, and low atom economy. Due to the abundance of naturally occurring essential-oil phenylpropenoids like estragole, eugenol, and safrole, which can easily be transformed into anethole, isoeugenol, and isosafrole by catalytic double bond isomerisation, the possibility of utilizing one of these β-methylstyrenes, *i.e*. anethole, together with 2-ethylhexyl acrylate in metathesis based methodology for the preparation of OMC looked promising and was investigated.

Model metathesis reactions between *trans*-β-methylstyrene and methyl acrylate over Grubbs 2nd generation catalyst, however, produced only the homo-metathesis product, *trans*-stilbene, in very high yields (>99%). Solvent, temperature and reactant ratio studies failed to change the course of the reaction towards the desired cross-metathesis product. Since Forman *et al*. reported the addition of phenol to the reaction mixture to enhance cross-metathesis over self-metathesis, the reaction was repeated with *p*-cresol (2 eq.) as additive. In order to prevent secondary metathesis reactions from occurring, the propene side-product was also stripped away by entrainment with argon, which led to the successful formation of methyl cinnamate in 38% yield.

In order to determine the general applicability of the new process, the electronic effect, if any, of substituents in the *para*-position of the β-methylstyrene and the steric/electronic influence of the alkyl group attached to the α,β-unsaturated carbonyl compound on the outcome of the reaction were investigated. *Trans*-*p*-methoxy-β-methylstyrene (*trans*-anethole) (1 eq.) and *trans*-4-trifluoromethylsulfonyloxy-β-methylstyrene (1 eq.) were therefore reacted with methyl acrylate (2 eq.) under the optimized reaction conditions [Grubbs 2nd

generation catalyst (0.5 mol%), *p*-cresol (0.25 eq.), refluxing DCM (10 mL), 2 hours] and it was found that an electron-donating group in the *para*-position caused a slight decrease in cross-metathesis product formation (36% vs 38% for unsubstituted *trans*-β-methylstyrene) whereas an electron-withdrawing group (triflate) in the same position enhanced cinnamate formation (43% vs 38%). The concomitant homo-metathesis reaction followed the opposite trend with the *p*-triflate suppressing stilbene formation (4% vs 18% for unsubstituted *trans*-β-methylstyrene) and a *p*-methoxy group enhancing the formation of the stilbene (50% vs 18%).

When the influence of the *O*-alkyl group attached to the α,β-unsaturated carbonyl moiety was investigated, it was found that the yield of the cinnamate product increased with increasing steric bulk of the alkyl group. For the reaction of unsubstituted *trans*-β-methylstyrene with methyl acrylate and *n*-butyl acrylate, respectively, the yield increased from 38 to 55%, while for reaction between *trans*-anethole and these acrylates it went from 36 to 41%. Substituting the ester *O*-alkyl moiety in the α,β-unsaturated system with an alkyl group (3-buten-2-one) and a hydrogen (acrolein), resulted in moderate yields of 34 and 32% for the reactions between the ketone and unsubstituted *trans*-β-methylstyrene and *trans*-anethole, respectively, while with acrolein only trace amounts (< 5%) of the cross–metathesis products were obtained. In all these reactions, the respective stilbenes were formed in 18 (for the reaction between methyl or *n*-butyl acrylate and *trans*-β-methylstyrene) to 58% (for the reaction of acrolein with *trans*-β-methylstyrene) yield. Finally, *trans*-β-methylstyrene and *trans*-anethole were reacted with 2-ethylhexyl acrylate to form 2-ethylhexyl cinnamate and the desired 2-ethylhexyl *p*-methoxycinnamate (OMC), which could be isolated as major products from the reaction in 64 and 47% yields, respectively. Due to the higher reactivity of *trans*-anethole, the cross-metathesis product (OMC) in this instance was accompanied by 32% of 4,4'-dimethoxystilbene.

In an effort to determine how *p*-cresol addition affects the catalytic cycle of Grubbs 2nd generation catalyst and thus how it influences product formation, a full NMR study of the addition of cresol to the catalyst, the catalyst and *trans*-β-

methylstyrene, the catalyst and methyl acrylate, as well as all the reactants together, was embarked upon. Despite severely restricted rotation, which necessitated the spectra to be recorded at 60 ^{o}C, room temp., and -40 ^{o}C, all the ^{1}H and ^{13}C NMR resonances in the spectra of the Grubbs II catalyst could be allocated unambiguously to the appropriate protons and carbon atoms. ^{31}P NMR studies allowed for the confirmation of a hydrogen bonding complex between cresol and the catalyst, while it also indicated some dissociation of the tricyclohexylphosphine from the catalyst to occur. The liberated tricyclohexylphosphine, however, prefers to react with the acrylate in a 1,4-addition process rather than forming a complex with the cresol as was postulated by Forman *et al.* This was confirmed by the preparation of the zwitterionic phosphonium salt through reaction of tricyclohexylphosphine with methyl acrylate in the presence of LiCl. Addition of cresol to the reaction mixture enhances the formation of the salt in its protonated form, while it also induces accelerated formation of oligomeric forms of the initially formed monomeric zwitterionic phosphonium salt.

Although Forman *et al.* proposed the addition of phenols to stabilize the Grubbs catalyst by slowing down the dissociation of the tricyclohexylphosphine from the metal and once dissociated, prevents the phosphine from binding to the metal again, this explanation does not allow for the fact that the more reactive styrene analogue becomes less reactive than the acrylate moiety when cresol is added to the reaction mixture, as is evident from the fact that cresol addition enhances cross-metathesis. It was determined during the current study that the cross-metathesis products (cinnamates) are indeed the result of the primary metathesis process and are not formed through secondary metathesis of the stilbene products. In order to explain the formation of the cross-metathesis over homo-metathesis products in the presence of cresol, it is proposed that an associative mechanism rather than a dissociative process is prevailing when cresol is added to the reaction mixture. In this instance the co-ordination number of the ruthenium temporarily increases from 5 to 6 to allow for the additional ligand to be attached to the metal centre. The catalyst complex

therefore becomes sterically more crowded and the steric size of the incoming ligand (reactant) would play a decisive role in its ability to react with the metal centre in the first step of the reaction. Since acrylate represents a mono substituted alkene and the alkyl group resides in a remote location with regard to the reaction centre, it would be sterically less demanding when compared to *trans*-β-methylstyrene and lead to enhanced formation of the cross-metathesis product. This assumption was proven by substituting methyl acrylate with methyl crotonate during the reaction and the resulting drop in cross-metathesis product from 38 to 31% yield observed. Support for this proposal comes from results by Fogg and co-workers, who reported cross-metathesis to be the dominant reaction when β-methylstyrenes were reacted with acrylates over the Hoveyda-Grubbs catalyst.

Finally, with a number of cinnamates (OMC, methyl *p*-methoxycinnamate, methyl cinnamate, *n*-butyl cinnamate, *n*-butyl *p*-methoxycinnamate, and 2-ethylhexyl cinnamate) and 3-buten-2-ones [4-phenyl-3-buten-2-one and 4-(4-methoxyphenyl)-3-buten-2-one] available, it was decided to evaluate the UV-B blocking properties of these compounds through utilization of UV spectroscopy in an effort to determine if OMC would, in principle, be the best sunscreen component of the series. By comparing the UV spectra of OMC to that of the other compounds, it was determined that methyl cinnamate, *n*-butyl cinnamate, methyl *p*-methoxycinnamate and *n*-butyl *p*-methoxycinnamate could be promising candidates in the development of new and maybe better sunscreen lotions and should be subjected to biological evaluation processes.

Keywords:
metathesis, Grubbs 2nd generation catalyst, cresol, *trans*-β-methylstyrene, acrylate, cinnamate, associative mechanism, ultra-violet spectroscopy.